Regulation of Autophagy, Endoplasmic Reticulum and Unfolded Protein Response by Glucocorticoids in Physiology and Disease

Sangkab Sudsaward

School of Environment & Life Sciences

College of Science and Technology

Biomedical Research Centre

The University of Salford, UK

Submitted in partial fulfilment of the requirements of the Degree of Doctor of Philosophy, 2018

TABLE OF CONTENTS

LIST OF TABLES

LIST OF FIGURES

ACKNOWLEDGEMENTS

I would like to take this special opportunity to express my sincere appreciation and gratefulness to my supervisor, Professor Marija Krstic-Demonacos for all supports, guidance and advice during my PhD life, Dr Costas Demonacos for his invaluable suggestion and for his constant, in addition to allowing me access to his laboratory to complete some experiments.

Inside our laboratory, I would like to extend my heartfelt thanks to all our colleague in Salford University and from Manchester University who contributed to this accomplishment and for their friendship and support at our group meetings and for helping me find what I needed when carrying out work.

I would like to acknowledge the Faculty of Medical Sciences, Naresuan University, and The Royal Thai Government for the grant and scholarship and time for PhD study.

Finally, I would like to express my sincere gratitude and deep appreciation to my family, especially my parents and my wife for their love, unfailing support, continuous encouragement, and long-term patient to my success.

Sangkab Sudsaward

DECLARATION

No portion of the work referred to in this thesis has been submitted in support of an application for another degree or qualification at this or any other university or institute of learning.

COPYRIGHT STATEMENT

The author of this thesis (including any appendices and/or schedules to this thesis) owns any copyright in it (the "Copyright") and he has given The University of Salford the right to use such Copyright for any administrative, promotional, educational and/or teaching purposes.

i. Copies of this thesis, either in full or in extracts, may be made **only** in accordance with the regulations of the Clifford Whitworth Library, The University of Salford. Details of these regulations may be obtained from the Librarian. This page must form part of any such copies made.

ii. The ownership of any patents, designs, trademarks and any and all other intellectual property rights except for the Copyright (the "Intellectual Property Rights") and any reproductions of copyright works, for example graphs and tables ("Reproductions"), which may be described in this thesis, may not be owned by the author and may be owned by third parties. Such Intellectual Property Rights and Reproductions cannot and must not be made available for use without the prior written permission of the owner(s) of the relevant Intellectual Property Rights and/or Reproductions.

iii. Further information on the conditions under which disclosure, publication and exploitation of this thesis, the Copyright and any Intellectual Property Rights and/or Reproductions described in it may take place, is available from the Dean of the School of Environment and Life Sciences.

LIST OF ABBREVIATIONS

11β-HSD	11β-hydroxysteroid dehydrogenase
ABL1	ABL proto-oncogene 1
ACTH	Adrenocorticotropic hormone
AF	Activation function
AIF	Apoptosis-inducing factor
ALL	Acute lymphoblastic leukemia
AMBRA1	Activating molecule in Beclin-1-regulated autophagy
AML	Acute myeloid leukemia
AMPK	AMP-activated protein kinase
Apo/DR	Apoptosis / Death receptor ligands
ARID5B	AT-rich interaction domain 5B
ATF4	Activating transcription factor 4
ATF6	Activating transcription factor 6
ATG	Autophagy-related protein
AVP	Arginine vasopressin
Bak	Bcl-2-antagonist-killer protein
Bax	Bcl-2-associated X protein
Bcl-2	B-cell lymphoma 2
BCR	Breakpoint cluster region
BH	Bcl-2 homology
BIM	Bcl-2 like Protein 11
Bip	Binding immunoglobulin protein
BNIP3	Bcl-2 adenovirus E1a nineteen kDa interacting protein 3; a prodeath Bcl-2 family member
Bok	Bcl-2-related ovarian killer protein
BTZ	Bortezomib
CAD	Carbamoyl-phosphate synthetase 2, aspartate transcarbamylase, and dihydroorotase
CaMKKβ	Calcium-activated calmodulin-dependent kinase kinase-β
CAT	Catalase
CBG	Corticosteroid binding globulin

CBP	CREM-binding protein
CDC28	Cell division control protein 28
CDK5	Cyclin-dependent kinase 5
cDNA	Complementary deoxyribonucleic acid
CEBPE	CCAAT enhancer binding protein epsilon
CEM	Human lymphoblastoid cell line
CFIA / CFIB	Factor
CHOP	CCAAT/enhancer binding protein homologous protein
CLL	Chronic lymphoblastic leukemia
CLOCK/BMAL1	Circadian locomotor output cycle kaput / brain-muscle-arnt-like protein1
CLQ	Chloroquine
CMA	Chaperone-mediated autophagy
CML	Chronic myeloid leukemia
cMyc	Transcriptional regulator Myc-like
CoQ10	Coenzyme Q10
CREB	cAMP responsive element binding protein
CRH	Corticotropic releasing hormone
CRUK	Cancer research UK
CTLs	Cytotoxic T lymphocytes
CytC	Cytochrome c
DAPk	Death-associated protein kinase
DBD	Deoxyribonucleic acid-binding domain
DCC	Dextran coated charcoal
DD	Death domain
Dex	Dexamethasone
DIABLO	Direct inhibitor of apoptosis-binding protein with low pI
DISC	Death inducing signaling complex
DNA	Deoxyribonucleic acid
DRIP	Vitamin D receptor interacting protein
E2F1	E2F transcription factor 1
eIF2α	Eukaryotic initiation factor 2α
Endo-G	Endonuclease G
ER	Endoplasmic reticulum

ERAD	ER-associated protein degradation
ERK	Extracellular signal related kinase
ERSE	ER stress response element
ETC	Electron transport chain
ETV6	ETS-variant gene 6
FACS	Fluorescence-activated cell sorting
FADD	Fas associated death domain
FasL/FasR	First apoptosis signal ligand / First apoptosis signal receptor
FBS	Fetal bovine serum
FIP200	Focal adhesion kinase family-interacting protein of 200 kD
FKBP5	FK 506 binding protein 51
FKBP52 (FKBP4)	FK 506 binding protein 4
FSC	Forward scatter
GATA3	GATA binding protein 3
GBM	Glioblastoma
GCN2	General control nonderepressible-2
GCs	Glucocorticoids
GR	Glucocorticoid receptor
GRE	Glucocorticoid response element
GRP78	Glucose regulated protein 78
GRP94	Glucose regulated protein 94
GRwt	Glucocorticoid receptor wild type
GSH	Glutathione
GSK-3β	Glycogen synthase kinase 3β
HAT	Histone acetyltransferase
HCC	Hepatocellular carcinoma
HDACi	Histone deacetylase inhibitors
hGR	Human glucocorticoid receptor
HIF-1	Hypoxia-inducible factor-1
HL-60	Human promyelocytic leukemia - 60
HPA	Hypothalamus Pituitary axis
HRP	Horse radish peroxidase
HSP70	Heat shock protein 70
HSP90	Heat shock protein 90

HSPA8	Heat shock protein A8
IBD	Inflammatory bowel disease
IGF-1	Insulin-like growth factor 1
IKZF1	IKAROS family zinc finger 1
IL-1	Interleukin-1
IM	Imatinib mesylate
IRE1α	Inositol-requiring enzyme 1α
JNK	c-Jun N-terminal kinase
LAMP2A	Lysosomal-associated membrane protein 2A
LBD	Ligand-binding domain
LC3	Light chain 3
LKB1	Liver kinase B1
LPS	Lipopolysaccharide
MAPK	p38 mitogen-activated protein kinase
MDC	Monodansylcadaverine
MDS	Myeloid dysplastic syndrome
MM	Multiple myeloma
MMPA	Mitochondria membrane potential assay
MPT	Mitochondria permeability transition
mTORC1	Mammalian target of rapamycin complex 1
MTX	Methotrexate
NADPH	Nicotinamide Adenine Dinucleotide Phosphate Hydrogen
NF-kB	Nuclear factor kappa light chain enhancer of activated B cells
NIX or BNIP3L	BNIP3-like protein
NOXA	NADPH oxidase activator
NRB	Nuclear receptor binding
NTD	N-terminal domain
p/CAF	p300 / CBP-associated factor
p300/CBP	p300 / CREB-binding protein
p34	Cyclin-dependent kinase catalytic subunit p34
PAX5	Pair box gene 5
PE	Phosphatidylethanolamine
PERK	Pancreatic ER kinase-like ER kinase
PI	Propidium iodide

PI3K	Phosphoinositide 3-kinase
PKCθ	Phosphorylation of protein kinase Cθ
PKR	IFN-inducible double-stranded RNA-dependent protein kinase R
Ph	Philadelphia chromosome
PSMA	Prostate specific membrane antigen
PTMs	Post-translational modifications
PUMA	p53-upregulated modulator of apoptosis
PVDF	Polyvinylidene difluoride
PVN	Paraventricular nucleus
Rheb	Ras homolog enriched in brain
RIP	Receptor-interacting protein
RIPA	Radio-immunoprecipitation assay
RNA	Ribonucleic acid
RNase A	Ribonuclease A
ROS	Reactive oxygen species
ROT	Rotenone
RPM	Revolution per minute
RT-PCR	Reverse transcription polymerase chain reaction
SAHA	Suberoylanilide hydroxamic acid
SDS-PAGE	Sodium dodecyl sulphate-polyacrylamide gel electrophoresis
SERCA	Sarco-endo-plasmic reticulum Calcium ATPase
SERPIN	Serine proteinase inhibitor
Smac	Second mitochondrial-derived activator of caspase
SOD	Superoxide dismutase
SSC	Side scatter
STAT	Signal Transducers and Activators of Transcription
SUMO	Small Ubiquitin-like Modifier
SWI/SNF	SWItch/Sucrose Non-Fermentable
TBP	TATA binding protein
TG	Thapsigargin
TIM	TRAF-interacting motifs
TLRs	Toll-like receptors
TNF	Tumour necrosis factor
TNFR	Tumor necrosis factor receptor

TRADD	TNFR associated DD
TRAF	Tumor necrosis factor receptor associated factor
TRAIL-R	TNF-related apoptosis-inducing ligand-R
TRAP	Thyroid hormone receptor-associated protein
Tregs	Regulatory T cell
TSC	Tuberous sclerosis complex (TSC) tumor syndrome
ULK	UNC51-like kinase
UPR	Unfolded protein response
UVRAG	UV radiation resistance-associated gene protein
VPS34	Phosphatidylinositol 3-kinase
XBP1	X-box binding protein 1

ABSTRACT

Acute lymphoblastic leukemia (ALL) is the most frequent cancer in children, and although highly treatable, challenges remain due to significant side effects of therapy and the poor outcome for some patients. Synthetic glucocorticoid, Dexamethasone (Dex), has been used to treat several haematological malignancies including ALL. To understand better how GC-resistant leukemic cells respond to Dex treatment, combination treatment of Dexamethasone with Chloroquine (CLQ), Thapsigargin (TG), Rotenone (ROT) and Bortezomib (BTZ) were used to investigate the role of autophagy, endoplasmic reticulum stress (ER stress) and unfolded protein response (UPR) respectively, in acute lymphoblastic leukemia cell lines including CEM-C1-15, CEM-C7-14 and Molt4.

The results showed that autophagy inhibition by CLQ increased cell death and combination treatment with Dex exerted cytotoxic effect in all cells. These findings suggest that autophagy may play the important role to protect the ALL cells from GC-induced cell apoptosis, especially in GC-resistant cells. Furthermore, ER stress inducer, TG, treatment in the absence and presence of dexamethasone resulted in increase of ER chaperone proteins GRP78 and GRP94 in CEM-C7-14 cells. This is potentially related to increased cell death and may play a role in ER stress mediated cell apoptosis. Protein degradation inhibition by BTZ sensitised the ALL cells to the treatments and combination conditions had synergistic effect in all leukemic cells. Reactive oxygen species assay indicated that increased ROS levels correlate with the increase in CEM cells death in ROT only and combination treatment with Dex. Interestingly, ER chaperone proteins GRP78 and GRP94 increase in the protein but not mRNA expression levels in Dexamethasone treated glucocorticoid-sensitive cells. These results suggested that GR regulated chaperone protein levels by indirect mechanism.

Taken together, these findings suggest that autophagy may be acting as pro survival process in glucocorticoid resistant leukemia. In GC sensitive leukemia, mitochondria and ER are important for GCs dependent cell death and GCs mediated increase in the GRPs protein levels that could lead to cell apoptosis. These results, if confirmed in clinical samples may have prognostic, diagnostic and therapeutic future use in medicine.

CHAPTER 1 INTRODUCTION

Glucocorticoids (GCs) are the type of steroid hormones synthesized by the zona fasciculata layer of the adrenal gland. The secretion is controlled by adrenocorticotropic hormone (ACTH), which is produced in the brain (anterior pituitary gland) in response to stress signals. Glucocorticoid hormone found in the human blood stream is cortisol. The synthetic form of glucocorticoid, Dexamethasone, has been used to treat patients suffering from numerous diseases such as leukemia, inflammatory bowel disease (IBD), arthritis, asthma, allergies and other diseases because of their role in the regulation of cellular inflammatory responses, immunosuppression, cell cycle proliferation inhibition and cell apoptosis induction. Glucocorticoids bind to the glucocorticoid receptor (GR), which is member of the nuclear steroid receptor superfamily. This receptor plays the role as a ligand-dependent transcription factor to regulate the expression of glucocorticoid target genes and cellular response. Ligand-bound GR regulates the genes expression in the way of positive or negative response depending on the glucocorticoid response element sequences (GREs) or alternatively, by binding to the DNA indirectly through other transcription factors. This binding is leading to altered production of several intracellular cytokines and other proteins involved in inflammation, metabolism and cell death. Several proteins that regulate apoptosis such as Bcl2 family members have been described to be the target of GR (Inaba & Pui, 2010).

1.1 Overview of Glucocorticoid hormones function

Glucocorticoids are steroid hormones produced by adrenal gland in response to stress that have anti-inflammatory, metabolic and immunosuppressive effects. The main function of GCs is to mediate response to stress and control of glucose metabolism such as maintaining of normal glucose level and concentration in the blood by increased glucose production in cells, stimulation of fat breakdown metabolism and inhibition of glucose and fat storage in cells. Regarding anti-inflammatory effects, glucocorticoids inhibit all stages of the inflammatory response.

In the brain, glucocorticoids are controlled by the hypothalamic pituitary adrenal (HPA)-axis that is the set of complex structures including hypothalamus, pituitary gland and adrenal cortex that communicate through several hormones including corticotropin-releasing hormone (CRH), adrenocorticotropic hormone (ACTH) and cortisol (Figure 1-1). CRH released from paraventricular nucleus of hypothalamus stimulates anterior lobe of pituitary gland to release

ACTH hormone to subsequently induce adrenal cortex to produce glucocorticoid hormones (mainly cortisol in humans). Over expression of Glucocorticoids will inhibit the production of CRH at hypothalamus and ACTH at pituitary gland that act as negative feedback loop of HPA-axis response.

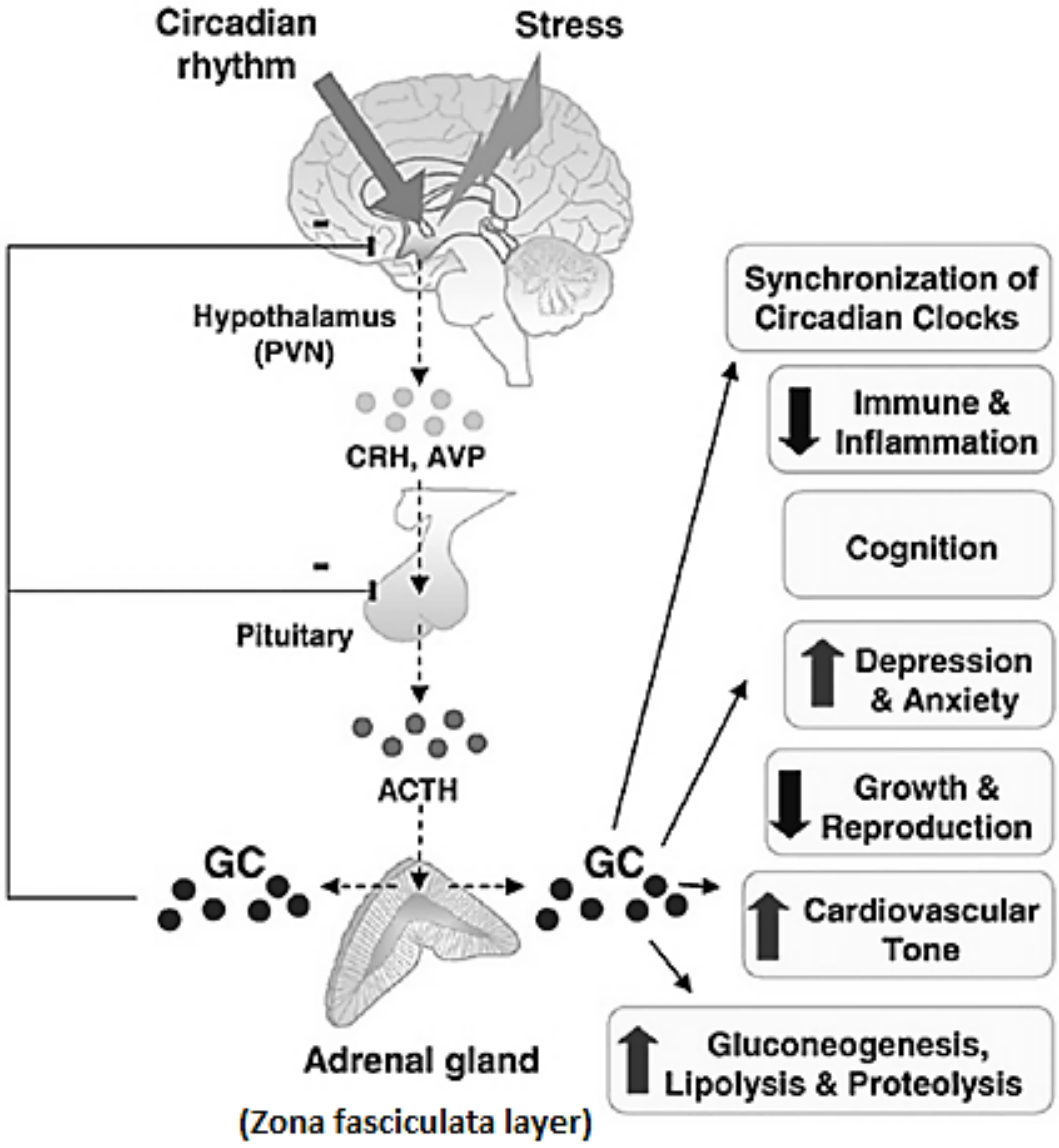

Figure 1-1 Neuroendocrine regulation of adrenal GCs and their physiological roles

Glucocorticoid hormones (GCs) are regulated by hypothalamus-pituitary-adrenal gland (HPA) axis that is an important neuroendocrine circuit system to control stress conditions by several hormones such as Corticotropin-releasing hormone (CRH), Arginine vasopressin (AVP) and Adrenocorticotropic hormone (ACTH). (adapted from (Chung et al., 2011))

After cortisol is released in the blood stream, it is bound to the plasma transporter glycoprotein known as corticosteroid binding globulin (CBG) or transcortin. CBG plays an important role to regulate concentration plasma cortisol by binding to cortisol in a 1:1 ratio and maintaining the concentration of free cortisol (Ho et al., 2006). In human, CBG peptide chain consists of 383 amino acids (50-60 kDa) with six position for N-glycosylation. CBG belongs to a non-inhibitory member of serine protease (SERPIN) family and the main function is transport of steroids and thyroid hormones in the blood to the target cells (Hammond et al., 1987; Irving et al., 2000; Pemberton et al., 1988; Sumer-Bayraktar et al., 2011). 80-90% of cortisol is bound to CBG while the free active GCs are loosely circulated in the serum (Siiteri et al., 1982). The main source of CBG is the liver where the CBG is produced by hepatocytes (Khan et al., 1984) and the CBG concentration in plasma is between 175-365 nmol/L (Nenke et al., 2016) while the plasma cortisol levels are saturated at 400-500 nmol/L (Ballard, 1979). The cortisol binding affinity can be changed by external factors such as inflammation and fever. The conformational change of CBG structure from intact S form (high affinity native form) to cleaved R form (low affinity cleaved form) (Klieber et al., 2007; Zhou, A. et al., 2006), when exposed to inflammatory protease (neutrophil protease), leads to loss of binding affinity of CBG for cortisol (Hammond et al., 1990; Pemberton et al., 1988) (Figure 1-2).

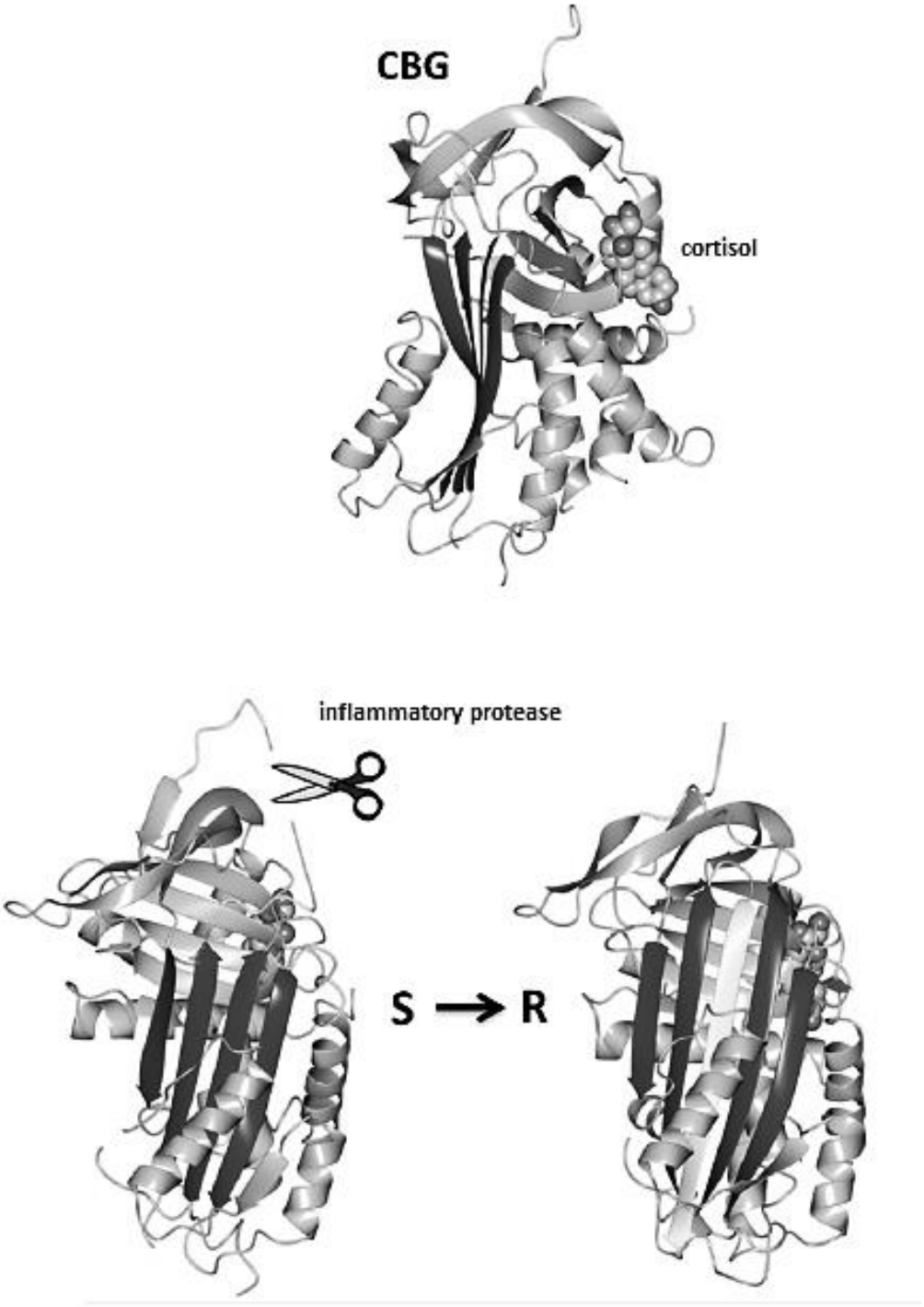

Figure 1-2 Corticosteroid binding protein structure and its conformational change after cleavage

The figure shows the cortisol binding region and the cleavage of reactive site of high affinity S from to low affinity R form of CBG that leads to cortisol release from CBG to become active free cortisol (adapted from (Henley et al., 2016)).

The cortisol is the active form of glucocorticoids and its concentration in tissues is regulated by 11β-hydroxysteroid dehydrogenase (11β-HSD) enzyme. This enzyme has two isoforms, 11β-hydroxysteroid dehydrogenase type 1 (11β-HSD1) and 11β-hydroxysteroid dehydrogenase type 2 (11β-HSD2), which regulate steroid hormones in the opposite way. Type 1 converts cortisone, inactive form of glucocorticoid metabolite, to cortisol while the conversion of cortisol to cortisone is regulated by 11β-HSD2 enzyme (Diederich et al., 2002) (Figure 1-3). 11β-HSD1 is expressed widely in many tissues, mainly in the liver, to facilitate GC action whereas 11β-HSD2 has a major role to prevent excess function of mineralocorticoids (MCs) in water and mineral homeostasis. Therefore, type 2 enzyme is mainly expressed in kidney, colon, salivary gland and placenta (Diederich et al., 2002; Gross & Cidlowski, 2008) (Figure 1-4).

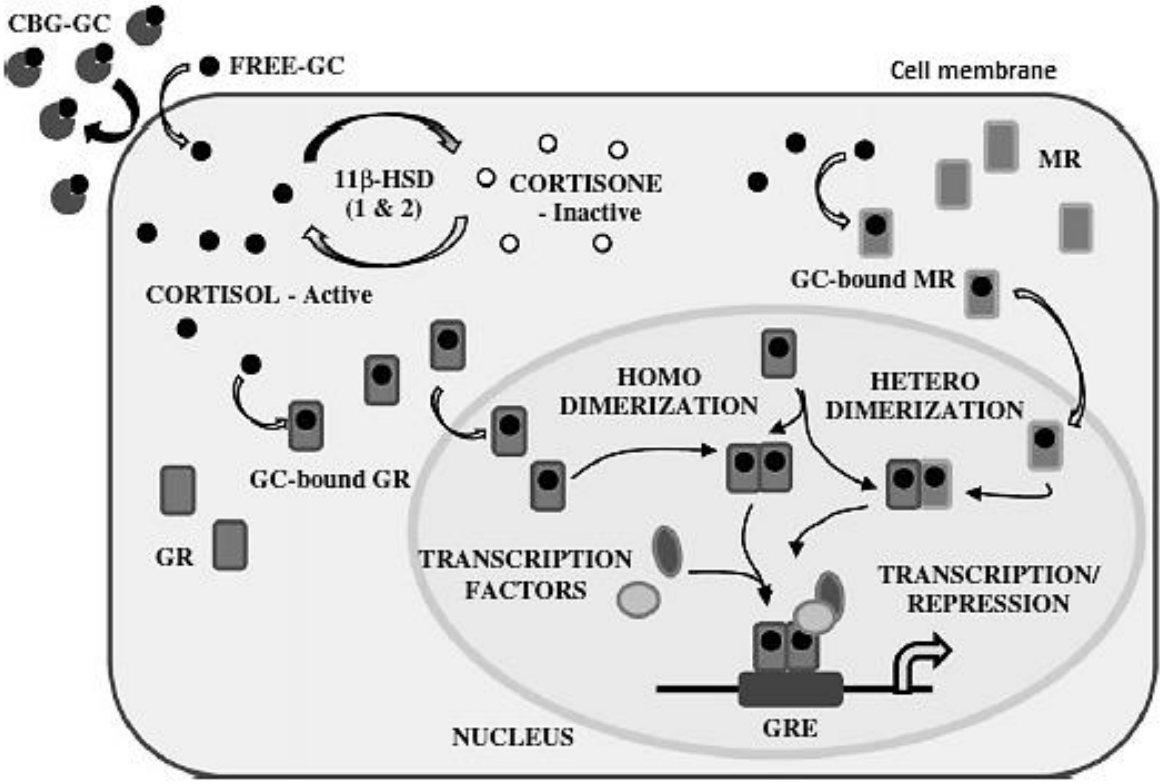

Figure 1-3 Molecular mechanism of cortisol action

The figure shows how cortisol is transported into the cell after dissociating from corticosteroid binding globulin (CBG). Most of GCs are bound by CBG in the blood, while the rest of GCs are in the free form. Unbound GCs are transported across the cell membrane and interact with the glucocorticoid receptor leading to GC-induced transcriptional regulation of target genes containing GREs regulatory sequence (adapted from (Sheriff et al., 2011)).

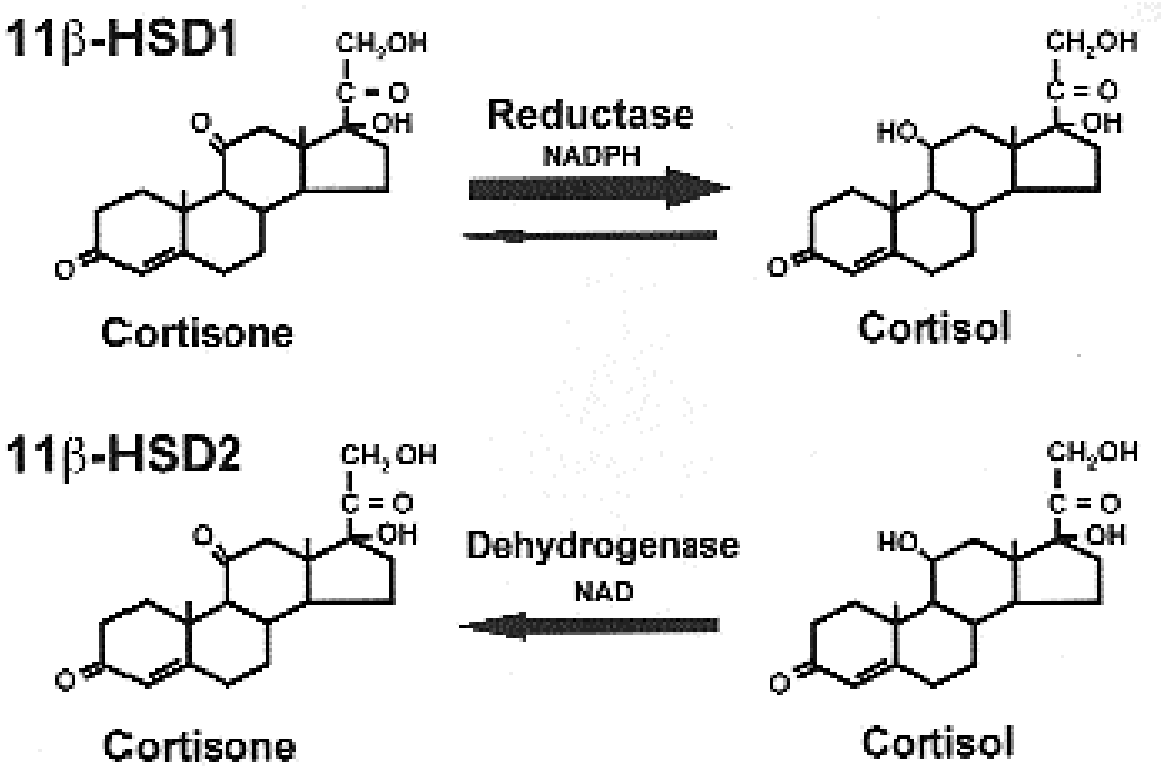

Figure 1-4 Interconversion of cortisone and cortisol by 11β-HSD isoenzyme

Type 1 11β-HSD (11β-HSD1) is NADPH-dependent reductase enzyme that converts inactive cortisone to active cortisol whereas type 2 11β-HSD (11β-HSD2), NAD-dependent dehydrogenase enzyme, regulates GC activity in the opposite way by converting cortisol to cortisone (adapted from (Espindola-Antunes & Kater, 2007)).

Corticosteroids are the steroid hormones that include glucocorticoid (GC) and / or mineralocorticoid. While mineralocorticoid effects are involved in electrolyte and water regulation, glucocorticoids predominantly affect carbohydrate, fat and protein metabolism, they have anti-inflammatory, immunosuppressive, and vasoconstrictive effects (Liu, D. et al., 2013a). In clinical practice, synthetic glucocorticoids are often used as they retain many properties of natural hormones but are more potent of stable. They are used as immunosuppressive drugs in the patients suffering from immune disorder diseases and hyper inflammatory responses such as allergies and asthma as well as leukemia. Corticosteroids also are used to replace cortisol in adrenal insufficiency patients suffering from Addison's disease, or after surgical removal of adrenal glands (Liu, D. et al., 2013a).

Glucocorticoids are among most widely used drugs in medicine. They have been used for a long time to treat numerous pathological conditions including asthma, allergies, skim conditions, some autoimmune diseases and in haematological disorders (Table 1). Their use in clinic is mostly based on their effects in inflammatory processes as they modulate mediators of inflammation to yield anti-inflammatory effect; they also affect immune system leading to their anti-inflammatory effects; glucocorticoids have anti-proliferative effects and cause cell death in white blood cells resulting in their use in leukemia treatment (Tables 1 and 2).

Table 1 Common clinical indications of glucocorticoids usage

Corticosteroids have been used to treat various inflammatory and autoimmune disorders indicated in this table (adapted from Liu et al., 2013).

Field of Medicine	Clinical use
Allery and Respiratory	Asthma, Allergic rhinitis, Anaphylaxis, Nasal polyps, Interstitial lung disease
Dermatology	Pemphigus vulgaris, Acute or severe contact dermatitis
Endocrine system	Adrenal insufficiency, Congenital adrenal hyperplasia
Gastroenterology	Ulcerative colitis, Crohn's disease, Autoimmune hepatitis
Hematology	Lymphoma / Leukemia, Hemolytic anemia, Idiopathic thrombocytopenic purpura
Rheumatology / Immunology	Rheumatoid arthritis, Systemic lupus erythematous, Polymyalgia rheumatica
Ophthalmology	Uveitis, Keratoconjunctivitis
Other	Multiple sclerosis, Organ transplantation, Cerebral edema

Table 2 List of glucocorticoids (GCs) effects on cellular response

The table shows the effects of glucocorticoids on cellular processes and mechanism of action of their effect.

Application	Mechanism of Action
Anti-inflammatory	Inhibit inflammation by blocking the action of inflammatory mediators (transrepression), or by inducing anti-inflammatory mediators (transactivation)
Immunosuppressive	Suppress delayed hypersensitivity reactions by directly affecting T-lymphocytes
Anti-proliferative	Inhibit of DNA synthesis and epidermal cell turnover
Vasoconstrictive	Inhibit the action of histamine and other vasoconstrictive mediators

1.2 Molecular biology of glucocorticoids function

In humans, GCs synthesis is induced by brain derived (hypothalamus) hormones. GCs play an important role for body metabolism by regulating a wide range of physiologic function and maintenance of basal and stress-related homeostasis (Chrousos et al., 2004). Around 20% of the genes that are expressed in human leukocytes are controlled by glucocorticoids in either positive or negative manner (Galon et al., 2002). The physiology and molecular cellular mechanisms involved with the effect of glucocorticoids are growth, nutrition metabolism, reproduction, immune system and inflammatory system (Clark et al., 1992; Galon et al., 2002). After release to blood stream and passing into cytoplasm of target cells, glucocorticoids exert their function by interacting with an intracellular protein, the glucocorticoid receptor (GR) (Chrousos et al., 2004; Galon et al., 2002; Zhou, J. & Cidlowski, 2005) which belongs to the steroid/thyroid/retinoic acid nuclear receptor superfamily of transcription factor proteins.

In general, transcription factors are group of proteins that control the rate of transcription of specific DNA sequence to generate messenger RNA during gene expression. The major steps of gene transcription are initiation, promoter escape, elongation, and termination. Briefly, RNA polymerase II together with transcription factors binds to DNA sequences within, promoter region, subsequently separating double stranded DNA and starting synthesis of new RNA chain. TATA box is the highly non-coding conserved DNA sequence for TATA box binding protein (TBP) (general transcription factor). TATA box usually is 25-35 base pairs upstream of

transcription start site. General transcription factors have DNA-binding domains to interact with specific DNA sequences and they also facilitate RNA polymerase II binding to the transcription start site. Several transcription factors involved with RNA polymerase II are transcription factor IID (TFIID), transcription factor IIA (TFIIA), transcription factor IIB (TFIIB), transcription factor IIF (TFIIF), transcription factor IIE (TFIIE), and transcription factor IIH (TFIIH) (Orphanides et al., 1996) (Table 3). In addition, transcription complexes require distal DNA sequences such as enhancers, silencers, and insulators to regulate gene transcription.

After first RNA bond is synthesized, RNA polymerase II moves away from promoter and drives RNA synthesis processes until approximately 10 nucleotides product is generated (Goldman et al., 2009). In the elongation step, RNA polymerase creates an RNA copy from 5′ to 3`using complementary base pairs except thymine that are replaced with uracil. Termination of RNA polymerase II transcription requires polyadenylation (poly-A) signal (within mRNA) to promote multi-component cleavage/polyadenylation complex including cleavage and polyadenylation factor (CPF), cleavage factors IA and IB (CFIA and CFIB). These complexes mediate cleavage and capping 3′ end with poly-A tail (Lykke-Andersen & Jensen, 2007).

Table 3 General transcription factors families and their properties

Several transcription factors have subunits compositions and are involved in transcription initiation step (adapted from (Orphanides et al., 1996)).

General transcription factor	Subunits[a]	Properties
TFIIA	37 kD (α) 19 kD (β) 13 kD (γ)	Antirepression; Required for activation
TFIIB	35 kD	Recruits pol II/TFIIF, start-site selection, zinc-ribbon, activator-induced conformational change
TFIID	38 kD (TBP)	Binds TATA element
	250 kD (TAFII250)	HMG-box, bromodomains, serine kinase
	150 kD (TAFII150)[b]	Binds downstream promoter regions
	135 kD (TAFII135)	
	95 kD (TAFII95)	WD-40 repeats
	80 kD (TAFII80)	Histone H4 similarity
	55 kD (TAFII55)	
	31 kD (TAFII31)	Histone H3 similarity
	28 kD (TAFII28)	
	20 kD (TAFII20)	Histone H2B similarity
TFIIE	56 kD	Zinc-binding domain; Promoter melting, recruits and modulates activity of TFIIH
	34 kD	
TFIIF	58 kD (RAP74)	Stimulates elongation, phosphorylated in vivo
	26 kD (RAP30)	σ homology, cryptic DNA-binding, prevents spurious initiation
TFIIH	89 kD (ERCC3)	3′–5′ helicase (essential for transcription), excision repair
	80 kD (ERCC2)	5′–3′ helicase (dispensible for transcription), excision repair
	62 kD (p62)	Excision repair
	44 kD (hSSL1)	Zinc-binding domain, excision repair
	40 kD (cdk7)	CTD-kinase, component of cdk7-activating kinase (CAK)
	37 kD (cyclin H)	cdk7 partner
	34 kD (p34)	Zinc-binding domain, homologous to hSSL1
	32 kD (MAT-1)	Ring-finger zinc-binding domain, CAK assembly factor

In the absence of GCs, GR forms the complexes with chaperone proteins including heat-shock protein 90 (hsp90) and 70 (hsp70) and co-chaperone binding protein (FKBP52) to inactivate the nuclear translocation region on the GR. After binding of GCs, the GR dissociates from its hetero-complexes and exposes nuclear translocation region that leads to the GR translocation to the nucleus. The homodimer GR binds to the glucocorticoid response elements (GRE) to activate transcription of the target genes. The monomer GR interacts with transcription factor proteins such as activation protein-1 (AP-1) or NF-κB resulting in gene inhibition (Inaba & Pui, 2010) (Figure 1-5).

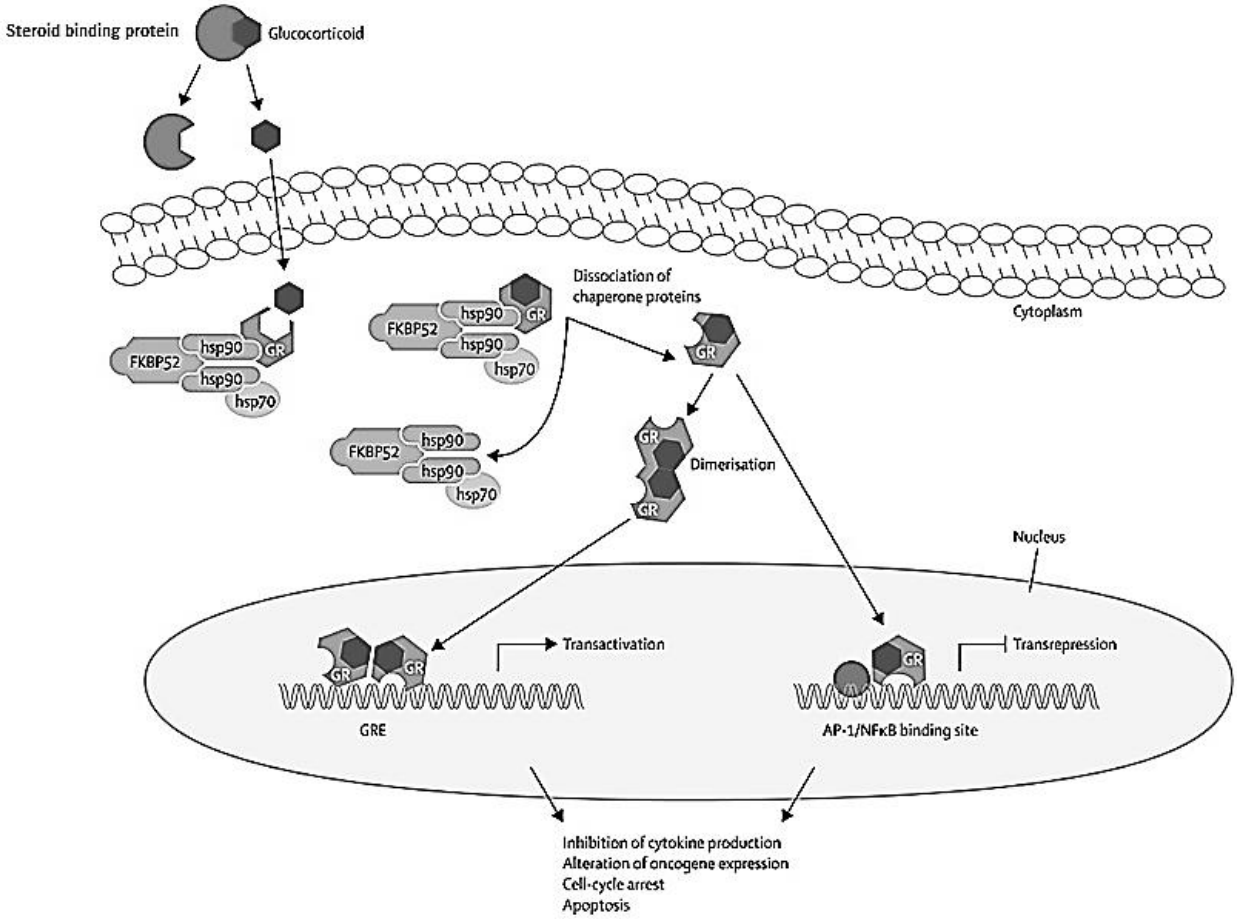

Figure 1-5 GR signalling pathway

GCs enter into cytoplasm where inactive form of GR is bound with their heterocomplexes chaperone heat shock protein 90 (HSP90), 70 (HSP70) and co chaperone protein FKBP52. After hormone binding, GR dissociates from chaperone complexes, unmasking nuclear localizing domain, and leading to nuclear translocation. Both homodimers and monomeric forms of GR bind to glucocorticoid response elements (GREs) to activate gene transcription or to inhibit transcription factors such as activation protein1 (AP-1) and nuclear factor-κB (NF-κB) (adapted from (Inaba & Pui, 2010)).

1.2.1 Glucocorticoid receptor gene and protein structure

The human glucocorticoid receptor (hGR) cDNA was isolated by expression cloning technique (Hollenberg et al., 1985) and it has nine exons located on chromosome 5. The splicing process produces two homologous receptor isoforms, α and ß hGR, which are identical through 727 amino acids from N terminus. The hGRα has an additional 50 amino acids while the hGRß contains additional 15 amino acids (Figure 1-6). The molecular weights of these

receptor isoforms are 97 and 94 kDA, respectively. The human GR is a modular protein that contains unique regions; the amino-terminal A/B region or N-terminal domain which is an immunogenic region involved in transcriptional regulation; C, D and E regions are the DNA-binding domain, the hinge region and ligand-binding domain, respectively (Nicolaides et al., 2010).

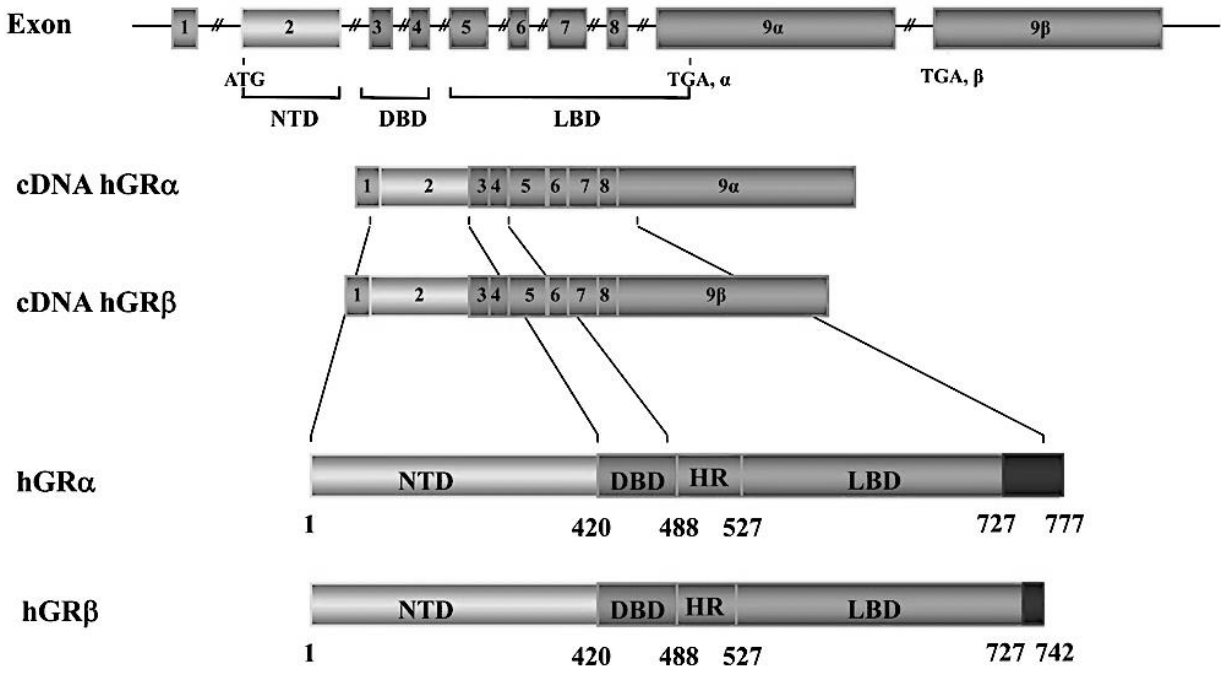

Figure 1-6 The human glucocorticoid receptor (hGR) gene.

The figure shows the alternative splicing of the hGR gene that gives rise to the two mRNA and protein isoforms, hGRα and hGRβ where the NTD; N-terminal domain DBD, DNA-binding domain; HR; hinge region, and LBD; ligand-binding domain are located (adapted from Nicolaides et al., 2010).

The hGRα N-terminal domain (NTD) consists of a major transactivation domain, referred as activation function (AF)-1 that is located from amino acids 77 to 262 of the human GRα. The AF-1 domain has been reported to be involved in the interaction of the receptor with initiation of transcription factors, such as RNA-polymerase II, TATA binding protein (TBP) and numerous TBP-associated proteins (TAFIIs), co-activation factor and chromatin modulators (Chrousos et al., 2004; Duma et al., 2006; Zhou, J. & Cidlowski, 2005).

The DNA-binding domain (DBD) of the hGRα is located between amino acids 420 and 480, which contains two zinc finger motifs binding to DNA sequences glucocorticoid response elements (GREs) in the promoter regions of target genes. The DBD is the most highly conserved part of the steroid receptor family and it also includes sequences that are important for receptor dimerization and nuclear translocation (Chrousos et al., 2004; Duma et al., 2006; Zhu, 2005).

The hinge region or D-region referred to as flexible region is located between the DNA binding domain and ligand binding domain. The amino terminus of hinge region shares the amino acid region with DBD and is involved in GR dimerization. The main function of D-region is to provide flexibility to the GR structure by allowing a single receptor dimmer to interact with several GREs (Duma et al., 2006; Zhu, 2005).

The hGRα ligand-binding domain (LBD) is located between amino acids 481 and 777, binds to glucocorticoids and plays an important role in hGRα activation. The LBD also contains a second transcription regulatory domain, known as AF-2, which is important for receptor dimerization, nuclear translocation and heat shock protein binding (Duma et al., 2006; Zhu, 2005).

1.2.2 Crystal structure of the ligand-binding domain of hGR

The crystal structure of the GRα ligand-binding domain (LBD) has 12 α-helixes and 4 small β-strands folding into a three-layer helical domain (Bledsoe et al., 2002). The structure has a space in the lower half of the ligand-binding domain, which is created by the arrangement of the helices 1 and 3 generating one side of a helical sandwich and helices 7 and 10 form the other side. The top half include helices 4, 5, 8, and 9 (Tanenbaum et al., 1998). The binding of ligand to LBD of hGRα can induce conformation changes of protein structure leading to a more compact structure and increases protein stability and electrophoretic mobility during non-denaturing conditions (Nicolaides et al., 2010). The helix (H) 12 has an important role to facilitate formation of the ligand-binding pocket and AF-2 surface interaction with coactivators after ligand binding and conformational changes have occurred (Lu & Cidlowski, 2005) (Figure 1-7).

Figure 1-7 Crystal structure shows the glucocorticoid receptor (GR) ligand binding domain area

The figure presents helix 12 (H12) area that has a crucial role for ligand binding. After hormone binding, the conformational change of GR facilitates coactivator complexes to interact with at cofactor area in LBF resulting in increase in gene expression. (adapted from (Veleiro et al., 2010)).

1.2.3 Transcriptional and translational regulation of hGR

The hGR gene is expressed into two alternative mRNA forms containing either exon 9α and 9β. The hGRα mRNA expresses multiple isoforms with different alternative translation initiation sites (multiple start codons) (Lu & Cidlowski, 2005). The all hGRα

isoforms have different transcriptional activity responding to GCs such as different distribution in the cytosol or nucleus in the absence of ligand, translocation into the nucleus in the presence of ligand, and unique transactivation or trans-repression patterns of the gene expression that was shown by microarray analysis (Lu & Cidlowski, 2005). The hGR gene contains three different promoter genes including A, B and C. Promoter A can be used with three untranslated exons, 1A1, 1A2 and 1A3, which have the specific unique promoter fragments (Breslin et al., 2001). The hGR gene can produce the same hGR proteins from the five different promoters and hGR protein levels can vary in different tissues that come from 256 different combinations of homo-and hetero- dimers produced from different promoters and isoforms (Chrousos & Kino, 2005).

1.2.4 Mechanism of transcriptional regulation by hGRα

After ligand binding and unmasking nuclear localizing sequence, GR enters to the nucleus and binds to DNA sequences, glucocorticoid responsive elements (GREs), to regulate gene transcription. There are several proposed models with glucocorticoid receptor transcriptional modulation including classical GRE, composite GRE, tethering GRE, negative GRE (nGRE), competitive nGRE, tethering nGRE and composite nGRE (Newton, 2000) (Figure 1-8).

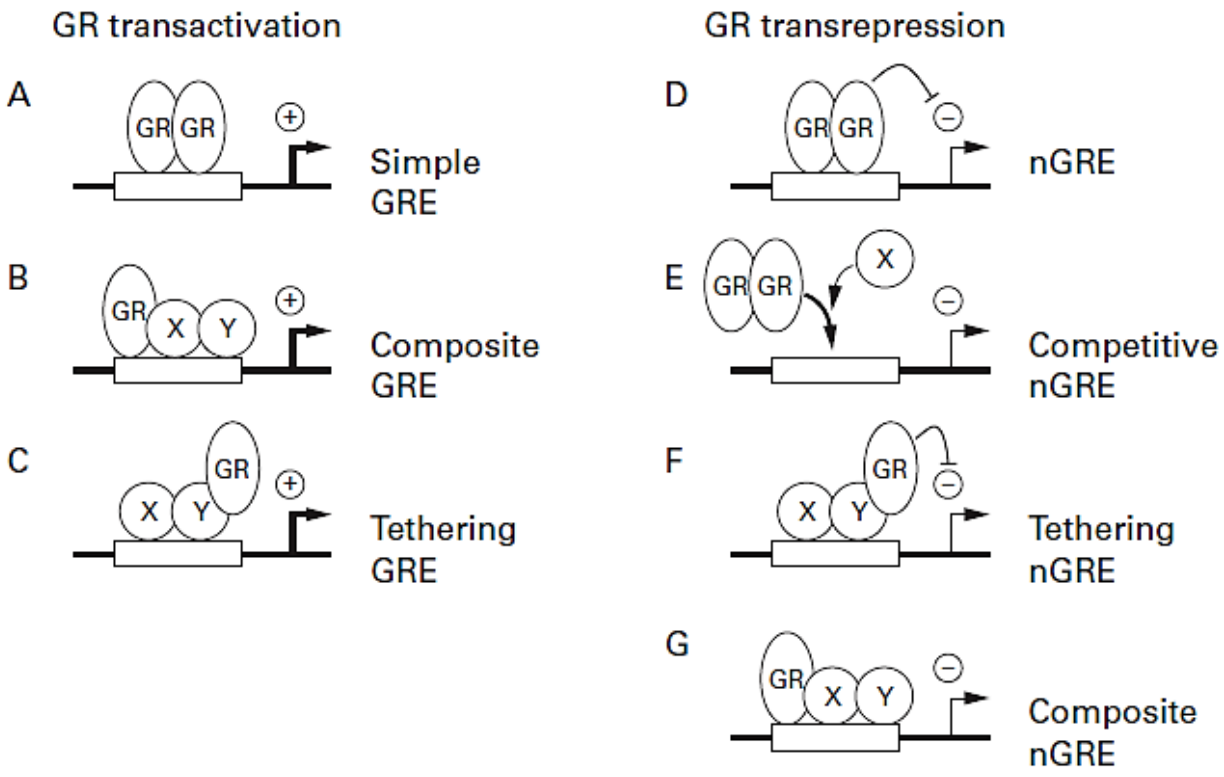

Figure 1-8 Glucocorticoid receptor mediated transcriptional activity models

There are many GR transcriptional regulation models including: homodimers GR bind to GRE (A); binding of GR and second transcription factor on DNA region (B); interaction of GR with secondary transcription factor not requiring GR binding to GRE (C); homodimers GR binding to nGRE to repress the transcription (D); GR competitive binding to nGRE to prevent binding factors required for transcription (E); interaction of GR with second transcription factor resulting in transcription repression not requiring GR binding to GRE (F); and interaction of GR and second transcription factor on DNA region resulting in transcription repression requiring DNA binding of both factors (adapted from (Newton, 2000)).

There are numerous genes known to be upregulated by GR (referred as transactivation) such as lipocortin I, p11/calpactin binding protein and β_2-adrenoreceptors, secretory leucocyte protease inhibitor (SLIPI) which have an important role in inflammatory response (Abbinante-Nissen et al., 1995; Flower & Rothwell, 1994; Yao et al., 1999). The negative regulation by glucocorticoids (referred as transrepression) are descripted to involve nuclear factor-κB (NK- κB) and Activator protein 1 (AP-1) proteins (Barnes, 1999; Barnes & Karin, 1997). The hGRα bound to GRE can stimulate the transcription of target genes and

activate the formation of the transcription initiation complex, such as the RNA-polymerase II via AF-1 and AF-2 domains (Beato & Sánchez-Pacheco, 1996).

In early steps of transcription, hGRα uses AF-1 and AF-2 domains to bind to nuclear receptor coactivators and chromatin-remodelling complexes. Many coactivators create the connection between the DNA-bound hGRα and the transcription initiation complex, and promote the glucocorticoid signal transmission to the RNA-polymerase II.

The transcription coactivator complexes comprise of p300 and homologous cAMP-responsive element-binding protein (CREB)-binding protein (CBP) that facilitate the core platforms of transcription process to receive signal for transcription from several transduction cascades such as nuclear receptors, CREB, AP-1, NF-κB, Ras-dependent growth factor, STATs and p53 (McKenna et al., 1999; McKenna & O'Malley, 2002). The p300/CBP-associated factor (p/CAF) is the another complex that interacts with p300/CBP and the final complex is p160 family of coactivators that have been reported as the initial molecules to be attracted to the DNA-bound hGRα and facilitate formation of other complexes such as p300/CBP and p/CAF proteins accumulation to the promoter region (Heck et al., 1994; Liu, J. & DeFranco, 2000; McKay & Cidlowski, 1999; Stocklin et al., 1996). The interaction occurs directly with both the AF-1 of human GRα via their carboxyl-terminal domain and the AF-2 of human GRα through multiple LXXLL motifs, which is located in the nuclear receptor-binding domain. Several other chromatin modulators can interact with human GRα through its transactivation domains (Heery et al., 1997) (Figure 1-9).

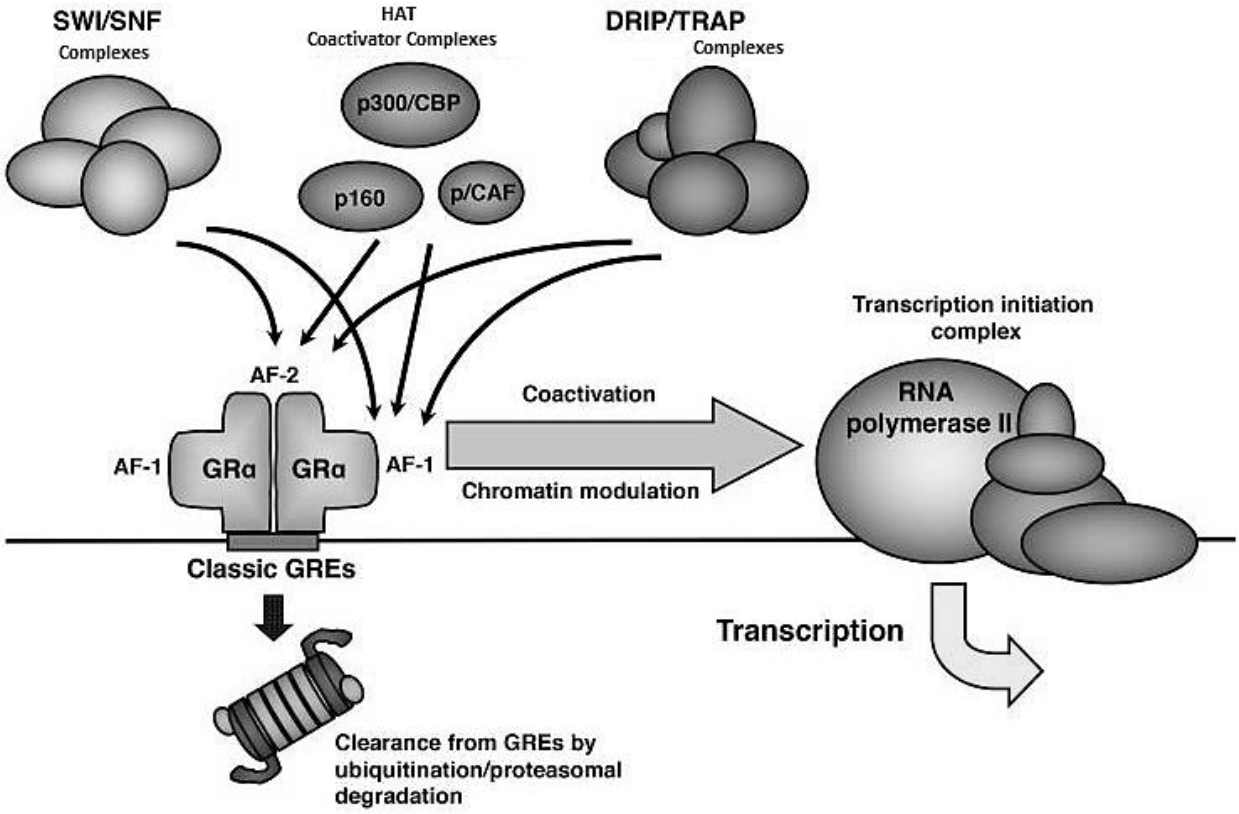

Figure 1-9 Proposed model of glucocorticoid receptor and coactivators interaction in the regulation of GR target genes transcription

The figure demonstrates the interaction of coactivators and other chromatin modulators involved in GREs transcription regulation by GR. Glucocorticoid receptor attracts several coactivator complexes including HAT complexes, SWI/SNF complexes and DRIP/TRAP complexes to the GR promotor to turn on transcription of GR target genes and facilitate formation of transcription initiation complex (adapted from (Charmandari et al., 2004)).

1.2.5 Post-translational modification of the GR

There are several types of GR protein modification after its protein translation. These comprise of phosphorylation, ubiquitination, acetylation and sumoylation processes. Post-translational modifications (PTMs) have an important role in GR stability, subcellular localization, and interaction with other proteins. Several phosphorylation sites, such as S113, S141, S203, S211, S226 and S404 have been found in human GR, most of sites are in the AF-1 domain of NTD (Ismaili & Garabedian, 2004; Krstic et al., 1997). In hGRα, some phosphorylation is hormone dependent, and this mechanism may determine turnover,

subcellular trafficking, specificity of target promoter, cofactor interaction, duration and strength of receptor signalling, and receptor stability (Nicolaides et al., 2010). Moreover, phosphorylation can stabilize the protein receptor during the absence of ligand, and also facilitate transcriptional activation. Finally, phosphorylation is involved in the non-genomic activation of cytoplasmic signalling pathways controlled by GR. Therefore; it is a versatile mechanism for modulating and integrating multiple receptor functions (Ismaili & Garabedian, 2004; Orti et al., 1993). Several protein kinases have been described to be involved in the phosphorylation of hGRα including the yeast cyclin-dependent kinase p34 CDC28 (Wang, Z. et al., 2002), the p38 mitogen-activated protein kinase (MAPK) (Miller et al., 2005), CNS-specific cyclin-dependent kinase 5 (CDK5) (Kino et al., 2007), the glycogen synthase kinase 3β (GSK-3β) (Rogatsky et al., 1998) and the c-Jun N-terminal kinase (JNK) (Itoh et al., 2002). Recent study indicated that S211 and S226 phosphorylation sites that were expressed differently in ALL cells have been involved in the regulation of GCs induced apoptosis in CEMs cells (Lynch et al., 2010).

After ligand binding, the ubiquitin/proteasome pathway plays a critical role in GR stability by directing GR to the proteasome complex for degradation processes. Several transcription factors including p53, cjun, cMyc and E2F1 and also transcription intermediate factors such as nuclear receptor coactivators, chromatin-remodelling factors are ubiquitinated and are degraded by the proteasome complex. The ubiquitination and proteasome degradation leads to decrease in activity of GR transcription (Dennis & O'Malley, 2005; Kinyamu et al., 2005). Ubiquitination also controls the GR motility in the nucleus (Deroo et al., 2002; Kino et al., 2004).

Acetylation plays an important role in GR induced transcriptional activity. Several sites of acetylation occur by several acetyltransferase enzymes at lysine residues in hinge region of GR (amino acid motif, KXKK). Recent studies indicated that circadian locomotor output cycle kaput / brain-muscle-arnt-like protein1 (CLOCK/BMAL1) transcription factors, act as acetyltransferase enzymes and repress GR action in target tissues after acetylation at the multiple lysine sites such as K480, K492, K494 and K495 (Nader et al., 2009). CLOCK are the important transcription factors that play crucial role for diurnal oscillation rhythms formation in circadian CLOCK system (Takahashi et al., 2008). GRα acetylation inhibits the binding of GR to the GRE regions resulting in decrease of GR-induced transcription (Figure 1-10). However, some studies found that mutation of GR lysine residues at 494 and 495 that are target for

acetylation resulted in down regulation of GR-responsive gene SLP1 when cells were treated with glucocorticoids (Wang, C. et al., 2011b).

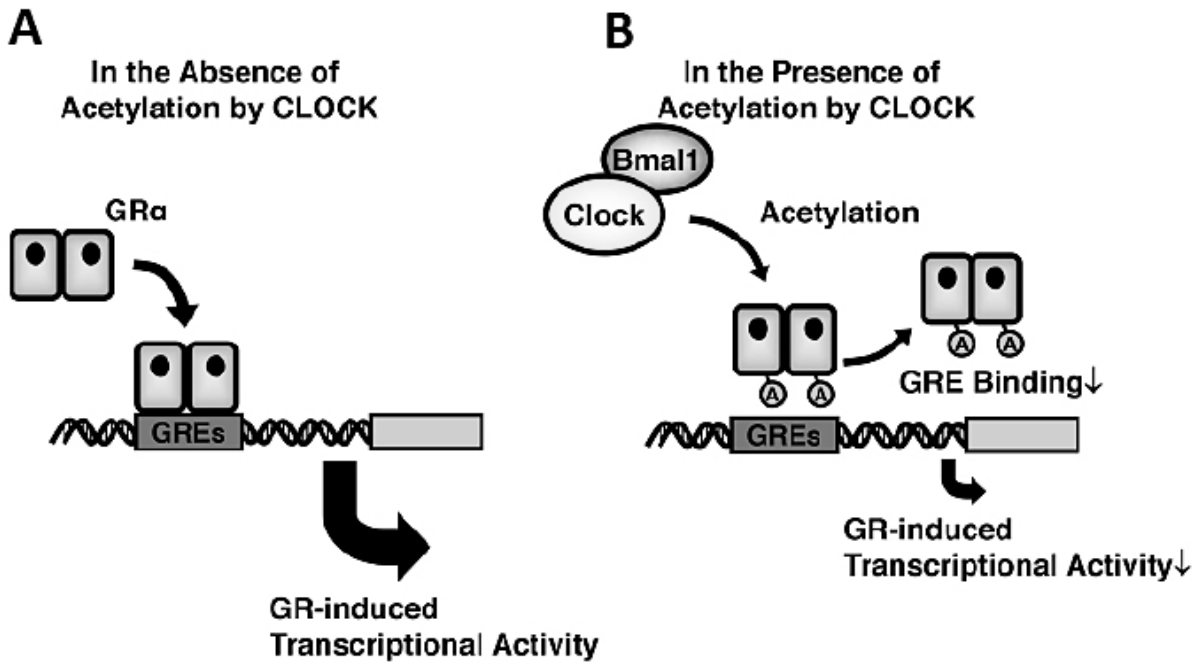

Figure 1-10 Acetylation regulation on GR-induced transcription activity
After CLOCK/BMAL1 acetylated GRα, the activity of GR binding to GREs was reduced resulting in down regulation of transcriptional activity on targeted genes (adapted from (Kino, 2000)).

Sumoylation is the post translational modification of GR mediated by small ubiquitin like modifier (SUMO) proteins that target the glucocorticoid receptor at K277, K293 (located in the NTD and are the major sites of modification) and K703 that is located in LBD region of GR (Figure 1-11). Sumoylation at K277 and K293 inhibits GR-induced transcriptional activity (Davies et al., 2008; Le Drean et al., 2002; Tian et al., 2002) while K703 site increases transcriptional activity of GR on GREs (Druker et al., 2013).

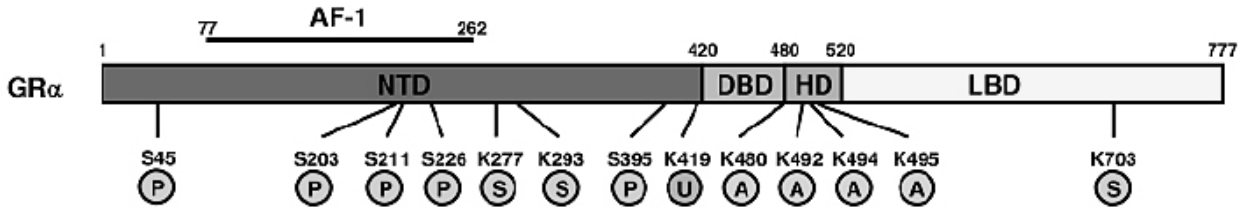

Figure 1-11 Post-translational sites of phosphorylation, acetylation, ubiquitination and SUMOylation

The figure shows the amino acid residue sites of modification by phosphorylation (P, serine amino acid position S45, S203, S211, S226, S395), acetylation (A, lysine amino acid position K480, K492, K494, K495), ubiquitination (U, lysine amino acid position K419), and SUMOylation (S, lysine amino acid position K227, K293, K703) (adapted from (Kino, 2000)).

1.2.6 Molecular mechanism of glucocorticoid resistance

Glucocorticoid are used to treat several inflammatory diseases and auto-immune disorders. However, glucocorticoid resistance can have negative effects on health of the patient and lead to decrease in efficacy of glucocorticoid therapy used in clinic. Several mechanisms are linked to the resistance including ligand induced down regulation of the GR receptor, dominant negative inhibition by ß-isoform, inhibition by the NF-κB (Schaaf & Cidlowski, 2002) (Figure 1-12) and alteration in other associated pathways such as alteration in apoptosis or autophagy.

There are several studies that showed that some steroid hormone treatment decreased GR expression in tissues and cultured cell lines such as HeLa cell (Lacroix et al., 1984), human lymphocytes (Schlechte et al., 1982), rat brain (Sapolsky et al., 1984), rat hepatoma cells and mouse fibroblasts (Dong, Y. et al., 1988). Some reports showed increase of GR expression after ligand binding to human leukemic T-cell (CEM-C7-14), human myeloma cell line OPM-2 and mouse thymoma cell line WEHI-7 (Antakly et al., 1989; Ashraf et al., 1991; Eisen et al., 1988; Gomi et al., 1990; Gruol et al., 1989). The ligand induced repression of GR mechanism is still unclear. However, some evidence showed the reduction of GR promoter activity through the sequences in GR promoter (region between -2838 and -1476) which are the same as the nGREs ((Drouin et al., 1989).

The alternative splicing presented ß-isoform of GR is another repression mechanism of GR resistance. The hGRß form does not interact with the ligand. Several hypothesises were proposed about resistance mechanism such as competition of hGRß and hGRα for GRE binding, interaction of hGRß with coactivators and the forming of inactive heterodimers between hGRß and hGRα (Leung et al., 1997; Oakley et al., 1999; Strickland et al., 2001) .

Crosstalk between GR and NF-κB is an important regulatory mechanism of glucocorticoid resistance in inflammatory diseases. Several studies indicated that certain GR target genes were inhibited by NF-κB subunit p65 and the activated form of NF-κB is required to repress hGRα (Schaaf & Cidlowski, 2002).

Additional mechanisms contributing to GCs resistance in leukemia are discussed later in this thesis (page 180-189).

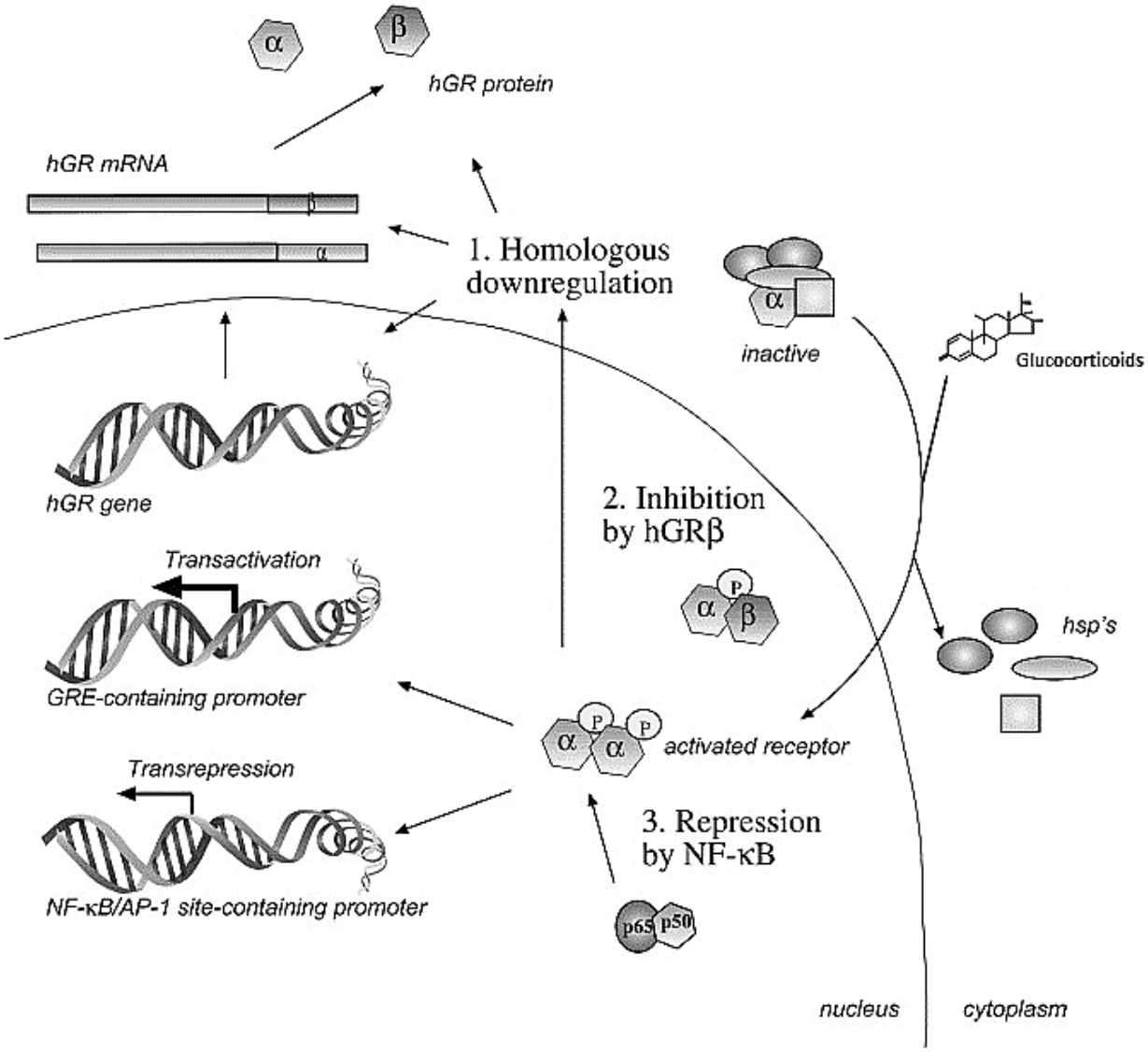

Figure 1-12 Proposed glucocorticoid resistance mechanism

Three mainly mechanisms involved in GC-resistance are 1) reduction of GR level, 2) hGRß isoform expression, and 3) repression of hGRα by transcription factor NF-κB (adapted from (Schaaf & Cidlowski, 2002)).

1.3 Leukemia

1.3.1 Introduction to cancer

Cancer is a group of diseases where normal process of cell proliferation is altered with potential to invade other parts of the body. There are more than 277 different types of disease and numerous gene mutations are involved in cancer pathogenesis. The alterations in oncogenes, tumor suppressor genes and genes involved in DNA repair play an important role in early stages of tumor formation (Imran et al., 2017). The process of normal cells becoming

malignant involves the sequential mutations that arise from genomic damaging. This can be the result of endogenous mechanism including inherited mutations but also numerous other processes such as errors in DNA replication, free radicals induced DNA instability, UV radiation and chemical carcinogens (Bertram, 2001). Microorganism infection such as viruses and bacteria are other carcinogenesis factors involving around 7% of all cancers (Parkin, 2006).

In men, the highest prevalence of cancer occurs in the prostate gland, lung tissue and bronchus, colon and rectum, and urinary bladder while the breast tissue, lung and bronchus, colon and rectum, uterine corpus and thyroid are the most common types of cancer in women (Siegel et al., 2016). In children, the highest prevalence types of cancer are blood cancer, brain and lymph nodes, respectively (Yoo & Chin, 2003). The characteristic of cancers are summarised by six hallmarks including sustaining proliferative signalling, evading growth suppressors, activating invasion and metastasis, enabling replicative immortality, inducing angiogenesis and resisting cell death (Hanahan & Weinberg, 2011).

1.3.2 Introduction to leukemia

In UK, around 8000 people are diagnosed with leukemia each year has high mortally. Disease is white blood cells disorder or blood cancer affecting white blood cells and bone marrow and is characterised by abnormal leucocytes proliferation. Loss of white blood cell function effects the immune system and disrupt normal functions. Different types of leukemia are classified based on morphology and disease progression. There are four main types of leukemia including acute myeloid leukemia (AML) that presented myeloblast abnormality, chronic myeloid leukemia (CML) that presented myelocytes abnormality including neutrophils, eosinophils, and basophils, acute lymphoblastic leukemia (ALL) with lymphoblasts abnormality, and chronic lymphoblastic leukemia (CLL) with lymphocytes abnormality. In acute stage, the number of abnormal cells increases rapidly while chronic stage occurs slowly. T and B cells are derived from leucocytes while neutrophils, basophils, eosinophils, and monocytes are originated from myeloid cell (Grigoropoulos et al., 2013). Signs and symptoms of patients with leukemia are related to bone marrow failure, spontaneous bruising or abnormal bleeding and anemia.

The most common cancer in children is ALL that has incidence rate at 3 to 100,000 population and 75% of patients are under 6 years (Swerdlow et al., 2008). Although children ALL is curable leukemia with combination chemotherapy with 85% long term survival, adult

patients have a poor prognosis because of intensive chemotherapy intolerance and toxicity of the treatment can be considerable (Hann et al., 2000).

Acute Lymphoblastic Leukemia (ALL) is the cancer of white blood cells that mainly affects children and teenagers. The ALL incident rate (around 1:100,000) in UK has been reported since the mid of the 1970s (Figure 1-13). Over 65% of ALL patients are young teenagers under 25 year old (Figure 1-14) and ALL is the frequent cause of death from cancer before 20 years of age (Smith, M. A. et al., 2010). Several genes mutation are linked to the risk factors of ALL while the hazardous environments are additional factors associated with ALL in children such as radiation and toxic chemical exposure. Combination chemotherapy reduced the clinical symptom and restored normal hematopoiesis activity in up to 90% of patients with ALL (Smith, M. A. et al., 2010). However, resistance to ALL Dexamethasone treated patients has been observed and the autophagy, endoplasmic reticulum stress and unfolded protein response may be involved in GC-induced ALL cell death (Bonapace et al., 2010) while the mechanism of the leukemic cell response to GC treatment is still not clear.

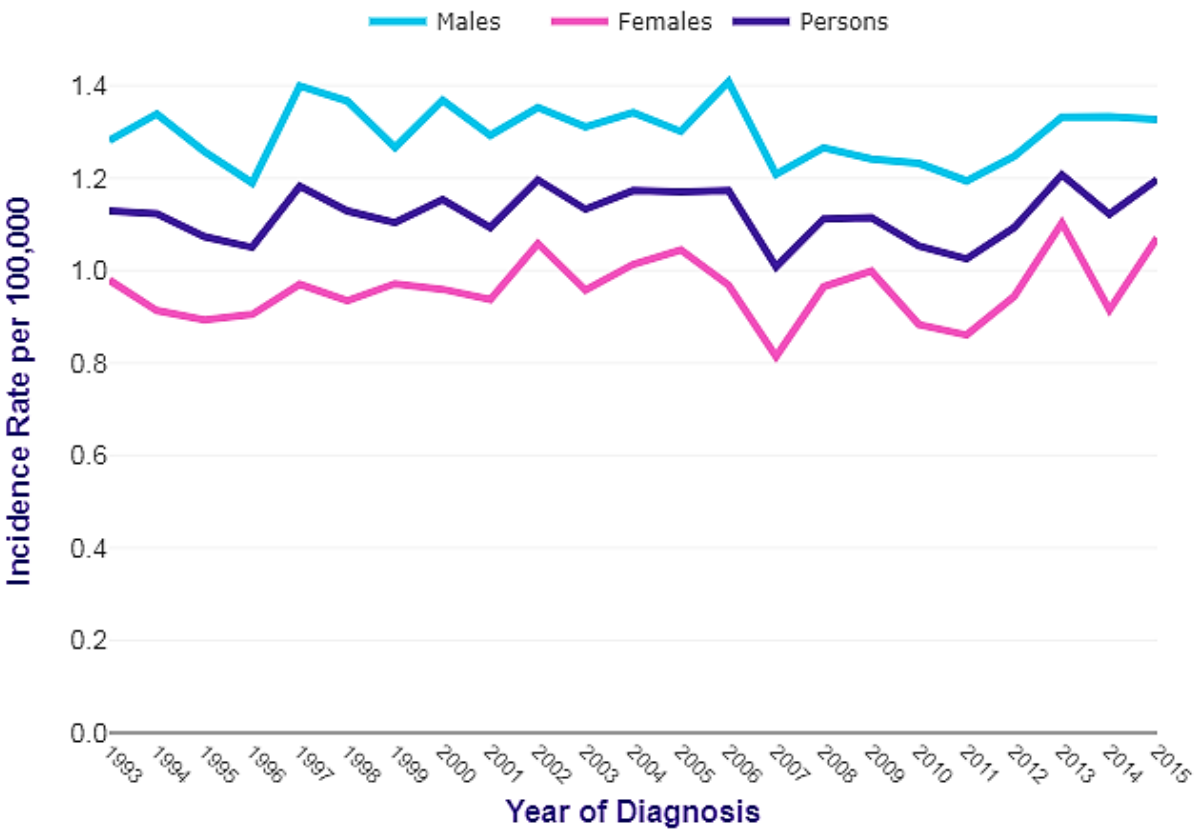

Figure 1-13 Acute Lymphoblastic Leukemia of European age-standardised incidence rates in Great Britain between 1993 and 2015

The graph provides acute lymphoblastic leukemia incidence rates according to gender that have increased by 13% in Great Britain since the late 1970s (CRUK, 2015).

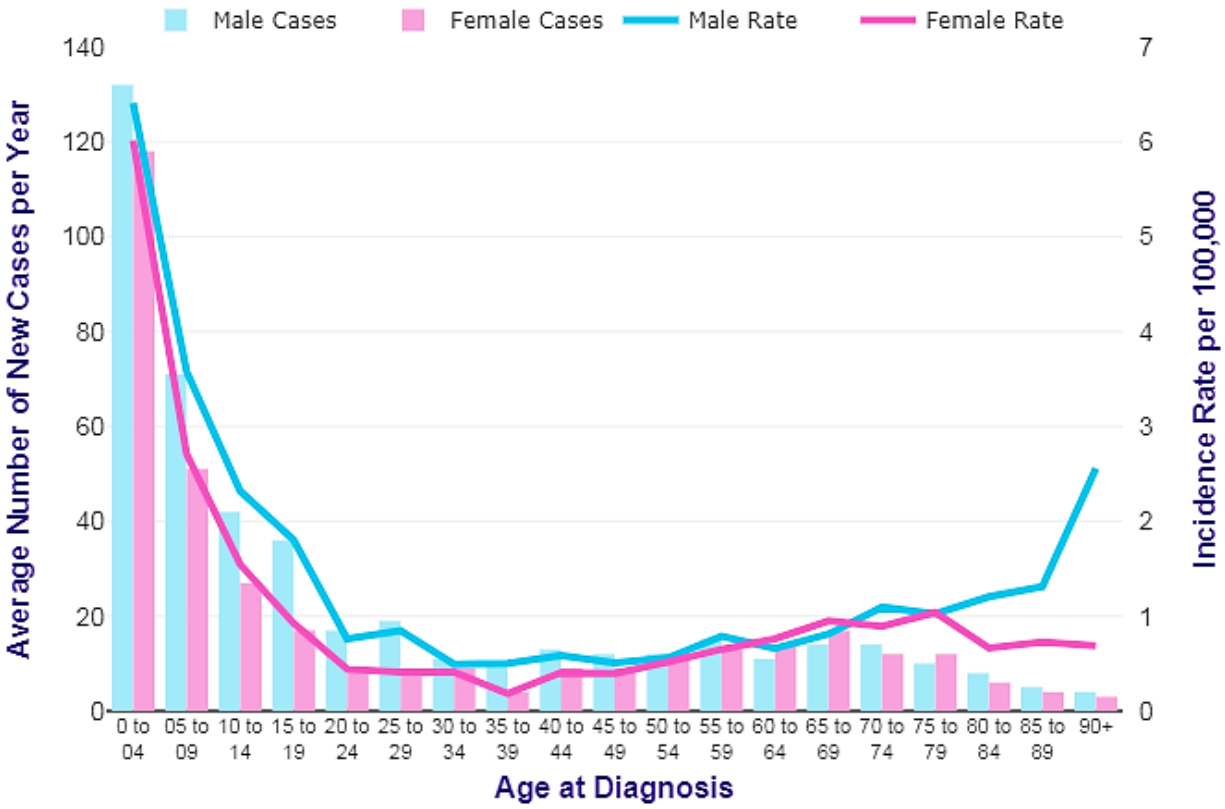

Figure 1-14 Acute Lymphoblastic Leukemia presented in average number of new cases per year and age-specific incidence rates, (CRUK, 2013 - 2015)

ALL incidence is strongly related to the age, which has the highest rates in children, teenagers and young adults. There are similar rates between male and female except age between 15 and 19 that the incident rate in male higher than female (CRUK, 2013 - 2015).

1.3.3 Risk factors and causes of ALL

Acute lymphoblastic leukemia is a malignant disorder of lymphatic stem cell, progenitor cell, in bone marrow. It affects not only children with the peak of prevalence 2 to 5 year old but also occurs in adults (Pui et al., 2008). The causes of ALL are not completely understood but risk factors can be multi-factorial such as infection, chronic inflammation, oxidative stress, environmental exposure to chemicals and radiation and genetic disorders (Greaves, M., 2006; Greaves, M. F. & Wiemels, 2003). In some childhood ALL cases have gross chromosomal mutation that can disrupt several genes that regulate normal haematopoiesis and lymphoid development have been identified (Inaba et al., 2013) which are related significantly with the patient's outcomes. Although the most patients with cancer have no recognized inherited factors, genomic studies have identified the polymorphism of several gene

that are associated with ALL including ARID5B, CEBPE, GATA3, and IKZF1 (Hunger & Mullighan, 2015a; Perez-Andreu et al., 2013; Trevino et al., 2009). Another rare germline mutation such as PAX5 and ETV6 have been found to be linked with familial ALL (Shah et al., 2013; Zhang, M. Y. et al., 2015) while few environmental risk factors are linked with ALL in children (Hunger & Mullighan, 2015a) (Figure 1-15).

There are several genetic alterations involved in ALL including change in chromosome number, chromosomal rearrangements (Philadelphia chromosome, Ph) resulting in gene expression inhibition or fusion proteins expression, DNA deletion, and mutation of DNA sequences (Harrison, 2009). The Philadelphia chromosome is the abnormal chromosome 22 causes of reciprocal translocation of genetic material with chromosome 9 (gene *ABL1* from chromosome 9 and *BCR* gene from chromosome 22). This genetic abnormality is found in chronic myeloid leukemia and acute lymphoblastic leukemia (Nowell & Hungerford, 1960; Secker-Walker et al., 1978).

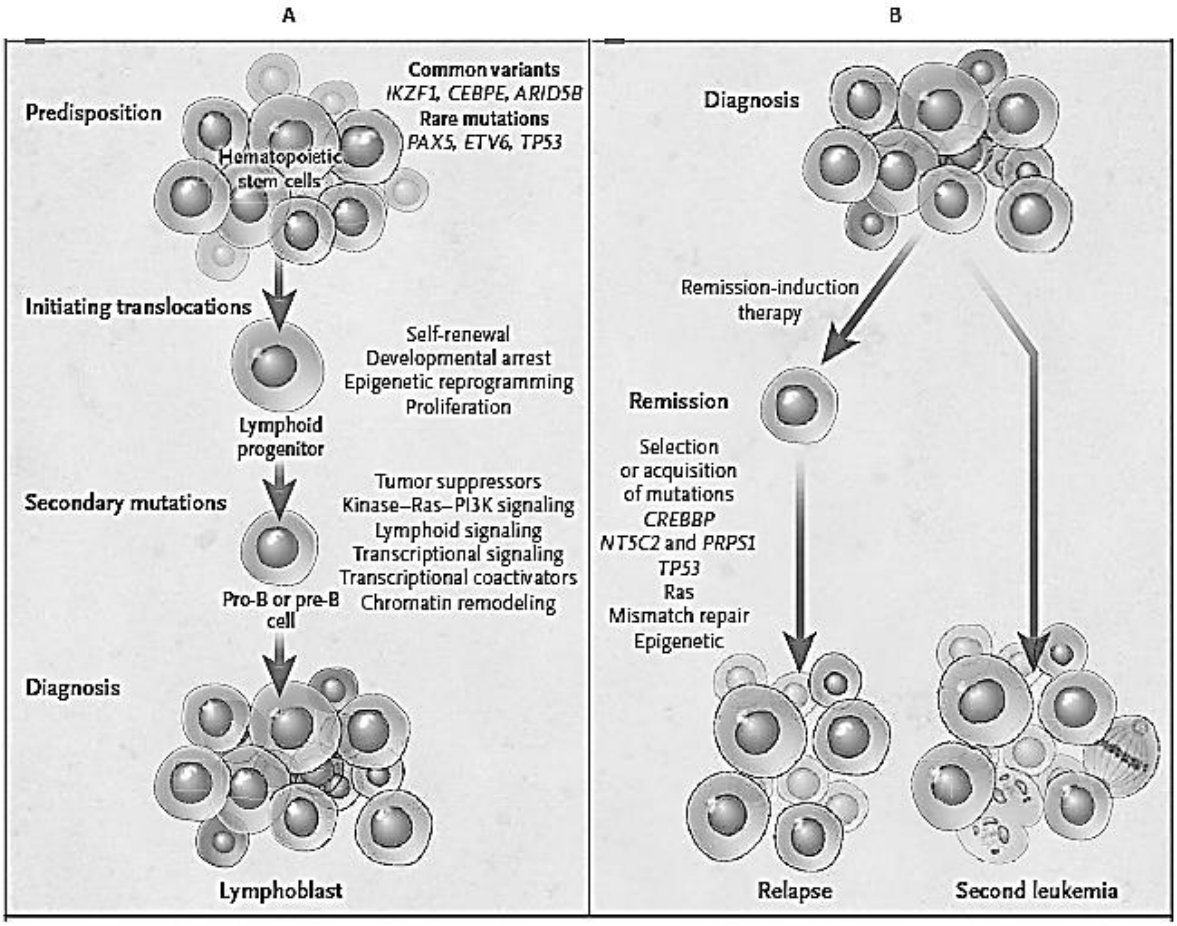

Figure 1-15 Genetic alterations resulting in the pathogenesis and relapse of ALL

Both common variants and rare mutations in several genes lead to lymphoid progenitor self-renewal, increased proliferation rate and affect tumor suppressors genes, transcriptional signalling, transcriptional coactivators alterations (A). ALL relapse can be caused by remission-induction therapy by leaving subclones that contained specific genes mutations resulting in chemotherapy resistance (B) (adapted from (Hunger & Mullighan, 2015b)).

1.3.4 ALL treatment

ALL patients can present the symptoms including bruising or bleeding, thrombocytopenia, pallor and fatigue, anemia, neutropenia that lead to infection (Hunger & Mullighan, 2015a). There are several techniques to detect the ALL such as morphological identification of lymphoblasts, immunophenotypic determination and development stage, and chromosomal analysis (Inaba et al., 2013; Pui et al., 2008).

Combination chemotherapy has been used for a long time to cure leukemia. (George et al., 1968). The treatment of ALL comprises 3 steps taking around 2 years, remission-induction as the first step, following by intensification, and continuation (Pui et al., 2008). The remission-induction phase is a period for 6 weeks treatment with chemotherapy agents such as glucocorticoids (prednisone or Dexamethasone), vincristine that inhibits microtubule formation in mitotic spindle resulting in cell cycle proliferation inhibition, and asparaginase, which is the hydrolase enzyme of endogenous L-asparagine resulting in inhibition of RNA and DNA synthesis. However, side effects can be found such as fever, nausea and vomiting, allergic reaction, and stomach cramping.

With these drug agents, normal haematopoiesis can be restored in 69-99% of children and 78-92% of adult patients (Hunger et al., 2012; Stanulla & Schrappe, 2009). Prednisolone has been used in ALL treatment while Dexamethasone is increasingly considered (Inaba & Pui, 2010). Some adverse effects from glucocorticoid treatment can be identified such as infection, osteonecrosis, fractures, psychosis, and myopathy, which is higher with Dexamethasone than with prednisone (Pui et al., 2012). In the intensification phase, high-dose of methotrexate (MTX) is used with mercaptopurine to reduce leukemic activity. However, some residual leukemic cell can be observed in patients that have drug resistance (Seibel et al., 2008). The final phase is continuation therapy that uses mercaptopurine (inhibits purine nucleotide synthesis) and methotrexate (inhibits Dihydrofolate reductase enzyme and also inhibits the binding of interleukin 1-beta to the cell surface receptor) weekly or without pulses of vincristine and Dexamethasone for 2 years (Inaba et al., 2013).

1.4 Cell death

Cell death normally occurs during cellular proliferation period to maintain and balance multi-cellular organisms. Disorders controlling cell death processes have pathological consequences and lead to embryogenesis disruption, neurodegenerative diseases, or development of cancer (Bröker et al., 2005). The cell has been considered dead according to molecular or morphological criteria when it has lost integrity of plasma membrane, the nucleus of cell has undergone fragmentation into apoptotic bodies and this cell fragments have been engulfed by adjacent cell (Kroemer et al., 2009).

There are several cell death types such as apoptosis, autophagy, necrosis, necroptosis and others and are mostly classified according to cell morphological features. In apoptosis mode, cell morphologies were identified as rounding-up of the cell, retraction of pseudopods,

reduction of cellular and nuclear volume, called pyknosis, nuclear fragmentation, plasma membrane blebbing, and presenting of the engulfment by resident phagocytes. The characteristics of autophagy are described as lack of chromatin condensation, several large vacuolization in cytoplasm, and double-membraned vacuoles accumulation. The last mode of cell death is necrosis that includes cytoplasmic swelling, plasma membrane rupture, cytoplasmic organelles swelling and moderate chromatin condensation (Kroemer et al., 2009) (Figure 1-16).

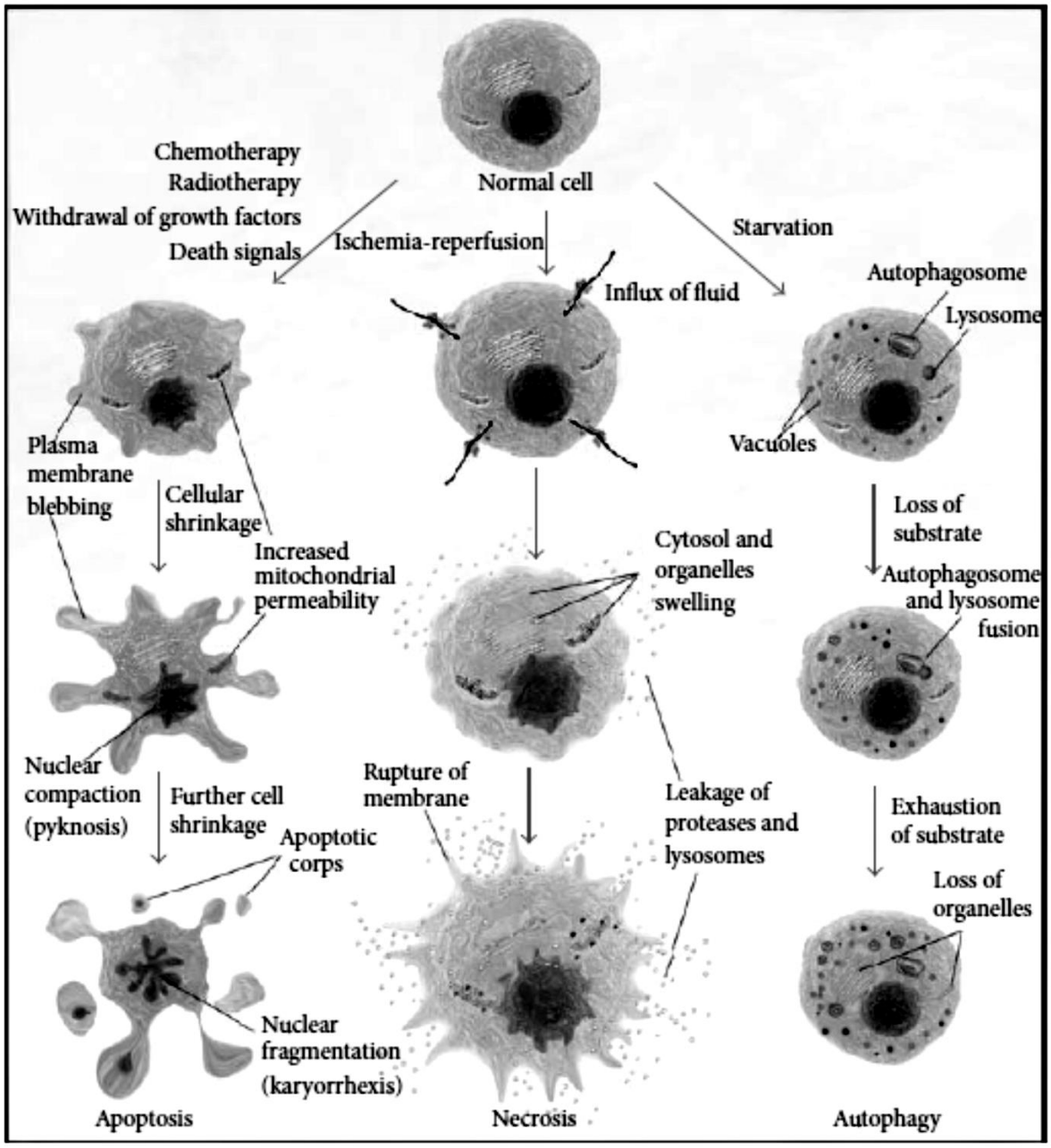

Figure 1-16 Major pathways of cell death

Programmed cell death mechanism can be divided into different paths depending on stimuli factors. Apoptosis pathway (left panel) is represented with cellular shrinkage and apoptotic body formations. The cytoplasmic organelles swelling and rupture of plasma membrane are the characteristic of necrotic cell (middle panel). The autophagic cell death is represented with vacuoles appearance and formation of auto-phagolysosome formation (right panel) (adapted from (Nunes et al., 2014)).

1.4.1 Apoptosis

In 1972, term “Apoptosis” has been used to describe a morphological alterations leading to cell death. Light and electron microscopy have been used to identify the various morphological changes occurring in apoptosis (Häcker, 2000). Cell shrinkage was observed, the cells were smaller in size and condensation of cytoplasm and organelles was seen by light microscopy in early stage of apoptosis (Kerr et al., 1972). The apoptotic cells were smaller than normal cells, and were stained with eosin dye in cytoplasm while the nuclear chromatin fragments were stained with purple (haematoxylin) dye.

1.4.1.1 Extrinsic apoptotic pathway

The mechanisms of apoptosis are complex and involve an energy-dependent cascade of molecular events. There are two important pathways utilised by cells undergoing apoptosis, the extrinsic or death receptor pathway and the intrinsic or mitochondrial pathway, while several proteins between these pathways have been identified to link them and have influence on both pathways (Igney & Krammer, 2002). In the early process of extrinsic signalling pathway, transmembrane death receptors that are members of the tumour necrosis factor (TNF) receptor gene superfamily have been crucial for apoptotic process (Locksley et al., 2001). TNF receptor family members share similar cysteine-rich extracellular domains that contains 80 amino acids located cytoplasmic domain, called “death domain” (Ashkenazi & Dixit, 1998). Briefly, tumor necrosis factor (TNF) is the molecule that binds to the receptors on cell membrane (tumor necrosis factor receptor, TNFR) resulting in gene activation, cell death and regulation of inflammatory processes. There are two main types of TNFR including death receptors that have intracellular region (death domain, DD) involved to induction of cell death, and TRAF domain which is involved in cell survival and inflammation (Cabal-Hierro & Lazo, 2012; Dempsey et al., 2003).

Death domain has an important role to transmit the death signal from the cell surface to the intracellular signalling processes that contain several ligands such as FasL/FasR, TRAIL-R1, TRAIL-R2, TNF-α/TNFR1, Apo3L/DR3, Apo2L/DR4 and Apo2L/DR5 (Ashkenazi & Dixit, 1998; Chicheportiche et al., 1997; Peter & Krammer, 1998; Rubio-Moscardo et al., 2005; Suliman et al., 2001). Activation of these receptors subsequently activates intracellular death domain association molecules such as Fas associated death domain (FADD) and TNFR associated DD (TRADD). The activation of DD signalling triggers caspase cascade pathways directly or via mitochondria results in cell apoptosis (Figure 1-17) (Dempsey

et al., 2003). However, TNF-R1 receptor also triggers anti-apoptotic signalling pathway by interacting with TRADD molecule that can also recruit TRAF2, TRAF1 and receptor-interacting protein (RIP) to induce inflammatory response and pro-apoptotic pathway such as nuclear factor κB (NF- κB) and Jun N-terminal kinase (JNK) (Hsu et al., 1996; Stanger et al., 1995).

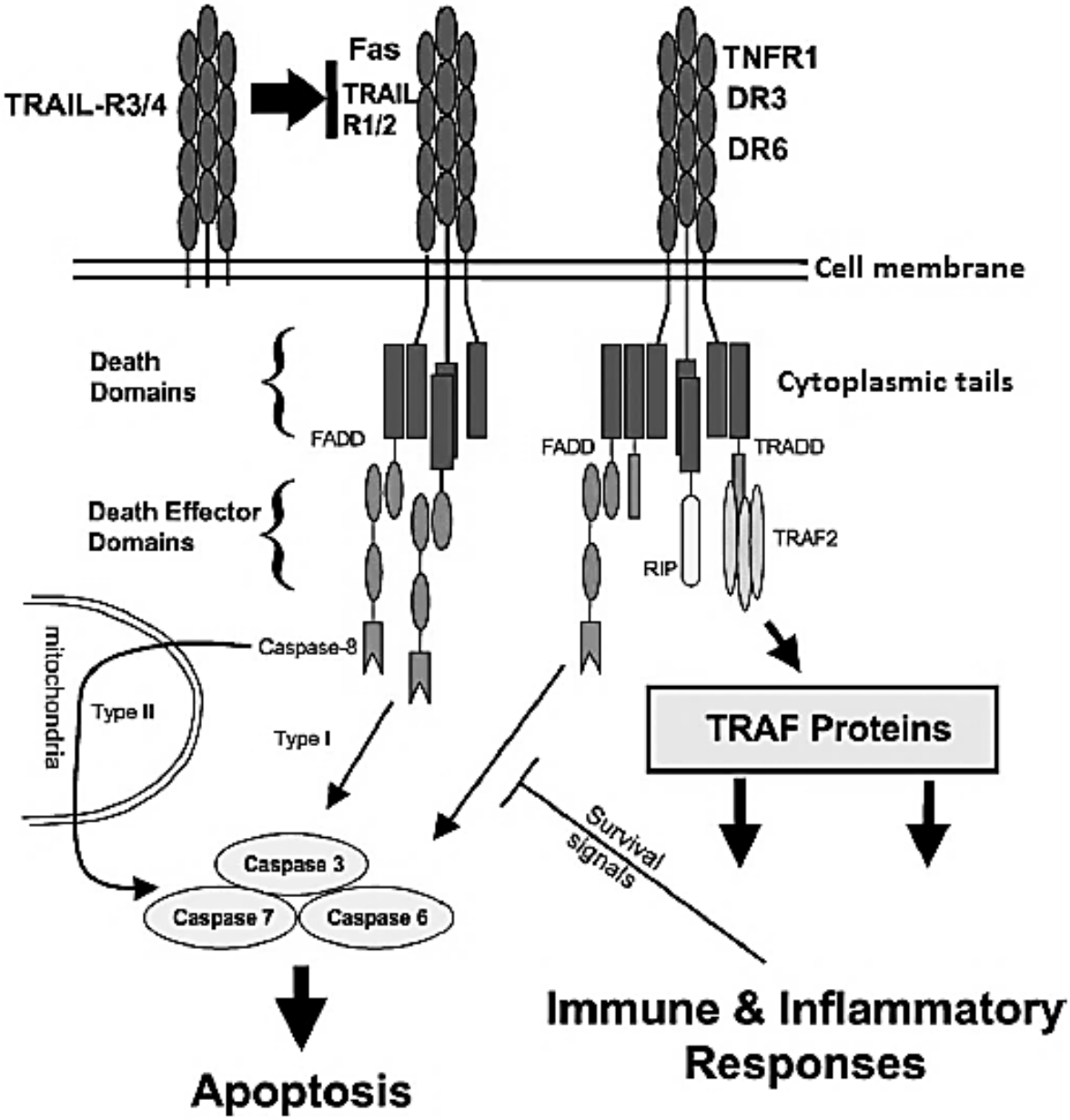

Figure 1-17 Death receptor mediated regulation of cell apoptosis

The figure shows death domain receptors and associated molecules involved in cell apoptosis regulation such as FADD, TRADD. Upon ligands binding, active FAS receptor interact with c-terminus DD of FADD molecule resulting in FADD activation. That triggers caspase-8 molecule to become active and subsequently activate downstream molecules including caspase-7, caspase-6, and caspase-3 (adapted from (Dempsey et al., 2003)).

In TRAFs pathway, there are several transmembrane receptors including TNF-R2, CD40, CD30, CD27, LTßR, Ox40, 4-IBB, BAFF-R, BCMA, etc. These receptors contain TRAF-interacting motifs (TIM) in cytoplasmic tails and activation of these molecules triggers

signal transduction pathway, nuclear factor κB (NF- κB), Jun N-terminal kinase (JNK), p38, extracellular signal-related kinase (ERK) and phosphoinositide 3-kinase (PI3K), for example, that are related in immune and inflammatory response (Dempsey et al., 2003). Tumor necrosis factor receptor associated factors (TRAFs) are the intracellular molecules (TRAF 1-6) that interact to several TNFR and IL-1/Toll-like receptor superfamily (Figure 1-18). All TRAFs have the conserved region at the c-terminus, TRAF domain, which contains 200 amino acid peptides and is divided into two sub-domains, TRAF-N and TRAF-C. TRAF domain is important part for interaction with its receptors or intracellular signalling molecules and it can produce homo-, hetero, or trimeric forms by association with TRAFs molecules such as TRAF1 and TRAF2 or TRAF3 and TRAF5 or TRAF6 (Cao et al., 1996; Pullen et al., 1998; Rothe et al., 1994). Previous studies indicated that RING finger domain is important for NF- κB activation while zinc finger domains are crucial for the activation of JNK and NF- κB (Brink & Lodish, 1998; Dadgostar & Cheng, 1998; Rothe et al., 1995; Takeuchi et al., 1996).

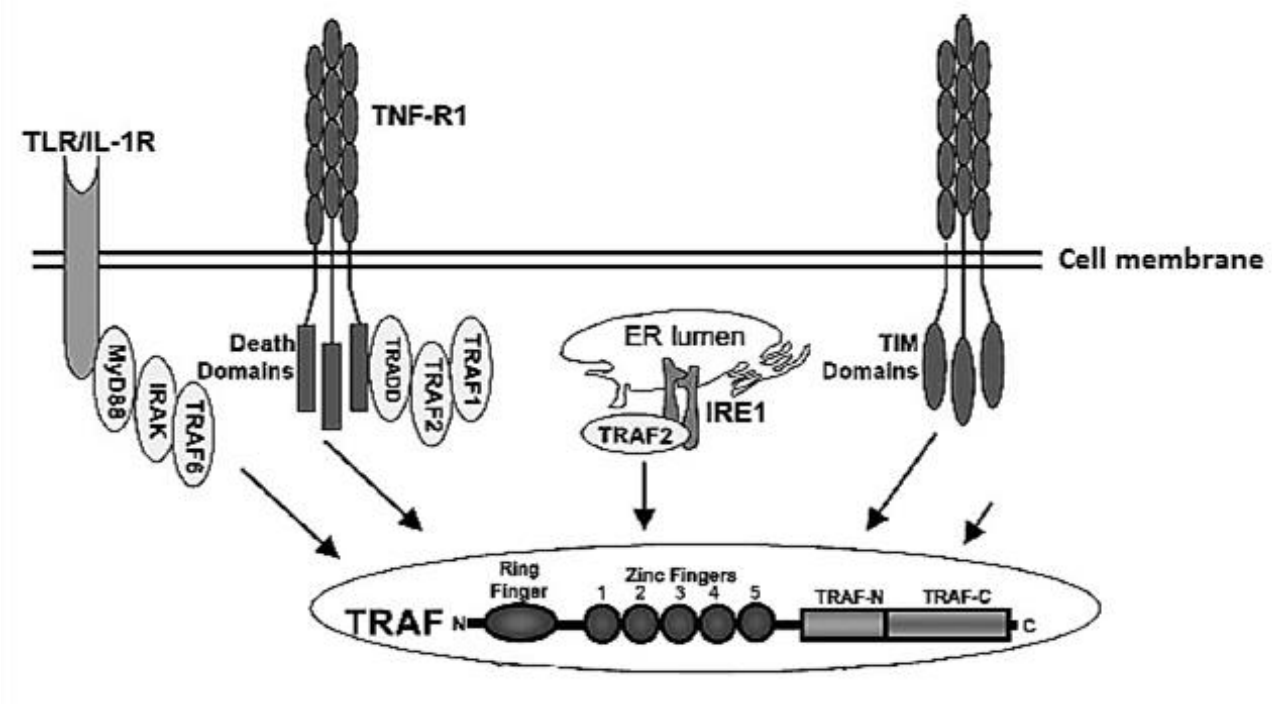

Figure 1-18 TRAFs interaction with transmembrane receptors

The figure shows the interaction of TRAFs with death receptor domain of TNF-R1, TIM domains and TLR/IL-1R receptor. TRAFs contain TRAF-N and TRAF-C domains at C-terminus that play an important role in intracellular signalling molecules and receptors interaction (adapted from (Dempsey et al., 2003)).

1.4.1.2 Intrinsic apoptotic pathway

Non-receptor-mediated apoptosis is the intrinsic signalling pathway that produces intracellular signals activating targets within the cell and mitochondria. The absence of growth hormone, factors, and cytokines is the negative signalling that can promote suppression of death programs dysfunction, thereby activating apoptosis. Several stimuli that have positive signalling regulation are ionising and UV radiation, toxic chemicals, hypoxia, hyperthermia, viral infections, and free radicals (Elmore, 2007) (Figure 1-19).

These stimuli interrupt the inner mitochondrial membrane leading to the mitochondrial permeability transition (MPT) pore to lose the mitochondrial transmembrane potential between inner and outer parts. Mitochondrial transmembrane potential alteration leads to release of the pro / anti apoptotic proteins from intermembrane space into cytoplasm (Saelens et al., 2004) such as cytochrome *c*, Smac/DIABLO, serine protease HtrA2/Omi that activate the caspase-dependent mitochondrial pathway via Apaf-1 and procaspase-9, apoptosome (Chinnaiyan, 1999; Du et al., 2000; Hill et al., 2004) and AIF, endonuclease G and CAD, which are released at the late stage of cell death and translocate to the nucleus to induce DNA fragmentation (Enari et al., 1998; Joza et al., 2001; Li, L. Y. et al., 2001).

The Mitochondrial electron transport chain produces the energy for cell metabolism and creates the mitochondrial membrane potential (MMP), which is the crucial parameter for mitochondrial functional evaluation (Chen, L. B., 1988; MITCHELL, 1961). The Mitochondrial membrane potential analysis is used to detect the alteration of the voltage between inner and outer membrane layers of mitochondria in cytoplasm. Changing of this voltage can cause the cell to become apoptotic or necrotic (Sakamuru et al., 2016). In healthy cells, inner mitochondrial membrane presents negative charge while positive charge is in outer layer.

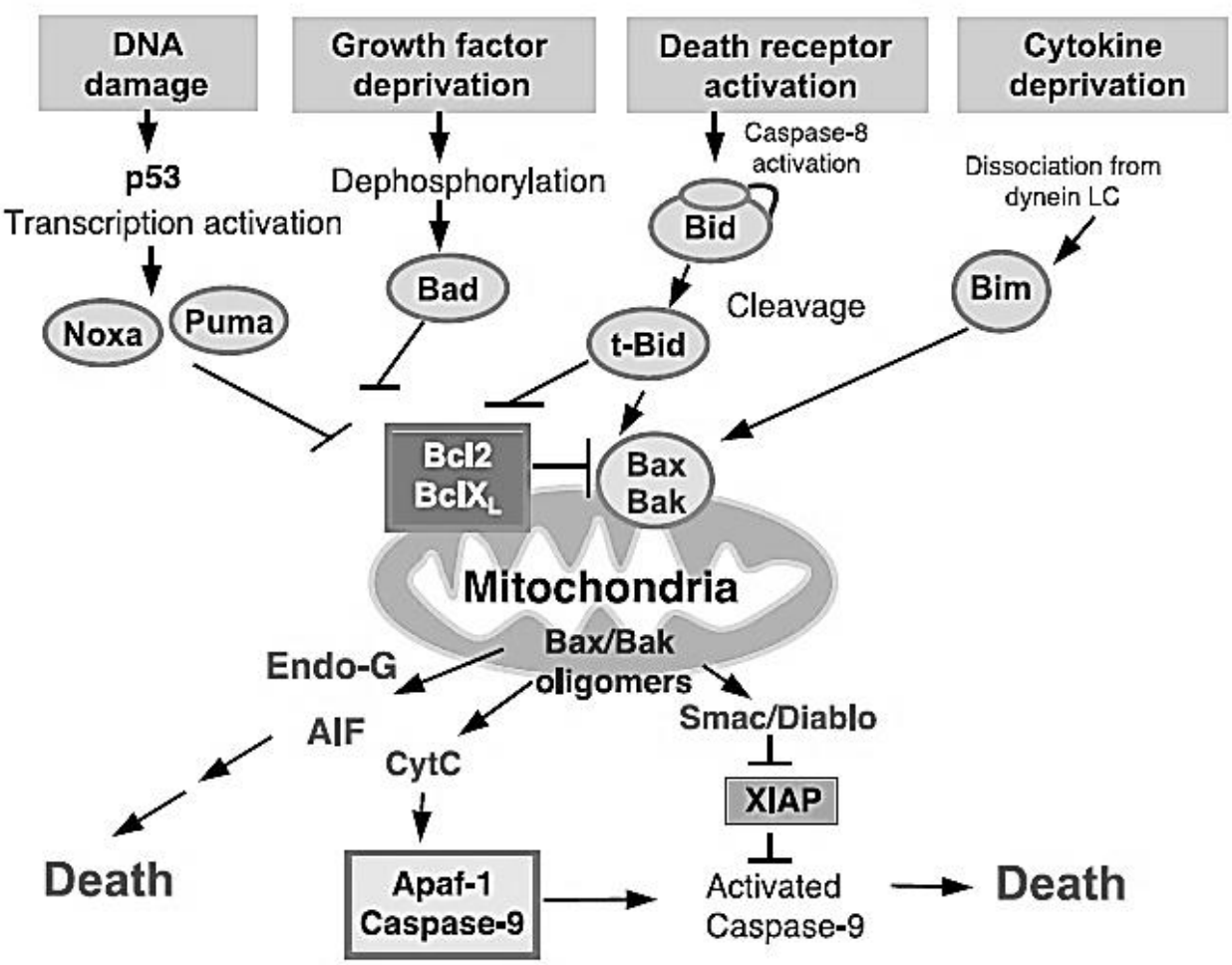

Figure 1-19 Proposed molecular function and regulation of Bcl-2 family members

The BH3-only members play a crucial role in apoptotic signalling regulation. Noxa, Puma, Bad, and Bid inhibit the anti-apoptotic activity of Bcl-2 / BclXL while Bax / Bak interaction with Bim / Bid facilitates caspase-dependent or –independent apoptotic signalling pathways including cytC, AIF, Endo-G and Smac/Diablo mechanism (adapted from (Chan & Yu, 2004)).

The regulation of mitochondrial-induced cell apoptosis is related with the Bcl-2 family proteins that control mitochondrial membrane permeability. Bcl-2 family presents Bcl-2 homology (BH) domains including BH1, BH2, BH3, and BH4. The anti-apoptotic members (Bcl-2, BclXL) consist of all BH domains, whereas pro-apoptotic members (Bax, Bak, and Bok) display BH1-3 domains (Chan & Yu, 2004) (Figure 1-20). In apoptotic signalling, BH3-only members play and crucial role as sensor molecules and relay signals to the mitochondria during apoptosis. At mitochondria, BH3-only molecules interact with Bax and Bak to promote

apoptosis, while the interaction with Bcl-2 / BclXL results in inhibition of anti-apoptotic activities. Multidomain pro-apoptotic members act as apoptotic signalling molecules by facilitating permeability of mitochondrial outer membrane and by releasing apoptotic factors such as cytochrome c (Cyt*C*), endonuclease G (Endo-G), apoptosis-inducing factor (AIF), and Smac/Diablo. These factors subsequently trigger cell death via caspase-dependent or – independent mechanism (Chan & Yu, 2004; Deng et al., 2003) (Figure 1-19).

The both extrinsic and intrinsic apoptotic pathways lead to the execution phase, final pathway of apoptosis. In this phase, execution caspases are activated and lead to cytoplasmic endonuclease becoming active form, which degrades nuclear material, and proteases by degrading the nuclear and cytoskeletal proteins. Another apoptotic pathway that is related to lymphocyte, especially cytotoxic T lymphocyte (CTLs) is perforin/granzyme pathway. Briefly, CTLs are able to mediate the secretion of transmembrane pore-forming molecule perforin after the target cells are infected with virus or the cells become a tumor cell, which will activate two serine protease enzymes, granzyme A and granzyme B. The activated granzyme B will subsequently mediate procaspase-10, and then execution pathway is activated while granzyme A will cleave the SET complex resulting in blocking DNA maintenance and chromatin structure integrity, leading to apoptosis (Elmore, 2007). (Figure 1-21)

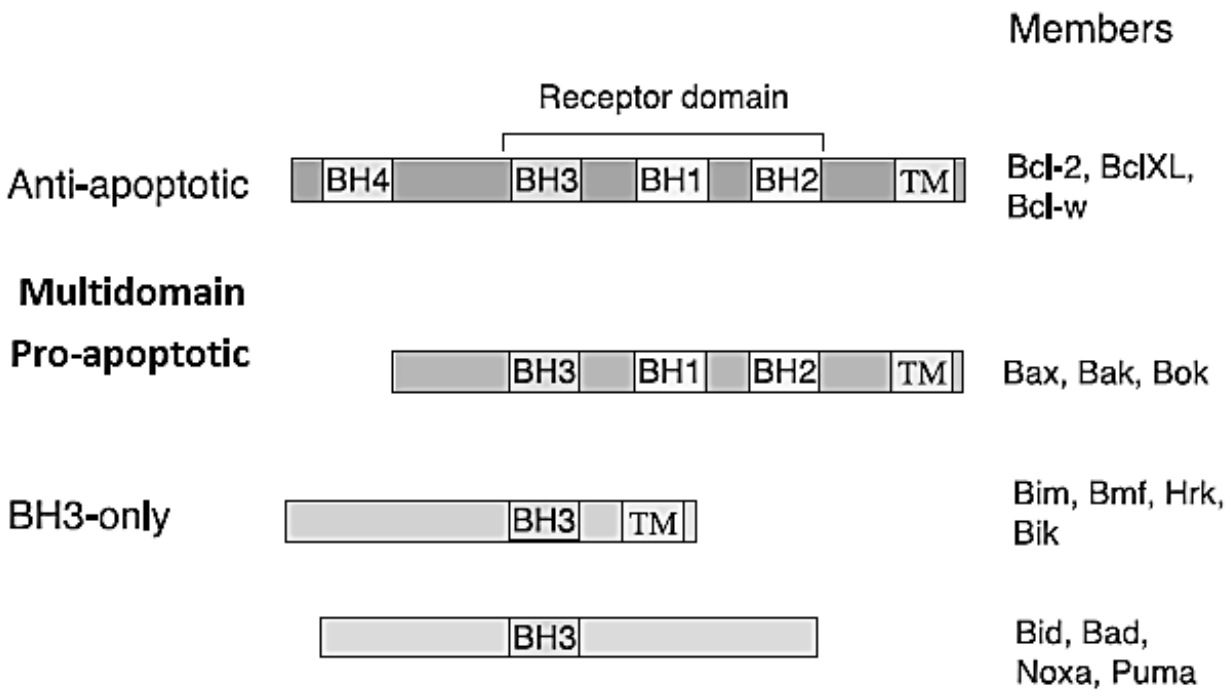

Figure 1-20 Bcl-2 family members

The figure shows four Bcl-2 homology (BH) domains and its members. The most members, except Bid, Bad, Noxa, and Puma, contain carboxyl-terminal hydrophobic region (transmembrane domain, TM) to facilitate intracellular membrane binding (adapted from (Chan & Yu, 2004)).

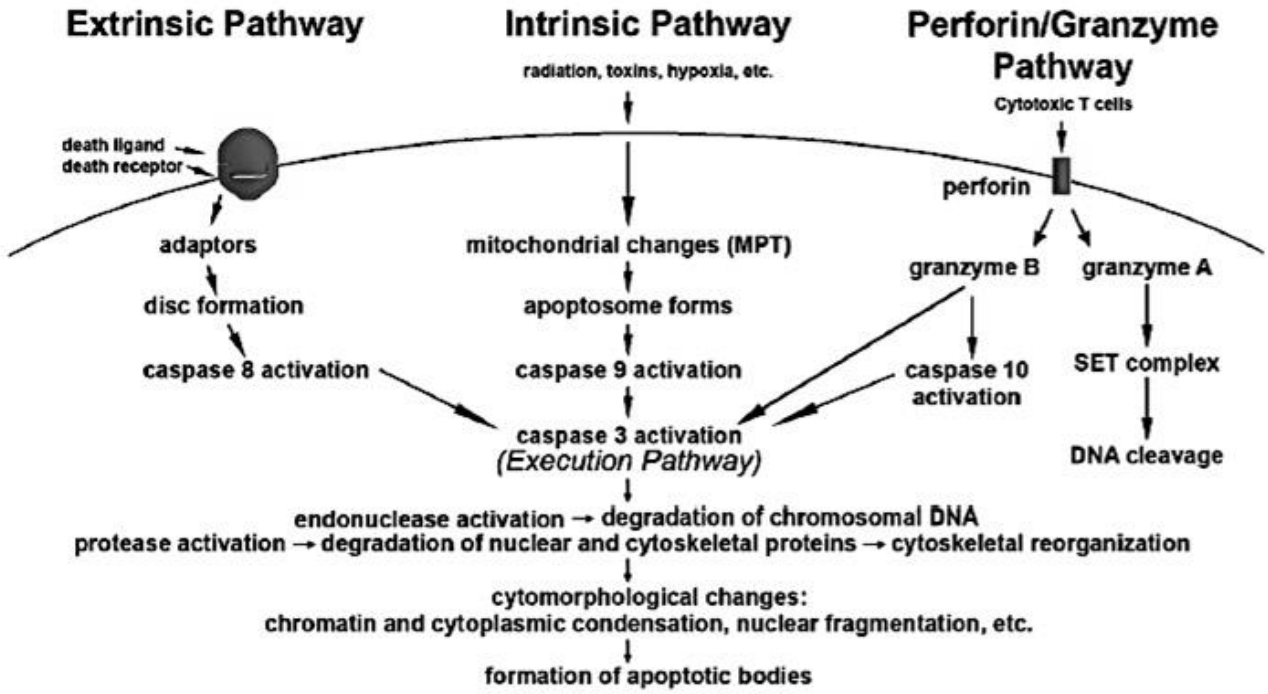

Figure 1-21 Diagram representations of apoptotic events

The two main apoptotic pathways, extrinsic and intrinsic, require specific signals to activate an energy-dependent cascade of molecular events including caspases 8, caspases 9, and caspases 10, which activate execution caspases 3 resulting in cyto-morphological features change (adapted form (Elmore, 2007)).

In haematological malignancies, Bcl-2 has an important role in cell development, progression, and chemosensitivity (Cory, 1995; Smets & van den Berg, 1996). Bcl-2 protein is encoded by B-cell lymphoma/leukemia-2 gene that is involved in apoptosis. In GCs induced cell apoptosis, increasing of Bcl-2 level protects the cell from the death by several stimuli (Reed, 1994). There are several reports indicating that Bcl-2 enhanced prosurvival role against GC-mediated apoptosis using gene transfection, as discussed in more details below (Alnemri et al., 1992a; Alnemri et al., 1992b; Hartmann et al., 1999; Smets et al., 1999; Smets et al., 1994). The Bcl-2 exerts its anti-apoptotic effects through with inhibition of caspase-activation protein such as Apaf-1, the regulation of cytochrome *c* release and intracellular calcium concentration by preventing Bax and Ca^{2+} activation from cytochrome *c* release (Adams, J. M. & Cory, 1998; Greenstein et al., 2002; Kluck et al., 1997).

1.4.2 Autophagy

Autophagy is a highly conserved cellular degradation and recycling processes in mammalian cells. Three principal types of autophagy, microautophagy, macroautophagy, and chaperone-mediated autophagy (CMA), deliver the cargos to the lysosome for degradation and recycling (Figure 1-22). Autophagy is an important process to maintain normal cellular homeostasis by removing unfolded, excessive proteins. In cellular stress conditions, nutrient starvation, low oxygen concentration, DNA damage, pathogen infection, and ER stress have been reported to increase the expression of protein involving autophagic pathway (Jia & Sowers, 2015; Mei et al., 2015). There are several reports that impairment of autophagy processes is involved in pathological conditions such as cancer, neurodegeneration, autoimmunity, and inflammation disorders (Levine et al., 2011; Mizushima et al., 2008; Winslow & Rubinsztein, 2008; Yang, L. et al., 2015).

While microautophagy is the processes of lysosome invagination of cytoplasmic contents, the chaperone-mediated autophagy engulfs both nonspecific and specific substrates to lysosome by recognizing KFERQ motif domain sequence of protein (Dice, 1990). Several targeted proteins such as glycolytic enzymes, transcription factors and inhibitors, calcium and lipid binding proteins, proteasome subunits, and vesicular trafficking proteins that contain KFERQ motif peptide sequence are unfolded by cytosolic chaperone (HSPA8) and are translocated to lysosomal membrane where they are degraded by lysosomal enzyme activities (Orenstein & Cuervo, 2010). At the lysosome membrane, lysosomal-associated membrane protein 2A (LAMP2A) receptor binds to protein substrate following targeted protein entering into lysosomal lumen (Cuervo & Dice, 1996).

Macroautophagy is a complicated degradative mechanism of cytoplasmic components such as misfolded protein and dysfunctional organelles that are formed into double-membrane vesicles (autophagosome) (Ma, T. et al., 2013).

In acute leukemia cells, macroautophagy has been reported to play an important role in promoting or suppressing acute leukemia cell proliferation or survival by activation and inhibition of autophagy (Evangelisti et al., 2014). Therefore, macroautophagy is referred to as autophagy throughout this report and is focus of investigation in this study.

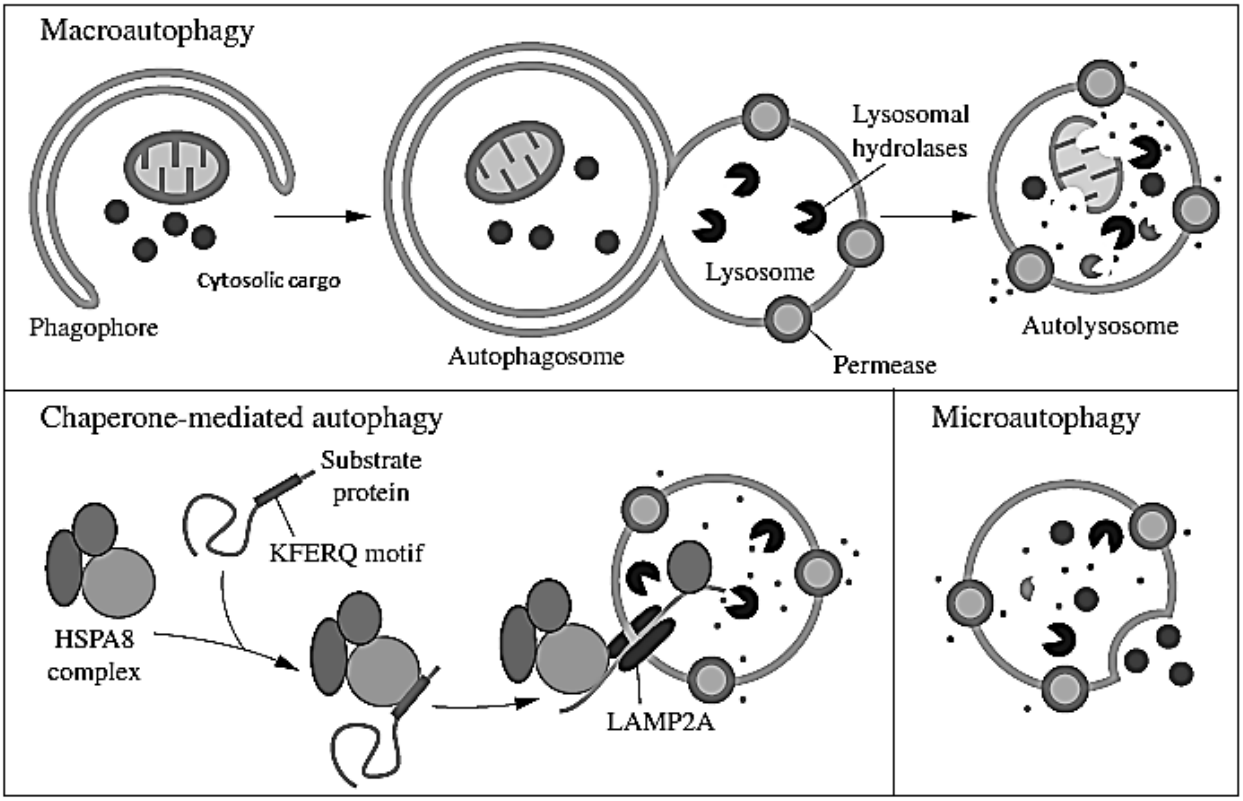

Figure 1-22 Three types of mammalian autophagy

The figure shows macroautophagy, microautophagy, and chaperone-mediated autophagy detected in mammalian cells. Macroautophagy forms double-membrane vesicles to transport cargo to the lysosome while chaperone-mediated autophagy targets individual targeted proteins with specific motif peptide sequence, KFERQ, by HSPA8 complex. Microautophagy is a directly uptake of cargo through lysosomal membrane invagination mechanism (adapted from (Parzych & Klionsky, 2014)).

1.4.2.1 Regulation of autophagy (macroautophagy) pathway

In early studies, yeast, Saccharomyces cerevisiae, was used as model to identify major molecular machinery of autophagy, Autophagy-related (ATG) proteins (Table 4). These proteins are involved in autophagic process in each step of activation (Nakatogawa et al., 2009). Several different phases of autophagy are induction, nucleation of autophagosome, elongation and completion, lysosomal fusion, and degradation (Denton et al., 2012).

Table 4 List of ATG proteins and their function

The key autophagy proteins and function in macroautophagy activation complex pathway (Bestebroer et al., 2013).

Complex	Components	General characteristics
ULK complex	ULK1/2 (Atg1)	Protein kinase
	ATG13	ULK1/2-binding protein
	FIP200 (Atg17)	Scaffold for ULK1/2 and ATG13
	ATG101	ATG13-binding protein
Autophagy-specific class III PtdIns3K complex	VPS34	PtdIns 3-kinase
	p150	VPS34 regulatory kinase
	BECLIN1 (Atg6)	Interacts with and is negatively regulated by BCL2 and BCL-XL
	ATG14L	Autophagy-specific subunit of the PtdIns3K complex
	AMBRA1	Interacts with and activates BECLIN1
	VMP1	ER transmembrane protein interacting with BECLIN1
Other factors	ATG2A	Interacts with WIPI4
	ATG9A	Transmembrane protein
	WIPI1-4 (Atg18)	PtdIns3P-binding proteins
	DFCP1	PtdIns3P-binding ER protein
ATG12-conjugation system	ATG12	Ubiquitin-like protein conjugated to ATG5
	ATG7	E1-like enzyme
	ATG10	E2-like enzyme
	ATG5	Conjugated by ATG12
	ATG16L1	Interacts with the ATG12-ATG5 conjugate and forming an oligomer, which promotes LC3 conjugation to PE
LC3-conjugation system	LC3A-C/ GABARAPL1-2/ GATE16 (Atg8)	Ubiquitin-like proteins conjugated to PE
	ATG4A-D	LC3 carboxy-terminal protease, deconjugating enzyme
	ATG7	E1-like enzyme
	ATG3	E2-like enzyme

The membrane induction and nucleation are the first events of autophagy that will form autophagosome, phagophore, for serving unfolded protein aggregates (Figure 1-23). Double membrane vacuole is formed by the nascent membrane that grows and fuses its edges during elongation phase. Then, the mature autophagosome subsequently fuses with the lysosomal membrane to form an autophago-lysosome. The luminal contents are degraded by acid hydrolase and are recycled through permeases inside autolysosome (Levine & Kroemer, 2008; Yang, Z. & Klionsky, 2010).

Two important regulators of induction autophagic phase are mammalian target of rapamycin complex1 (mTORC1) and AMP-activated protein kinase (AMPK) that were found in eukaryotic cells (Yang, Z. & Klionsky, 2010). It has been reported that mTORC1 is an important down-stream target protein of phosphoinositide 3-kinase (PI3K)/Akt pathway that were activated in haematological malignancies (Kelly et al., 2011; Martini et al., 2014; Polivka & Janku, 2014). The mTORC1 interacts with the UNC51-like kinase (ULK) multi-protein complex, which is the initial step for phagophore formation, resulting in inhibition of autophagy. Furthermore, inhibition of autophagy can occur via phosphorylation of ULK1 and ATG13 by mTORC1, therefore this modification leads to down regulation of autophagic activities (He & Klionsky, 2009). However, nutrient starvation or mTORC1 inhibition by rapamycin treatment have been reported to dissociate mTORC1 from ULK1/ULK2 complex, leading to inducing of down-stream complex and autophagic activities (He & Klionsky, 2009; Kroemer et al., 2010).

AMPK plays a critical role in positive regulation of the autophagic process by directly phosphorylating ULK1 at multiple sites including Ser 317, Ser 467, Ser 556, Thr 575, Ser 638, Ser 777, thus increasing ULK1 activity (Dunlop & Tee, 2013) and it also inhibits indirectly mTORC1 activity (He & Klionsky, 2009).

Autophagosome membrane formation during nucleation phase requires proteins and lipids to activate Beclin1 core complex. Complex is formed by Beclin1 and p150/hVps15 (English et al., 2009) resulting in production of PI 3-phosphate, which promotes autophagosome membrane nucleation. It has been identified that Beclin1 can lead to either activation or inhibition of autophagy by direct interaction with numerous binding partners such as ATG14L, AMBRA1, Bcl-2, Bcl-xL (Abrahamsen et al., 2012; Pattingre et al., 2005).

Vesicle elongation and autophagosome completion phases have two important ubiquitin-like conjugation systems. Both ATG7 and ATG3 proteins regulate the lipid

modification of Light Chain 3 (LC3) by conversion of cytosolic LC3 (LC3-I) into stable form, LC3-II, which conjugates with phosphatidylethanolamine (PE) (Tanida et al., 2004). Before conjugating with PE, LC3 is required to be cleaved initially by ATG4B protease. LC3 is involved in proteins and organelles-developing autophagosome. LC3 has been used as marker of autophagy when it is present in autophagosomes and in slow migration form, LC3-II, which is converted form of LC3-I (Denton et al., 2012). Another pathway contains ATG7 and ATG10 that promotes LC3 lipidation by using ATG12-ATG5-ATG16L complex (Walczak & Martens, 2013; Yang, Z. & Klionsky, 2010).

Finally, autophagosomes fuse with lysosomes (Ravikumar et al., 2010b), forming autophago-lysosomes, to degrade the engulfed contents by resident enzymes (Yang, Z. & Klionsky, 2010).

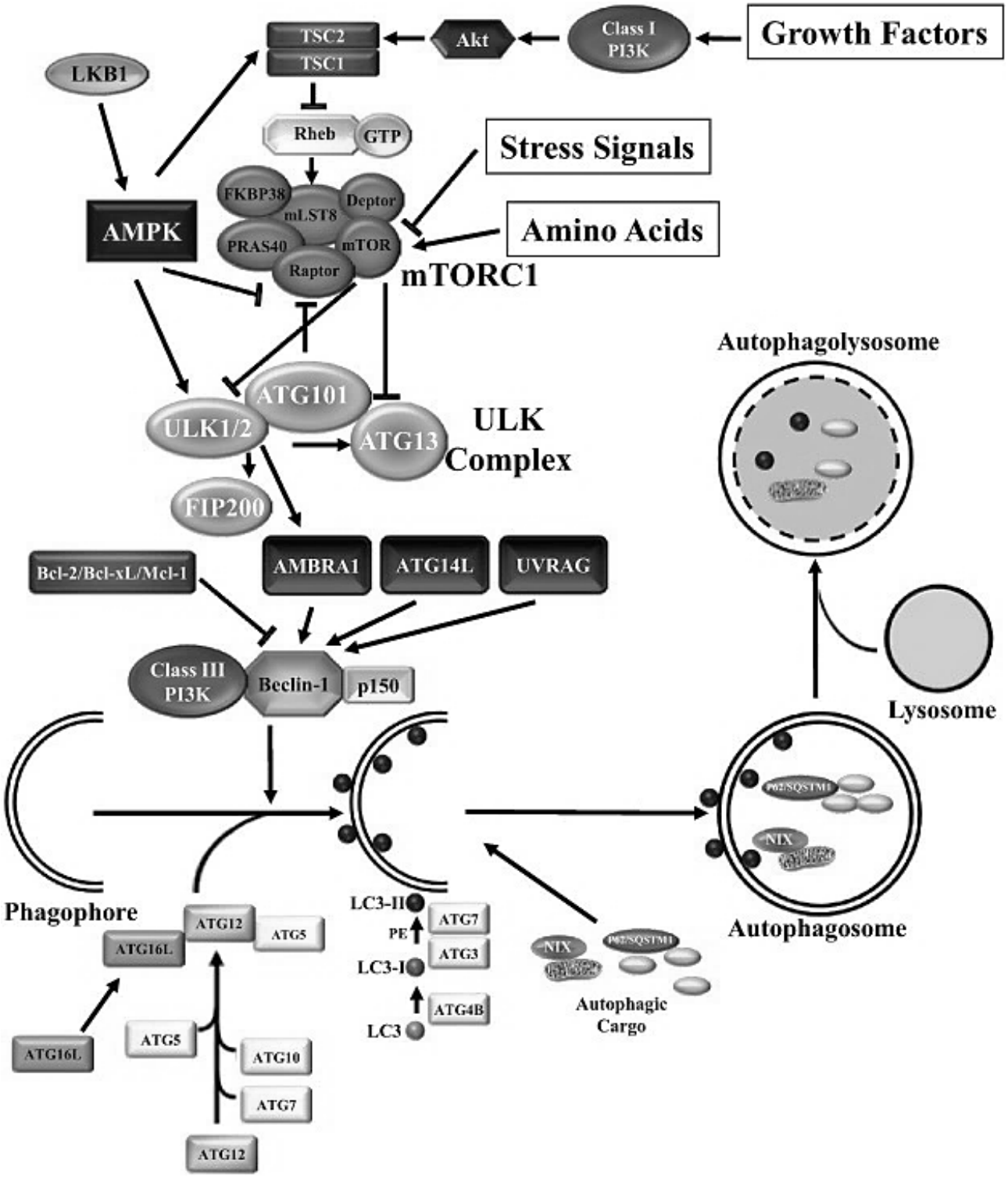

Figure 1-23 The regulation of autophagic molecular machinery

The figure represents the mTORC1 complex association and inhibition by ULK complex by the growth factors and amino acids by phosphorylating ATG13 and ULK1/2. To activate autophagy, stress stimuli or AMPK promote mTORC1 dissociation form ULK1/2 complex, leading to the formation of the phagophore (adapted from (Evangelisti et al., 2014)).

1.4.3 Autophagy and stress conditions

While ER plays an important role to facilitate protein folding and intracellular Ca^{2+} reservoir, exceeded folding capacity by ER stress stimuli leads to protein accumulation and induces ER stress and unfolded protein response activation. Several studies indicated that autophagy is induced by ER stress signalling pathway (Figure 1-24). The mechanisms of activation are dependent on specific stress condition and organism. In mammalian cells, GRP78 inhibition decreases autophagosome formation during ER stress and starvation condition, however, the conversion of LC3 I to LC3 II is not affected. This finding indicated that GRP78 in a crucial factor for autophagy in the phagophore expansion step (Li, J. et al., 2008). The c-Jun N-terminal kinase (JNK), downstream target of IRE1 transmembrane receptor, is the essential molecule for lipid conjugation of LC3 during misfolded proteins induced autophagy in cancer cells (Ding et al., 2007; Ogata et al., 2006). Recent study indicated that IRE1-JNK and REPK-eIF2α pathways are required for LC3 conversion and autophagic degradation of mutant proteins in ER (Fujita et al., 2007; Kouroku et al., 2007). Hypoxia and oxidative stress also play and crucial role in regulating autophagy. These conditions can induce autophagy and several signalling molecules have been reported to be involved in the autophagy activation such as hypoxia-inducible factor-1 (HIF-1), BNIP3, NIX and reactive oxygen species level (Chen, Y. et al., 2007, 2008; Sandoval et al., 2008; Schweers et al., 2007; Zhang, H. et al., 2008a).

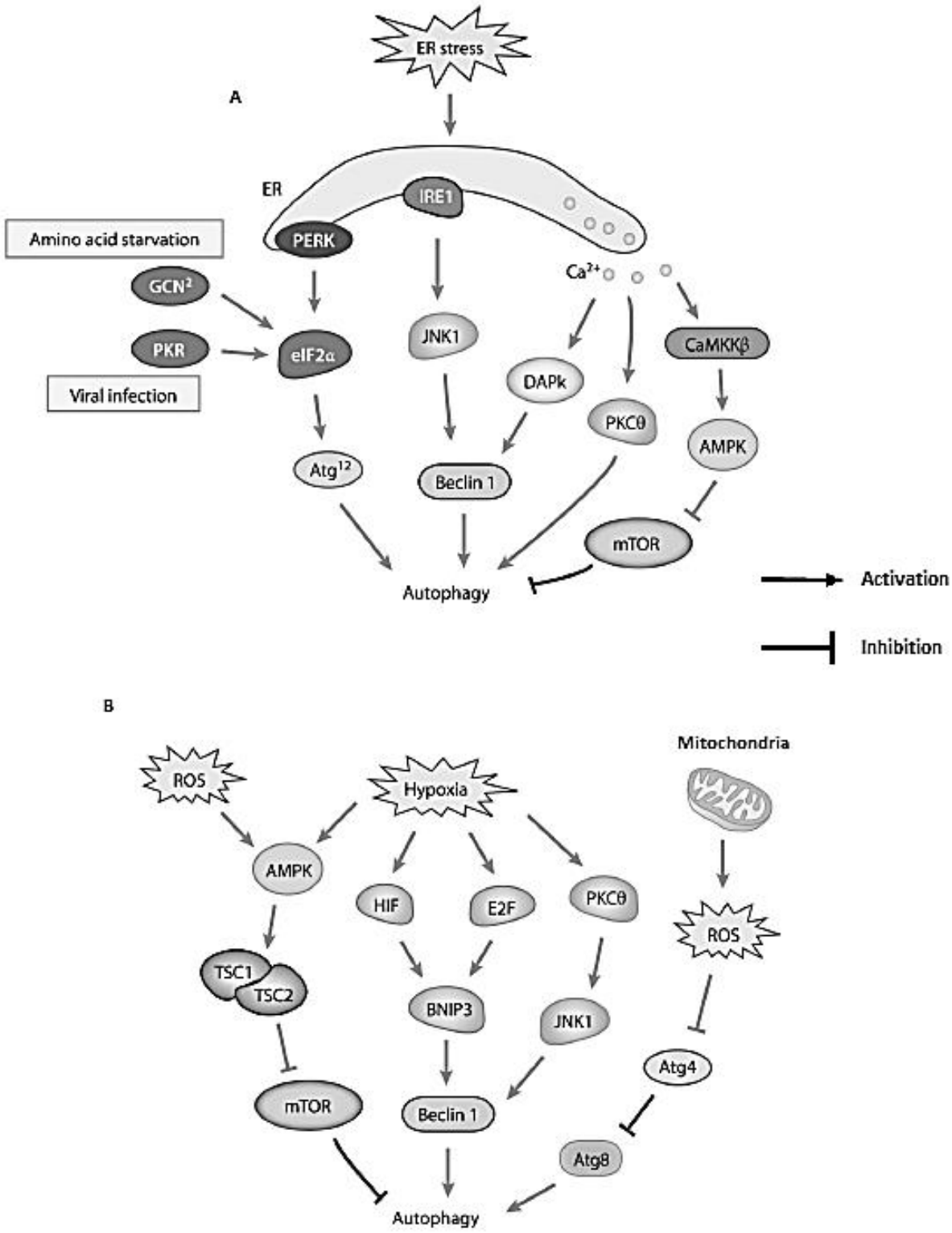

Figure 1-24 Regulation of autophagy in stress conditions

The figures show autophagy is induced by ER stress condition (A) via PERK-eIF2α, IRE1-JNK1 and Ca^{2+} release pathways, and (B) by hypoxia, oxidative stress (ROS) stimuli. Several molecules are involved in this pathway such as HIF, E2F, JNK1 and BNIP3 (adapted from (He & Klionsky, 2009)).

1.5 Endoplasmic reticulum stress and unfolded protein response

The endoplasmic reticulum (ER) is the cytoplasmic organelle that is involved in protein folding, translocation and post-translocation modifications. Impairment or imbalance in the ER environment occurs upon several stimuli including physiological and pathological causes such as nutrient deprivation, oxidative stress, glycosylation change, calcium depletion, damaging of DNA, and energy level alteration. This can lead to ER stress with subsequent accumulation of unfolded or misfolded proteins inside the ER organelle (Yadav et al., 2014). In case of unresolved ER stress conditions, cell can be lead to death via apoptosis (Tabas & Ron, 2011). ER stress causes an increase in Bcl2-like1 (BIM) transcription, p53-upregulated modulator of apoptosis (PUMA), NADPH oxidase activator (NOXA), and BH3-only proteins while imbalance between anti- and pro-apoptotic Bcl-2 family members occurs.

ER stress has been found to restore homeostasis and to be involved in making the adjacent environment suitable for tumour survival and expansion (Martinon, 2012). During tumorigenesis, the high proliferation rates of cancer cells are required to increase ER activity or protein folding, assembly and transport that can induce physiological ER stress (Lee, A. S., 2007). There are three ER stress signalling pathways including inositol-requiring enzyme 1α (IRE1α), activating transcription factor 6 (ATF6) and pancreatic ER kinase-like ER kinase (PERK) that are localized in the ER membrane and are involved with tumorigenesis (Yadav et al., 2014) (Figure 1-25). X-box binding protein (XBP1), down-stream signalling pathway, and IRE1α have been found to promote cancer progression (Koong et al., 2006). It has been reported that protein XBP1 is increased in several types of human cancer including breast cancer, hepatocellular carcinoma and pancreatic adenocarcinoma (Koong et al., 2006). Another ER stress pathway, PERK/eukaryotic initiation factor 2α (eIF2α)/ATF4, also have an important role to contribute in the progression of cancer cell (Koumenis et al., 2002). For developing anti-cancer drugs, ER stress has become a potential target mechanism to reduce adaptation to hypoxia, inflammatory response, and angiogenesis that causes drug resistance (Kraskiewicz & FitzGerald, 2012).

ATF4, XBP1, and PERK regulation or inhibition has been reported to be involved in cancer therapies (Luo & Lee, 2013; Wang, Y. et al., 2012). ER chaperone and UPR component, glucose regulated protein 78 (GRP78), has been recently reported to be over-expressed in several tumour types such as breast cancer, lung tumor, liver cell, brain tumor, colon cancer, ovarian cancer, glioblastoma, and pancreatic cancers (Yadav et al., 2014). However, there are

several studies that have reported ER stress response is directly involved in pro-apoptotic mechanism in either UPR-dependent or –independent manners (Moenner et al., 2007). Agents that induced ER stress are also potential anticancer therapies (Rosati et al., 2010). The cytosolic domain of IRE1α connects with the Bax/Bak apoptotic pathway. This binding leads to IRE1α becoming activated (Hetz et al., 2006). Induction of breast cancer-derived MCF-7 cell death occurring through the activation of ER stress-induced apoptosis and is mediated by Bim protein (Puthalakath et al., 2007).

1.5.1 Regulation of unfolded protein response in ER stress

Unfolded protein response (UPR) is cyto-protective mechanism of cell to balance the misfolded or unfolded proteins under ER stress. Tumour cells will undergo apoptosis when ER stress is prolonged and failure of UPR controlling ER homeostasis has been identified. During UPR process, cells maintain appropriate processes of protein folding in the ER by the dissociation of Grp78/binding immunoglobulin protein (Bip) from 3 membrane-bound ER stress protein sensors, including PERK, ATF6, and IRE1α (Szegezdi et al., 2006). Activation of these sensors occurs after Grp78/Bip protein is dissociated from sensing proteins and PERK is the first sensor protein to activate eIF2α by phosphorylation mechanism (Harding et al., 2000; Shi et al., 1998). These processes result in transcription factor NF-kB inhibition during cellular stress. ATF6 is cleaved in Golgi apparatus before it translocate in the nucleus to regulate gene expression (Schindler & Schekman, 2009). After IRE1 activation, the spliced XBP1 protein translocates into the nucleus and subsequently activates genes expression that are involved with chaperones proteins or folding enzymes involved in protein folding, secretion or ER-associated protein degradation (ERAD) (Acosta-Alvear et al., 2007; Lee, A. H. et al., 2003) (Figure 1-25).

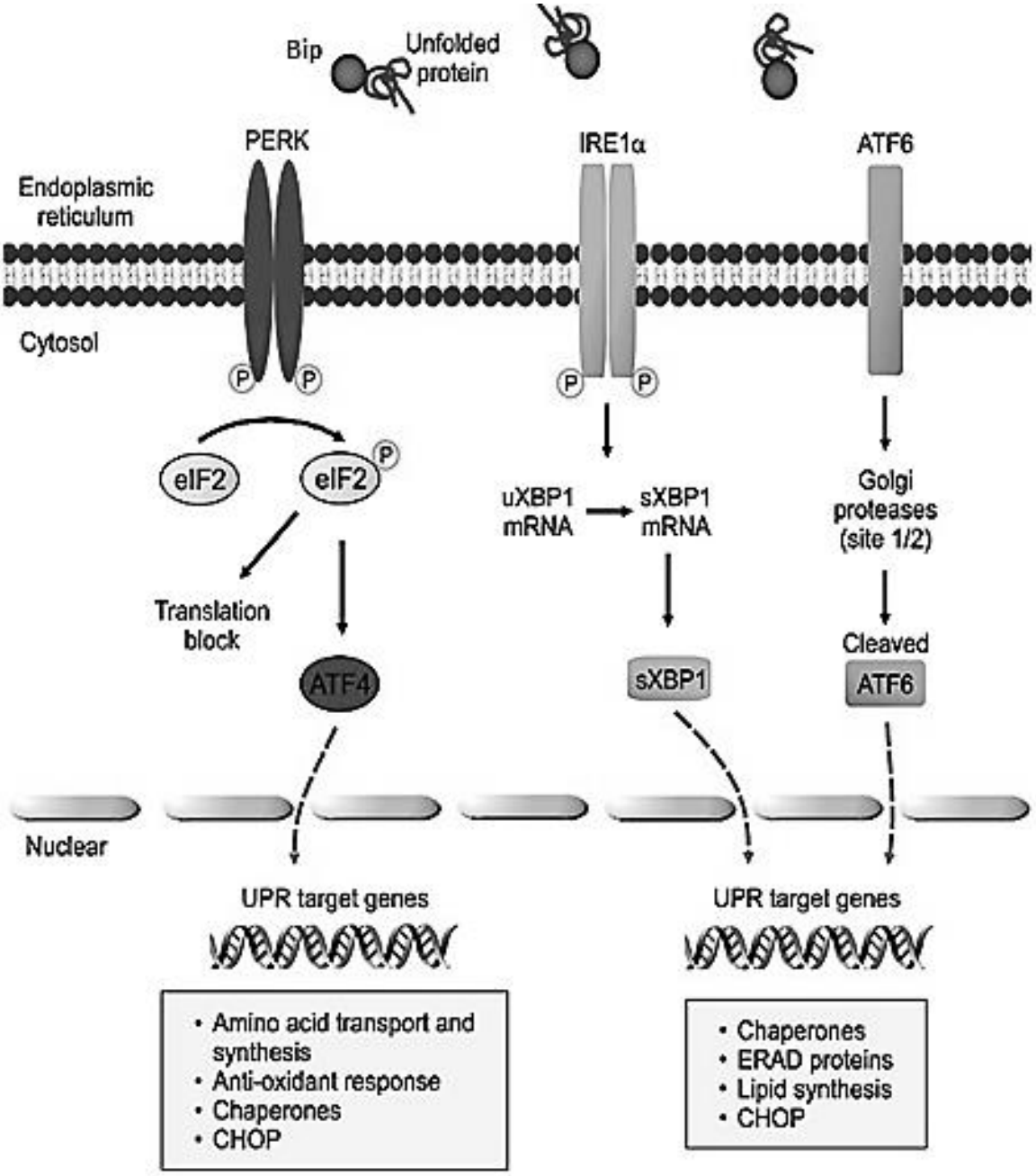

Figure 1-25 Mechanism of UPR during endoplasmic reticulum (ER) stress

Dissociation of glucose-regulated protein 78/binding immunoglobulin protein (Bip) from membrane bound sensing protein activates inositol-requiring enzyme 1α (IRE1α), activating transcription factor 6 (ATF6), and pancreatic ER kinase-like ER kinase (PERK). Several proteins involved in transcription activation of desired gene are activated by active form of membrane sensing proteins resulting in UPR target genes transcription such as CCAAT/enhancer binding protein homologous protein (CHOP) and ER-associated protein degradation (ERAD) (adapted from (Yadav et al., 2014)).

1.6 Glucose regulated proteins (GRPs)

The glucose regulated proteins (GRPs) are known as stress inducible chaperone proteins that mainly are located in the endoplasmic reticulum and the mitochondria. Recent studies indicated that GRPs play an important role in control of signalling, proliferation, invasion, apoptosis, inflammation and immune response and can be translocated to other locations such as cell surface membrane and vesicle membrane that are secreted outside the cell (Gonzalez-Gronow et al., 2009; Gray & Vale, 2012; Ni et al., 2011; Sato et al., 2010).

Glucose regulated proteins, GRP78 (Bip / HSPA5), GRP94 (gp96 / HSP90B1), GRP170 (ORP150), and GRP75 (HSPA9) are stress- related chaperone heat shock protein (HSP) family (Figure 1-26). These GRPs play a crucial role in regulation of protein quality and metabolic balance by facilitating protein folding, assembly and export unfolded or misfolded proteins to degrade. Furthermore, GRPs also maintain ER and mitochondrial homeostasis in the physiological and pathological conditions (Lee, A. S., 2014). Previous studies reported that GRPs are overexpressed in cancer cell lines and are involved in cancer proliferation and metastasis process (Lee, A. S., 2007; Miao et al., 2013). While GRP78 regulates cancer cell viability and apoptosis (Wang, M. et al., 2009), GRP94 is involved in the process of tumorigenesis and implicated with insulin-like growth factor 1 (IGF-1), Toll-like receptors (TLRs) and integrins (Marzec et al., 2012). There are several studies that indicated that ER stress induced GRP78 cell surface expression that is involved in the regulation of PI3K-AKT oncogenic signalling pathway (Liu, R. et al., 2013b; Zhang, Y. et al., 2010; Zhang, Y. et al., 2013). GRP94 and GRP170 expressed on cell surface play an important role in antigen presentation and they also have secreted form that can induce innate and adaptive immune response (Luo & Lee, 2013; Ni & Lee, 2007; Wang, X. Y. & Subjeck, 2013). GRP94 has an important role in immune system by inducing the maturation and activation involved in immune responses and by secreting pro-inflammatory cytokines leading to help antigen presenting cell (MHC class I) to promote the antigen (Luo & Lee, 2013).

Glucose regulated proteins, GRP78, GRP94 are heat shock protein (HSP) family that are mainly found in the endoplasmic reticulum (ER) and in the mitochondria, which are the important organelles controlling protein quality and metabolic balance (Marzec et al., 2012; Ni & Lee, 2007; Wadhwa et al., 2002; Wang, X. Y. & Subjeck, 2013). In some cancers, cell surface GRP78 forms a complex with TGF-β to induce regulatory T cell (Tregs) that inhibit immune system and promote cancer progression by supressing immune response against the

tumor (Oida & Weiner, 2010). Some cancer cells secrete GRP78 into mature dendritic cells leading to Tregs cell production (Corrigall et al., 2009).

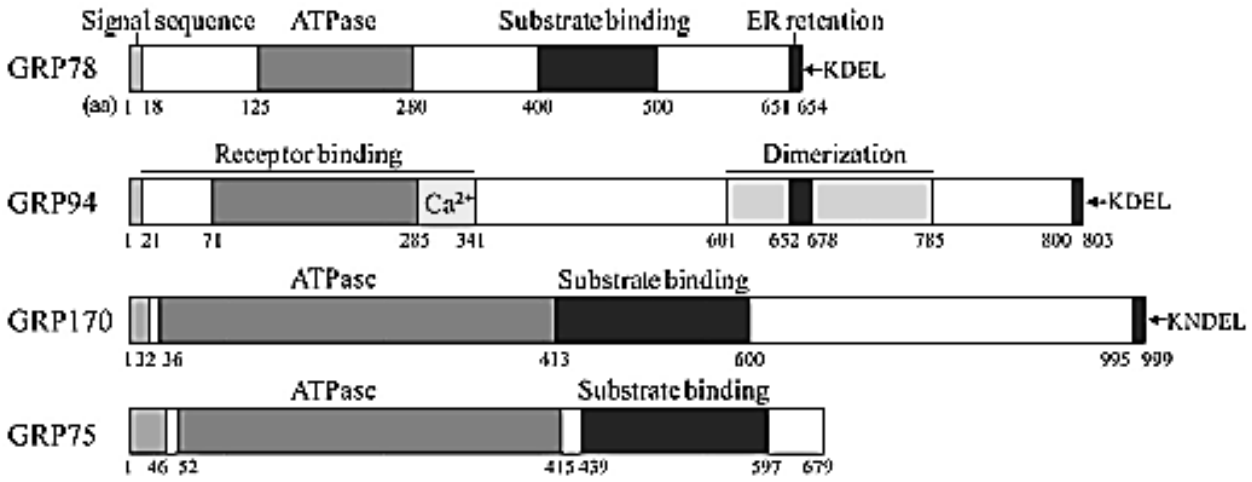

Figure 1-26 Functional domains of glucose regulated proteins (GRPs)

The figure shows several domains of GRPs including ATPase activity, substrate binding site, ER retention peptides (KDEL) and Ca^{2+} binding domain. All GRPs share ATPase and substrate binding domains while Ca^{2+} binding domain, dimerization domain and receptor binding domain are presented only in GRP94 (adapted from (Lee, A. S., 2014)).

1.6.1 ER stress and GRPs regulation

GRPs are expressed constitutively at basal level and maintain homeostasis through different mechanism. During ER stress condition, the induction of GRPs is used as stress indicator and this overexpression has become the crucial issue to investigate intracellular signalling pathway due to ER stress; it can also be interconnected to the nucleus to activate transcription of unfolded protein response (UPR)-associated gene. In cancer cell, ER stress triggered by intrinsic and extrinsic stimuli such as metabolism alteration, aggressive proliferation, starvation, hypoxia, acidosis, viral infection, and genetic mutations, is related to GRPs expression and regulation that is yet to be elucidated (Luo & Lee, 2013; Ma, Y. & Hendershot, 2004). Several studies reported that GRP78 binds to all three ER stress transmembrane sensors including PRKR-like endoplasmic reticulum kinase (PERK), inositol-requiring enzyme 1 (IRE1) and ATF6 under normal condition to regulate unfolded protein response (Luo & Lee, 2013; Wang, M. et al., 2009) (Figure 1-27). GRP activation also is involved in autophagy by upregulation ER chaperones during metabolic stress response

(Mathew et al., 2009). Under ER stress, alternative splicing of GRP78 is triggered to produce cytosolic isoform (GRP78va) that regulates PERK signalling sensor and facilitate leukemia cell survival (Ni et al., 2009). ER stress also regulates GRP78 localization to the mitochondria where mitochondrial-associated GRP78 can bind to RAF1 to regulate mitochondrial permeability and to protect the cell by ER stress induced apoptosis (Shu et al., 2008). GRP94 is linked to Ca2+ homeostasis pathway that can protect the cancer cells from apoptosis (Reddy, R. K. et al., 1999).

In the immune response, there are several studies reported that GRPs are involved in the regulation of major histocompatibility complex (MHC) class I molecules to promote cancer cell survival by immune suppression activation or inhibition of cancer cell survival by pro-inflammatory activation. GRP78 interacts with MHC class I molecules on cell surface to regulate Gs-mediated cAMP production and the pro-inflammatory COX-2PGE-cAMP signalling cascade (Misra et al., 1993; Misra & Pizzo, 2013). In some cancers, GRP78 in T-cell interacts with cell surface TGF-ß to induce regulatory T cells (Tregs) that play an important role for immune suppression and promote cancer cell progression (Oida & Weiner, 2010). Secreted GRP78 also modulates human monocyte differentiation into dendritic cells subsequently inducing Tregs generation (Corrigall et al., 2009). (Figure 1-28)

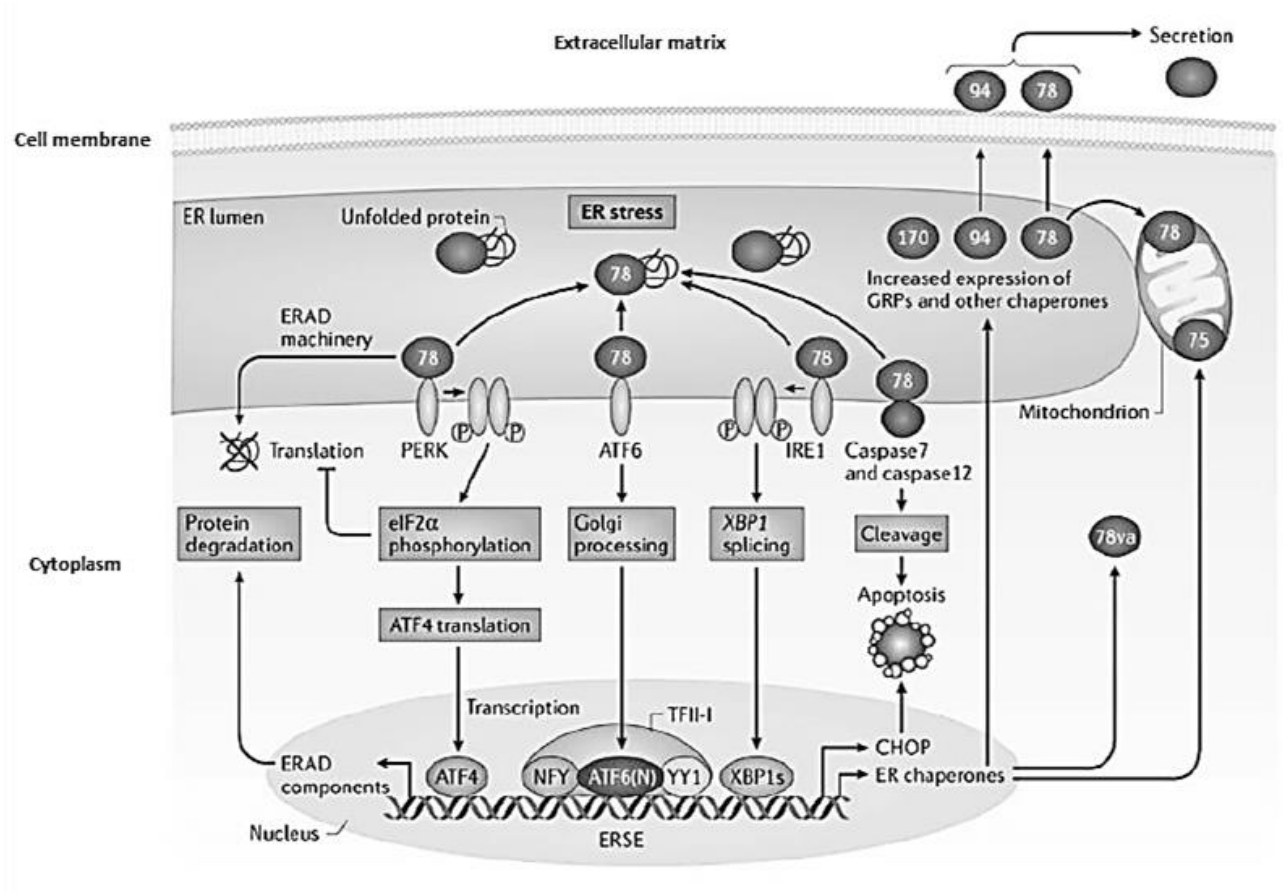

Figure 1-27 Regulation of GRPs in ER stress and UPR conditions

GRP78 located in ER lumen plays a crucial role in UPR signalling regulation by binding and maintaining to the ER stress sensors (PERK, ATF6 and IRE1) under un-stress condition. Upon ER stress, GRP78 dissociates from stress sensors and interacts with misfolded proteins subsequently triggering stress sensors activation and translocation to nucleus. ERSE is the target gene for unfolded protein response and several proteins such as pro-apoptotic transcription factor (CHOP) and ER chaperones are activated and resulting in cell apoptosis (adapted from (Lee, A. S., 2014)).

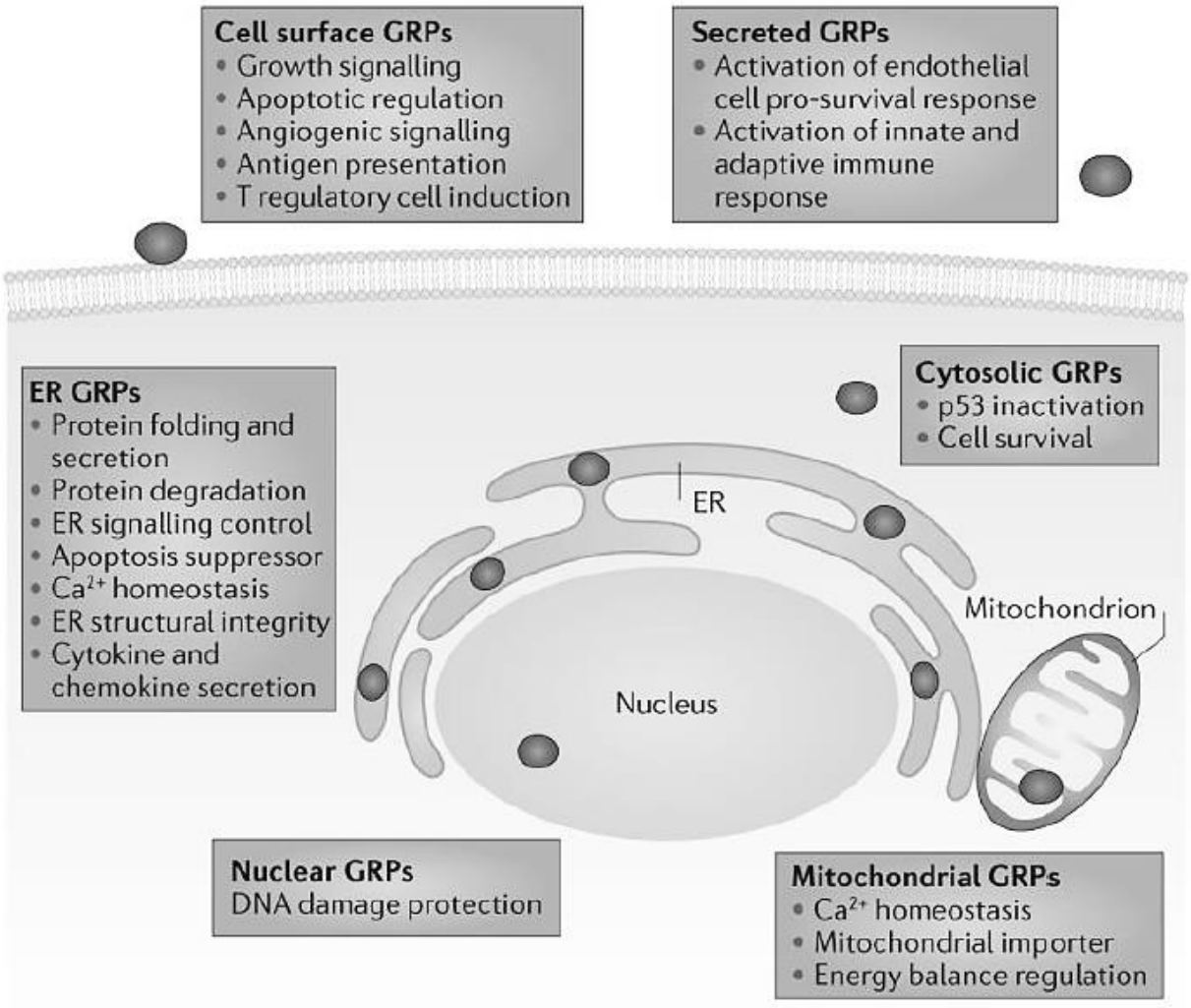

Figure 1-28 GRPs regulation in Cell survival and immune response

GRP78, GRP94 and GRP170 chaperone proteins are mostly found in ER lumen and mitochondria. GRP78 and GRP94 are translocated to cell surface and secreted outside cell upon ER stress or pathological stress. Cell surface GRPs affect growth, apoptosis and immune system (adapted from (Lee, A. S., 2014)).

1.7 Reactive oxygen species (ROS) and leukemia

Reactive Oxygen Species are the group of active molecules and free radicals (oxidants) including O_2, H_2O_2, OH^-, NO and etc. that are derived from oxygen molecule. These molecules are produced during mitochondrial electron transport chain of aerobic respiration processes. In general, ROS are eliminated by host cell protecting mechanism (antioxidants molecules such as superoxide dismutase (SOD), glutathione (GSH), catalase (CAT) and Coenzyme Q10 (CoQ10) (Udensi & Tchounwou, 2014). Imbalance between ROS production and repairing active and free radical molecules can induce oxidative stress (OS) (Finkel, 2003).

OS has been known to induce carcinogenesis but it also induces cancer cell apoptosis which has been used in cancer therapy (Kumar, S. et al., 2014). During cancer treatment, chemotherapeutic drugs and radiation creates ROS and induced OS. Chronic OS alters crucial cellular functions and triggers several types of cancer such as prostate cancer, melanoma, acute lymphoblastic leukemia (ALL), myeloid leukemia, and myelodysplastic syndrome (MDS) (Battisti et al., 2008; Farquhar & Bowen, 2003; Fried & Arbiser, 2008; Kumar, B. et al., 2008; Lau et al., 2008; Renschler, 2004; Weinberg & Chandel, 2009). However, ROS triggers tumorigenesis by anti-apoptosis mechanism, promoting cell survival, proliferation, migration metastasis and chemotherapeutic resistance (Arnold et al., 2007; Maraldi et al., 2009; Naughton et al., 2009; Trachootham et al., 2009; Wu et al., 2008). In leukemia, several observations indicated that activities of antioxidant enzymes are decreased in ALL patients such as SOD, CAT and GSH. The alterations in antioxidants activity disrupts free radical removal and interferes with biological protection mechanism (Flora, 2009).

1.8 Mechanism of GC induced leukemic cell death

GC-induced apoptosis is an important molecular response that has been used in lymphoid malignancies therapy (Gaynon & Carrel, 1999). There are several reports indicating that intrinsic apoptosis pathway is involved in GC-induced leukemia apoptosis. The extrinsic pathway inhibitor, *crmA*, had no substantial effect on GC-induced apoptosis in ALL (Geley et al., 1997; Smith, K. G. et al., 1996). Other molecules involved in GC-induced intrinsic pathway of apoptosis in thymocyts are APAF-1 (Cecconi et al., 1998; Yoshida, H. et al., 1998), Bax and Bak (Rathmell et al., 2002), Bim (Bouillet et al., 1999), Puma and Noxa (Villunger et al., 2003). The knockout (KO) Bcl-$2^{-/-}$ mice showed the effect of GC induced lymphoid apoptosis indicated that anti-apoptotic proteins such as Bcl-2, Bcl-X_L and Mcl-1 are the crucial factor to prevent GC-induced apoptosis (Veis et al., 1993). Further studies indicated that Bax and Bak

are an important proteins for GC-induced apoptosis; this was shown by using KO $Bax^{-/-}$ $Bak^{-/-}$ mice treated with GC and the result showed the thymocytes from KO mice were resistant to GC-induced apoptosis (Rathmell et al., 2002).

Moreover, microarray-based expression profiling of cells in cells treated with GC-s identiified a number of genes were regulated by GR and these can be grouped into three classes 1); death and survival regulation genes 2); cellular distress response genes and 3); non-death response genes (Ploner et al., 2005). There are several genes regulated by GCs in CEM cells apoptosis including NFκB inhibitor α (IκB- α), FK506 binding protein 5 (FKBP 51), BCL2-like 11 (BIM), GILZ, HIF-1 responsive RTP801 (Dig-2), Glucocorticoid receptor α (GR- α), Interleukin 7 receptor, and TGF-β II receptor α, which increase gene expression levels, while the group of genes repressed by GC are Solute carrier family 16 (MCT-1), Tubulin β polypeptide, c-Myc, and Integrin α 4 (antigen CD49D) (Chauhan, D. et al., 2002; Chauhan, S. et al., 2003; Obexer et al., 2001; Tonko et al., 2001; Webb et al., 2003; Yoshida, N. L. et al., 2002).

In addition, mitochondria has been reported as the target organelle for GR translocation to be involved in GC-induced apoptosis. GR has been detected in the mitochondria in several cell types (Demonacos et al., 1995; Koufali et al., 2003; Psarra et al., 2005; Scheller et al., 2003; Scheller et al., 2000). Recent study in various T lymphoid cell lines indicated that only GC-sensitive cells but not in GC-resistant cells were observed the mitochondrial translocation of GR while nuclear GR translocations were observed in both cell types (Sionov et al., 2006a). Further studies demonstrated that GR is located mainly to the inner mitochondrial membrane and mitochondrial GRE elements have been found in the mitochondrial genome which may involve in mitochondrial transcription and energy metabolism (Roussel et al., 2004; Scheller et al., 2003; Scheller et al., 2000; Tome et al., 2004). The binding of GR with mitochondrial membrane may regulate mitochondrial membrane potential and subsequently be involved in ROS generation and transient Ca+ mobilization that are crucial for the apoptotic response (Scheller et al., 2000; Sionov et al., 2006b; Zhang, L. et al., 2006) and the regulation between mitochondria and endoplasmic reticulum in apoptotic processes has been studied (Walter & Hajnoczky, 2005).

Recently, autophagy has been reported to play an important role in drug resistant therapy including hepatocarcinoma cancer, lung cancer, and multiple myeloma (Guo et al., 2013; Lamy et al., 2013; Xi et al., 2011). In murine lymphoma cells, mTOR inhibitor, Dig-2, expression

level increased in Dex treated cells and subsequently activated autophagy processes. Further studies showed Dig-2 knockdown increased levels of dexamethasone induced cell death (Molitoris et al., 2011). Although inhibition of autophagy by chloroquine or 3-methyladenine (3-MA) increased amount of GC-resistant lymphoid cells to apoptosis, the mechanism of GC-induced apoptosis and regulation of autophagy processes are still unclear (Jiang et al., 2015).

1.9 Drugs used in this project

1.9.1 Dexamethasone

Dexamethasone is the synthetic steroid drug which is used in the treatment of anti-inflammatory disorders, including rheumatism, skin diseases, severe allergies, asthma, brain swelling etc. (Figure 1-29). It also is used in the patients suffering with autoimmune diseases. In cancer treatment, Dexamethasone is used as chemotherapeutic agent especially in haematological malignancies such as multiple myeloma and acute lymphoblastic leukemia. The Dex chemotherapeutic effect is through binding to the receptor (GR receptor) to induce tumor cell death. In this study, 1 μM concentration of Dexamethasone is used to treat all cell lines with or without combination treatment with other drugs.

Dexamethasone was purchased from Enzo Life Science Company. The molecular formula is $C_{22}H_{29}FO_5$ with molecular weight at 392.5. The powder form can be prepared in ethanol, DMSO or methanol.

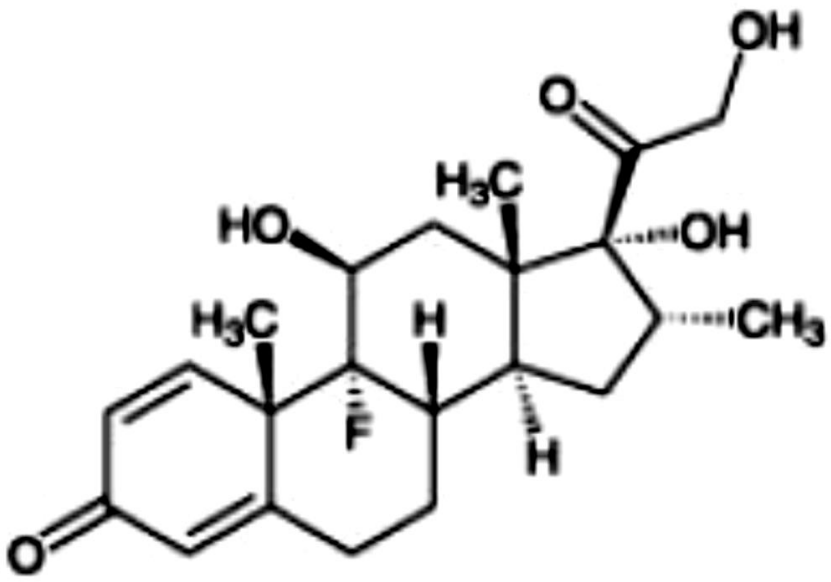

Figure 1-29 The chemical structure of Dexamethasone

(Adapted from Enzo Life Science product data sheet, BML-El126)

1.9.2 Chloroquine

Chloroquine is an antimalarial chemotherapy that belongs to the quinolone family (Figure 1-30). It was used as an antimalarial drug compound. The action of this drug inhibits parasite cell proliferation by binding to heme and forming toxic complex, which results in the cell and parasite becoming lysed. Chloroquine enters the cell to bind with lysosome and it will neutralize acidic property inside lysosome. The disruption of lysosomal pH inhibits the fusion of autophagosome with lysosome to form autophago-lysosome that is the end process of autophagy (Kimura et al., 2013).

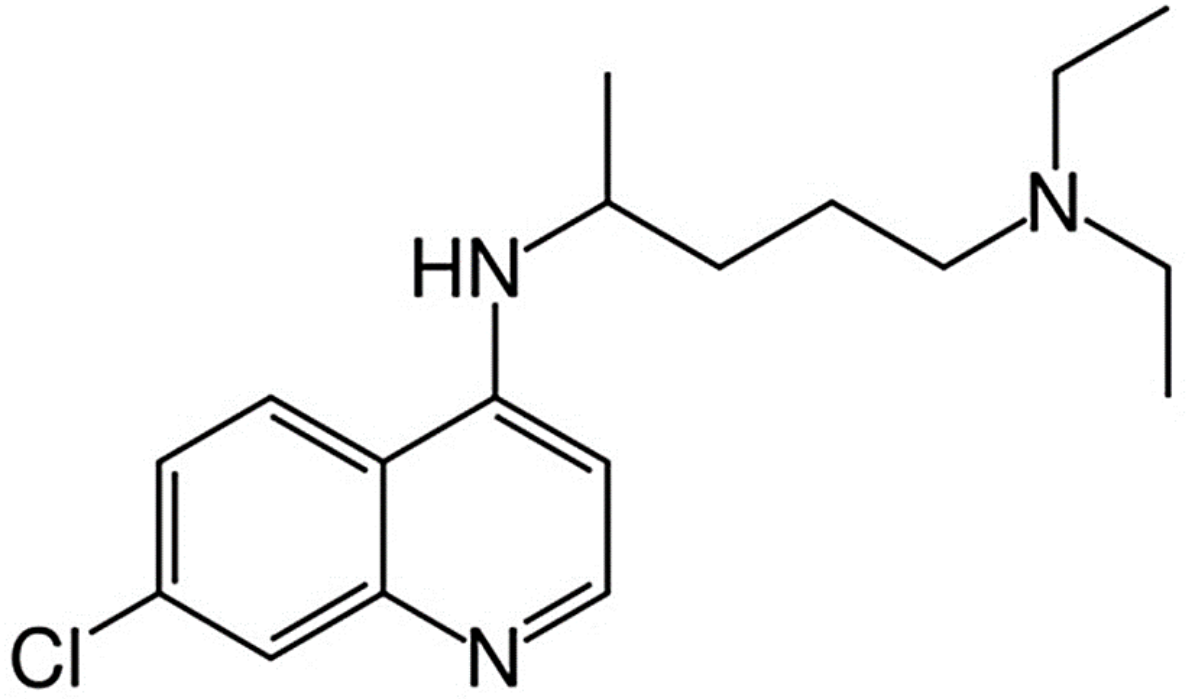

Figure 1-30 The chemical structure of Chloroquine

The chemical structure composes of $C_{18}H_{26}ClN_3$. This drug has 319.877 g/mol in molecular weight. It can be used as antimalarial drug and anti-inflammatory agent. The drug's action inhibits enzyme heme polymerase leading to accumulate the toxic heme within the parasite (Xu et al., 2016).

1.9.3 Thapsigargin

Thapsigargin is used to inhibit sarco (endo)-plasmic reticulum Ca^{2+} ATPase (SERCA) pump, which is located on membrane of sarco (endo)-plasmic reticulum (Figure 1-31). The SERCA pump controls Calcium concentration between cytoplasm of the cell and endoplasmic reticulum by pumps calcium ions from cytosol into ER lumen (Møller et al., 2010). This inhibition raises intracellular calcium concentration that disrupts cellular homeostasis. Accumulation of cytoplasmic calcium can induce mitochondrial morphological change and cell apoptosis via ER stress induced cytochrome C release and caspases activation (Hom et al., 2007). 1 μM and 10 μM thapsigargin have been used in this study to treat ALL cells with or without Dexamethasone.

The drug was purchased from Sigma Company with the molecular formula $C_{34}H_{50}O_{12}$ while the molecular weight is 650.75. Thapsigargin (TG) is extracted from the plant called *Thapsiagarganica L.* by HPLC technique.

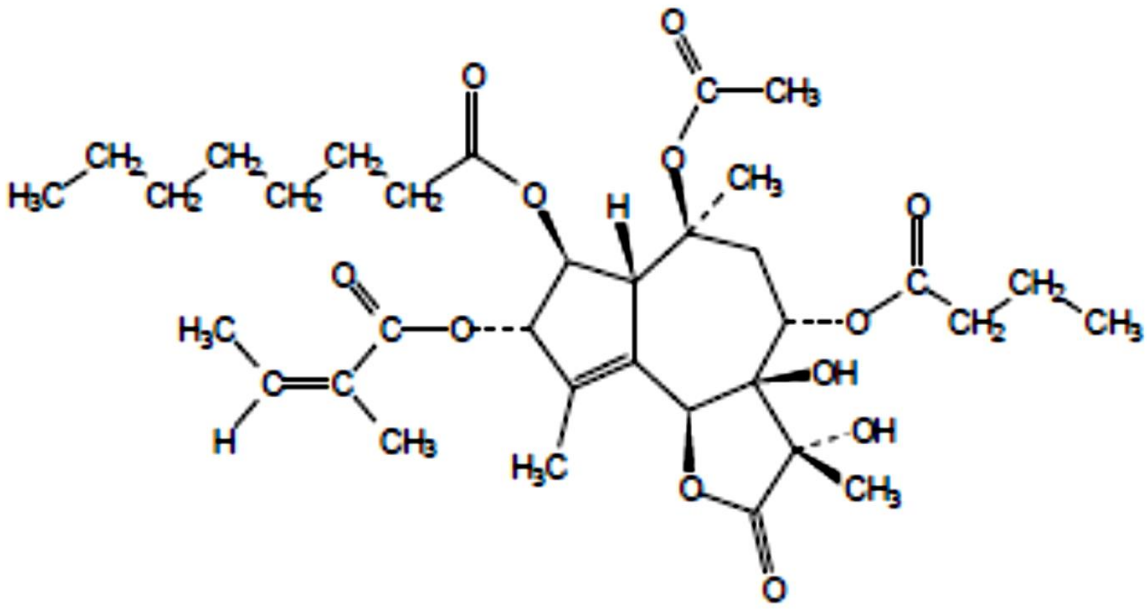

Figure 1-31 The molecular structure of Thapsigargin

Carbon atoms on the structure interact with SERCA pump by hydrophobic bond while the oxygen atoms create hydrogen bonds with the backbone of SERCA pump. These interactions block Calcium homeostasis occurring between cytoplasm and ER lumen and leading to apoptosis activation by cascade pathways (adapted from Sigma (Doan et al., 2015)).

1.9.4 Rotenone

Rotenone (ROT) is a natural botanical compound extracted from *Derris sp.* Root (Figure 1-32). The drug is widely used as an insecticide and herbicide as it acts by inhibiting the electron transfer at the mitochondrial complex I, where is the major source of ATP production. Inhibition of this electron transport chain has been found to induce cell death and to increase mitochondrial ROS production (Li, N. et al., 2003). 1 μM and 10 μM concentration of rotenone has been used with or without Dexamethasone combination to treat cells.

The molecular structure contains $C_{23}H_{22}O_6$ while 394.4 is the molecular weight of this drug (Sigma). Rotenone is soluble in DMSO at 0.5 mg/ml.

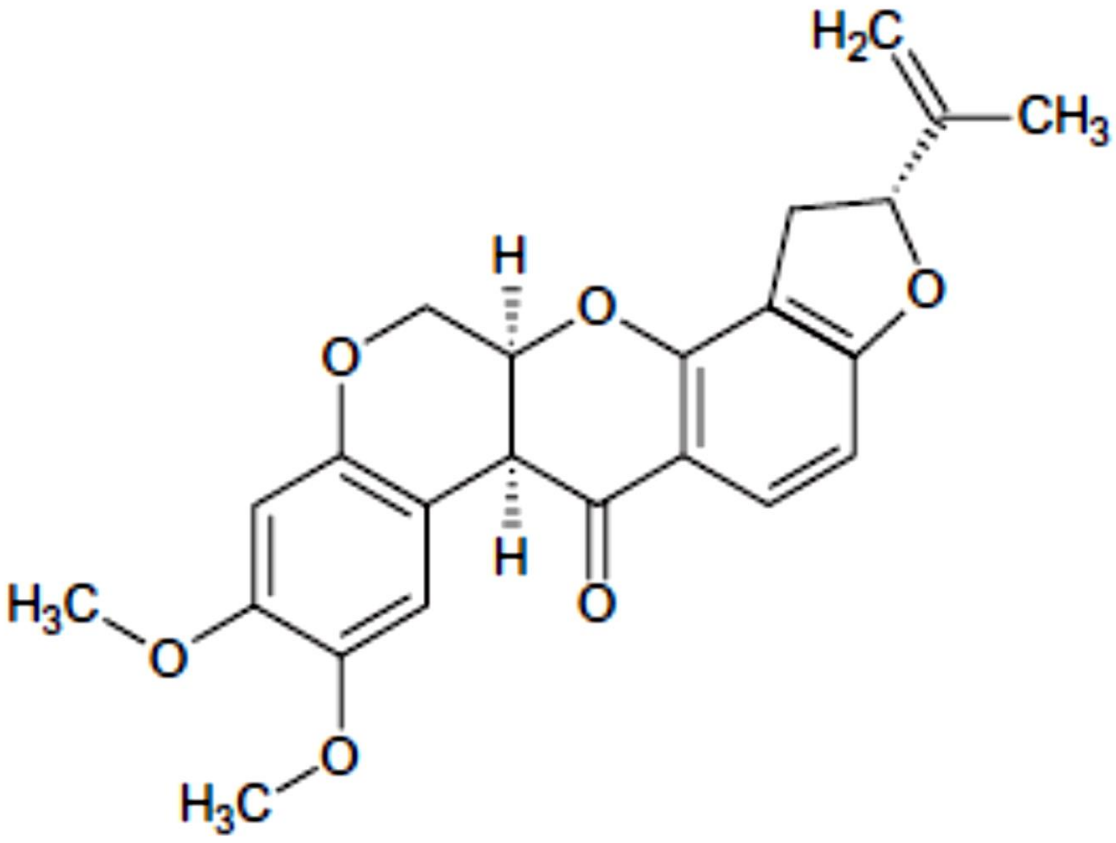

Figure 1-32 The figure shows chemical structure of Rotenone

The Rotenone structure contains 5 carbon rings and it is colourless crystal powder. The yellow colour could be visible when it is oxidized by the light (Gupta, 2012).

1.9.5 Bortezomib

The Proteasome is a cylindrically shaped multi-subunit structure that controls degradation of proteins involved in cell cycle regulation, cell differentiation, transcriptional regulation, and cell apoptosis (Figure 1-33). Ubiquitin-proteasome inhibitor, Bortezomib, inhibits 26S proteasome resulting in apoptosis in many malignant cell types (Horton et al., 2006). Bortezomib has cytotoxic effect in T-ALL cells including Jurkat, Molt4 and CEM cells lines with the IC_{50} values 13.0±2.9, 4.5±0.24 and 3.5±0.24 nM respectively (Koyama et al., 2014). Horton and colleagues demonstrated that T-ALL cell lines are very sensitive to single Bortezomib treatment after 48 hrs using MTT assay (Horton et al., 2006). In this study, 2 nM and 5 nM concentration of bortezomib have been used with or without Dexamethasone.

Bortezomib was purchased from Santa Cruz Company that contains $C_{19}H_{25}BN_4O_4$ in molecular structure. The molecular weight is 384.24.

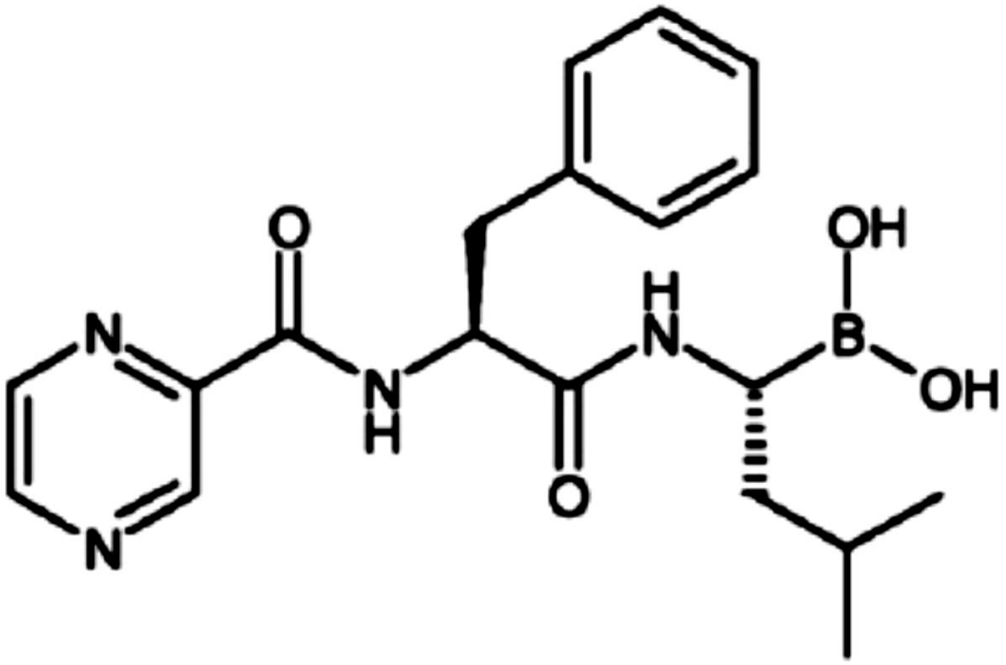

Figure 1-33 The chemical structure of Bortezomib

The figure represents chemical structure of Bortezomib that is a specific proteasome inhibitor. This drug has been approved for use in multiple myeloma and mantle cell lymphoma patients (Ying et al., 2013).

1.10 Project aims

In this study we hypothesise that autophagy, ER stress and UPR play important role in GR function. Therefore the aim of this research is to elucidate the relationship between autophagy and glucocorticoids in human ALL cell lines, CEM-C1-15 and CEM-C7-14 and Molt4. Autophagic proteins such as LC3 I and II, Beclin1 will be analysed in the experiment. This study will also investigate the contribution of endoplasmic reticulum stress and unfolded protein response to the resistance in glucocorticoid therapy by observing ER stress related protein such as GRP78 and GRP 94, which play an important role as protein chaperones responding to unfolded protein accumulation.

Several drugs have been used with Dexamethasone to investigate the autophagy and ER stress response relationship including chloroquine, that acts as autophagic inhibitor reagent, thapsigargin which induces ER stress by blocking calcium pump on ER membrane, rotenone that induces reactive oxygen species generation and bortezomib that induces the ER stress and unfolded protein response by inhibition of proteasome function.

Cell viability assay such as MTS, cell cycle analysis and mitochondrial membrane potential assay will be used to test cytotoxicity of leukemia cells, cell cycle distribution and cell death, respectively. Western blotting technique will be used to investigate protein expression level while RT-qPCR will determine mRNA expression level.

It is hoped that these findings will contribute to better understanding of glucocorticoid molecular mechanism of action, effects on white blood cells and glucocorticoid resistance ultimately leading to improved therapeutic schemes for leukemia.

CHAPTER 2 MATERIALS AND METHODS

2.1 Chemicals

Table 5 List of chemicals used in the project.

This table also provides catalogue number and supplier names.

Chemicals	Company	Catalog number
Acrylamide (ProtoGel)	Fisher, UK	12381469
Ammonium per sulphate (APS)	Sigma, UK	215589-500G
Bovine serum albumin (BSA)	Roche, UK	10711454001
β-Glycerol phosphate (BGP)	Sigma, UK	154804-51-0
β-Mercaptoethanol (HSCH2CH2OH)	Sigma, UK	M6250-250ML
Bromophenal blue	Sigma, UK	B8026-5G
Chemiluminescent substrate (West FEMTO Max. Sensitivity substrate, SuperSignal)	Fisher, UK	11859290
Chemiluminescent substrate (West PICO Chemiluminescent Substrate, SuperSignal)	Fisher, UK	10743105
Dextran Coated Charcoal (DCC) stripped serum	(Hyclone)	SH30068.03
Dimethylsulphoxide (DMSO)	Fisher, UK	D/4121/PB08
Dithiothreitol (DTT)	Sigma, UK	10708984001
Ethylene-diamine-tetraacetatic acid (EDTA)	Sigma, UK	60-00-4
Fetal bovine serum (heat inactivated) (FBS)	Fisher, UK	11550356

Chemicals	Company	Catalog number
Fetal Bovine Serum charcoal stripped	Fisher, UK	10706143
HEPES	Sigma, UK	BP310-100
IGEPAL CA-630 (NP-40)	Sigma, UK	18896-100ML
L-Glutamine	SLS, UK	LZBE17-605E
Penicillin/Streptomycin	Lonza, UK	DE17-602E
Phenylmethylsulphonylfluoride (PMSF)	Sigma, UK	10837091001
PBS (10X concentration)	Fisher, UK	BP399-20
PBS tablets	SLS, UK	79382-50TAB
Propidium iodide solution (1 mg/ml)	Sigma, UK	P4864-10ML
RG Developer 2 x 5l - ready to use	Labtech international Ltd.	RGDEV
RG Fixer 2 x 5l - ready to use	Labtech international Ltd.	RGFIX
Skimmed milk	Marvel	3023034
Sodium dodecyl sulphate (SDS)	Fisher, UK	S/5200/53
Sodium ortho vandate (NaOV)	Sigma, UK	S6508-50G
Sodium pyrophosphate (NaPPi)	Sigma, UK	221368-100G
Tetra methyl ethylene diamine (TEMED)	Sigma-Aldrich, UK	T9281-50 ml
Trypan blue solution	Fluka, UK	93595-50ML

Chemicals	Company	Catalog number
X-ray film SUPER RX 100 NIF sheets 18x24	Fuji Films, UK	47410 19289
X Ray Film 18x24cm Double Sided	SLS UK	MOL7016

2.2 Protein marker, antibodies, and drugs

Table 6 List of protein markers, antibodies and drugs used in the project

This table also provides catalogue number and supplier names.

Products	Company	Catalog number
β-Actin rabbit polyclonal antibody	Abcam, UK	ab8227
β-Actin mouse monoclonal antibody	Invitrogen	MA5-14739
Beclin-1 rabbit monoclonal antibody	Cell signalling, UK	#3495
Bortezomib	Santa cruz biotechology	sc-217785
CellTiter 96 Aqueous MTS reagent powder 250 mg	Promega, UK	G1112
Chloroquine diphosphate salt	Sigma, UK	C6628-25G
DAPI staining (Solution-8)	Chemometec, UK	910-3008
DAPI staining (Solution-12)	Chemometec, UK	910-3012
Dexamethasone	Enzo Life Science	BML-El126
ECL Anti-Rabbit IgG, Horseradish Peroxidase linked from donkey	GE Healthcare,UK	LNA934V
ECL Anti-mouse IgG, Horseradish Peroxidase linked from sheep	GE Healthcare,UK	LNA931V

Products	Company	Catalog number
GRP78 mouse monoclonal antibody	Santa cruz biotechology	sc-376768
GRP 94 mouse monoclonal antibody	Santa cruz biotechology	sc-53929
High Pure RNA Isolation kit	Roche Diagnostics Ltd.	11828665001
JC-1 staining (Solution-7)	Chemometec, UK	910-3007
LC3 rabbit polyclonal antibody	Cell signalling,UK	#4108
Molecular Probe Carboxy-H2DCFDA 25 mg	Fisher Scientific UK	11500146
PageRuler™ Prestained Protein Ladder	Thermo Fischer Scientific, UK	26616
Phenazine methyl sulfate (PMS)	Scientific Laboratory Supplies	P9625-500MG
Reactive Oxygen Species (ROS) Assay kit 520 nm	eBioscience, UK	88-5930
Re-blot mild antibody stripping solution (10X)	Millipore, UK	2502
Ribonuclease A (RNase A)	Sigma, UK	R4875
Rotenone	Sigma, UK	R8875-1G
SensiFAST SYBR no-ROX Mix	Bioline Reagent Ltd.	BIO-98005
TaqMan High Capacity RNA to cDNA kit	Fisher Scientific UK	10704217
Thapsigargin	Sigma, UK	T9033-0.5MG

2.3 Buffers and Reagents

Table 7 List of buffers and reagents used in this project

This table provided the buffers and reagents used in this thesis study

Buffers and Reagents	Composition
High salt lysis buffer (HSLB)	45mM HEPES pH 7.5, 400mM NaCl, 1mM EDTA pH 8.0, 10% Glycerol, 0.5% NP40 – IPEGAL, 1mM DTT, 1 mM PMSF, 2mM Sodium Orthovanadate (NaOV), 1X Protease inhibitors (PI) 1mg/ml (1000X), 20 mM ß-glycerol phosphate (BGP), 5 mM Sodium Pyrophosphate (NaPPi)
Radio-Immunoprecipitation Assay (RIPA) buffer (product code: R-0278)	20 mM Tris-HCl, pH 8.0, 150 mM sodium chloride 1.0% Igepal CA-630 (NP-40), 0.5% sodium deoxycholate, 0.1% sodium dodecyl sulfate
3x SDS loading buffer	187 mM Tris pH 6.95, 30% Glycerol, 6% SDS, 15% 2-mercapto ethanol, 0.01% bromophenol blue
10X western running buffer	250 mM Tris, 1.9 M glycine, 350 mM SDS
10X western transfer buffer	220 mM Tris, 750 mM glycine
Blocking buffer	5% skimmed milk in 1X PBS
0.1% PBS tween	0.1% Tween in 1X PBS
0.1% Sodium dodecyl sulfate (SDS)	0.1 g SDS was dissolved in 100 ml distilled water
10% Sodium dodecyl sulfate	10 g SDS was dissolved in 100 ml distilled water
0.2M EDTA pH 8.0	18.61 g EDTA was dissolved in 100 ml distilled water and pH was adjusted to 8.00 with Sodium hydroxide (NaOH) before adding distilled water to the final volume.
1M Tris pH 6.95	12.14 g Tris was dissolved in 100 ml distilled water and pH was adjusted to 6.95 with concentration hydrochloric acid (HCl) before adding distilled water to the final volume.

Buffers and Reagents	Composition
1.5M Tris pH 8.95	18.21 g Tris was dissolved in 100 ml distilled water and pH was adjusted to 8.95 with concentration hydrochloric acid (HCl) before adding distilled water to the final volume.
200 mM Sodium pyrophosphate (NaPPi)	8.92 g NaPPi in 100 ml distilled water
10% Ammonium persulfate	1 g ammonium persulfate was dissolved in distilled water and adjusted the final volume to 10 ml.
1M Sodium Orthovanadate (NaOV)	1.84 g NaOV was dissolved in 8 ml of distilled water and pH was adjusted to 10.
1M HEPES pH 7.5 for 100 ml	23.83 g of HEPES was dissolved in 80 ml distilled water then the solution was adjusted pH for 7.5 by NaOH. Distilled water was added to 100 ml.
1M Dithiothreitol (DTT)	1.5 g DTT was dissolved in 8 ml of distilled water and mixed it until the solution was mixed completely. Then adjusted the volume by adding distilled water to 10 ml.
0.5 M EDTA pH 8.0	93.05 g of EDTA was dissolved in 400 ml distilled water. Then adjusted pH with sodium hydroxide (NaOH) to 8.0 and filled up with distilled water to 500 ml.
100mM PMSF	0.09 g of PMSF was dissolved in 5 ml of absolute ethanol.

2.4 Primers used in Quantitative Reverse Transcription Polymerase Chain Reaction

The primers used in the project were purchased from Eurofins Company. The details for DNA sequence are listed below.

Table 8 List of Primers used for RT-qPCR Assay

All primers were ordered from Eurofins Company.

Primer	DNA Sequence (5`to 3`)	Tm (°C)
BECLIN1 forward	TTGGCACAATCAATAACTTCAGGC	59.3
BECLIN1 reverse	CCGTAAGGAACAAGTCGGTATCTC	62.7
LC3B forward	TGTCCGACTTATTCGAGAGCAGCA	62.7
LC3B reverse	TGTGTCCGTTCACCAACAGGAAGA	62.7
GRP78 forward	TGCCGTTCAAGGTGGTTG	56.0
GRP78 reverse	CCAAATAAGCCTCAGCGG	56.0
GRP94 forward	CTGGGTCCAGCAGAAAAGAG	59.4
GRP94 reverse	CACTCCTTCCTTGGCAACAT	57.3
RPL19 forward	ATGTATCACAGCCTGTACCTG	57.9
RPL19 reverse	TTCTTGGTCTCTTCCTCCTTG	57.9

2.5 Mammalian cell types

There are three human haematological malignant cell lines that were used in the experimental research including ALL CEM-C1-15 and Molt4 which are resistant to glucocorticoids and CEM-C7-14 which is sensitive to glucocorticoid treatment. Molt4 cell line is derived from acute lymphoblastic leukemia patient that carried the mutated genes including CDKN2A, NOTCH1, NRAS, PIK3R1, PTEN and TP53 (ATCC No. TCP-1010). CEM cell lines were derived from lymphoblastic cells of acute lymphoblastic leukemia patient containing several gene mutations (Foley et al., 1965). CEM C1 and CEM C7 are clones isolated from the original CEM cell line and are glucocorticoid resistant and glucocorticoid sensitive, respectively (Medh et al., 2003). The sensitive clones of CEM cell have been identified after the cells were treated with 1 μM Dexamethasone for 4-5 days, when their proliferation was inhibited and they became pyknotic shape and lysed (Medh et al., 1998; Norman & Thompson, 1977). The steroid resistant cells were isolated using semisolid agarose medium which contained 1μM Dexamethasone (Harmon & Thompson, 1981). These cells contained receptor

for glucocorticoids identical to CEM wild-type cells (Zawydiwski et al., 1983). However, CEM C1 (clone 15) was re-isolated in 1998 by Reem D. Medh to test the mechanism of Dexamethasone and forskolin synergism. In the genotypic alteration, CEM cell lines were found to have missense mutation of both alleles of the p53 genes that would inhibit normal function of cells (Cheng & Haas, 1990). The Molt4 cell line is another human acute T-lymphoblastic leukemia and the karyotypic study has shown there were structural abnormalities of chromosomes that effected several genes (Ma, X. C. et al., 2014)

2.6 Cell culture protocols

2.6.1 Growth media

Roswell park memorial institute-1640 (RPMI-1640) media purchased from Sigma, UK with catalogue number R1383 was used to maintain human cell line including CEM-C1-15, Molt4 and CEM-C7-14. Media was prepared by adding 10% of fetal bovine serum, 1% of penicillin/streptomycin and 1% L-glutamine making enrichment medium that was kept at 4° C.

Dextran Coated Charcoal (DCC) or Fetal Bovine Serum Charcoal Stripped media were used before adding Dexamethasone in any experiments to decrease the levels of various hormones that can affect studies. To prepare the DCC containing media, RPMI-1640 media was supplemented with 10% fetal bovine serum charcoal stripped from Sigma, UK (catalogue number 6765-100ML), 1% of penicillin/streptomycin and 1% L-glutamine. The complete media can be kept in 4°C for a long term use.

2.6.2 Maintenance of cell culture

Cells were maintained in 25 cm^2 tissue culture flasks (T25) or in 75 cm^2 tissue culture flasks (T75) and sub-cultured every 2-3 days when they were 70-80% confluent. In this step, suspended cells were centrifuged in room temperature as 2,000 revolution per minute (RPM) for 3 minutes then the supernatant was discarded. The pellets were re-suspended in 2 ml of complete fresh medium and transferred into a new culture flask containing 8 ml of medium to maintain 1:5-10 dilutions ratio. For sterile environment, class II laminar flow microbiological safety cabinet (Walker Safety Cabinets Ltd. Serial number: 50000657) was used. During maintenance, cells were incubated in the incubator with 37°C and 5% carbon dioxide (CO_2) concentration (Sanyo CO_2 Incubator: MCO-17AIC, Serial number: 10908824).

2.6.3 Freezing and thawing of suspended cell

In the first step, the fetal bovine serum was warmed in 37°C water bath. Once warmed, 2 ml DMSO was added into 8 ml FCS making 20% DMSO solution. Next, cells were pelleted by centrifugation at 2,000 rpm for 3 minutes at room temperature. Then, pellets were resuspended in 1 ml fresh FCS and 1 ml 20% DMSO solution. The DMSO prevents cells forming intracellular ice crystals. Finally, cells suspension was aliquoted into cryovial tubes and then transferred to -80°C respectively.

For defrosting or thawing the cells, warmed RPMI-1460 media containing 10%FCS, 1% L-glutamine and 1% penicillin/streptomycin was added to T25 flask and transferred the 1 ml cells directly into flask. The cells were incubated in the 37°C incubator with 5% CO_2 for 24 hours and the media was changed with fresh completed RPMI-1460 medium to avoid cytotoxic effect of the DMSO residue on the cells. Then the cells were maintained until 70-80% confluence in T25 flask.

2.6.4 Cell counting using a haemocytometer

Microscopic chamber slide with a small (3mm × 3mm) square etched onto surface was used to determine the number of cells before extracting the protein from cells. Cells were diluted in the first step with complete medium at the dilution ratio 1:12 (10 µl of cell suspension and 110 µl of fresh RPMI-1460 medium). The cell suspension was diluted with trypan blue dye with the ratio 1:2 by mixing 10 µl of cell suspension with 10 µl of dye and the cell suspension was loaded into the haemocytometer (C-Chip DHC-N01, from Digital Bio Company) and observed under 10X objective lens microscope (Figure 2-1). Generally, the total number of cells was counted in the four large corner squares and the cell concentration was calculated as

Cell concentration (cells/ml) = average cell count from 4 corners × dilution factor × 10,000

The cell counting was used to obtain the number of cells to optimize cell concentration for Dexamethasone treatment in any future experiments such as cell viability assay, protein extraction technique and cell cycle analysis by flow cytometry.

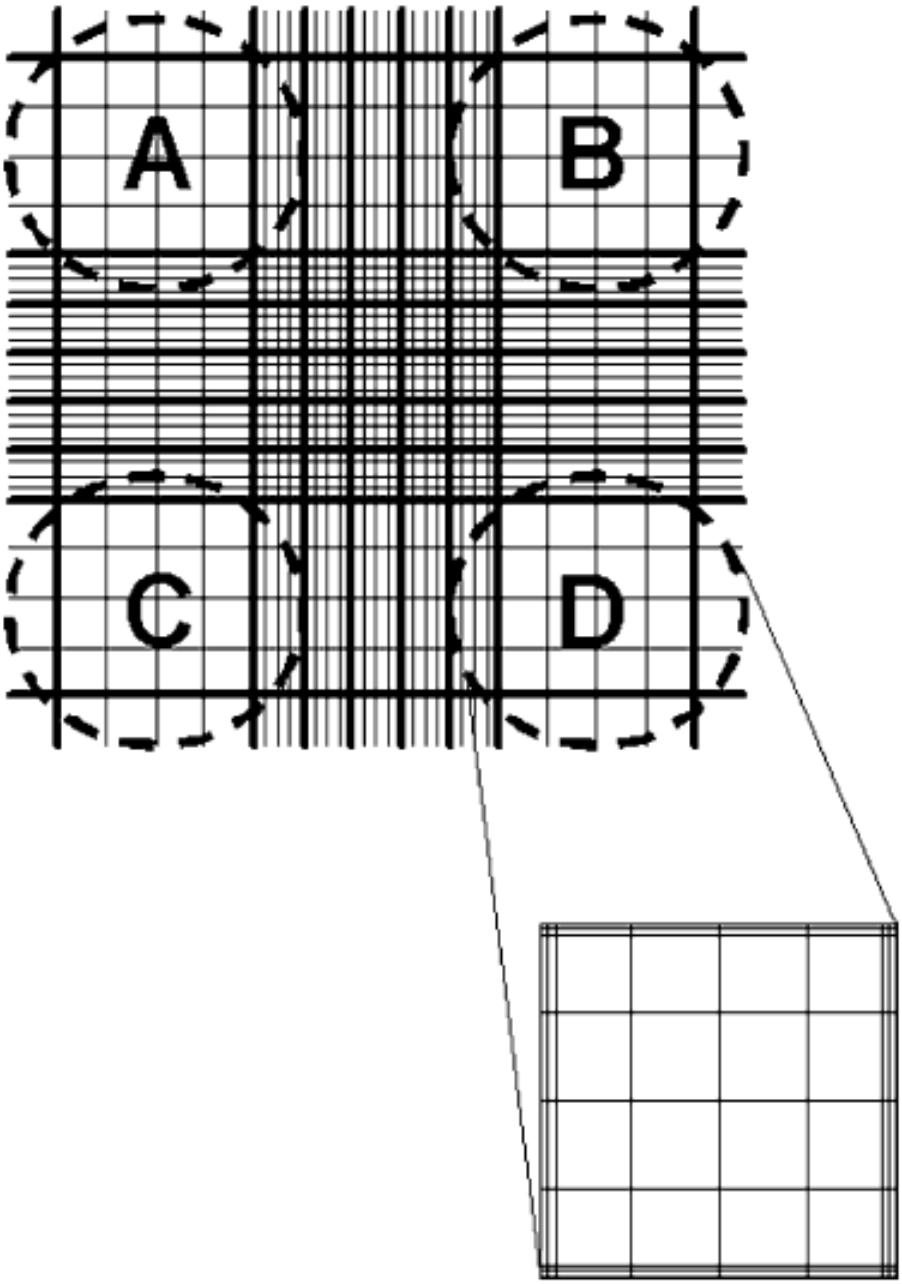

Figure 2-1 The figure shows outline of four corners in haemocytometer (C-Chip)

The outline is focusing on the grid with 10X magnification on objective lens. A, B, C and D represent the corners where alive cells were counted *(Louis & Siegel, 2011).*

2.7 Cell viability assay using MTS dye

To determine the effect of studied drugs on cell, cell-based assay using negatively charged compound, MTS, was applied in this study. MTS does not penetrate into cytoplasm of the living cell while the activity of alive cell will transfer electron from the cytoplasm or cell membrane to intermediate electron acceptor reagent such as Phenazine methyl sulfate (PMS) and Phenazine ethyl sulfate (PES) and then these reagents can convert tetrazolium compound in the culture medium to the soluble form of formazan reagent (Berridge et al., 2005). The soluble formazan will turn the medium to dark brown colour that is visible in the experiment plate. The MTS compound was purchased from Promega Company, CellTiter 96 Aqueous MTS reagent (Figure 2-2). It can be summarized that more alive cells were growing in the medium more dark brown colour was visible.

2.7.1 Cell seeding into 96 wells plate

After counting the cell using C-Chip, 50,000 cells were seeded into flat bottom 96 wells plate containing 50 µl of DCC-RPMI medium. Then, the drug dilutions were prepared before loaded into 96 wells plate for 50 µl. Dexamethasone was prepared for maximal concentration at 20 µM and then the concentration was diluted in half 6 times. The Thapsigargin concentration started at 40 µM as same as Rotenone while the maximal concentration of Bortezomib was 20 µM. The untreated condition is set as row A and the maximal drug concentration was loaded in row H (the bottom of the 96 wells plate) while the rest of diluted condition were loaded from row Q to row B, respectively. Once the drugs have been added, the plate was left in the incubator for 24 and 48 hrs.

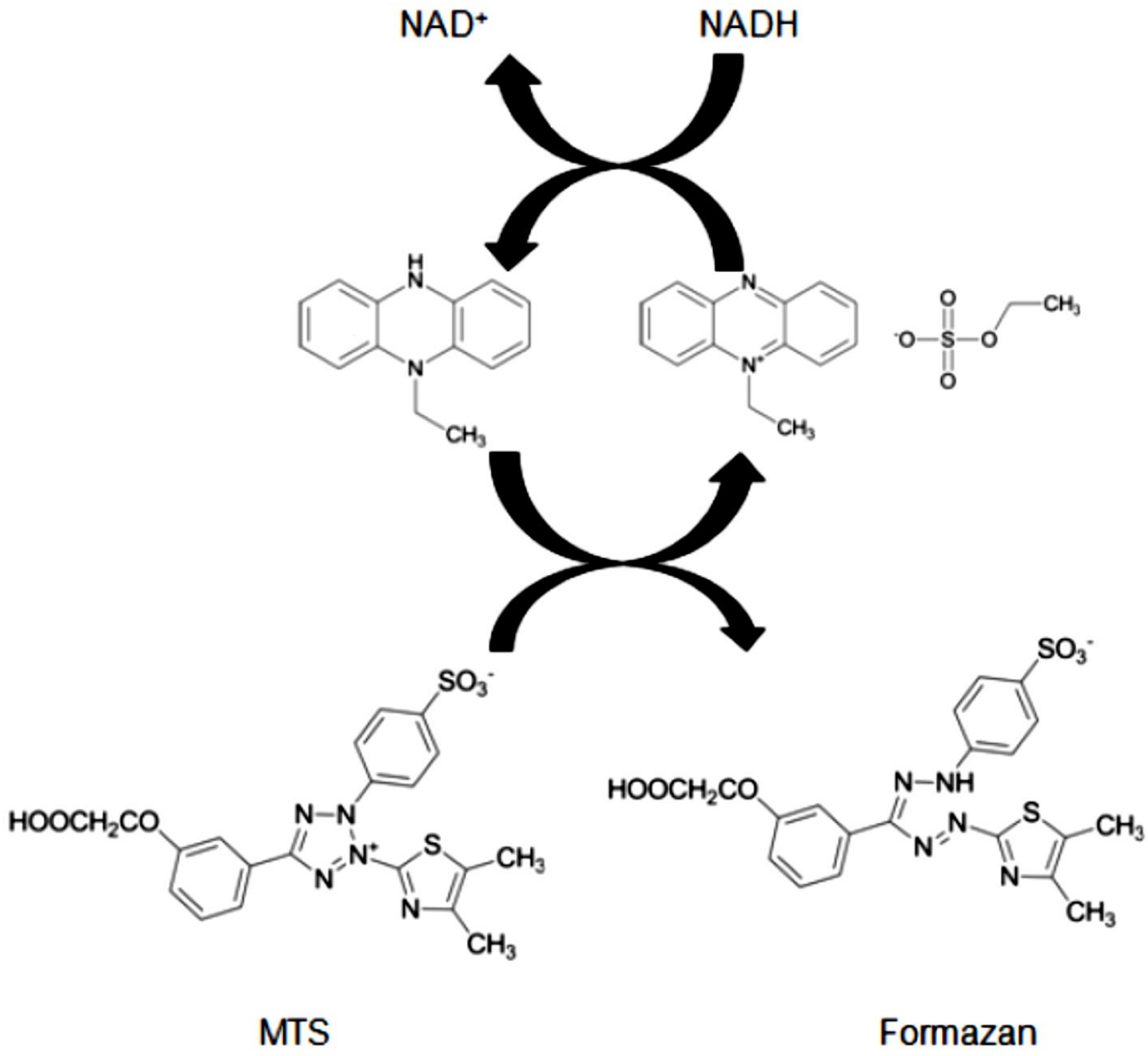

Figure 2-2 The principle of the MTS assay

Figure shows that intermediate reagent accepts the electron from NADH in the cytoplasm of alive cell to activate soluble formazan from MTS dye. The figure was adapted from cell viability assay guideline (Terry L Riss, Published May 1, 2013; Last Update: July 1, 2016.).

2.7.2 MTS dye incubation periods and optical density (OD) interpretation

Once the incubation with drugs was completed, the 20 µl MTS working solution was added to the wells. The working MTS solution was prepared by mixing 2 ml of 2 mg/ml in PBS of MTS solution with 100 µl PMS solution at 0.92 mg/ml concentration in 1X PBS. This was performed in the dark as it is a light sensitive dye. The plate was incubated in the incubator at 37°C for 4 hours. Once the dye has converted the colour to dark brown, the MTS plate was read on the microplate reader (Multiskan Ascent Thermo Labsystems 354, SN: 354-01134), using Ascent software Multiskan. The absorbent values were set at 490 nm in wavelength to detect MTS dye and 690 nm for the 96 well plate background compensation absorbance.

The OD values obtained by measurement at 690 nm (background) were subtracted from 490 nm (sample) reading. The experiment was carried out in triplicate to get the accurate value. Then the average of each treatment is divided by the average value for the control and multiplied by 100. The percentage of growth curve was plotted to observe the trend of cell proliferation and the concentration of the drug that inhibits cell growth.

2.8 Cell Cycle Analysis

2.8.1 Cell preparation for flow cytometry

The cells were plated at 3×10^6 per well and the drug was added at desired concentration. Then cells were incubated at 37°C with 5% CO_2 concentration for 48 hours. Once the incubation period was finished, the cells were transferred to new tubes and were centrifuged at 2,000 rpm for 3 minutes, and then supernatant was discarded. In the next step, the cells were re-suspended in 1 ml cold 1x PBS, transferred to new Eppendorf tube and centrifuged at 2,000 rpm for 3 minutes. Supernatant was discarded and the 500 µl cold ethanol was added to cells before mixing by vortex for approximately 10 seconds. Then, the cells were incubated at 4°C for 30 minutes before the 50 µl of a 100 µg/ml solution of ribonuclease A (RNase A) was added, and then the cells were left at room temperature for 15 minutes. Before using the FACS machine, 300 µl of 50 µg/ml propidium iodide solution was added to the samples and incubated for 15 minutes.

2.8.2 Cell cycle analysis using flow cytometry

Cell cycle analysis by quantifying DNA content was one of the earliest applications of flow cytometry. This analysis is based on the ability to stain the cellular DNA that is directly

proportional to the amount of DNA within the cell. The most common DNA binding dye used to measure DNA is Propidium Iodide (PI), which binds to DNA groove and double stranded RNA. The 10,000 cells were collected and were analysed by flow cytometry. The forward scatter (FSC) and side scatter (SSC) were set to identify single cell. This can be performed by using pulse area and pulse width signals detection which can be set on FACS software. The DNA contents are converted into the signal using PE channel from the software.

Cell division has 2 mainly processes including DNA replication and segregation into two cells. In the interphase, the cell is preparing for DNA synthesis, G1, and then the replication of DNA occurs in S phase followed by G2 phase, respectively (Vermeulen et al., 2003). In this way, cells that are in S phase will present more DNA contents than cells in G1. The cell will absorb proportionally more dye and fluorescent intensity will be higher while the cells in G2 phase will be approximately twice as bright as cell in G1 phase. In healthy cell, SubG1 is not presented in the graph obtained from flow cytometry while in cell death condition, DNA fragments will be stained with PI and were shown in the area before G1 phase, SubG1, during analysis (Figure 2-3).

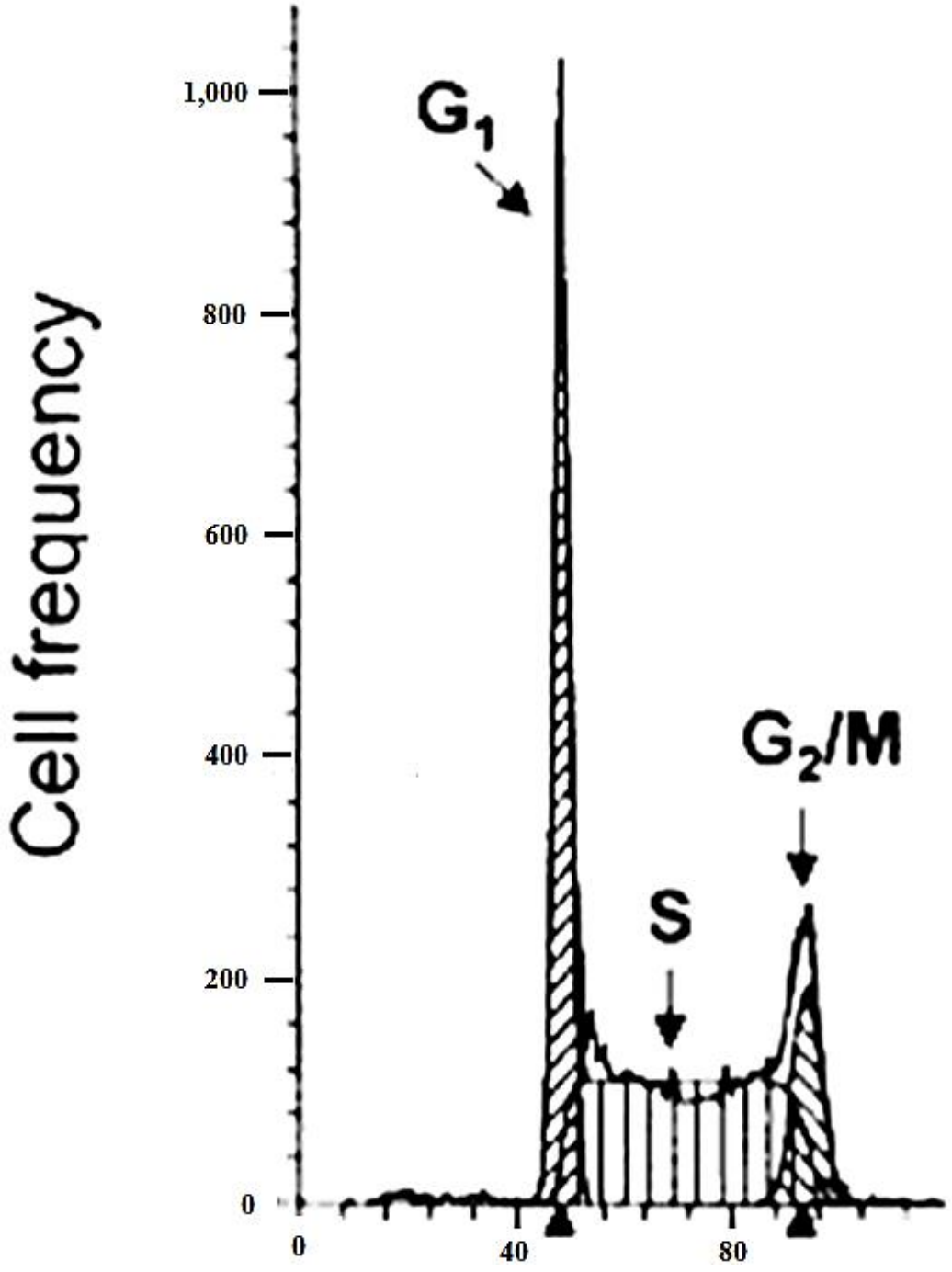

Figure 2-3 Typical DNA content histogram obtained from PI staining method

The figure represents DNA content distribution indicating cell cycle phases including G1, S, G2/M phases (Pozarowski & Darzynkiewicz, 2004).

2.9 Mitochondrial Membrane Potential (MMP) Assay

The principle of this method is based on the dye, JC-1, that has positive molecular charge and passes through the cell membrane and mitochondrial membrane into the matrix of mitochondria. The dye will bind to inner membrane and form aggregated JC-1 that can be detected as red fluorescence signal. In early apoptosis cells, the inner membrane will lose transmembrane potential (negative charge) that the dye will be presented in monomeric form and the green signal can be detected by fluorescence.

2.9.1 Cell preparation for MMP Assay

3×10^6 cells of CEM-C1-15, Molt4 and CEM-C7-14 were seeded in 6 well plates before the combination treatments were applied for 48 hrs. After that, cells were suspended in 1 ml medium or PBS at approximately 1×10^6 cells/ml. 6.25 µl of solution 7 (JC-1 dye, Figure 2-4) was added directly to each sample and incubated 20 minutes at 37°C. The stained cells were centrifuged at 400 g for 5 minutes at room temperature and supernatant was removed completely without disturbing cell pellet. Then, samples were washed twice with 1 ml 1X PBS by pipetting. After centrifuging the sample at 400 g for 5 minutes at room temperature, the pellets were resuspended in 250 µl of solution 8 (DAPI) by pipetting and the samples were analysed immediately by NucleoCounter NC-3000.

2.9.2 MMP Measurement using NucleoCounter NC-3000

8-chamber slide (NC-Slide A8) was used by loading 10 µl of each sample into the chamber of slide and then the loaded slide was placed on the tray of the NucleoCounter NC-3000. Using image analysis, the NC-3000 software was used to analyse the different form of cationic JC-1 dye (5, 5, 6, 6-tetracholo-1, 1, 3, 3-tetraethylbenzimidazol-carbocyanine iodide) since this dye can be detected as green and red fluorescence intensity according to mitochondrial membrane potential voltage. The mitochondrial probe, JC-1, has a positive charge while the intact inner mitochondria contains negative charge. In case of disruption of mitochondrial membrane potential or loss of the mitochondrial membrane potential such as apoptosis, JC-1 localizes to the cytoplasm in its monomeric green fluorescence form that has an emission wavelength of 529 nm. In the case of healthy cell, the dye becomes aggregated red fluorescent form which can emit the fluorescence at 590 nm (Chazotte, 2011). The red/green fluorescence intensity ratio was determined by NC-3000 software where decreasing of red/green ratio refers as apoptosis. Example is shown in the Figure 2-5.

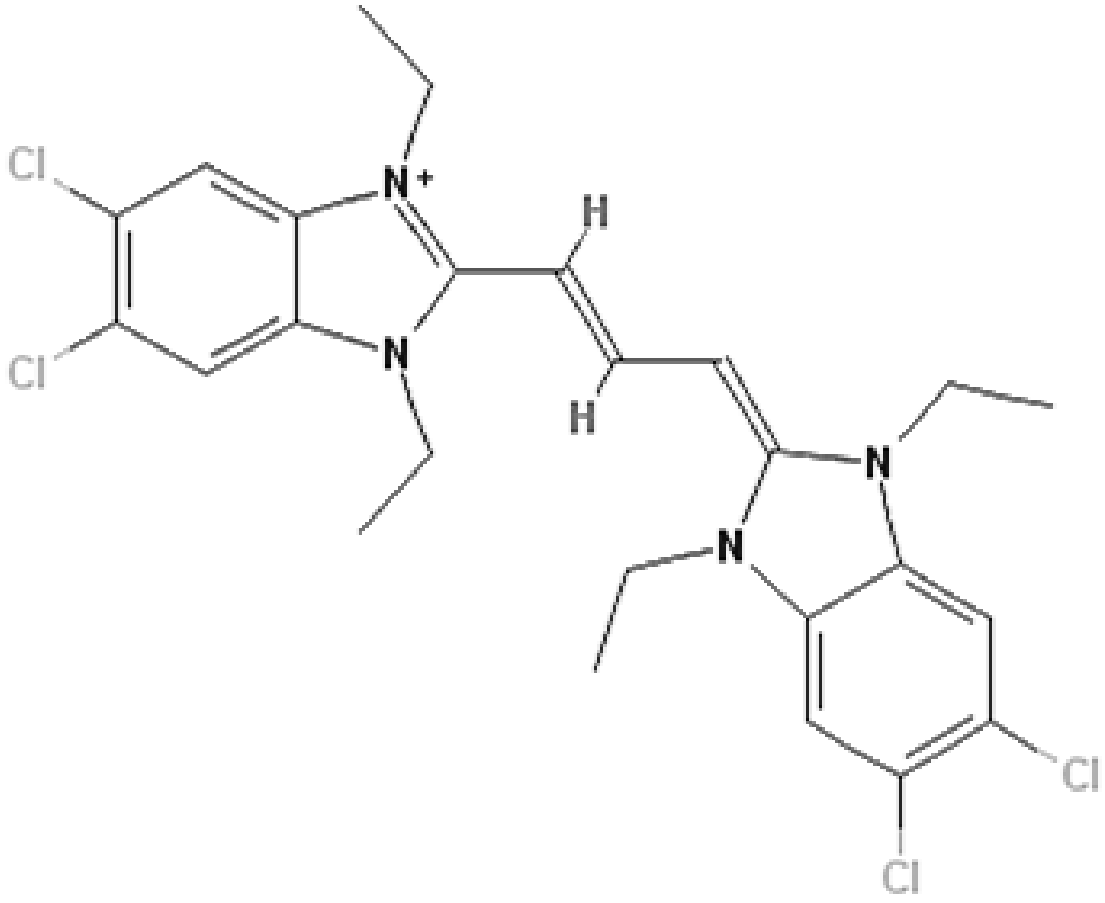

Figure 2-4 Chemical structure of JC-1 dye using in MMP Assay

The figure was adapted from PubChem website with compound CID 5492929 (https://pubchem.ncbi.nlm.nih.gov/image/fl.html?cid=5492929)

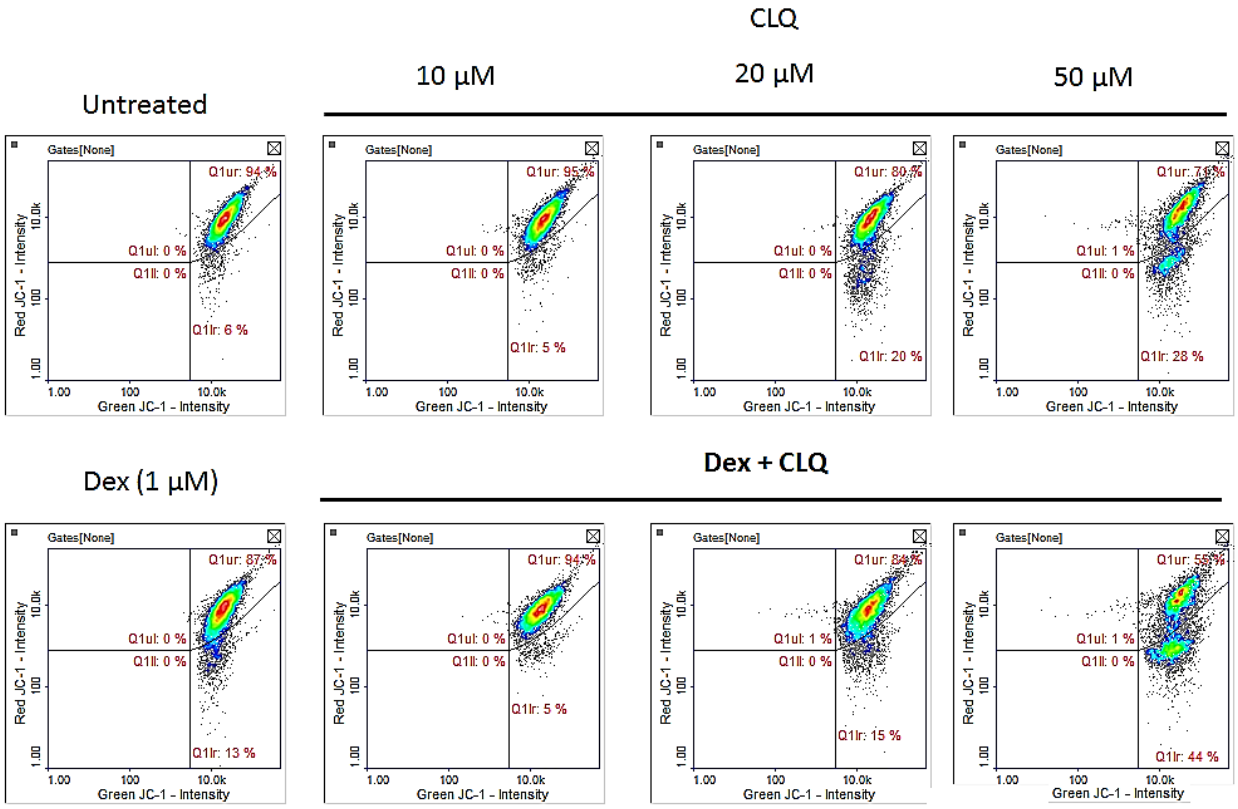

Figure 2-5 Figure is the sample showing the ratio of red/green fluorescent intensity profiles and percent of cell death in chloroquine treated CEM-C1-15

The figures showed the fluorescent signal of healthy cells in the upper right quadrant (QUR) and cell death in lower right quadrant (QLR) presenting in each condition including untreated, 1 µM Dex, 10, 20, 50 µM CLQ and combined Dex with 10, 20, 50 µM CLQ, respectively.

2.10 Reactive Oxygen Species (ROS) Assay

ROS production levels play an important role in the cell signalling pathways such as apoptosis, gene expression and cell signalling cascades activation (Hancock et al., 2001). In this study, Carboxy-H2DCADA (Invitrogen C400) probe was used to detect total reactive oxygen species generated in leukemic cells treated with various drugs (Figure 2-6). The probe containing 2′, 7′-dichlorofluorescein (DCF) and calcein is non-fluorescent compound until the acetate groups are removed by intracellular esterase and oxidation occurs inside the cell. This oxidation process can be detected by determination of the increase in fluorescent signal with flow cytometer using excitation sources and filters for FITC channel (excitation wavelength 520 nm, emission wavelength 488 nm).

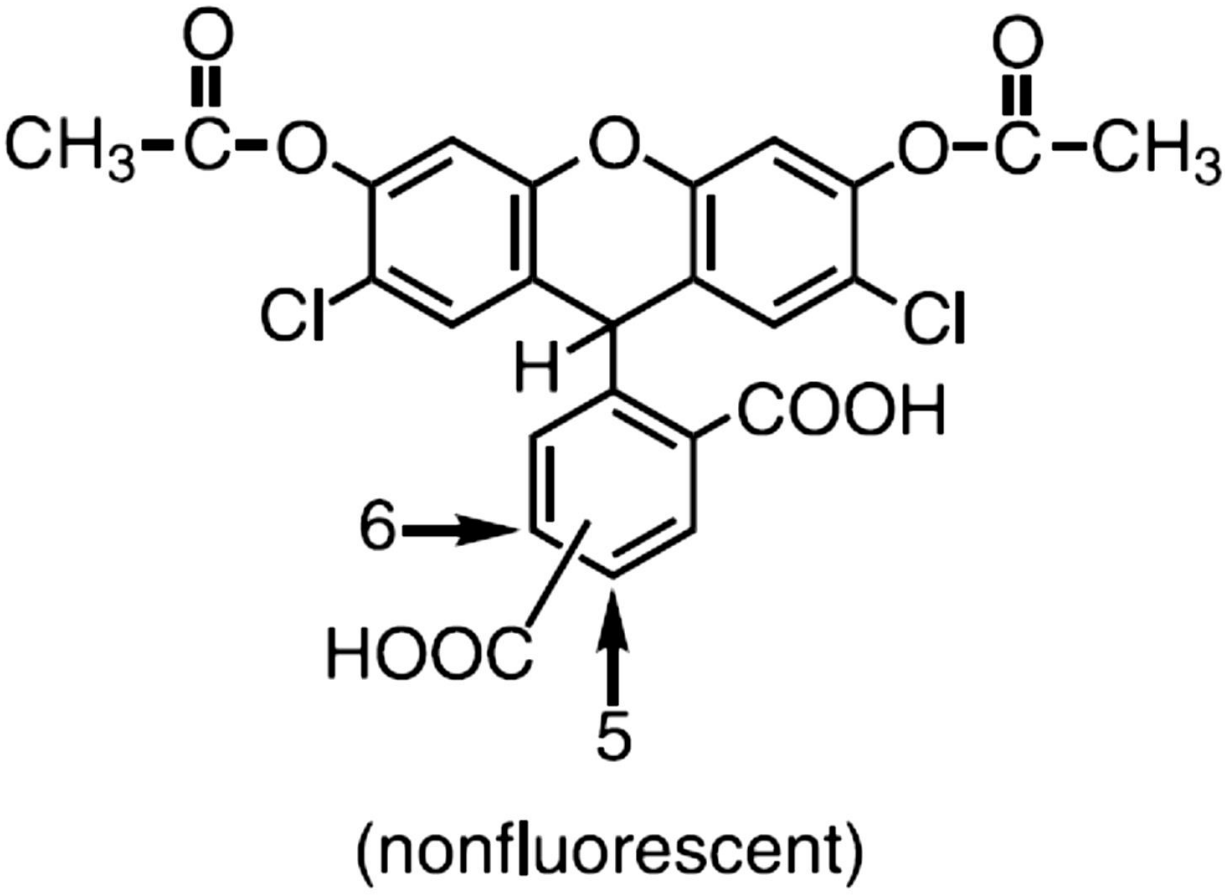

Figure 2-6 The structure of carboxy-H2DCFDA molecular probe

The figure was adapted from Invitrogen Reactive Oxygen Species (ROS) Detection Reagents Kit Manual Protocol. (https://assets.thermofisher.com/TFS-Assets/LSG/manuals/mp36103.pdf)

2.10.1 Cell preparation for ROS Assay

3× 10^6 cells of CEM-C1-15, Molt4 and CEM-C7-14 were seeded in 6 well plates before the combination treatments were applied using desired drug concentration and 24 hrs incubation time point. After the incubation periods, the cells were transferred into new 15 ml centrifuge tube to collect the cell suspension. The tubes were centrifuged at 2,000 RPM for 3 minutes before supernatant was discarded. 1 ml cold 1X PBS was used to re-suspend cell pellets and then transferred all pellets into new Eppendorf tubes and centrifuged again at 2,000 RPM for 3 minutes at 4°C for pellet collecting. Before adding 100 µl of working carboxy-H2DCFDA dye to the pellets, 100 mM stock dye was diluted into 100 µM working dye by

adding 2 µl of stock dye into 2 ml 1X PBS. After re-suspending the pellets, the cells were incubated for 30 – 60 minutes at 37°C with 5% CO_2 in the dark. Then, the dye was discarded by centrifuging the pellets at 2,000 RPM for 3 minutes. The cells were washed by cold PBS for 1 ml and the pellets were collected before 1 ml cold PBS was used to resuspend the cells. The cells were then analysed by flow cytometry using FITC channel.

2.10.2 ROS Assay analysis using flow cytometer

This analysis is based on the intensity of the fluorescent signal emitted from the dye inside the cells containing ROS products. The 10,000 cells were collected and were analysed by flow cytometry. The forward scatter (FSC) and side scatter (SSC) were set to identify cell population. The appropriate filter FITC channel was selected to determine the fluorescent signal intensity. The FITC-A signal was collected by using geo-mean (the signal obtained at the peak of the intensity graph) and was analysed by Excel program to interpret the total ROS production in the cell during desired treated conditions comparing to untreated.

2.11 Protein Expression Analysis

2.11.1 Protein extracts preparation

CEM-C1-15, Molt4 and CEM-C7-14 were counted by using haemocytometer and approximately 2×10^6 cells/ml were split into each 6 wells plate containing DCC-FCS RPMI medium. The cells were treated without/with combination treatment of 1µM Dexamethasone and other drugs that related to inhibition of autophagolysosome formation (Chloroquine), ER stress inducer (Thapsigargin and Rotenone) and proteasome inhibitor (Bortezomib) in different concentration. Then, cells were incubated at 37°C with 5% CO_2 for 48 hours to allow the drug taking their effects. Then the cells were transferred to new centrifuge tubes and spun at 2,000 rpm for 3 minutes. Supernatants were discarded and re-suspended with 1 ml cold 1x PBS before transfer of the cells to new eppendorf tube and centrifuged to discard supernatant. Radio-Immunoprecipitation Assay Buffer (RIPA buffer) was added into harvested cells for 100 µl and re-suspended completely as the buffer solubilized wide range of proteins including cytoplasmic proteins, nuclear proteins and membrane bounded proteins (Ngoka, 2008). Then, lysates were incubated 20 minutes at 4°C on a rotating platform on ice, followed by centrifugation at 13,000 rpm for 15 minutes at 4°C. Supernatant was transferred to a new Eppendorf tube without disturbing the cell lysate that placed on ice to preserve protein lysate. The protein concentration

was measured by using spectrophotometer at the wavelength absorbance 595 nm followed by Bradford assay.

Bradford assay is a colorimetric assay measuring protein concentration using Bio-Rad protein assay reagent. The working solution was prepared as 800 µl distilled water and 200 µl Bradford reagent (Bio-Rad) and 2 µl of protein extracted sample. The mixed solutions were added in a semi-micro cuvettes (VWR) and mixed gently by using parafilm to cover top of cuvette and inverted all cuvettes to avoid air bubbles. 2 µl RIPA buffer was used as blank to calibrate the spectrophotometer. The protein samples were duplicated for each extract for a good practice and an average value used. Samples were incubated at room temperature for 5 minutes and then the protein concentration was determined the absorbance at 595 nm wavelength.

Following this step, each protein concentration was calculated following protein standard curve as protein concentration references and 3x SDS loading buffer was added as half volume of protein sample to denature secondary and tertiary protein structures. To making the protein standard curve, Bovine Serum Albumin (BSA) was dissolved in RIPA buffer to make various desired concentration tubes from 0.5 µg/µl to 5 µg/µ. The absorbance at 595 nm wavelength in each tube was measured according and the regression equation was used to calculate protein concentration.

2.11.2 Protein separation by SDS-PAGE

Sodium dodecyl sulphate-polyacrylamide gel electrophoresis (SDS-PAGE) is a technique used to separate protein according to size in an electric field. SDS is an anionic detergent, which denatures the proteins by covering around the polypeptide backbone resulting in the protein becoming negatively charged and moving towards the positive electrode in an electric field according to the polypeptide mass. 10% resoling gel was prepared and the gel casting apparatus (Mini-Protean 3 Bio-Rad, UK) was set up according to manufacturer's instruction. The gel was placed into electrophoresis tank (Bio-Rad) and then the tank was filled with 1x SDS running buffer. Before loading samples into the wells, the comb was removed and samples were boiled at 95°C for 5 minutes using hotplate. 5 µl of Protein molecular weight marker (PageRuler™ Prestained Protein Ladder) and 40 µg of total protein samples were loaded onto the well using a Hamilton microliter syringe or 2 µl pipette tip. The gel was run for

20 minutes at 80V then at 110V for 95 minutes or until the samples nearly reached the end of the gel.

2.11.3 SDS-PAGE preparation

Table 9 List of reagents used in 10% and 12% resolving gels preparation

This table showes components for resolving part of SDS-PAGE preparation used in this study

Reagents	10% Resolving gel	12% Resolving gel
30% (w/v) Acrylamide-bisacylamide	9.33 ml	11.2 ml
1.5M Tris-HCl (pH 8.95)	7 ml	7 ml
10% SDS	0.28 ml	0.28 ml
0.2M EDTA	0.28 ml	0.28 ml
10% Ammonium persulfate	157 µl	157 µl
Distilled water	10.74 ml	9.7 ml
TEMED	17 µl	17 µl

These solutions were mixed and loaded into a protein gel casting apparatus (Mini-PROTEAN 3 Bio-Rad, UK) which was set up according to manufacturer's instruction. The 0.1%SDS solution was added on surface of gel protecting gel oxidation and was poured off when gel was completely set for 30-45 minutes.

Table 10 List of reagents used in stacking gel preparation

This table provided the reagents used to prepare stacking part of SDS-PAGE

Reagents	Stacking gel
30% (w/v) Acrylamide-bisacylamide	1.67 ml
1M Tris-HCl (pH 6.95)	1.25 ml
10% SDS	100 µl
0.2M EDTA	100 µl
10% Ammonium persulfate	157 µl
Distilled water	6.73 ml
TEMED	17 µl

These solutions were mixed and poured on the surface of resolving gel and the 10 wells comb was placed immediately. Gel was completely set after 30-45 minutes.

2.11.4 Western blotting and detection of proteins

Western blot is used to detect the specific protein in a mixture by adding specific antibodies against a desired protein. Basically, primary antibody binds to the target protein and secondary antibody, which is labelled with a fluorescent probe detected by light detection, which binds to the primary antibody.

Before transferring protein from the gel to membrane, a sandwich of filter paper, gel, polyvinylidene difluoride (PVDF) membrane (Millipore, UK) and one more layer of filter paper were prepared in a cassette, which was placed between electrodes immersed in 1x SDS transfer buffer. The membrane was soaked in methanol for 30 seconds and the filter paper in 1x SDS-PAGE transfer buffer before placing in the cassette. The set of cassette and icebox were placed in the tank with 1x SDS-PAGE transfer buffer and stirrer bar was used to keep buffer and membrane cool. The transferring was set for 2 hour at 0.4 amps and ice was changed after an hour of running. Next, membrane was blocked with 5% skimmed milk in 1x PBS for an hour to prevent the nonspecific binding. After blocking, the nitrocellulose membrane was incubated with a primary antibody (dilution at 1:1,000 – 1:2,000) in 2.5% skimmed milk /1x PBS / 0.1%

Tween on a rocking platform overnight at 4°C. Next day, the membrane was washed 3 times with 1x PBS / Tween (0.1%) buffer for 10 minutes interval. Then, the membrane was incubated with Horse Radish Peroxidase (HRP) conjugated secondary antibody (antibody dilution 1:5,000) dissolved in 10 ml of 2.5% skimmed milk /1x PBS / Tween (0.1%) and washed 3 times again with 1x PBS / Tween (0.1%) buffer for 10 minutes interval. Protein bands were visualized by incubating PVDF membrane with Supersignal West Pico or West Femto Chemiluminescent substrates and the protein bands were captured on film using x-ray developer in the dark room.

The intensity of protein bands was analysed using ImageJ software. Then the % of intensity was compared to the control condition to determine the effect of drugs on ALL cell lines.

2.11.5 Membrane stripping

The membrane can be re-probed multiple times before it is subjected to another desired antibody by stripping the membrane. This method unbinds of the first primary antibody and allows the other primary antibody to bind specific protein on the membrane. To strip the blot, 10 ml of 10% SDS solution was added into universal tube following 3.2 ml of 1M Tris pH 6.95 and distilled water was added up to 50 ml. Under chemical hood, 2-mercaptoethanol was added and mixed by inverting the tube before placing the tube in the 50°C water bath for 30 minutes. Solution was discarded under hood and PBS / 0.1% Tween was used to wash the membrane 3 times and the membrane blocking process was carried out as normal.

Primary and secondary antibodies can be gently removed from PVDF membrane by using re-blot plus mild stripping buffer. Before stripping the blot, stripping solution was diluted by adding 18 ml distilled water into 2 ml of 10X re-blot solution (Merck Millipore, catalog number 2502). Then, membrane was placed into plastic tray with appropriate amount of 1X stripping solution. 15-20 minutes of incubation time of stripping processes was applied into membrane on the rotor machine. Normal blocking procedure using 5% skimmed milk in 1X PBS was done for 1 hour. After blocking, the blot was ready for reprobing with desired antibodies.

2.12 Quantitative reverse transcription polymerase chain reaction (RT-qPCR)

RT-qPCR is the method used to determine gene expression profiling starting with RNA. Real time PCR technique is a sensitive method for detection and quantification nucleic acids.

The fluorescent DNA binding dye, SYBR® Green I, was used in this study. Generally, SYBR® Green I dye will bind to double-strand DNA only and after binding has occurred, the dye will emit fluorescence signal and the intensity that correlates with amplified DNA will be detected by Rotor-Gene® Q. Three essential steps of this technique are total RNA isolation, conversion of total RNA to cDNA by reverse transcriptase enzyme and finally quantitative real time polymerase chain reaction (Peirson & Butler, 2007). The result obtained from experiment was analysed and compared using linear phase of exponential graph before it reached the plateau phase.

2.12.1 Cell preparation for total RNA isolation

CEM-C1-15, Molt4 and CEM-C7-14 were counted by using haemocytometer (C-Chip) and approximately 2×10^6 cells/ ml were seeded into 6 wells plate containing 3 ml of DCC-FCS RPMI medium. The cells were treated without / with combination treatment of 1μM Dexamethasone with other drugs using maximal dose including 10 μM thapsigargin, 5 nM bortezomib. Then, cells were incubated at 37°C with 5% CO_2 for 24 hours to allow the drug taking their effects.

2.12.2 Total RNA isolation and purification

After the incubation periods, the cells were transferred to new sterile Eppendorf tubes and then pellets were harvested by centrifugation at 2,000 RPM for 3 minutes. Pellets were resuspended by adding 200 µl sterile 1X PBS followed by adding 400 µl Lysis/Binding Buffer and then the cells were vortexed for 15 seconds. The pellets were transferred to a high pure filter tubes (Roche® High Pure RNA Isolation Kit) and the cell lysates were collected by centrifuging the tube at 8,000 ×g for 15 seconds. After discarding the flowthrough, 100 µl DNase I mixed buffer (90 µl DNase I incubation buffer and 10 µl DNase I) was added on the each filter membrane and the membrane was incubated for 15 minutes at room temperature to allow the enzyme DNase to eliminate genomic DNA on the membrane. Once the incubation time has been finished, 500 µl Wash Buffer I was added to the filter tube and then the tube was centrifuged at 8,000 ×g for 15 seconds. After the flowthrough was discarded, 500 µl of Wash Buffer II was added to the filter tube before the flowthrough was discarded again by centrifuging the tube at 8,000 ×g for 15 seconds. Additionally, washing step was applied by adding 200 µl Wash Buffer II into the filter tube and centrifuged again at maximum speed (approx. 13,000 ×g) for 2 minutes to remove any residual washing buffer. Then, the filter tube

was inserted into clean, sterile 1.5 ml micro-centrifuge tube before 50 µl of Elution Buffer was added into the centre of filter membrane. The tube was centrifuged for 1 minute at 8,000 ×g to collect the purified total RNA that can be used directly in reverse transcription process (Roche Diagnostics GmbH, High Pure RNA Isolation Manual Leaflet). The concentration and purity of the total RNA were measured by using ThermoScientific NanoDrop™ machine.

2.12.3 Total RNA conversion to cDNA by reverse transcription method

Before adding 1 µg of total RNA into the reaction tube, total RNA stock solution was diluted to 1 µg by adding Nuclease-free water up to 10 µl of total volume. In this study, High-Capacity RNA-to-cDNA™ Kit was used to create cDNA strand. The RT mixture including 2X RT Buffer mix, 20X RT Enzyme mix and Nuclease-free H_2O were prepared following product information sheet guideline. 9 µl of total RNA sample was added into RT master mixed reaction tube to fill up total volume 20 µl in each reaction tube the RT reaction tubes were kept on ice at all times until next step was performed. After sealing the tube with caps, the RT tube was briefly centrifuged to spin down the sample and to eliminate any air bubbles. The reaction tube was loaded to the PCR machine and sample tube was incubated at 37°C for 60 minutes followed by heating the sample at 95°C for 5 minutes and holding the sample at 4°C until the RT tubes were collected. After finishing the cycle, the cDNA was ready for real time PCR application or long-term storage in the freezer (-20°C).

2.12.4 Quantitative real time polymerase chain reaction assay

Before the cDNA sample was added into the tube containing qPCR mixture, the primers used in this experiment were reconstituted by adding desired nuclease-free water to make 100 µM stock solution tube. The working primer sample was prepared by diluting the stock primer with nuclease-free water to make 10 µM. The SensiFAST SYBR® No-ROX Kit was used to determine the amount of cDNA template. The master mix qPCR tube was prepared by mixing 10 µl of 2X SensiFAST SYBR® with 0.8 µl forward primer, 0.8 µl reverse primer, 2 µl cDNA template and 6.4 µl nuclease-free water to make 20 µl reaction tube. Then, the duplicated reactions were loaded into Qiagen Rotor-Gene Q Centrifuge machine. The qPCR thermal cycle parameters were set according to the company leaflet guideline (cycle 1: 95°C 2 minutes, Cycles 2 – 40: 95°C 5 seconds for denaturation step, 60°C 15 seconds for annealing / extension steps). After the reaction reached completion, the melting curve analysis has been done before the threshold cycle was collected and was analysed. At the end of processes,

amplification plot where the x-axis represents the PCR cycle and y-axis is the fluorescence signal of the amplified cDNA was selected the appropriate fluorescence threshold. At this point, threshold cycle (*Ct*) was determined to further analysis.

2.13 Computer programs

2.13.1 Multiskan ascent software for ascent multiskan microplate reader

Multiskan Ascent Software is the software to determine the colour intensity by using the filter to detect the optical density (OD) or an absorbent at 490 nm and 690 nm wavelength. The 96 well plate was used in this method and MTS dye was used to determine alive cell metabolism.

2.13.2 ImageJ software

ImageJ is the free analysis software, which can be downloaded from the website: http://imagej.nih.gov/ij/download.html. It can be used to measure and to compare the density of scanned picture or x-ray protein band from western blot technique. The suitable x-ray film for this software should be transparency film. ImageJ is the semi-quantitative tool and the selected area obtained from the experimental result can lead to different values so the average value of three independent choices of scanned area was calculated before a statistical test programs.

2.13.3 BD FACSuite

The BD FACSuite is the software which was used with flow cytometry machine (BD FACSVerse^{TM}). This software has been used to analyse the cell cycle of CEM-C1-15, CEM-C7-14 cell lines and Molt4 cell after treating with drugs and it can also be applied to analyse autophagic cell activities, cell death and apoptosis events.

2.13.4 NucleoView NC-3000

The NucleoView NC-3000 is the software which was used to analyse mitochondrial membrane potential assay that detects the change of mitochondrial membrane voltage between inner and outer layers after drug treatment. Results obtained from this software can be applied to analyse early apoptosis and late apoptosis events.

2.13.5 Rotor-Gene Q series software

To determine mRNA expression level, quantitative reverse transcription polymerase chain reaction (RT-qPCR) was used in this study. The software called Rotor-Gene® Q series which was installed in Rotor Gene Machine was used to determine the threshold cycle (*Ct* value). All results obtained from experiments were further analysed in excel.

2.14 Statistical analysis

Mean ± standard error of the mean (SEM) of the quantitative data from at least three independent experiments were calculated and displayed as error bars in bar charts. Statistical analysis was conducted by using Graph-Pad Prism Software. The difference in experimental data was analysed by student *t.test* when comparing to untreated group to obtain *p-value*. Less of equal to 0.05 *p-value* was considered statistically significant.

CHAPTER 3 CELL VIABILITY ASSAYS

3.1 Introduction to cell viability assay

The inhibition of lymphoid cells growth by steroid hormones, glucocorticoids, has been found to be important for treatment of haematological malignancies and lympho-proliferative diseases (Claman, 1972; Goldin et al., 1971). However, important problem of glucocorticoid usage is the occurrence of side effects and the drug resistance to the treatment. The combination treatment with other drug compounds is the potential way to increase the successful therapy in patients.

The purpose of this set of experiments was to determine the optimal dose and duration for cytotoxic effect of glucocorticoid and other drugs including Chloroquine (inhibits autophagy), Thapsigargin (causes ER stress), Rotenone (increases ROS) and Bortezomib (inhibits proteasome and causes ER stress and unfolded protein response) treatments in order to maximize cytotoxic effects on leukemic cells (CEM-C1-15, CEM-C7-14 and Molt4).

3.2 Determination cytotoxic effect of individual and combined drugs treatment on leukemia cells using MTS assay

To determine the optimal dose and incubation time period of chemotherapeutic agents as mentioned above, MTS assay was performed after 24 hrs and 48 hrs treatment with glucocorticoid alone or in combination conditions.

3.2.1 Cell viability of leukemia cells treated with Dexamethasone and Chloroquine

The synthetic steroid compound, Dexamethasone (Dex), and anti-malarial drug, Chloroquine (CLQ), which also has the autophagic flux inhibition effect were tested to determine the concentration and incubation period needed to inhibit cell proliferation and to induce cell death. The most effective doses obtained from Dexamethasone treated alone, chloroquine treated alone and combination treated conditions were chosen to treat the cells throughout the study.

CEM-C1-15, CEM-C7-14 and Molt4 cells were treated with Dexamethasone using wide range of concentrations between 0.15625 µM and 10 µM. The doses of Chloroquine (CLQ) used in this test were between 1.5625 µM and 100 µM (Ramakrishnan &

Houston, 1984; Verras et al., 2015). Cells were treated for 24 hrs and 48 hrs to determine optimal time to allow drugs taking their effects. The results obtained using 24 hrs treatment showed that Dex did not substantially inhibit cell proliferation in CEM-C1-15 cells with CEM-C7-14 and Molt4 showing greater Dex sensitivity respectively. However, no Dex concentration showed inhibition greater than 50% in all three cell lines tested (Figure 3-1 A-C, full black line). CLQ treated alone decreased cell proliferation in CEM-C1-15, CEM-C7-14 and Molt4 cell lines (Figure 3-1, A-C, grey line). The concentrations that inhibited CEM-C1-15 and CEM-C7-14 cell growths at 50% (IC_{50}) were calculated for each cell line (38.5 µM and 37.7 µM, respectively) (Table 11). The IC_{50} was calculated using *CompuSyn* software which is the point where straight line passes through the y-axis at 50% cell viability and x-axis when the drug concentrations were represented as logarithm value.

To analyse the effect of combination drug treatment, Combination index (CI) was considered, where CI<1, =1 and >1 indicates synergism, additive effect and antagonism, respectively (Zhang, N. et al., 2016). The combination treatment showed synergistic effect in CEM-C1-15 in all combinations of drugs concentration (Table 12 A), CEM-C7-14 in all combination treatments except the maximal dose of Dex and CLQ (Table 14 A), and in Molt4 (Table 16 A) with Dex concentration greater than 1.25 µM and CLQ dose above 12.5 µM (Figure 3-1, A-C, black dashed line).

At 48 hrs incubation time, Dexamethasone decreased the percent of cell death in CEM-C1-15 and Molt4 cells but the greater effect was observed in CEM-C7-14. CLQ alone inhibited the CEM-C1-15, CEM-C7-14 and Molt4 proliferations with IC_{50} at 22.0, 21.7 and 35.1 µM, respectively. Cytotoxic effects increased when combination treatments were applied (Figure 3-1, D-F, black dashed line). In CEM-C1-15, the synergistic effects were observed in several combination treatments except in minimal dose treatment with 0.3125 µM of Dex and 3.125 µM of CLQ (Table 13 A). Synergistic effect were also observed in CEM-C7-14 at all combined treatments excluding maximal doses (10 µM of Dex with 100 µM of CLQ) (Table 15 A) while this effects in Molt4 were observed if Dex concentration was above 1.25 µM and CLQ concentration is higher than 12.5 µM (Table 17 A).

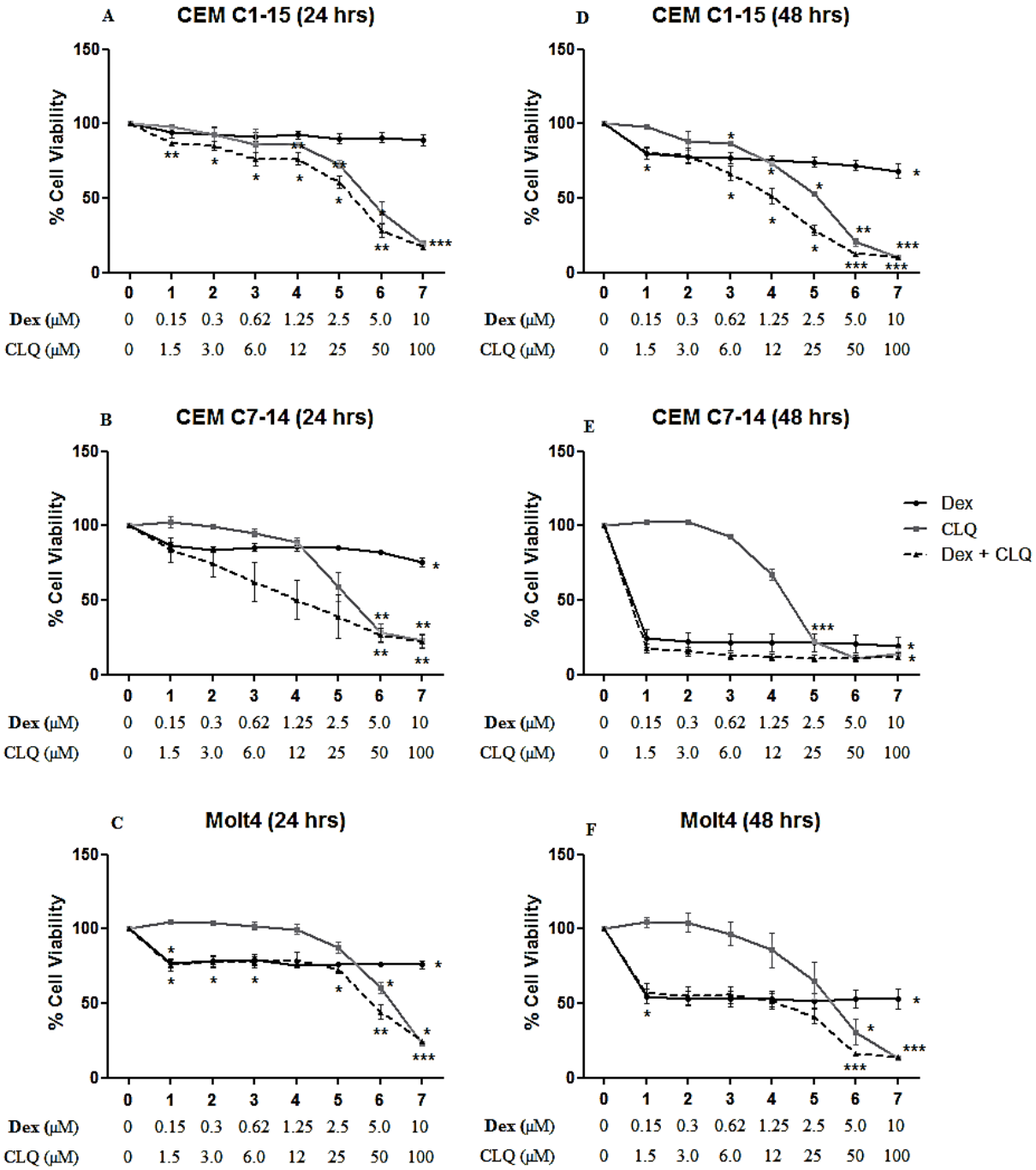

Figure 3-1 Cytotoxicity curves of CEM-C1-15, CEM-C7-14 and Molt4 cells treated with Dexamethasone and Chloroquine

Cells were treated with different concentrations of Dex alone (black line), CLQ alone (grey line) and combination (black dashed line) for 24 hrs (A to C) and 48 hrs (D to F). Cell viability was determined using MTS assay and data expressed relative to untreated sample. The results are representative of 3 independent experiments. Error bars represent ± SEM (* $p < 0.05$, ** $p < 0.01$, *** $p < 0.001$, *student t.test*). Each sample was compared to untreated control.

3.2.2 Cell viability of leukemia cells treated with Dexamethasone and Thapsigargin

CEM-C1-15, CEM-C7-14 and Molt4 cells were treated with Dexamethasone and thapsigargin to investigate the role of ER stress in glucocorticoid signalling. Dex was used at increasing concentrations from 0.15625 µM to 10 µM. The doses of Thapsigargin (TG) used in this test were between 0.3125 µM and 20 µM (Krysov et al., 2014; Rosati et al., 2010) and cells were treated for 24 hrs and 48 hrs. The results showed that 24 hrs treatment with Thapsigargin alone decreased the cell viability in all three cell lines in a dose dependent manner (cell viability was between 1% and 48%). However, no single drug treatment inhibited cell proliferation more than 50% when cells were treated for 24 hrs (Figure 3-2, A-C). The combination treatment with Dexamethasone and Thapsigargin exerted cytotoxic effect in CEM-C7-14 with CI value less than 1 in all combined conditions indicating synergistic effect (Table 14 B), while synergistic effects fluctuated in CEM-C1-15 and Molt4 cells (Tables 12 B and 16 B).

After 48 hrs incubation time, Thapsigargin treatments significantly increased the cell proliferation inhibition in all cell lines. Dex also decreased cell viability in resistant cell and Molt4 while CEM-C7-14 were highly inhibited by Dex with minimal dose used.

Additionally, combination treatments enhanced cytotoxicity effects in three cell lines when compared to the single drug treatment (Figure 3-2, D-F). IC_{50} which was calculated for Thapsigargin treatment in CEM-C1-15, CEM-C7-14 cells was 1.99 µM and 4.27 µM respectively, while IC_{50} was very low calculated from Molt4 (0.06 nM). The combination index showed synergistic effects in CEM-C1-15 and CEM-C7-14 at all concentrations, while drug antagonism was observed in Molt4 if the Dex and TG concentration was more than 0.625 µM and 1.25 µM, respectively (CI>1) (Tables 13 B, 15 B and 17 B).

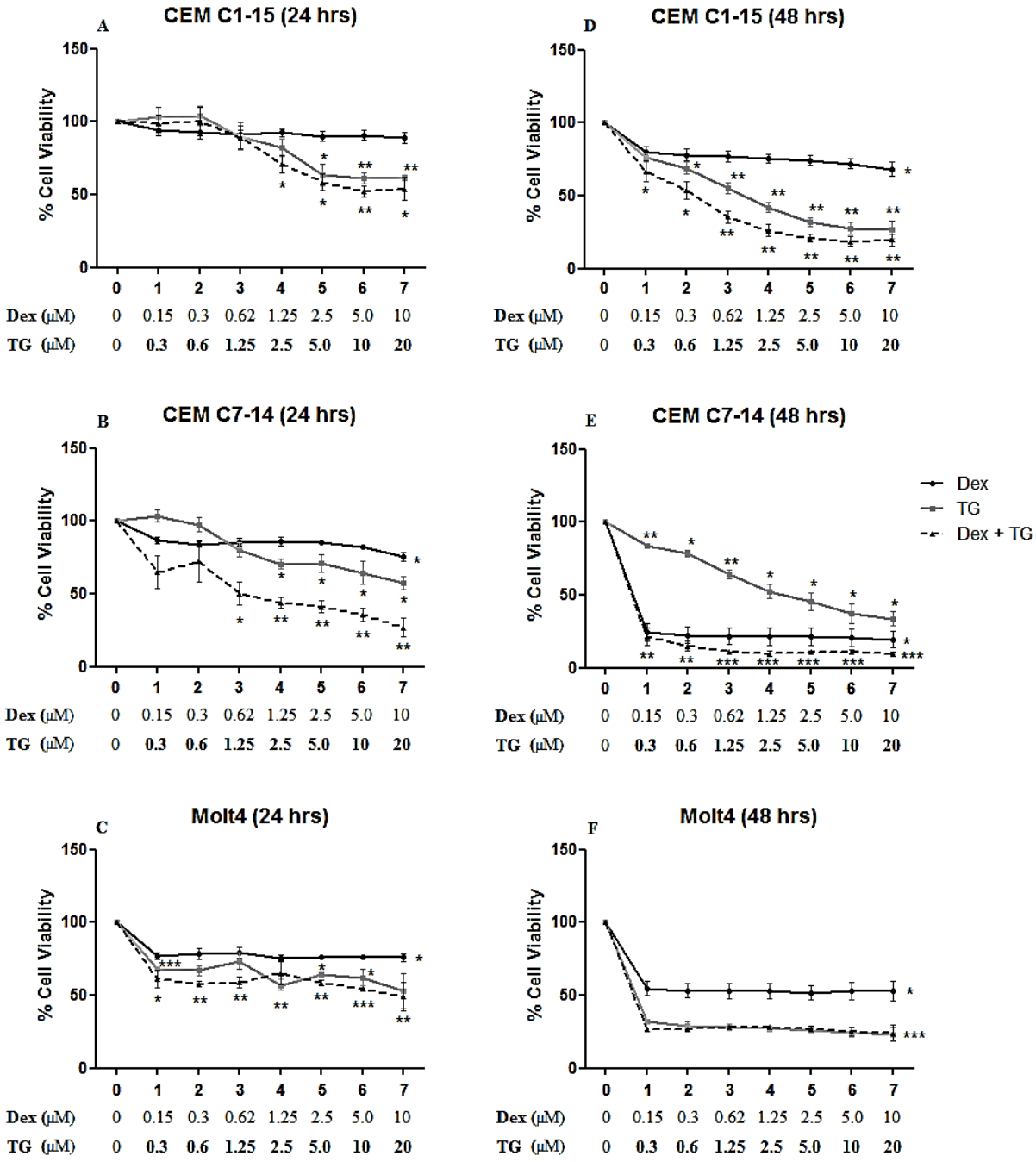

Figure 3-2 Cytotoxicity curves of CEM-C1-15, CEM-C7-14 and Molt4 cells treated with Dexamethasone and Thapsigargin

Cells were treated with different concentrations of Dex alone (black line), TG alone (grey line) and combination (black dashed line) for 24 hrs (A to C) and 48 hrs (D to F). Cell viability was determined using MTS assay and data expressed relative to untreated sample. The results are representative of 3 independent experiments. Error bars represent ± SEM (* $p < 0.05$, ** $p < 0.01$, *** $p < 0.001$, *student t.test*). Each sample was compared to untreated control.

3.2.3 Cell viability of leukemia cells treated with Dexamethasone and Rotenone

CEM-C1-15, CEM-C7-14 and Molt4 cells were treated with Dexamethasone with concentrations mentioned above and with Rotenone to analyse the role of ROS in glucocorticoid receptor function. The doses of Rotenone (ROT) used in this test were between 0.3125 µM and 20 µM (Roedding et al., 2012; Velez et al., 2016) and the samples were analysed after 24 hrs and 48 hrs. The results showed that 24 hrs treatment with Rotenone alone did not substantially inhibit cell proliferation in Molt4 cell with CEM-C1-15 and CEM-C7-14 showing greater Dex sensitivity respectively (Figure 3-3, A-C). However, IC_{50} for Rotenone was calculated in CEM-C7-14 at 16.61 µM (Table 11). The combination treatment showed synergistic effect observed in CEM-C1-15 and CEM-C7-14 at all concentrations (CI<1) (Tables 12 C and 14 C).

In 48 hrs of incubation time, Rotenone treatment alone showed significant cell growth inhibition in all cell lines more than 50%, especially in CEM-C1-15 (Figure 3-3, D-F). The IC_{50} values for Rotenone in CEM-C1-15, CEM-C7-14 and Molt4 cells were 0.10 µM, 0.47 µM and 0.68 µM, respectively.

The combination treatments enhanced the cytotoxicity effects on three cell lines when compared to the single drug treatment. The synergistic effect has been indicated by the combination index calculated from *CompuSyn* software with CI<1 at all combined doses (Tables 13 C, 15 C and 17 C).

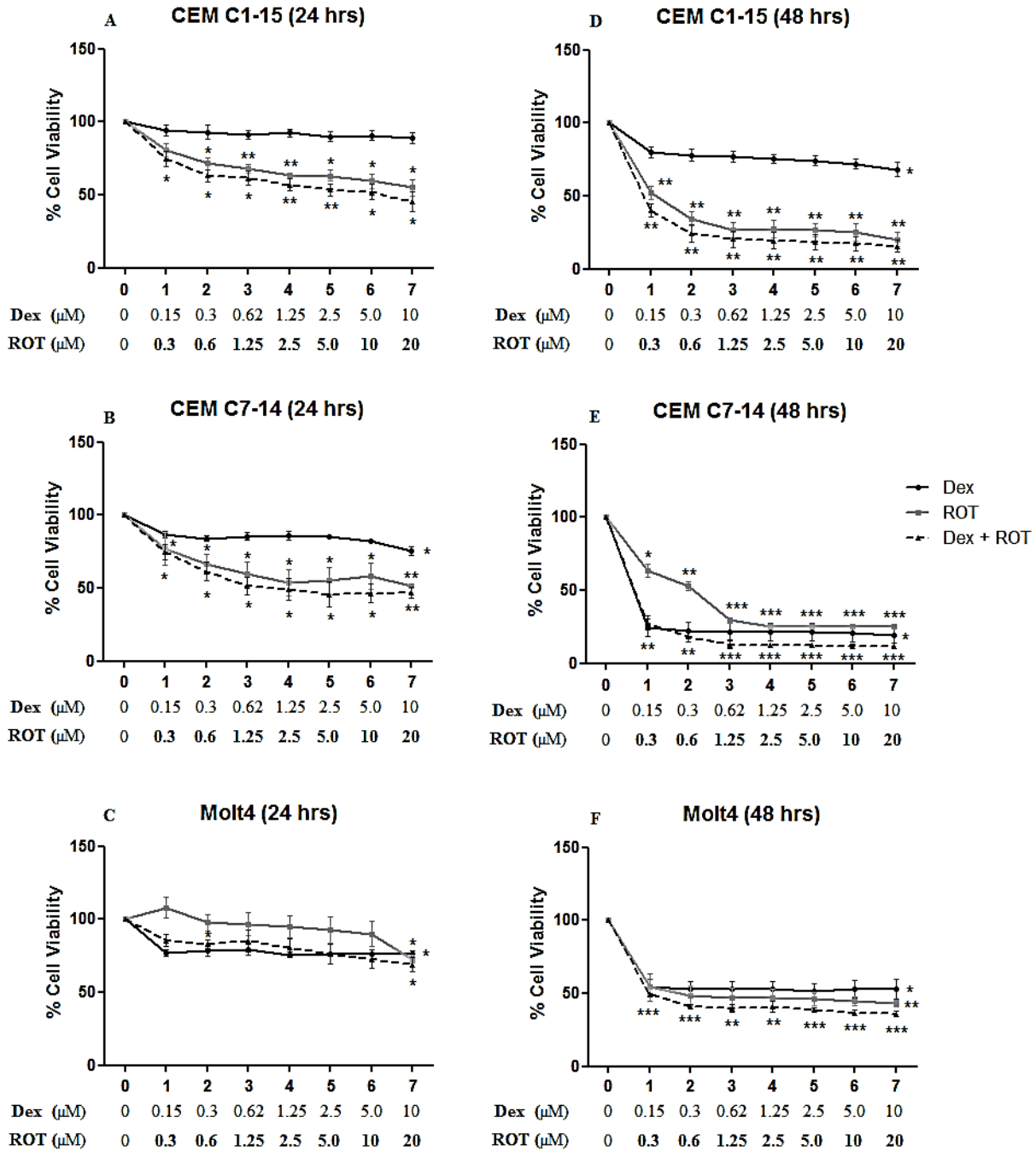

Figure 3-3 Cytotoxicity curves of CEM-C1-15, CEM-C7-14 and Molt4 cells treated with Dexamethasone and Rotenone

Cells were treated with different concentrations of Dex alone (black line), ROT alone (grey line) and combination (black dashed line) for 24 hrs (A to C) and 48 hrs (D to F). Cell viability was determined using MTS assay and data expressed relative to untreated sample. The results are representative of 3 independent experiments. Error bars represent ± SEM (* $p < 0.05$, ** $p < 0.01$, *** $p < 0.001$, *student t.test*). Each sample was compared to untreated control.

3.2.4 Cell viability of leukemia cells treated with Dexamethasone and Bortezomib

CEM-C1-15, CEM-C7-14 and Molt4 cells were treated with Dexamethasone concentrations as above and Bortezomib to examine the role of proteasome and ER stress in GR signalling. The doses of Bortezomib (BTZ) used in this test were between 0.15625 nM and 10 nM (Dai et al., 2011; Wang, A. H. et al., 2011a) and cells were treated for 24 hrs and 48 hrs. The results upon 24 hrs incubation time showed that Bortezomib inhibited CEM-C1-15 proliferation more than 50% at 5 nM and 10 nM, while the combination treatment with Dex enhanced cytotoxic effect in all three cell lines (Figure 3-4, A-C). IC_{50} was calculated for only CEM-C1-15 cell line at 4.0 nM (Table 11).

In 48 hrs incubation period, Bortezomib treatment led to a decrease of more than 50% cell viability in CEM CEM-C1-15 and Molt4 with 5 nM and 10 nM, respectively. However, the drug did not have significant effect in glucocorticoid-sensitive cells at the maximal concentration (10 nM) (Figure 3-4 E, grey line). When drugs were combined, synergistic effects were observed in CEM-C1-15 at 2.5 µM of Dex and 2.5 nM BTZ, CEM-C7-14 at all concentrations treated cells and Molt4 cells at all concentration except 1.25 µM of Dex and 1.25 nM of BTZ (Tables 13 D, 15 D and 17 D).

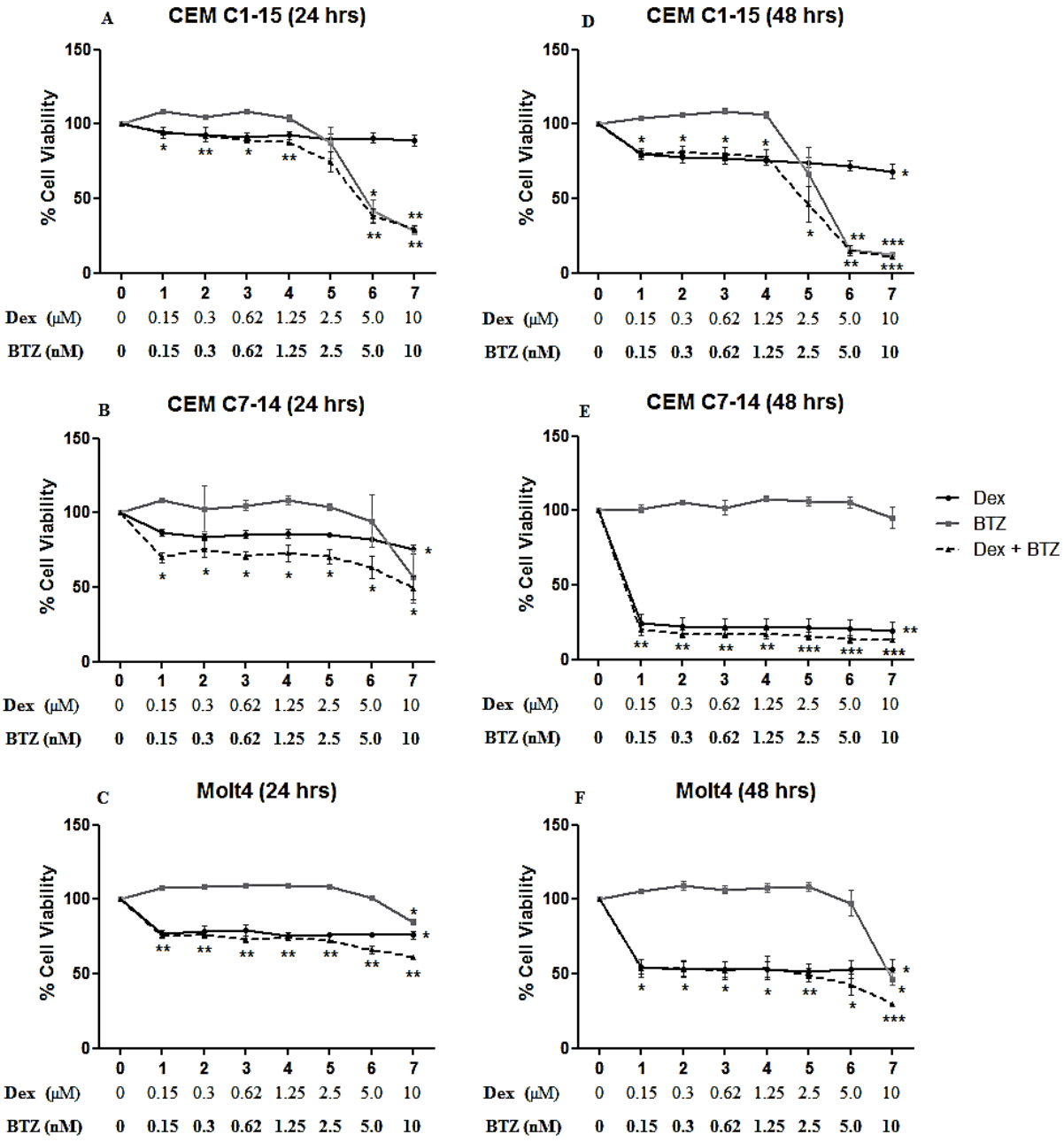

Figure 3-4 Cytotoxicity curves of CEM-C1-15, CEM-C7-14 and Molt4 cells treated with Dexamethasone and Bortezomib

Cells were treated with different concentrations of Dex alone (black line), BTZ alone (grey line) and combination (black dashed line) for 24 hrs (A to C) and 48 hrs (D to F). Cell viability was determined using MTS assay and data expressed relative to untreated sample. The results are representative of 3 independent experiments. Error bars represent ± SEM (* $p < 0.05$, ** $p < 0.01$, *** $p < 0.001$, *student t.test*). Each sample was compared to untreated control.

3.2.5 Conclusion

All drugs including CLQ, TG, ROT and BTZ reached 50% of inhibition of ALL cells proliferation at different concentrations, while the combination treatment exerted their cytotoxic effects on ALL cells. IC_{50} values obtained from MTS assay vary according to type of cell lines and the duration of the incubation time (Table 11). TG and ROT treatments sensitized leukemic cells when cells were treated individually or in combination with studied compounds. BTZ induced apoptosis of CEM-C1-15 cells that was greater than Molt4 and CEM-C7-14 cells. Moreover, 48 hours of incubation time had higher cytotoxic effects than 24 hours treatment.

Drug doses including 1 µM Dexamethasone, 10, 20, and 50 µM Chloroquine, 1 and 10 µM Thapsigargin, 1 and 10 µM Rotenone, 2 and 5 nM Bortezomib have been selected to use in further experiments.

Table 11 IC_{50} obtained using MTS assay in CEM-C1-15, CEM-C7-14 and Molt4 cells

The table shows IC_{50} after 24 hrs incubation time (A) and 48 hrs incubation time (B) with Dexamethasone, Chloroquine, Thapsigargin, Rotenone and Bortezomib drugs treatment. IC_{50} values were calculated using *CompuSyn* software.

A

Drugs (24 hrs)	IC_{50}		
	CEM-C1-15	CEM-C7-14	Molt4
Dex (µM)	-	-	-
CLQ (µM)	38.5	37.7	84.3
TG (µM)	15.0	14.4	126.5
ROT (µM)	34.9	16.6	111.1
BTZ (nM)	7.6	101.9	-

B

Drugs (48 hrs)	IC_{50}		
	CEM-C1-15	CEM-C7-14	Molt4
Dex (µM)	-	<0.001	-
CLQ (µM)	22.0	21.7	35.1
TG (µM)	1.9	4.2	<0.001
ROT (µM)	0.1	0.4	0.6
BTZ (nM)	4.0	-	123.7

Table 12 Combination index (CI) upon 24 hrs combination treatment of CEM-C1-15 cell

The synergistic values in CEM-C1-15 combination treatments Dex (µM) and CLQ (µM) (A), Dex (µM) and TG (µM) (B), Dex (µM) and ROT (µM) (C) and Dex (µM) and BTZ (nM) (D) were considered by using combination index (CI) where CI<1, =1 and >1 indicates synergism, additive and antagonism effects, respectively.

A

Dose Dex	Dose CLQ	Effect	CI
0.15625	1.5625	0.129	0.20486
0.3125	3.125	0.15	0.34935
0.625	6.25	0.239	0.42848
1.25	12.5	0.236	0.86895
2.5	25.0	0.394	0.93135
5.0	50.0	0.718	0.59340
10.0	100.0	0.827	0.70003

B

Dose Dex	Dose TG	Effect	CI
0.15625	0.3125	0.013	165251.
0.3125	0.625	0.01	2275204
0.625	1.25	0.107	0.60022
1.25	2.5	0.29	0.36361
2.5	5.0	0.415	0.44943
5.0	10.0	0.479	0.71704
10.0	20.0	0.46	1.53268

C

Dose Dex	Dose ROT	Effect	CI
0.15625	0.3125	0.251	0.61616
0.3125	0.625	0.368	0.14511
0.625	1.25	0.385	0.21924
1.25	2.5	0.431	0.20962
2.5	5.0	0.466	0.24234
5.0	10.0	0.482	0.37804
10.0	20.0	0.546	0.28000

D

Dose Dex	Dose BTZ	Effect	CI
0.15625	0.15625	0.057	2.69041
0.3125	0.3125	0.077	0.70538
0.625	0.625	0.112	0.37297
1.25	1.25	0.122	0.65612
2.5	2.5	0.255	0.66660
5.0	5.0	0.617	0.47447
10.0	10.0	0.705	0.72948

Table 13 Combination index (CI) after 48 hrs combination treatment of CEM-C1-15 cells

The synergistic values in CEM-C1-15 combination treatments Dex (µM) and CLQ (µM) (A), Dex (µM) and TG (µM) (B), Dex (µM) and ROT (µM) (C) and Dex (µM) and BTZ (nM) (D) were considered by using combination index (CI) where CI<1, =1 and >1 indicates synergism, additive and antagonism effects, respectively.

A

Dose Dex	Dose CLQ	Effect	CI
0.15625	1.5625	0.196	1.41112
0.3125	3.125	0.216	1.34232
0.625	6.25	0.334	0.48758
1.25	12.5	0.487	0.58930
2.5	25.0	0.716	0.58745
5.0	50.0	0.875	0.56775
10.0	100.0	0.894	0.99437

B

Dose Dex	Dose TG	Effect	CI
0.15625	0.3125	0.334	0.53327
0.3125	0.625	0.464	0.40377
0.625	1.25	0.646	0.21727
1.25	2.5	0.74	0.19876
2.5	5.0	0.79	0.24332
5.0	10.0	0.815	0.36857
10.0	20.0	0.803	0.84512

C

Dose Dex	Dose ROT	Effect	CI
0.15625	0.3125	0.598	0.67502
0.3125	0.625	0.757	0.09135
0.625	1.25	0.795	0.08226
1.25	2.5	0.806	0.12799
2.5	5.0	0.817	0.19697
5.0	10.0	0.825	0.32305
10.0	20.0	0.844	0.39121

D

Dose Dex	Dose BTZ	Effect	CI
0.15625	0.15625	0.202	1.00256
0.3125	0.3125	0.19	3.40278
0.625	0.625	0.203	3.84444
1.25	1.25	0.223	3.52242
2.5	2.5	0.54	0.56630
5.0	5.0	0.85	0.48718
10.0	10.0	0.892	0.79629

Table 14 Combination index (CI) after 24 hrs combination treatment of CEM-C7-14 cells

The synergistic values in CEM-C7-14 combination treatments Dex (µM) and CLQ (µM) (A), Dex (µM) and TG (µM) (B), Dex (µM) and ROT (µM) (C) and Dex (µM) and BTZ (nM) (D) were considered by using combination index (CI) where CI<1, =1 and >1 indicates synergism, additive and antagonism effects, respectively.

A

Dose Dex	Dose CLQ	Effect	CI
0.15625	1.5625	0.163	0.23749
0.3125	3.125	0.256	0.16416
0.625	6.25	0.378	0.22599
1.25	12.5	0.495	0.33544
2.5	25.0	0.609	0.50273
5.0	50.0	0.735	0.70182
10.0	100.0	0.778	1.21330

B

Dose Dex	Dose TG	Effect	CI
0.15625	0.3125	0.354	0.03958
0.3125	0.625	0.277	0.11444
0.625	1.25	0.497	0.08775
1.25	2.5	0.561	0.13572
2.5	5.0	0.587	0.24408
5.0	10.0	0.643	0.38530
10.0	20.0	0.731	0.51094

C

Dose Dex	Dose ROT	Effect	CI
0.15625	0.3125	0.254	2.19029
0.3125	0.625	0.385	0.29752
0.625	1.25	0.487	0.09466
1.25	2.5	0.51	0.12611
2.5	5.0	0.544	0.13809
5.0	10.0	0.535	0.32408
10.0	20.0	0.533	0.67157

D

Dose Dex	Dose BTZ	Effect	CI
0.15625	0.15625	0.301	0.00443
0.3125	0.3125	0.243	0.01710
0.625	0.625	0.291	0.01918
1.25	1.25	0.27	0.04694
2.5	2.5	0.294	0.07485
5.0	5.0	0.367	0.09427
10.0	10.0	0.504	0.09628

Table 15 Combination index (CI) after 48 hrs combination treatment of CEM-C7-14 cells

The synergistic values in CEM-C7-14 combination treatments Dex (µM) and CLQ (µM) (A), Dex (µM) and TG (µM) (B), Dex (µM) and ROT (µM) (C) and Dex (µM) and BTZ (nM) (D) were considered by using combination index (CI) where CI<1, =1 and >1 indicates synergism, additive and antagonism effects, respectively.

A

Dose Dex	Dose CLQ	Effect	CI
0.15625	1.5625	0.821	0.03448
0.3125	3.125	0.847	0.05813
0.625	6.25	0.874	0.10277
1.25	12.5	0.882	0.19752
2.5	25.0	0.892	0.37460
5.0	50.0	0.892	0.74920
10.0	100.0	0.879	1.60432

B

Dose Dex	Dose TG	Effect	CI
0.15625	0.3125	0.787	0.10494
0.3125	0.625	0.851	0.00762
0.625	1.25	0.888	0.00858
1.25	2.5	0.902	0.01330
2.5	5.0	0.893	0.03144
5.0	10.0	0.89	0.06629
10.0	20.0	0.905	0.10036

C

Dose Dex	Dose ROT	Effect	CI
0.15625	0.3125	0.724	32.6424
0.3125	0.625	0.818	0.03561
0.625	1.25	0.872	0.01987
1.25	2.5	0.877	0.03537
2.5	5.0	0.878	0.06909
5.0	10.0	0.884	0.11941
10.0	20.0	0.882	0.25090

D

Dose Dex	Dose BTZ	Effect	CI
0.15625	0.15625	0.802	0.02039
0.3125	0.3125	0.827	0.00245
0.625	0.625	0.827	0.00489
1.25	1.25	0.83	0.00684
2.5	2.5	0.843	0.00272
5.0	5.0	0.866	2.34E-4
10.0	10.0	0.866	4.68E-4

Table 16 Combination index (CI) after 24 hrs combination treatment of Molt4 cells

The synergistic values in Molt4 combination treatments Dex (µM) and CLQ (µM) (A), Dex (µM) and TG (µM) (B), Dex (µM) and ROT (µM) (C) and Dex (µM) and BTZ (nM) (D) were considered by using combination index (CI) where CI<1, =1 and >1 indicates synergism, additive and antagonism effects, respectively.

A

Dose Dex	Dose CLQ	Effect	CI
0.15625	1.5625	0.241	0.05822
0.3125	3.125	0.223	1.24387
0.625	6.25	0.22	4.39506
1.25	12.5	0.209	80.7937
2.5	25.0	0.273	0.57969
5.0	50.0	0.558	0.50543
10.0	100.0	0.752	0.55538

B

Dose Dex	Dose TG	Effect	CI
0.15625	0.3125	0.389	0.05734
0.3125	0.625	0.423	0.04294
0.625	1.25	0.412	0.11768
1.25	2.5	0.348	1.56649
2.5	5.0	0.414	0.44444
5.0	10.0	0.457	0.26266
10.0	20.0	0.509	0.12301

C

Dose Dex	Dose ROT	Effect	CI
0.15625	0.3125	0.144	5.923E7
0.3125	0.625	0.172	81377.4
0.625	1.25	0.148	7.825E7
1.25	2.5	0.194	2013.29
2.5	5.0	0.238	0.70248
5.0	10.0	0.274	0.32015
10.0	20.0	0.312	0.50226

D

Dose Dex	Dose BTZ	Effect	CI
0.15625	0.15625	0.245	0.00846
0.3125	0.3125	0.239	0.05183
0.625	0.625	0.269	8.21E-4
1.25	1.25	0.257	0.00824
2.5	2.5	0.278	0.00176
5.0	5.0	0.338	0.00148
10.0	10.0	0.389	0.00181

Table 17 Combination index (CI) after 48 hrs combination treatment of Molt4 cells

The synergistic values in Molt4 combination treatments Dex (µM) and CLQ (µM) (A), Dex (µM) and TG (µM) (B), Dex (µM) and ROT (µM) (C) and Dex (µM) and BTZ (nM) (D) were considered by using combination index (CI) where CI<1, =1 and >1 indicates synergism, additive and antagonism effects, respectively.

A

Dose Dex	Dose CLQ	Effect	CI
0.15625	1.5625	0.434	2943.58
0.3125	3.125	0.45	67.1507
0.625	6.25	0.443	946.273
1.25	12.5	0.486	0.38015
2.5	25.0	0.589	0.57632
5.0	50.0	0.84	0.53850
10.0	100.0	0.863	0.96790

B

Dose Dex	Dose TG	Effect	CI
0.15625	0.3125	0.73	0.11694
0.3125	0.625	0.732	0.20980
0.625	1.25	0.719	0.84284
1.25	2.5	0.721	1.51617
2.5	5.0	0.729	1.97515
5.0	10.0	0.748	1.38039
10.0	20.0	0.759	1.46630

C

Dose Dex	Dose ROT	Effect	CI
0.15625	0.3125	0.506	0.34452
0.3125	0.625	0.59	0.01396
0.625	1.25	0.602	0.01577
1.25	2.5	0.594	0.04619
2.5	5.0	0.614	0.03541
5.0	10.0	0.634	0.02664
10.0	20.0	0.64	0.03956

D

Dose Dex	Dose BTZ	Effect	CI
0.15625	0.15625	0.463	0.90454
0.3125	0.3125	0.467	0.59873
0.625	0.625	0.478	0.06237
1.25	1.25	0.461	12.5966
2.5	2.5	0.509	0.01938
5.0	5.0	0.574	0.02815
10.0	10.0	0.7	0.02893

3.3 Determination of cell cycle phases of leukemia cells treated with individual and combined drugs using cell cycle progression analysis

In order to determine effect of the studied compounds on ALL cell death and cell cycle progression, desired drugs concentrations were used to treat CEM-C1-15, CEM-C7-14 and Molt4 cells for 48 hrs. Cells then were stained with propidium iodide dye before flow cytometry was used to determine the percentage of cells in each cell cycle phase including subG1 (DNA fragmentation referred to cell death), G1, S and G2/M phases (Figure 3-5).

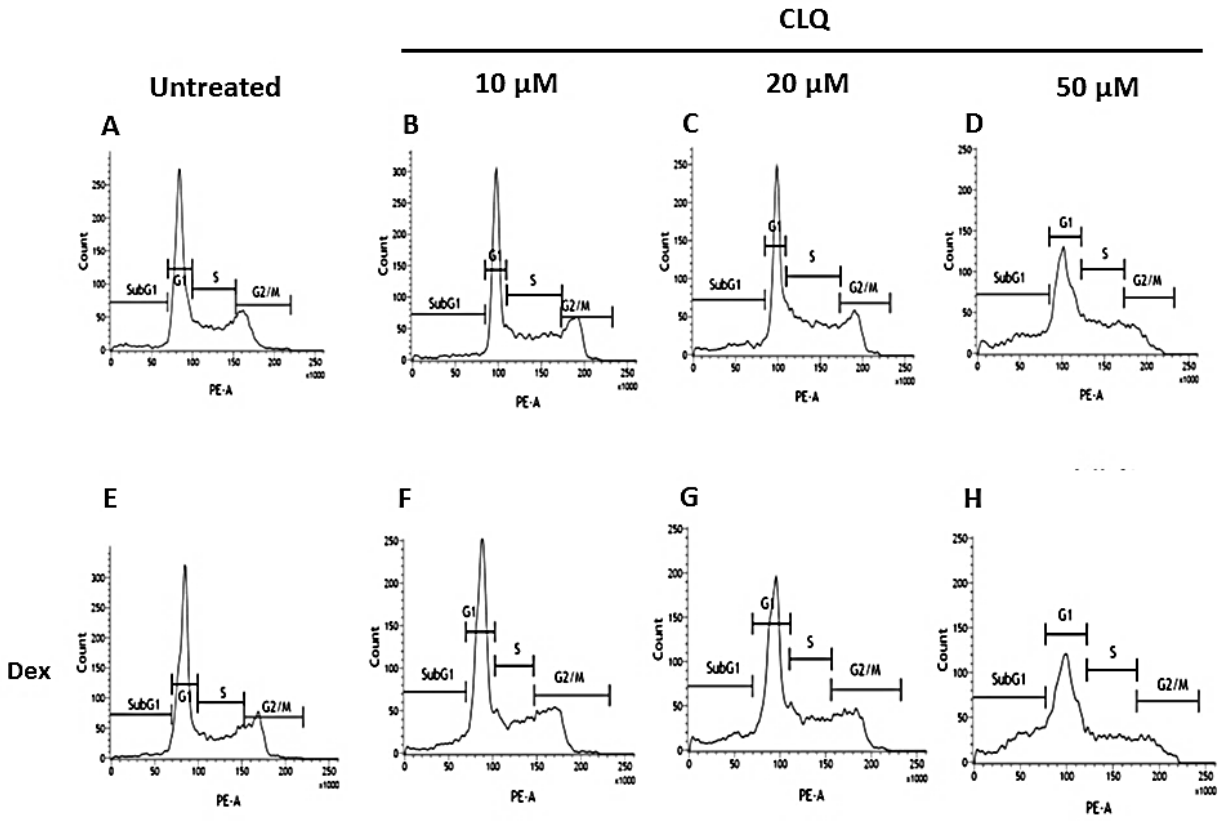

Figure 3-5 The representative results obtained from flow cytometry to analyse the cell cycle distribution pattern in CEM-C1-15 cells treated with Chloroquine

Graphs showed DNA content against cell numbers in SubG1, G1, S and G2/M phases in all treatments including untreated group (A), 10 µM (B), 20 µM (C) and 50 µM (D), of Chloroquine, 1 µM Dexamethasone (E), combination treatments of Dex with 10 µM (F), 20 µM (G) and 50 µM (H) Chloroquine, respectively.

3.3.1 Determination of cell cycle profiles in Dexamethasone and Chloroquine treated leukemia cells

To investigate the role of Autophagy in the glucocorticoid hormones mediated cell cycle progression control, Dex and CLQ were used individually and in combination to measure effect on ALL cell viability and cell cycle profile. After seeding the cells in 6-well plates, all treatments have been performed for 48 hrs. The PI-stained cells were loaded into flow cytometry and BD FACSuite software has been used to analyse all experiments. After gating, the percent of cells in each phase was compared to untreated sample and data were displayed using histogram charts. The results showed that Dex increased percentage of CEM-C7-14 cells in SubG1 phase to a greater extent than in CEM-C1-15 and Molt4, respectively (Figure 3-6 A, compare lane 1 and 2). CLQ alone increased SubG1 phase in dose-dependent manner in CEM resistant and sensitive cells while Molt4 cell were not affected by CLQ (Figure 3-6 A, lanes 3 to 5 compare black, light grey and grey bars). The combination treatments caused substantial increase in fragmented DNA in CEM-C1-15 and CEM-C7-14 while in Molt4 cells increase in SubG1 phase was not observed. Increase in G1 phase was observed in Dex treated Molt4 cells and marginal decrease in CEM-C1-15 and CEM-C7-14 cells (Figure 3-6 B, lanes 2, 6 to 8 grey bars). S phase substantially decreased in the Dex treated Molt4 cells (Figure 3-6 C, lanes 2, and 6 to 8 light grey and grey bars). Furthermore, G2/M phase was decreased by Dex treatment alone in CEM-C7-14 and Molt4 while combined conditions with CLQ resulted in decrease of G2/M in CEM-C1-15 and CEM-C7-14 cells (Figure 3-6 D, lane 2, 6 to 8 light grey and grey bars).

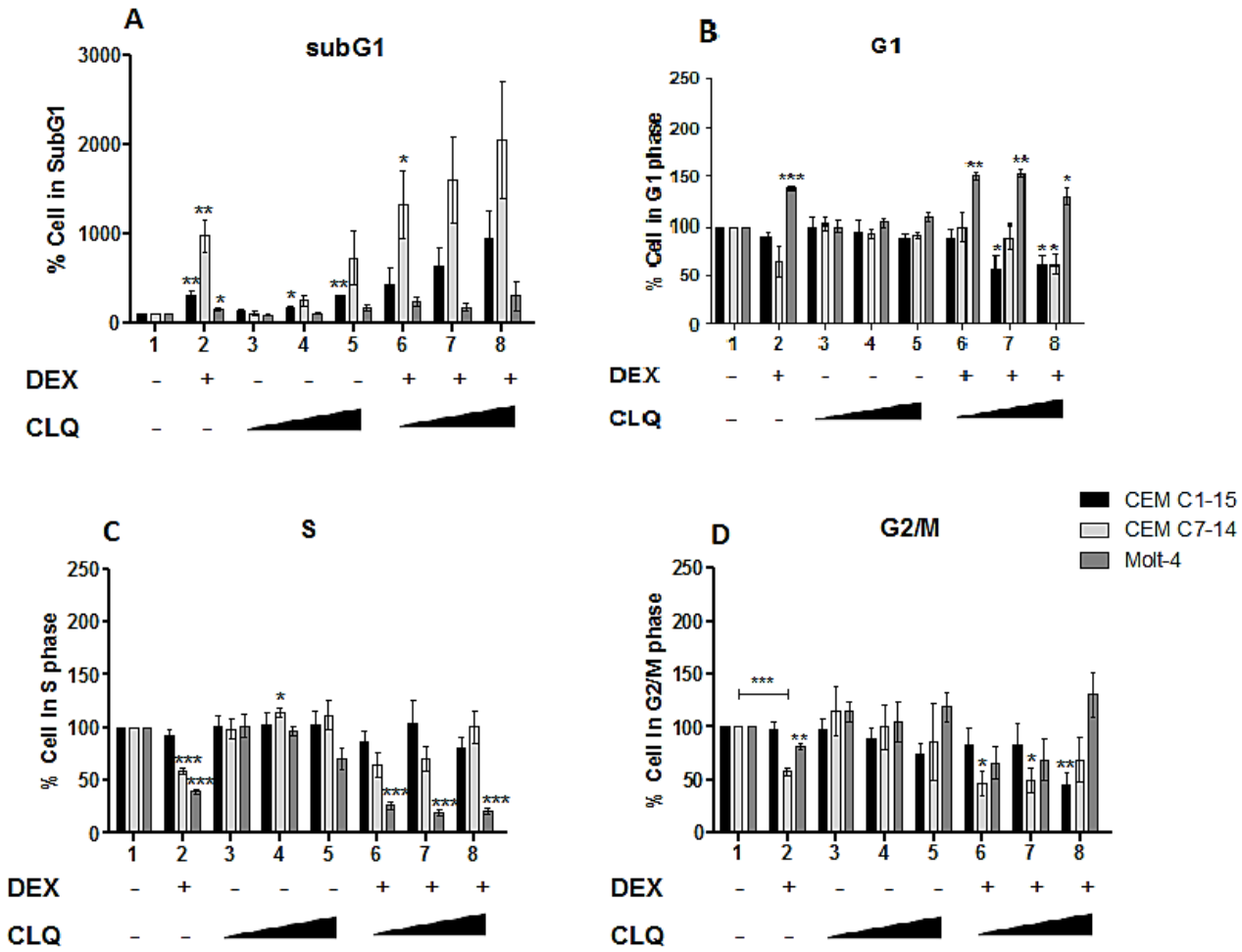

Figure 3-6 Cell cycle phase distribution in CEM-C1-15, CEM-C7-14 and Molt4 Chloroquine and Dex treated cells

CEM-C1-15 (black bars), CEM-C7-14 (light grey bars) and Molt4 (dark grey bars) were treated with indicated concentration of Dex and CLQ for 48 hrs. Cells were either untreated (lane 1), or treated with 1 μM Dex (lane 2), 10, 20 and 50 μM Chloroquine (lanes 3-5), and combination of 1 μM Dex with 10, 20 and 50 μM Chloroquine (lanes 6-8). Cell cycle phases were gated and values for SubG1 (A), G1 (B), S (C) and G2/M phases (D) across different treatments were expressed as a percentage of control group. The results are representative of 3 independent experiments. Error bars represent ± SEM (* $p < 0.05$, ** $p < 0.01$, *** $p < 0.001$, *student t.test*). Each sample was compared to untreated control.

3.3.2 Determination of cell cycle phases in Dexamethasone and Thapsigargin treated leukemia cells

In order to determine potential crosstalk of glucocorticoid hormones and ER stress, Dex and TG were used individually and in combination to measure effect on ALL cell viability and cell cycle progression. Dex and TG were added for 48 hrs (concentrations were mentioned above), and flow cytometry carried out as described above. Results indicated that TG increased SubG1 phase in C1-15 cells higher than in C7-14 and Molt4 cells. Moreover, the combination treatments increased SubG1 in all cell lines (Figure 3-7 A, lanes 5 and 6 compare to lane 1). G1 phase significantly decreased when TG was used to treat CEM-C1-15 cells (Figure 3-7 B, lanes 3 to 6 black bars) while the increase in G1 was observed in Molt4 (Figure 3-7 B, lanes 2 to 6 grey bars). The percent of cells in G2/M phase decreased significantly in CEM-C1-15 and CEM-C7-14 with combination treatments (Figure 3-7 D, lanes 5 and 6 black and light grey bars compare to lane 1).

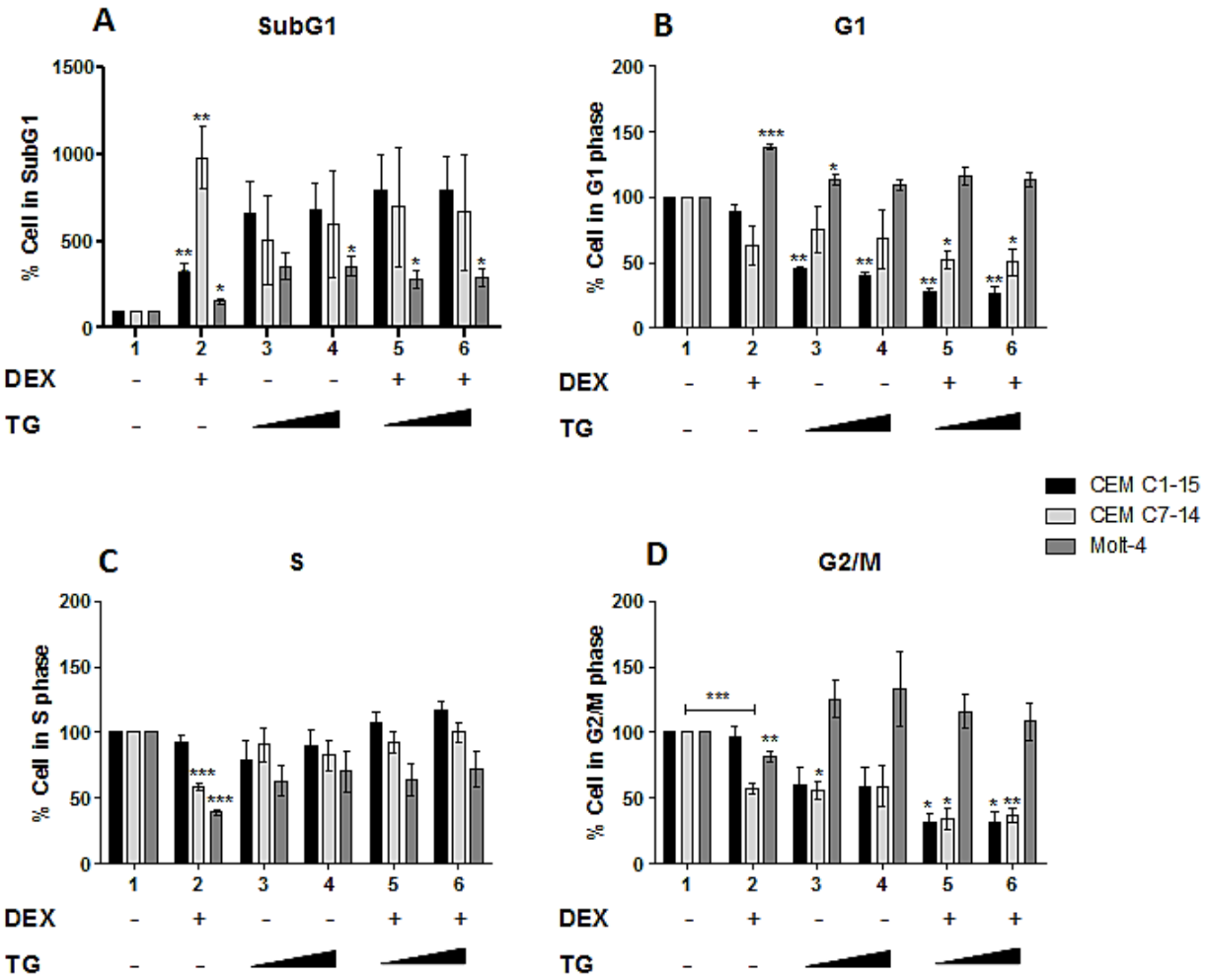

Figure 3-7 Cell cycle phase distribution in CEM-C1-15, CEM-C7-14 and Molt4 Thapsigargin and Dex treated cells

CEM-C1-15 (black bar), CEM-C7-14 (light grey bar) and Molt4 (dark grey bar) were treated with Dex and TG in different conditions for 48 hrs. Cells were either untreated (lane 1), or treated with 1 μM Dex (lane 2), 1 and 10 μM Thapsigargin (lanes 3-4), and combination of 1 μM Dex with 1 and 10 μM Thapsigargin (lanes 5-6). Cell cycle phases were gated and values for SubG1 (A), G1phase (B), S phase (C) and G2/M phase (D) across different treatments were expressed as a percentage of control group. The results are representative of 3 independent experiments. Error bars represent ± SEM (* $p < 0.05$, ** $p < 0.01$, *** $p < 0.001$, *student t.test*). Each sample was compared to untreated control.

3.3.3 Determination of cell cycle phases in Dexamethasone and Rotenone treated leukemia cells

To investigate the role of oxidative stress in the function of glucocorticoid hormones, Dex and ROT were used individually and in combination to measure effect on ALL cell viability and cell cycle progression. Cells were treated with Dex and ROT for 48 hrs and analysed by flow cytometry. The results showed that SubG1 phase substantially increased in ROT treated CEM-C1-15 and CEM-C7-14 cells and the combination treatment led to further increase in SubG1 phase in CEM cells in a dose dependent manner (Figure 3-8 A, lanes 3 to 6 black and light grey bars compare to lane 1). G1 phase was decreased significantly in ROT and combined treatment with Dex in CEM-C1-15 and CEM-C7-14 cells (Figure 3-8 B, lanes 3 to 6 black and light grey bars). In addition, Dex increased G1 phase in Molt4 cells but this accumulation of cells in G1 phase was decreased when ROT was added (Figure 3-8 B, grey bars compare lane 2 and lanes 3 to 6). Dex had inhibitory effect on S phase in CEM-C7-14 and Molt4 cells. ROT alone increased G2/M phase in all cells with significant effects observed only in Molt-4, while inhibitory trend was observed in G2/M when the combined drugs were used (Figure 3-8 D, compare lanes 3 and 4 to lanes 5 and 6).

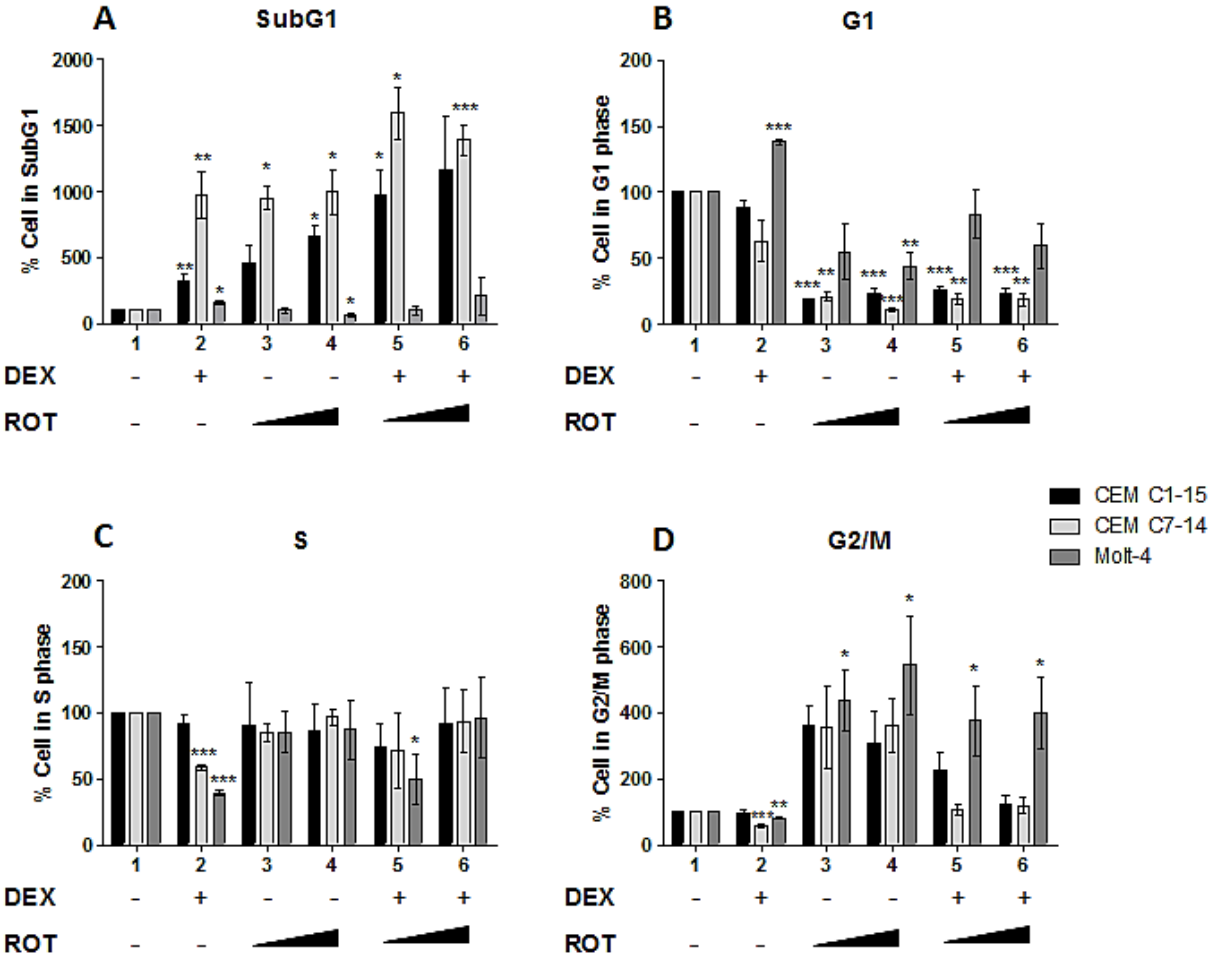

Figure 3-8 Cell cycle phase distribution in CEM-C1-15, CEM-C7-14 and Molt4 Rotenone and Dex treated cells

CEM-C1-15 (black bar), CEM-C7-14 (light grey bar) and Molt4 (dark grey bar) were treated with Dex and ROT in different conditions for 48 hrs. Cells were either untreated (lane 1), or treated with 1 μM Dex (lane 2), 1 and 10 μM Rotenone (lanes 3-4), and combination of 1 μM Dex with 1 and 10 μM Rotenone (lanes 5-6). Cell cycle phases were gated and values for SubG1 (A), G1phase (B), S phase (C) and G2/M phase (D) across different treatments were expressed as a percentage of control group. The results are representative of 3 independent experiments. Error bars represent ± SEM (* $p < 0.05$, ** $p < 0.01$, *** $p < 0.001$, *student t.test*). Each sample was compared to untreated control.

3.3.4 Determination of cell cycle phases in Dexamethasone and Bortezomib treated leukemia cells

To investigate the role of ER stress and unfolded protein response in the function of glucocorticoid hormones, Dex and BTZ were used individually and in combination to measure effect on ALL cell viability and cell cycle progression. Dex and Bortezomib were incubated with cells for 48 hrs and flow cytometry used to obtain SubG1 and cell cycle phases. The results showed that SubG1 phase increased in CEM-C7-14 and Molt4 cells when BTZ was used alone (Figure 3-9 A, lanes 3 and 4 light grey and grey bars compare to lane 1) while increase in SubG1 was observed in CEM-C1-15 (Figure 3-9 A, lanes 4 and 5 black bars). The combination treatment with Dex substantially increased SubG1 in CEM cells (Figure 3-9 A, lanes 5 and 6 black and light grey bars). G1 phase substantially increased in Molt4 when Dex was added while decreasing of S phase was observed in CEM-C7-14 and Molt4 (Figure 3-9 B and C). In CEM-C1-15 and CEM-C7-14, decrease of G1 phase was observed in combined treatment of Dex and BTZ (Figure 3-9 B, lanes 5 and 6 black and light grey bars). G2/M phase decreased in CEM-C7-14 when treated with Dex alone and combined drug conditions (Figure 3-9 D, lanes 2 and 5 to 6 light grey bars).

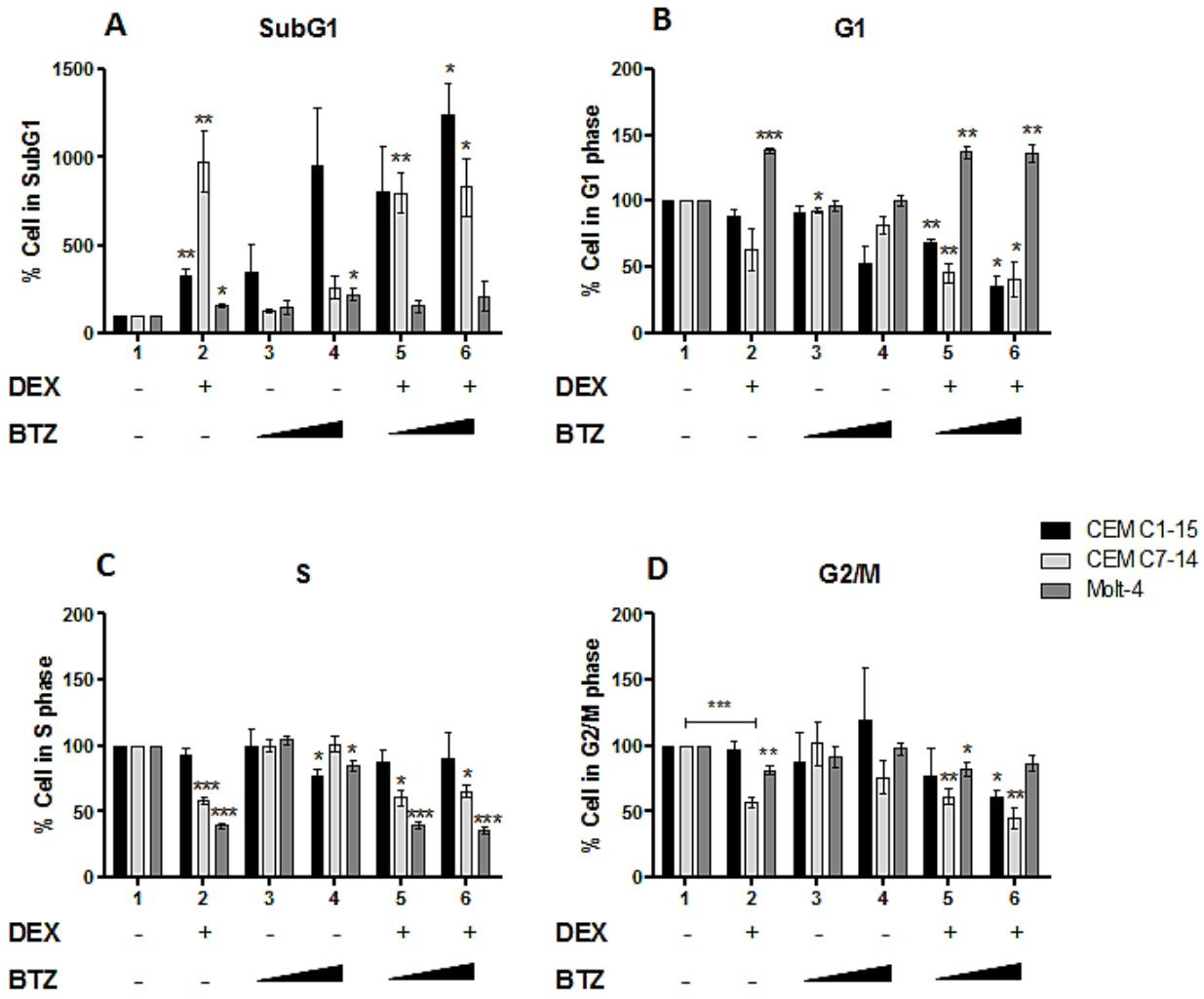

Figure 3-9 Cell cycle phase distribution in CEM-C1-15, CEM-C7-14 and Molt4 Bortezomib and Dex treated cells

CEM-C1-15 (black bar), CEM-C7-14 (light grey bar) and Molt4 (dark grey bar) were treated with Dex and BTZ in different conditions for 48 hrs. Cells were either untreated (lane 1), or treated with 1 μM Dex (lane 2), 2 and 5 nM Bortezomib (lanes 3-4), and combination of 1 μM Dex with 2 and 5 nM Bortezomib (lanes 5-6). Cell cycle phases were gated and values for SubG1 (A), G1phase (B), S phase (C) and G2/M phase (D) across different treatments were expressed as a percentage of control group. The results are representative of 3 independent experiments. Error bars represent ± SEM (* $p < 0.05$, ** $p < 0.01$, *** $p < 0.001$, *student t.test*). Each sample was compared to untreated control.

3.3.5 Conclusion

Dexamethasone mediated increase in SubG1 was higher in CEM-C7-14 than in CEM-C1-15 and Molt4, whereas stronger effects were observed in combination treatments with Chloroquine, Thapsigargin, Rotenone and Bortezomib. Dex also increased G1 phase in Molt4 while lower number of CEM-C1-15 and CEM-C7-14 cells were observed in G1 phase. Dex significantly decreased S and G2/M phases in CEM-C7-14 and Molt7 cells. Increase in SubG1 in a dose dependent manner was observed in CLQ and ROT treated cells, however cell death did not increase when BTZ was used in CEM-C7-14 and Molt4 cells. Finally, ROT alone increased G2/M phase in ALL cells while TG increased G2/M phase only in Molt4.

3.4 Determination of mitochondrial membrane potential alteration in leukemia cells treated with individual and combined drugs

Mitochondria is the crucial organelle involved in cellular physiology and is the source of intracellular energy (ATP). It produces the ATP through oxidative phosphorylation processes during electron transport chain (Chance & Williams, 1956). During the ATP synthesis, series of redox reactions generate the gradient of electrochemical voltage that also creates the mitochondrial membrane potential (MMP), which becomes the important parameter to detect and to determine mitochondrial function (Chen, L. B., 1988; MITCHELL, 1961). The alteration of mitochondrial membrane potential is linked to cell apoptosis. Several cell membrane permeable fluorescent dyes such as 3, 3′-dihexyloxacarbocyanine iodide, rhodamine-123, and JC-1 have been used to detect the change of MMP that were associated with various disorders (Lemasters et al., 2002; Sakamuru et al., 2012).

3.4.1 MMP alteration in Dexamethasone and Chloroquine treated leukemia cells

To investigate the role of Autophagy in the role of glucocorticoid hormones in mitochondrial mediated processes, Dex and CLQ were used individually and in combination to measure the disruption of mitochondrial membrane potential on ALL cells. After seeding the cells in 6-well plates, cells were treated with indicated drugs concentrations for 48 hrs, stained with JC-1 and loaded into A8 slide. Cells were analysed using NucleoCounter. The percent of cell death presenting in lower right quadrant (QLR) in each condition was noted and normalised to control group. Results showed that Dexamethasone alone substantially changes the mitochondrial membrane potential in CEM-C7-14 cells (Figure 3-10 B lane 2), while slight increase was observed in CEM-C1-15 cells. However, the mitochondrial membrane voltage was not affected by Dex in Molt4 cells. Only 50 μM Chloroquine alone significantly increased MMP alteration in all cell lines (Figure 3-10 A-C lane 5) and further increase was observed when CLQ was combined with Dex in CEM-C1-15 and CEM-C7-14 (Figure 3-10 A and B lanes 7-8). In Molt4, the combination conditions did not increase the MMP alterations.

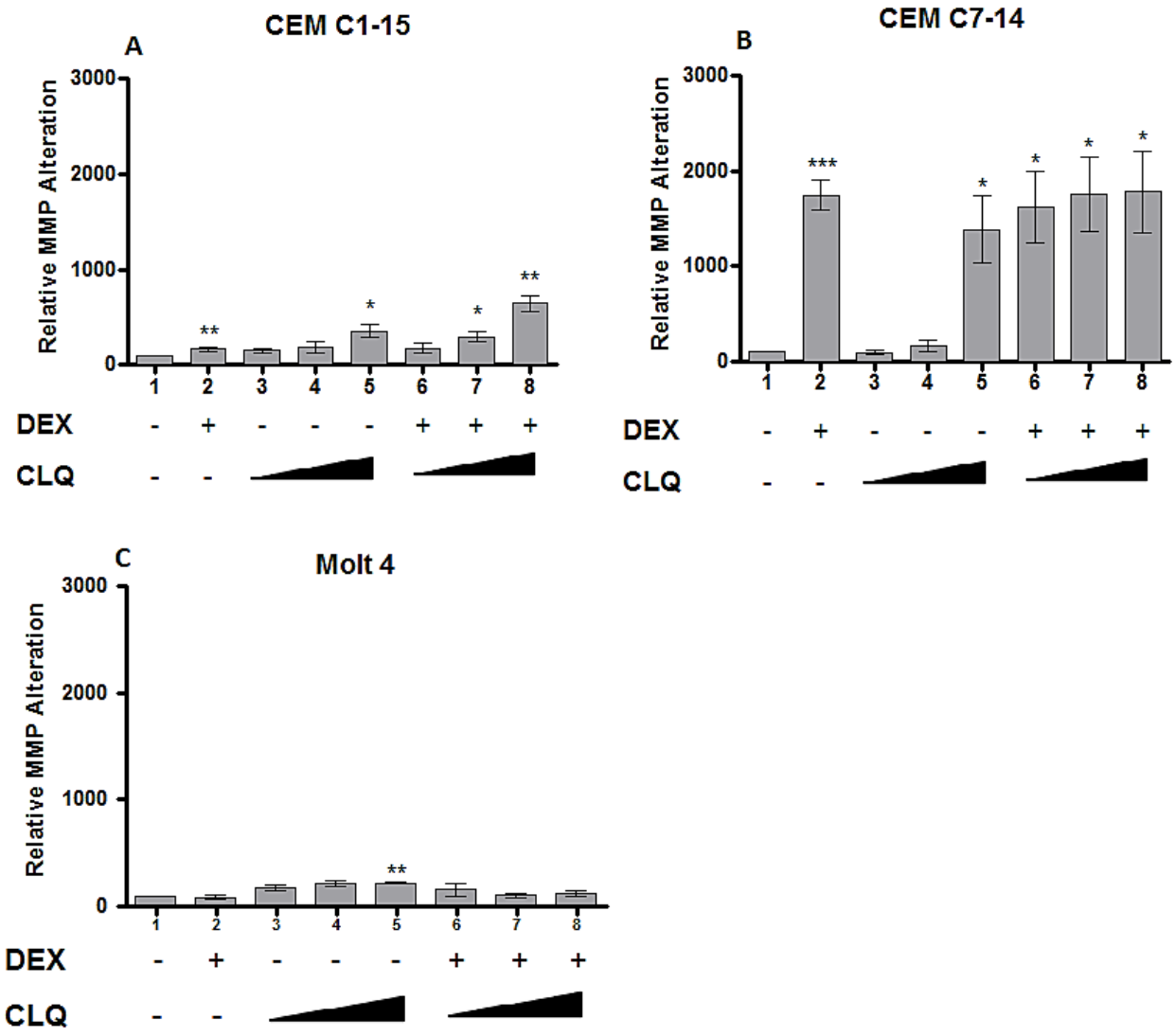

Figure 3-10 Mitochondrial membrane alterations observed in CEM-C1-15, CEM-C7-14 and Molt4 Dexamethasone and Chloroquine treated cells

The figures show the relative MMP alterations in CEM-C1-15 (A), CEM-C7-14 (B) and Molt4 (C) cells in different conditions including untreated group (lane 1), 1 μM Dex (lane 2), 10, 20 and 50 μM Chloroquine (lanes 3-5), and combination treatment of 1 μM Dex with 10, 20 and 50 μM Chloroquine (lanes 6-8). The results are representative of 3 independent experiments. Error bars represent ± SEM (* $p < 0.05$, ** $p < 0.01$, *** $p < 0.001$, *student t.test*). Each sample was compared to untreated control.

3.4.2 MMP analysis in Dexamethasone and Thapsigargin treated cells

To investigate the role of ER stress and unfolded protein response in the role of glucocorticoid hormones in mitochondrial functions, Dex and TG were used individually and in combination to measure the mitochondrial membrane potential alteration on ALL cells. Cells were treated as mentioned above 48 hrs. The results showed that in CEM-C1-15 cells increase in MMP was caused by 10 μM TG treatment (Figure 3-11 A lane 4), in CEM-C7-14 cells this increase was more substantial than in CEM-C1-15 and Molt4 cells when cells were treated with Dex and TG individually (Figure 3-11 B). The combination treatments increased MMP in CEM cells no significant alterations were observed.

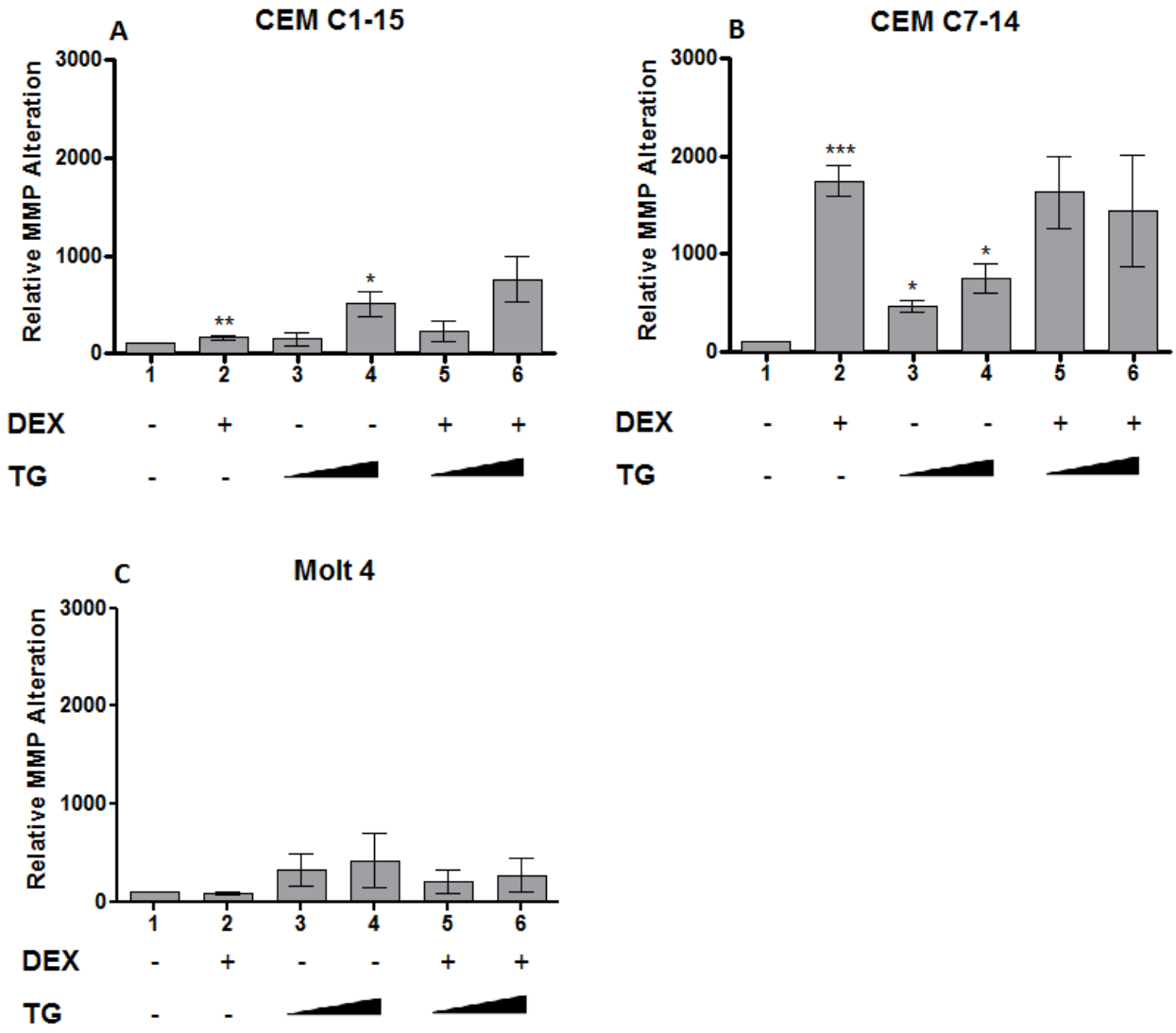

Figure 3-11 Mitochondrial membrane alterations observed in CEM-C1-15, CEM-C7-14 and Molt4 Dexamethasone and Thapsigargin treated cells

The figures show the relative MMP alterations in CEM-C1-15 (A), CEM-C7-14 (B) and Molt4 (C) cells in different conditions including untreated group (lane 1), 1 μM Dex (lane 2), 1 and 10 μM Thapsigargin (lanes 3-4), and combination treatment of 1 μM Dex with 1 and 10 μM Thapsigargin (lanes 5-6). The results are representative of 3 independent experiments. Error bars represent ± SEM (* $p < 0.05$, ** $p < 0.01$, *** $p < 0.001$, *student t.test*). Each sample was compared to untreated control.

3.4.3 MMP analysis in Dexamethasone and Rotenone treated cells

To investigate the role of oxidative stress and glucocorticoid hormones in mitochondrial functions, Dex and ROT were used individually and in combination to measure the alteration of mitochondrial membrane voltage on ALL cells. After treating the cells with studied drugs for 48 hrs, Nucleocounter was used to determine MMP as described above. The results showed that Rotenone alone substantially increased MMP in CEM-C1-15 and CEM-C7-14 cells (Figure 3-12 A and B lanes 3-4), while marginal increase was observed in Molt4. The combination conditions increased the percent of MMP alterations to a greater extent in CEM cell lines (Figure 3-12 A and B lanes 5-6), while the Molt4 cells were not affected by combined drugs (Figure 3-12 C lanes 5-6).

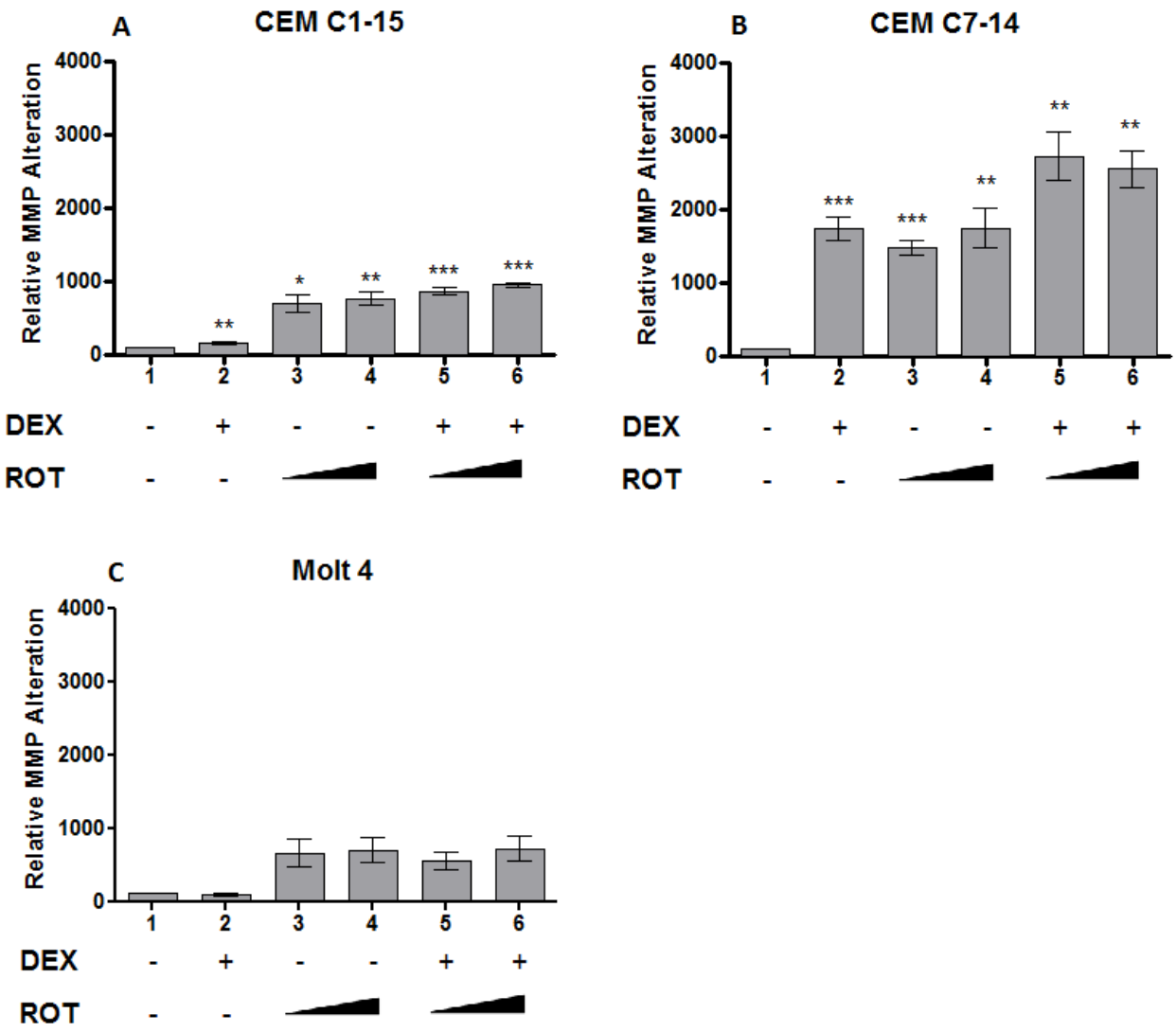

Figure 3-12 Mitochondrial membrane alterations observed in CEM-C1-15, CEM-C7-14 and Molt4 Dexamethasone and Rotenone treated cells

The figures show the relative MMP alterations in CEM-C1-15 (A), CEM-C7-14 (B) and Molt4 (C) cells in different conditions including untreated group (lane 1), 1 μM Dex (lane 2), 1 and 10 μM Rotenone (lanes 3-4), and combination treatment of 1 μM Dex with 1 and 10 μM Rotenone (lanes 5-6). The results are representative of 3 independent experiments. Error bars represent ± SEM (* $p < 0.05$, ** $p < 0.01$, *** $p < 0.001$, *student t.test*). Each sample was compared to untreated control.

3.4.4 MMP analysis in Dexamethasone and Bortezomib treated cells

To investigate the role of ER stress and unfolded protein response in the function of glucocorticoid hormones and in mitochondrial processes, Dex and BTZ were used to treat cells for 48 hrs individually and in combination, and the mitochondrial membrane alterations on ALL cells measured as described above. The results indicated that 5 nM Bortezomib increased MMP alterations in CEM-C1-15, CEM-C7-14 cells and Molt4 cells but only in CEM-C1-15 significant values were observed (Figure 3-13 A). Combination treatment significantly increased MMP alterations only in CEM-C1-15 and CEM-C7-14 cells (Figure 3-13 A and B lanes 5-6).

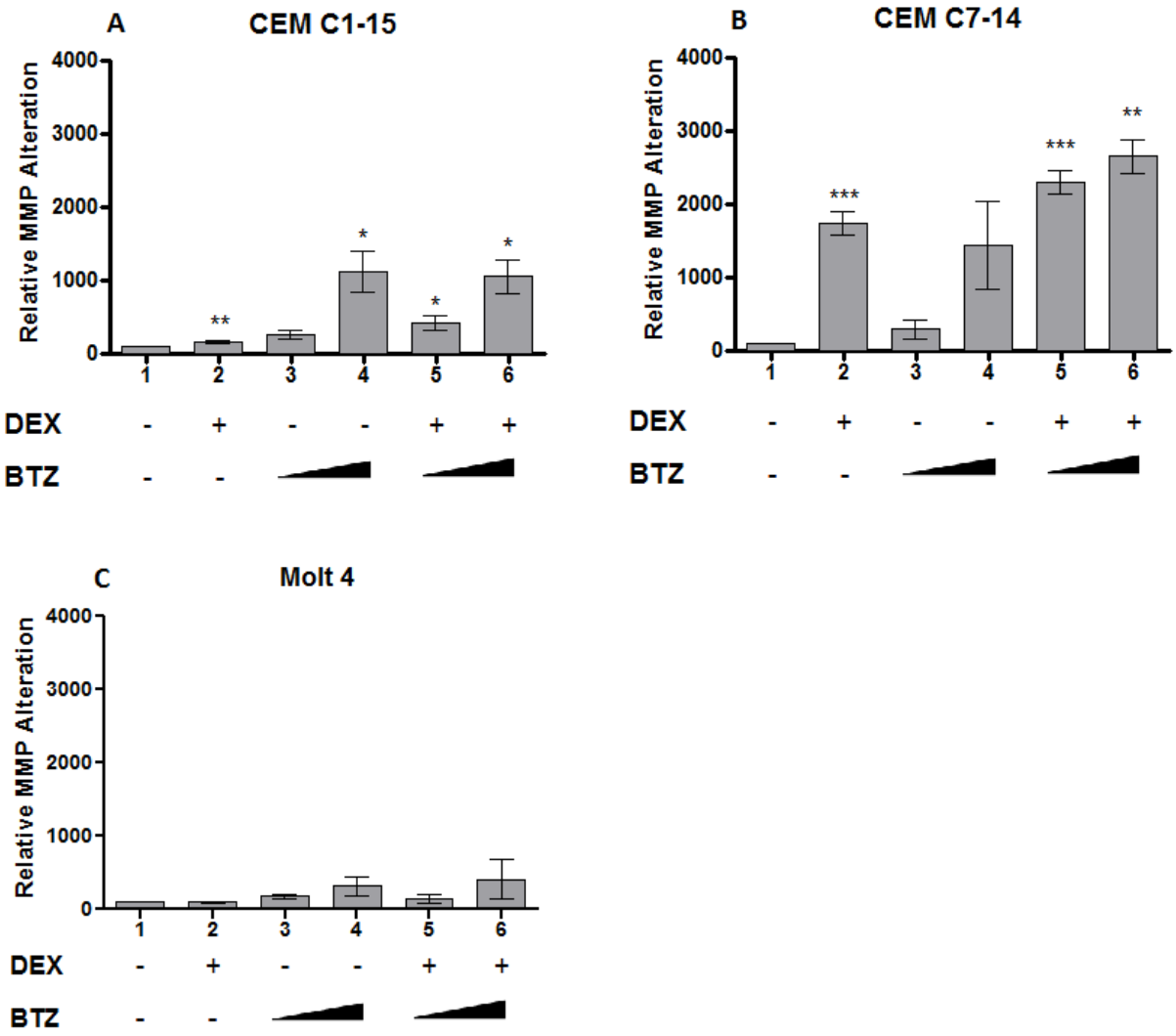

Figure 3-13 Mitochondrial membrane alterations observed in CEM-C1-15, CEM-C7-14 and Molt4 Dexamethasone and Bortezomib treated cells

The figures show the relative MMP alterations in CEM-C1-15 (A), CEM-C7-14 (B) and Molt4 (C) cells in different conditions including untreated group (lane 1), 1 μM Dex (lane 2), 2 and 5 nM Bortezomib (lanes 3-4), and combination treatment of 1 μM Dex with 2 and 5 nM Bortezomib (lanes 5-6). The results are representative of 3 independent experiments. Error bars represent ± SEM (* $p < 0.05$, ** $p < 0.01$, *** $p < 0.001$, *student t.test*). Each sample was compared to untreated control.

3.4.5 Conclusion

Dexamethasone substantially increased the mitochondrial membrane potential alterations in glucocorticoid-sensitive cells while the marginal changes of mitochondrial membrane voltage were observed in CEM-C1-15 cells. However, Dex did not change MMP in Molt4 cells. Chloroquine interrupted mitochondrial membrane voltage when used at high dose in all three cell lines while combined drugs with Dex have stronger effects in CEM-C7-14 and CEM-C1-15. CEM-C1-15 and CEM-C7-14 MMP alterations were affected by Thapsigargin and Rotenone alone treatments in a dose dependent manner. Combination treatments of Dex and ROT increased MMP alteration in CEM-C7-14 and CEM-C1-15 but not in Molt4.

CHAPTER 4 REACTIVE OXYGEN SPECIES PRODUCTION IN LEUKEMIA

4.1 Overview of reactive oxygen species generation in leukemia

In redox homeostasis, Reactive Oxygen Species (ROS) level plays an important role in cell proliferation, survival and genomic mutation in leukemic cell. The increased ROS levels disrupt oxidative pathway leading to genomic instability and leukemogenesis (Irwin et al., 2013). The major source and target of ROS in leukemic cells are in the mitochondrial electron transport chain (ETC) and the variety of genomic and mitochondria mutations play the critical role to increase ROS levels in leukemic cells (Carew et al., 2003; Quillet-Mary et al., 1997; Silva et al., 2011). In order to determine ROS generation in ALL cells treated with studied compounds indicated drugs concentrations were used to treat CEM-C1-15, CEM-C7-14 and Molt4 cells for 24 hrs. Cells were then stained with carboxy-H2DCFDA dye to determine the total reactive oxygen species generation by flow cytometry. The percent of total ROS signal intensity was normalized to control group.

4.2 Determination of reactive oxygen species levels in Dexamethasone and Chloroquine treated leukemia cells

In order to investigate the role of autophagy and ROS generation in glucocorticoid treatment, Dex and CLQ were used individually and in combination to measure ROS levels in ALL cells. After seeding the cells in 6-well plates, Dex and CLQ were added for 24 hrs and stained cells analysed using flow cytometry. The results showed that Dex significantly decreased the total ROS levels in CEM-C7-14 cells, caused marginal reduction in Molt4 cells, whereas in CEM-C1-15 cells there was no change in ROS levels (Figure 4-1 A to C, lane 2). CLQ alone at 20 and 50 μM decreased ROS level only in CEM-C1-15 cells (Figure 4-1 A lane 4-5). The combination with Dex decreased ROS generation in CEM-C1-15 and CEM-C7-14 cells at all combined drug treatments except 50 μM CLQ in CEM-C7-14 cells (Figure 4-1 B lane 8).

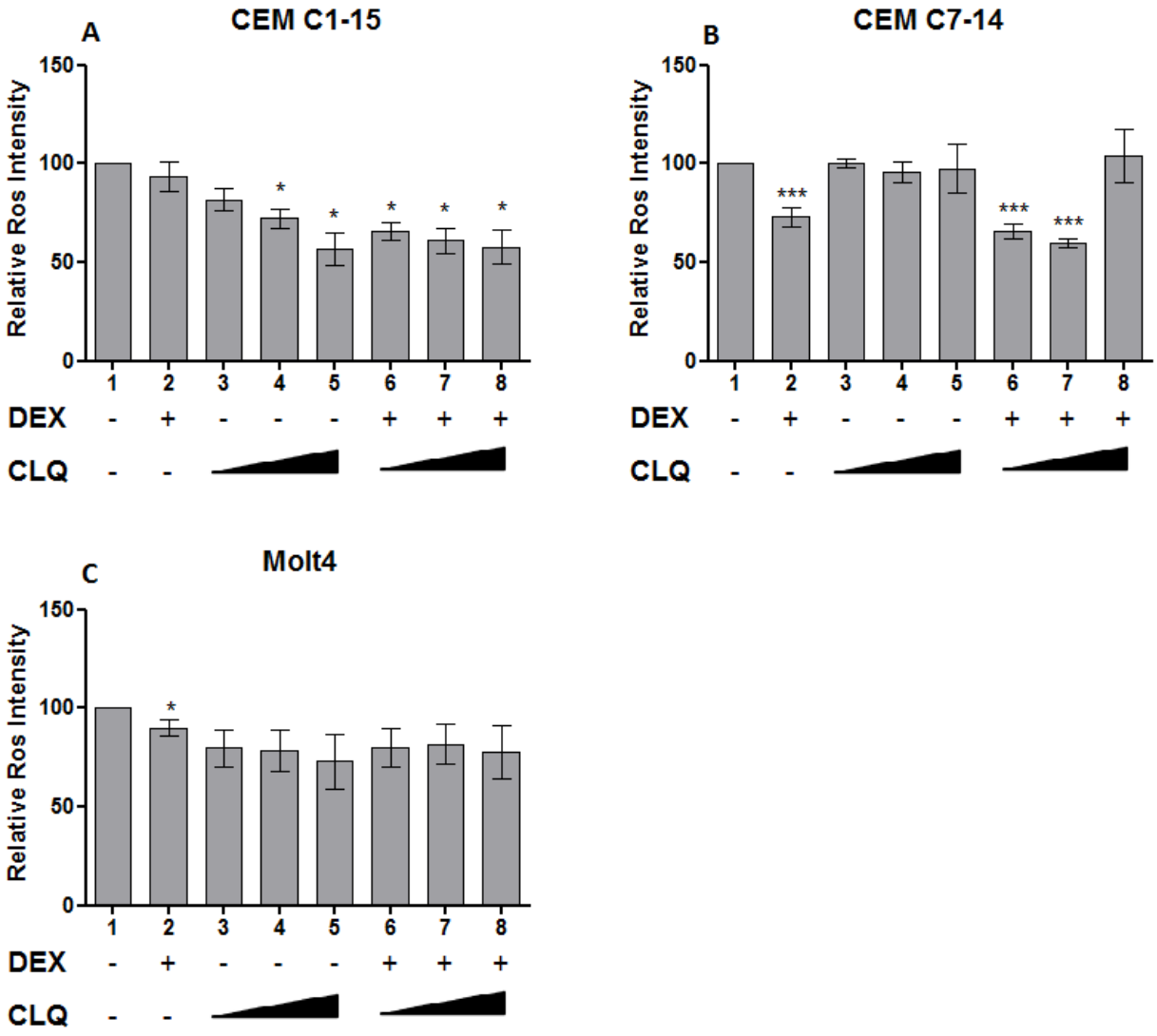

Figure 4-1 Reactive oxygen species generation in CEM-C1-15, CEM-C7-14 and Molt4 cells treated with Chloroquine and Dexamethasone

The figures show the relative ROS generation intensity in CEM-C1-15 (A), CEM-C7-14 (B) and Molt4 (C) cells in different conditions including untreated group (lane 1), 1 μM Dex (lane 2), 10, 20 and 50 μM Chloroquine (lanes 3-5), and combination treatment of 1 μM Dex with 10, 20 and 50 μM Chloroquine (lanes 6-8). The results are representative of 3 independent experiments. Error bars represent ± SEM (* $p < 0.05$, ** $p < 0.01$, *** $p < 0.001$, *student t.test*). Each sample was compared to untreated control.

4.3 Reactive oxygen species generation in Dexamethasone and Thapsigargin treated leukemia cells

In order to investigate the role of ER stress and glucocorticoid treatment in ROS signalling, Dex and TG were used individually and in combination to measure ROS level in ALL cells. Cells were treated with Dex and TG for 24 hrs and analysed using flow cytometry. The results indicated that TG alone significantly decreased ROS generation in all cells (Figure 4-2 lane 3 and 4) and the combination with Dex also decreased ROS level in three cell lines (Figure 4-2 lane 5 and 6).

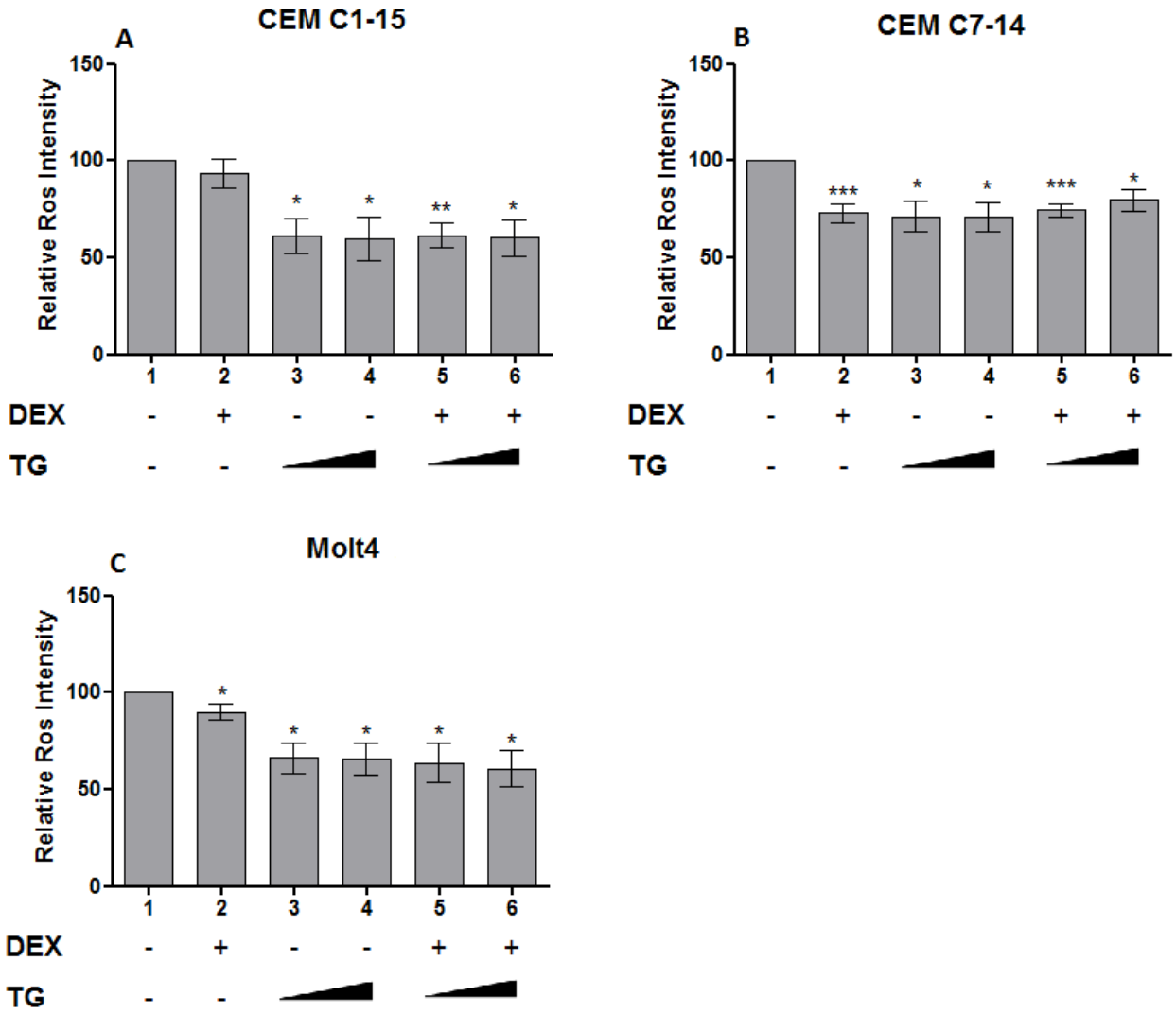

Figure 4-2 Reactive oxygen species generation in CEM-C1-15, CEM-C7-14 and Molt4 cells treated with Thapsigargin and Dexamethasone

The figures show the relative ROS generation intensity in CEM-C1-15 (A), CEM-C7-14 (B) and Molt4 (C) cells in different conditions including untreated group (lane 1), 1 μM Dex (lane 2), 1 and 10 μM Thapsigargin (lanes 3-4), and combination treatment of 1 μM Dex with 1 and 10 μM Thapsigargin (lanes 5-6). The results are representative of 3 independent experiments. Error bars represent ± SEM (* $p < 0.05$, ** $p < 0.01$, *** $p < 0.001$, *student t.test*). Each sample was compared to untreated control.

4.4 Reactive oxygen species generation in Dexamethasone and Rotenone treated leukemia cells

In order to determine the role of oxidative stress and ROS generation in glucocorticoid treatment, Dex and ROT were used individually and in combination to measure ROS level in ALL cells. Dex and ROT were added for 24 hrs to leukemia cells and flow cytometer used for analysis. The results showed that ROT alone substantially increased ROS production in CEM-C1-15 and CEM-C7-14 cells in dose dependent manner (Figure 4-3 A and B, lane 3 and 4) and the combination treatment with Dex significantly increased ROS level in CEM-C1-15 and CEM-C7-14 cells (Figure 4-3 A and B, lane 5 and 6). However, decreased ROS production in Dex and 1 μM ROT CEM-C7-14 treated cells when compared to ROT alone has been observed (Figure 4-3 B lane 3 and 5). Molt4 cells did not change ROS levels when treated with ROT alone or when ROT was combined with Dex.

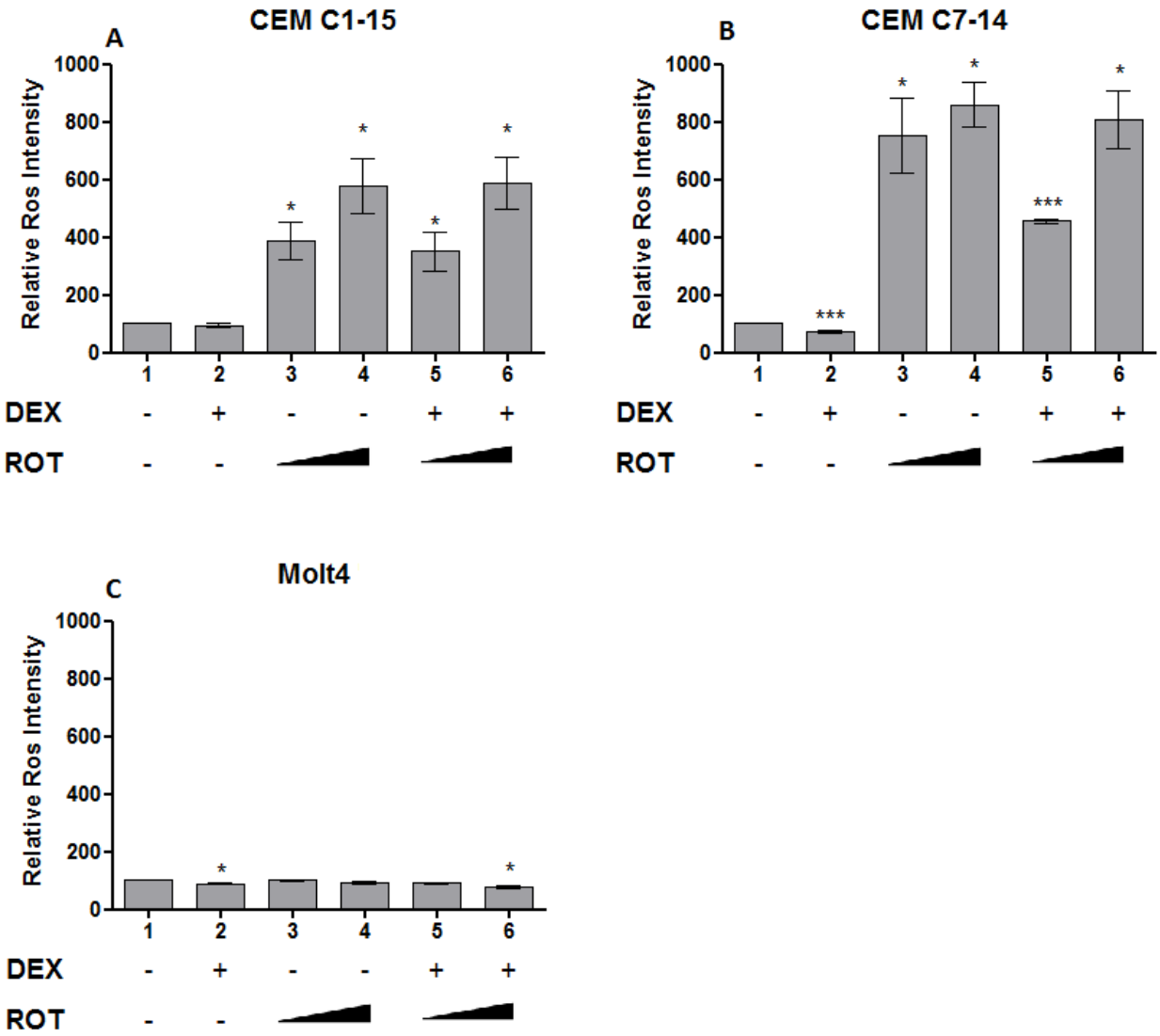

Figure 4-3 Reactive oxygen species generation in CEM-C1-15, CEM-C7-14 and Molt4 cells treated with Rotenone and Dexamethasone

The figures show the relative ROS generation intensity in CEM-C1-15 (A), CEM-C7-14 (B) and Molt4 (C) cells in different conditions including untreated group (lane 1), 1 μM Dex (lane 2), 1 and 10 μM Rotenone (lanes 3-4), and combination treatment of 1 μM Dex with 1 and 10 μM Rotenone (lanes 5-6). The results are representative of 3 independent experiments. Error bars represent ± SEM (* $p < 0.05$, ** $p < 0.01$, *** $p < 0.001$, *student t.test*). Each sample was compared to untreated control.

4.5 Reactive oxygen species generation in Dexamethasone and Bortezomib treated leukemia cells

In order to determine the role of unfolded protein response and ROS generation in glucocorticoid treatment, Dex and BTZ were used individually and in combination to measure ROS level in ALL cells. Dex and BTZ were added for 24 hrs to leukemia cells and results obtained using flow cytometer. The results showed that ROS production decreased significantly in BTZ alone treatment in CEM-C1-15 cells at 2 nM BTZ and CEM-C7-14 cells at 2 and 5 nM (Figure 4-4 A and B, lane 3 and 4) while BTZ did not change ROS level in Molt4 cells. The combination treatment with Dex significantly decreased ROS generation in CEM cells in dose dependent manner (Figure 4-4 A and B, lane 5 and 6) but not in Molt4 (Figure 4-4 C lane 5 and 6).

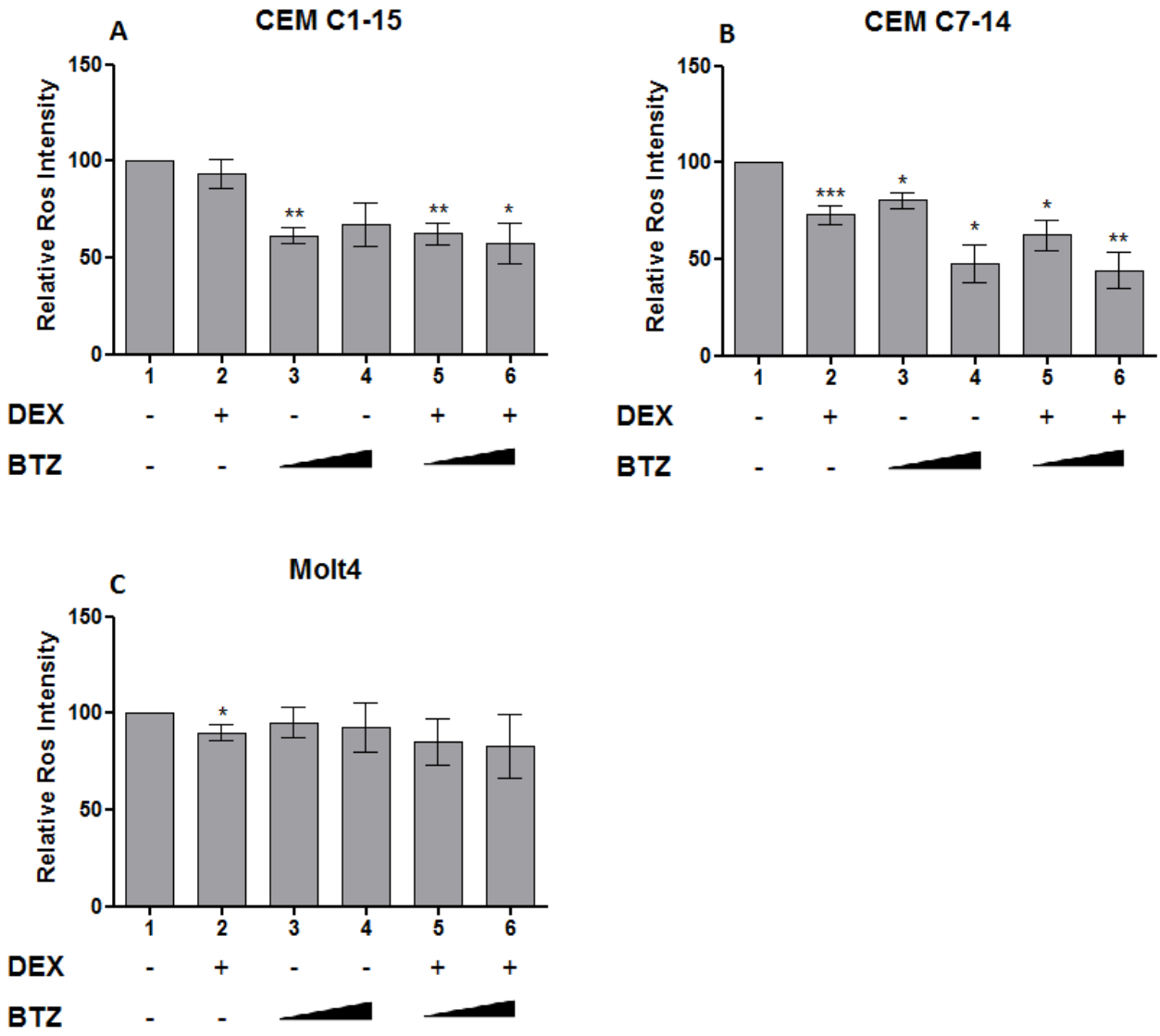

Figure 4-4 Reactive oxygen species generation in CEM-C1-15, CEM-C7-14 and Molt4 cells treated with Bortezomib and Dexamethasone

The figures show the relative ROS generation intensity in CEM-C1-15 (A), CEM-C7-14 (B) and Molt4 (C) cells in different conditions including untreated group (lane 1), 1 μM Dex (lane 2), 2 and 5 nM Bortezomib (lanes 3-4), and combination treatment of 1 μM Dex with 2 and 5 nM Bortezomib (lanes 5-6). The results are representative of 3 independent experiments. Error bars represent ± SEM (* $p < 0.05$, ** $p < 0.01$, *** $p < 0.001$, *student t.test*). Each sample was compared to untreated control.

4.6 Conclusion

Dexamethasone treatment significantly decreased reactive oxygen species (ROS) levels in GC-sensitive cells and Molt4 after 24 hrs. However, there was no alteration of ROS level in CEM-C1-15 cells treated with Dex. Chloroquine decreased ROS production only in CEM-C1-15 cells when the single treatment was performed whereas the combination treatment decreased ROS in CEM cells. Thapsigargin caused decrease in ROS levels in all cell lines when used alone and in combination with Dex. Rotenone substantially increased ROS generation in CEM cells in dose dependent manner in both individual and combination treatments. Bortezomib decreased ROS production in CEM cells but not in Molt4.

CHAPTER 5 AUTOPHAGY, ER STRESS AND UNFOLDED PROTEIN RESPONSE IN LEUKEMIA CELLS

5.1 Analysis of individual and combined drugs treatments on protein expression levels in leukemia cells

To investigate the effect of drugs on endogenous protein expression alteration, the immunoblotting technique was used. Cell lysates were collected for protein extraction after 48 hrs of incubation with studied drugs and western blots were performed to detect ER stress related chaperone protein levels including GRP94 and GRP78 or autophagic protein levels such as Beclin1 and LC3. Protein intensities quantification was carried out using ImageJ software and statistical analysis carried out using GraphPad prism software.

5.1.1 Protein expression levels in Dexamethasone and Chloroquine treated leukemia cells

In order to determine effect of steroids and autophagy inhibition on endogenous protein levels, Dexamethasone 1 µM and Chloroquine 10, 20 and 50 µM individual and in combination were used to treat CEM-C1-15, Molt4 and CEM-C7-14 cells. Endogenous protein intensities of GRP94, GRP78, Beclin1, LC3 I and II were analysed using actin as loading control (Figure 5-1). The results indicated that Dex alone significantly increased GRP94 protein expression level in CEM-C7-14 cells, there were no changes in CEM-C1-15 and Molt4 cells (Figure 5-2 A, lane 2 compare to lane 1). GRP94 protein levels were not changed in CLQ alone treatment except in CEM-C1-15 cells, which significantly increased GRP94 expressions, but increasing trends of GRP94 level were observed in CEM-C7-14 when combined with Dex (Figure 5-2 A, lanes 6 to 8 grey bars). In addition, GRP78 level significantly increased in Dex alone treated GC-sensitive cells (Figure 5-2 B, lane 2 grey bar) and the increasing trend of GRP78 protein was observed in CEM-C7-14 when CLQ was used with combination conditions (Figure 5-2 B, lanes 6 to 8 grey bars).

Beclin1 levels were not changed by Dex treatment in all cells (Figure 5-2 C, lane 2). LC3 II / LC3 I ratio, which can be used to analyse the autophagy process, significantly increased in Molt4 cells but decreased in CEM-C7-14 cells treated by Dex alone (Figure 5-2 D, lane 2 light grey bar and grey bar). There were increasing trends of LC3 II / LC3 I ratio in CLQ alone treated cells and in combination conditions with Dex in all cells (Figure 5-2 D, lanes 3 to 8 compare to lane 1).

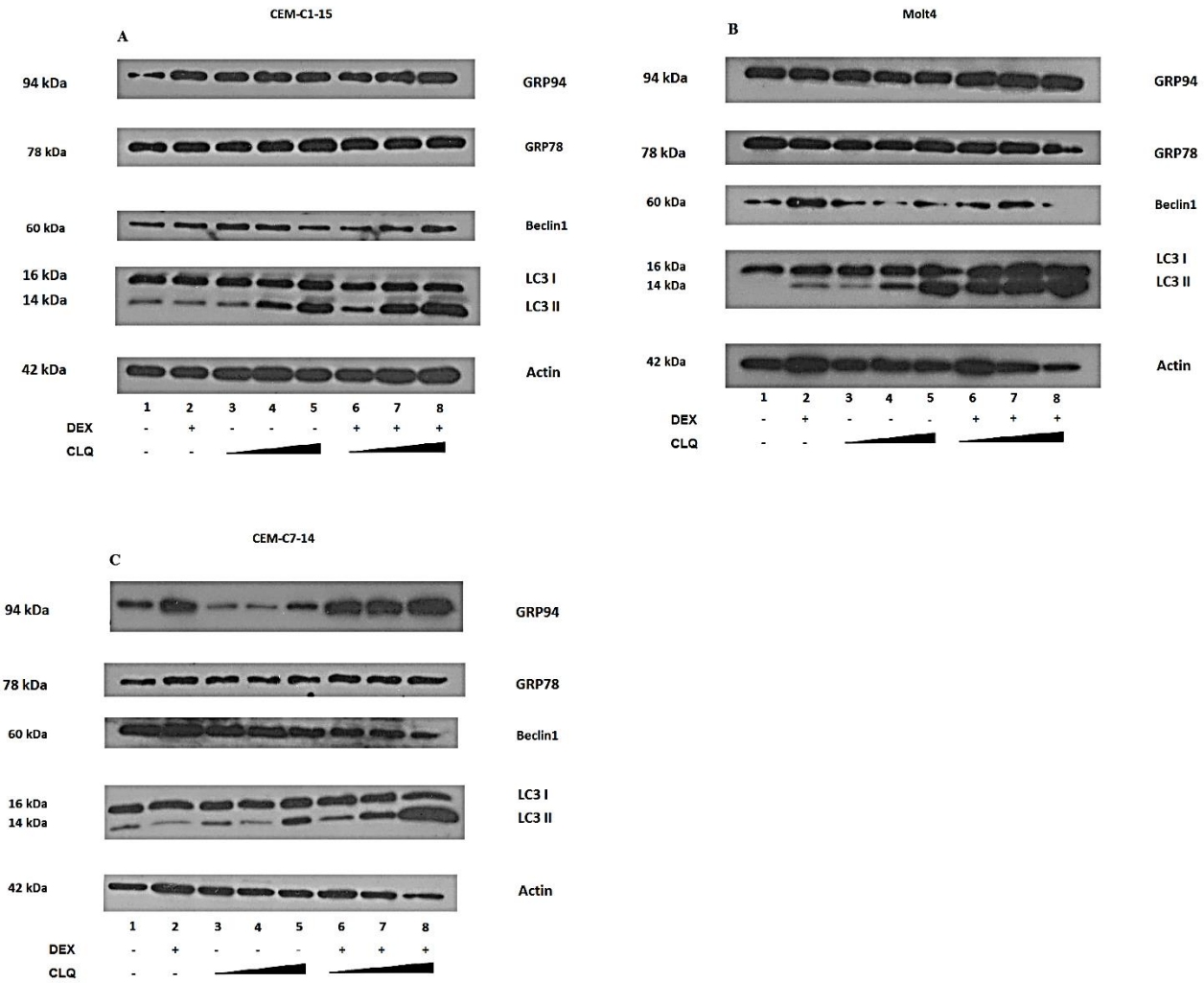

Figure 5-1 Protein levels in CEM-C1-15, CEM-C7-14 and Molt4 cells treated with Chloroquine and Dexamethasone

The figures show representative protein intensities of GRP94, GRP78, Beclin1, LC3 and Actin as loading control protein in CEM-C1-15 (A), Molt4 (B) and CEM-C7-14 (C) cells in different conditions including untreated group (lane 1), 1 μM Dex (lane 2), 10, 20 and 50 μM of Chloroquine (lanes 3-5), and combination treatment of 1 μM Dex with 10, 20 and 50 μM Chloroquine (lanes 6-8), respectively.

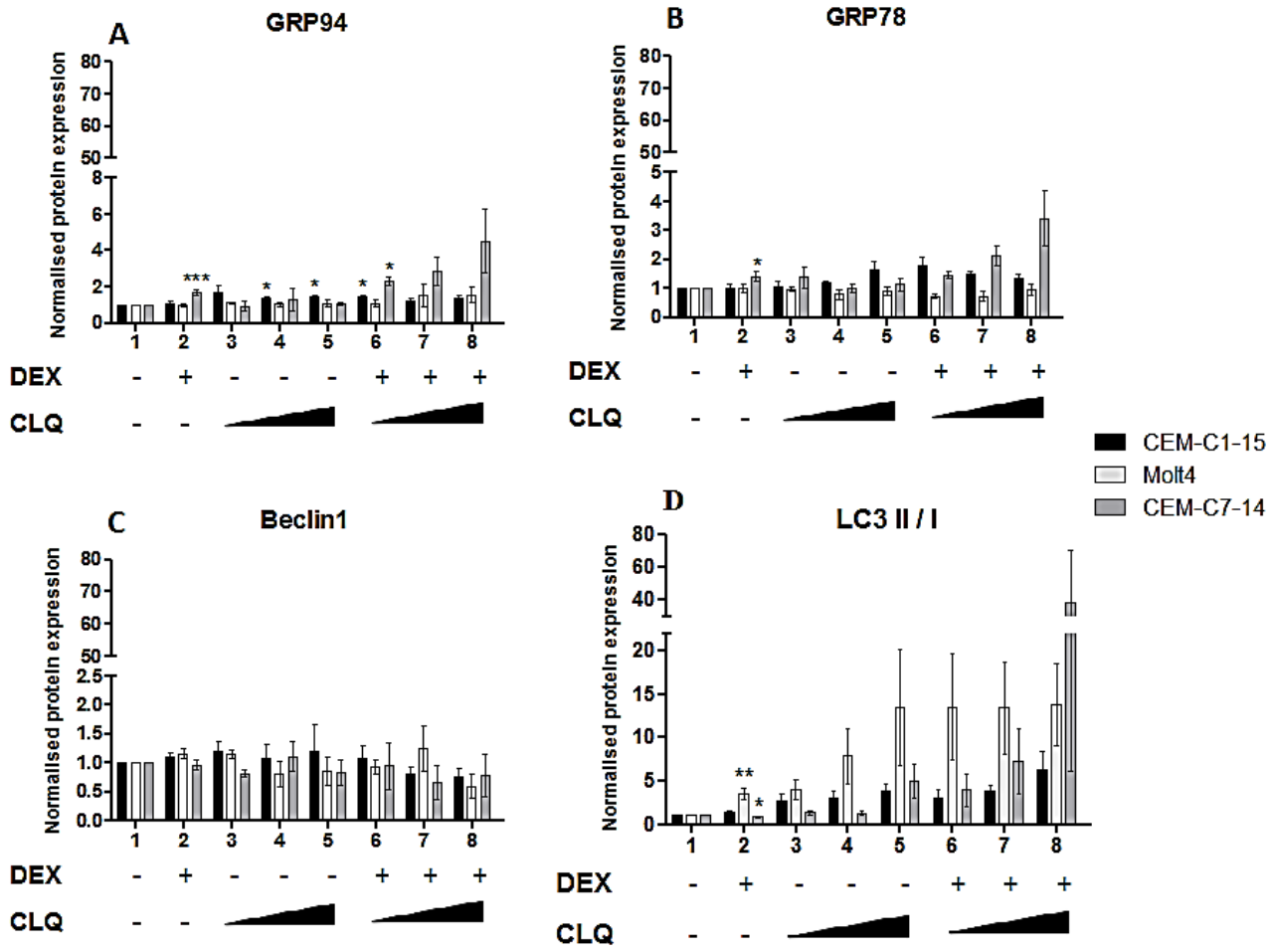

Figure 5-2 Protein expression levels in CEM-C1-15, Molt4 and CEM-C7-14 Chloroquine and Dex treated cells.

The figures show the relative protein intensities of GRP94 (A), GRP78 (B), Beclin1 (C) and LC3 II / I (D) in CEM-C1-15 (black bars), Molt4 (light grey bars) and CEM-C7-14 (grey bars) cells in different conditions including untreated group (lane 1), 1 μM Dex (lane 2), 10, 20 and 50 μM Chloroquine (lanes 3-5), and combination treatment of 1 μM Dex with 10, 20 and 50 μM Chloroquine (lanes 6-8). The results are representative of 3 independent experiments. Error bars represent ± SEM. (* $p < 0.05$, ** $p < 0.01$, *** $p < 0.001$, *student t.test*). The values were normalised to the corresponding actin loading control and each sample was compared to untreated control.

5.1.2 Protein expression levels in Dexamethasone and Thapsigargin treated leukemia cells

In order to determine effect of glucocorticoid and ER stress conditions on endogenous levels of proteins that mark ER stress and autophagy processes, Dexamethasone 1 μM and Thapsigargin 1 and 10 μM were used to treat individually and in combination leukemia cells as described above (Figure 5-3).

The results indicate that GRP94 and GRP78 proteins expression levels were increased substantially by TG and Dex in combination treatment of GC-sensitive cells (Figure 5-4 A and B, lanes 5 and 6 grey bars compare to lane 1). In TG alone treated Molt4 cells, GRP94 levels were increased (Figure 5-4 A, lanes 3 and 4 light grey bars). Beclin1 protein levels increased in TG alone and combination treated CEM-C7-14 cells while decreasing trend was observed in CEM-C1-15 and Molt4 cells (Figure 5-4 C, lanes 3 to 6). TG alone and combined with Dex increased LC3 II / I ratio in GC-resistant cells (Figure 5-4 D, lanes 3 to 6 black bars and light grey bars) while TG alone increased LC3 II / I ratio in GC-sensitive cells (Figure 5-4 D, lanes 3 and 4 grey bars). Finally, Dex decreased LC3 expression in GC-sensitive cell in combination treatments (Figure 5-4 D, lanes 2, 5 and 6 grey bars compare to lane 1).

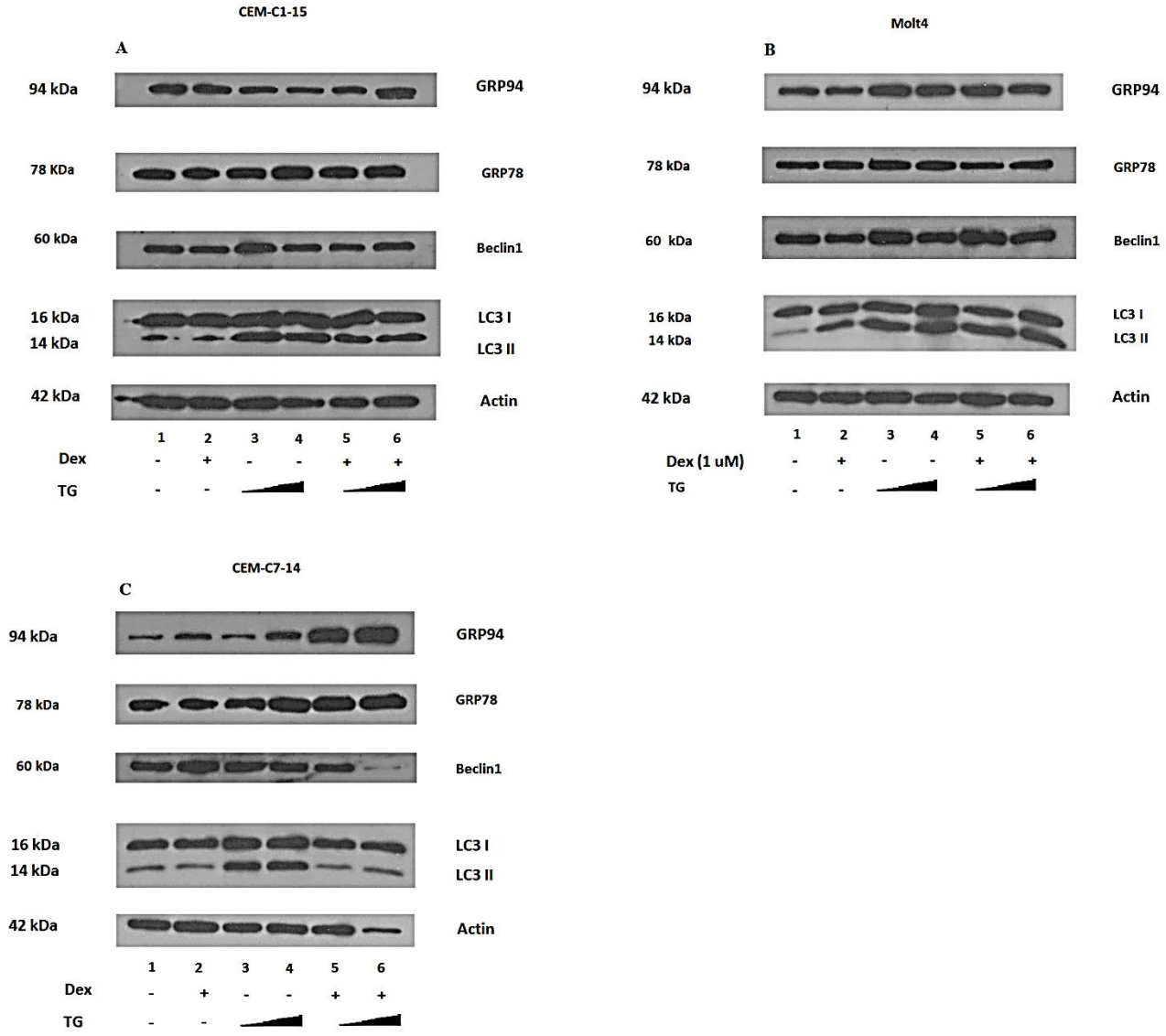

Figure 5-3 Protein levels in CEM-C1-15, CEM-C7-14 and Molt4 cells treated with Thapsigargin and Dexamethasone

The figures show representative protein intensities of GRP94, GRP78, Beclin1, LC3 and Actin as loading control protein in CEM-C1-15 (A), Molt4 (B) and CEM-C7-14 (C) cells in different conditions including untreated group (lane 1), 1 μM Dex (lane 2), 1 and 10 μM of Thapsigargin (lanes 3-4), and combination treatment of 1 μM Dex with 1 and 10 μM Thapsigargin (lanes 5-6), respectively.

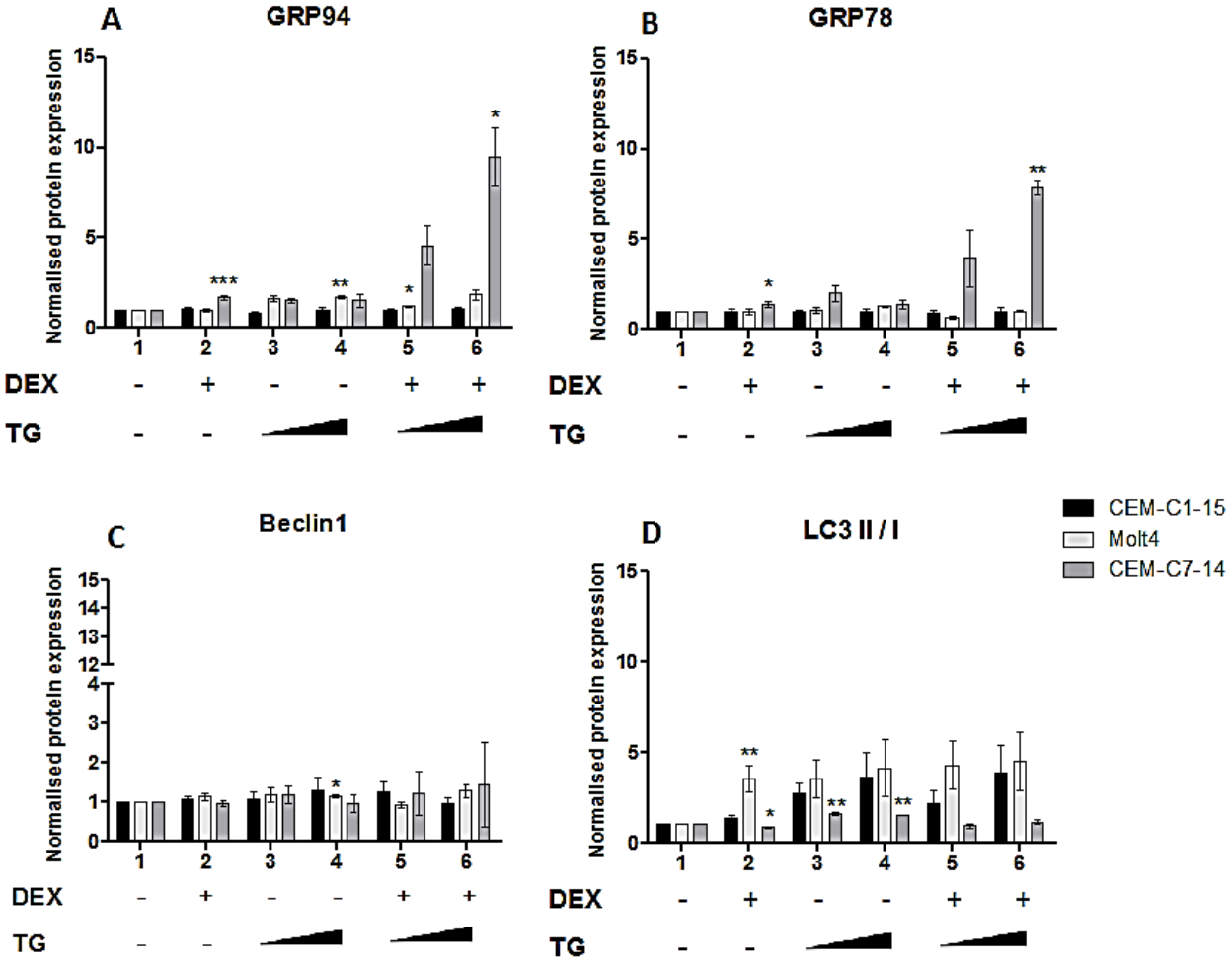

Figure 5-4 Protein expression levels in CEM-C1-15, Molt4 and CEM-C7-14 Thapsigargin and Dex treated cells

The figures show the relative protein intensities of GRP94 (A), GRP78 (B), Beclin1 (C) and LC3 II / I (D) in CEM-C1-15 (black bars), Molt4 (light grey bars) and CEM-C7-14 (grey bars) cells in different conditions including untreated group (lane 1), 1 μM Dex (lane 2), 1 and 10 μM Thapsigargin (lanes 3-4), and combination treatment of 1 μM Dex with 1 and 10 μM Thapsigargin (lanes 5-6). The results are representative of 3 independent experiments. Error bars represent ± SEM. (* $p < 0.05$, ** $p < 0.01$, *** $p < 0.001$, *student t.test*). The values were normalised to the corresponding actin loading control and each sample was compared to untreated control.

5.1.3 Protein expression levels in Dexamethasone and Rotenone treated leukemia cells

To investigate effect of glucocorticoid and reactive oxygen species production on endogenous levels of proteins that mark ER stress and autophagy processes, Dexamethasone 1 μM and Rotenone 1 and 10 μM were used to treat individually and in combination leukemia cells and follow protein levels as described above. (Figure 5-5).

The results indicate that GRP94 expression levels were increased by ROT alone and combination treatment in CEM cells (Figure 5-6 A, lanes 3 to 6 black bars and grey bars compare to lane 1). The opposite trends were observed in Molt4 cells treated with ROT alone and in combination conditions (Figure 5-6 A, lanes 3 to 6 light grey bars). GRP78 levels were increased in CEM-C7-14 cells treated with ROT alone and in combination conditions while no significant changes were observed in Molt4 cells (Figure 5-6 B, lanes 3 to 6 light grey bars and grey bars). Beclin1 levels had increased trends in Molt4 cells while increased trends of Beclin1 levels were observed in CEM-C1-15 cells treated with ROT alone and in combination treatments (Figure 5-6 C, lanes 3 to 6 light grey bars and black bars). There were no changes of Beclin1 expression levels in Dex and ROT treated CEM-C7-14 cells. The LC3 expression ratios did not change significantly in ROT alone and combination conditions treated cells when compared to control (Figure 5-6 D, lanes 3 to 6 compare to lane 1).

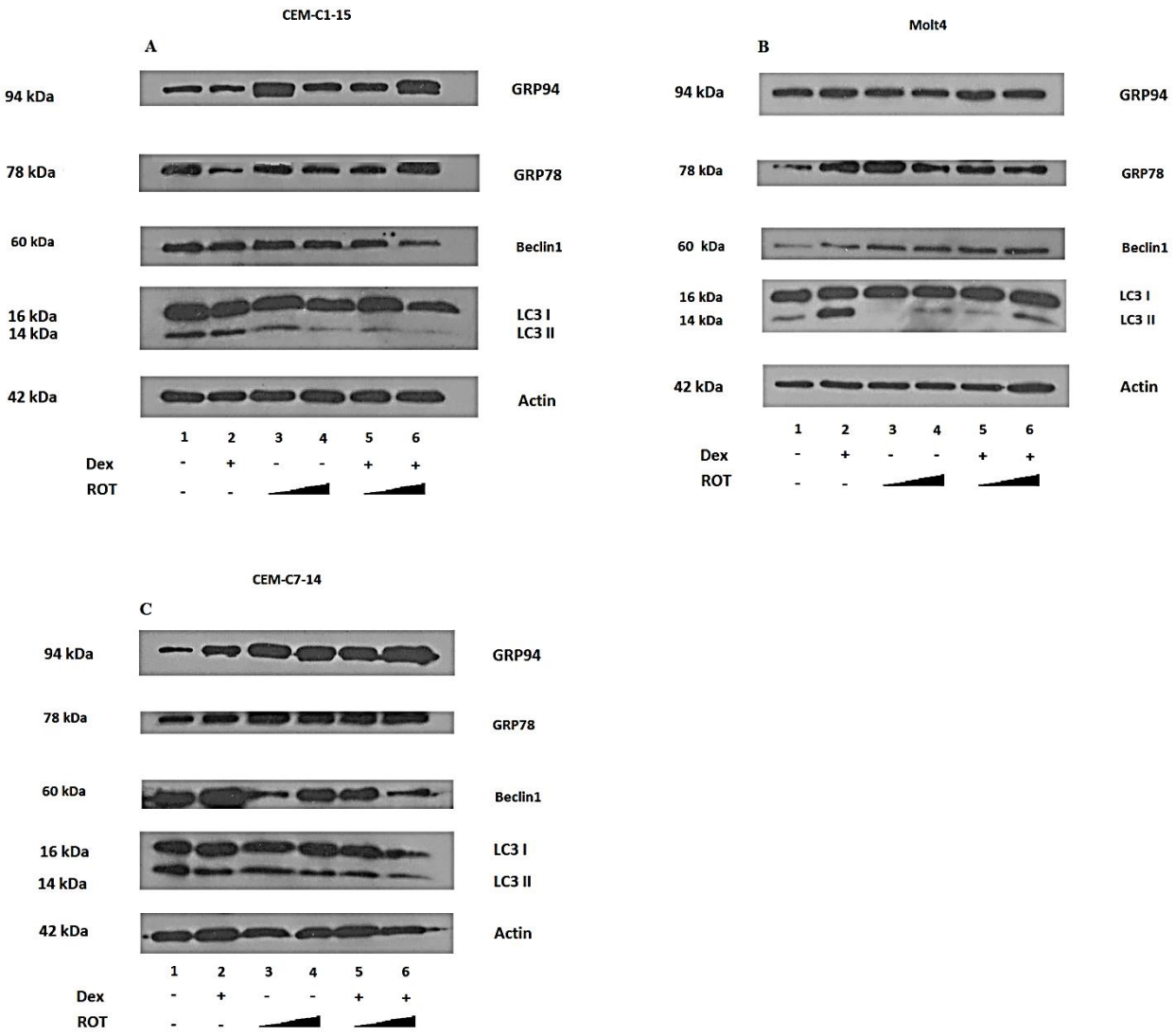

Figure 5-5 Protein levels in CEM-C1-15, CEM-C7-14 and Molt4 cells treated with Rotenone and Dexamethasone

The figures show representative protein intensities of GRP94, GRP78, Beclin1, LC3 and Actin as loading control protein in CEM-C1-15 (A), Molt4 (B) and CEM-C7-14 (C) cells in different conditions including untreated group (lane 1), 1 μM Dex (lane 2), 1 and 10 μM of Rotenone (lanes 3-4), and combination treatment of 1 μM Dex with 1 and 10 μM Rotenone (lanes 5-6), respectively.

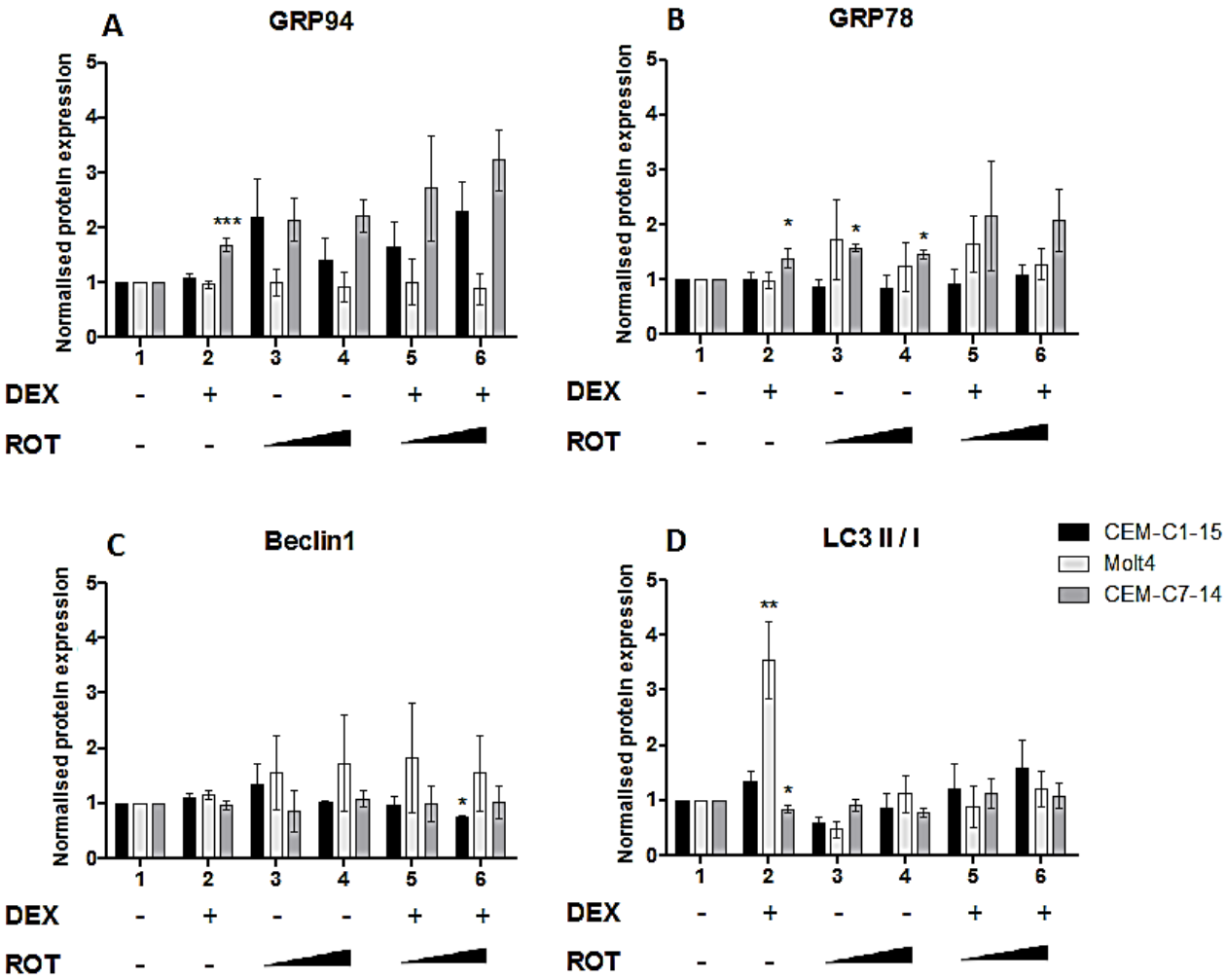

Figure 5-6 Protein expression levels in CEM-C1-15, Molt4 and CEM-C7-14 Rotenone and Dex treated cells

The figures show the relative protein intensities of GRP94 (A), GRP78 (B), Beclin1 (C) and LC3 II / I (D) in CEM-C1-15 (black bars), Molt4 (light grey bars) and CEM-C7-14 (grey bars) cells in different conditions including untreated group (lane 1), 1 μM Dex (lane 2), 1 and 10 μM Rotenone (lanes 3-4), and combination treatment of 1 μM Dex with 1 and 10 μM Rotenone (lanes 5-6). The results are representative of 3 independent experiments. Error bars represent ± SEM. (* $p < 0.05$, ** $p < 0.01$, *** $p < 0.001$, *student t.test*). The values were normalised to the corresponding actin loading control and each sample was compared to untreated control.

5.1.4 Protein expression levels in Dexamethasone and Bortezomib treated leukemia cells

In order to determine effect of glucocorticoid, ER stress and unfolded protein response on endogenous levels of proteins that mark ER stress and autophagy processes, Dexamethasone 1 µM and Bortezomib 2 and 5 nM were used to treat individually and in combination leukemia cells as described previously (Figure 5-7).

The results show that GRP chaperone proteins were increased in CEM-C1-15 cells treated with 5 nM BTZ alone and in combination with Dex (Figure 5-8 A and B, lanes 4 and 5 black bars). Decreased protein expression level of Beclin1 were observed in BTZ alone and combination treated CEM-C1-15 cells, while there was no change in expression levels in Molt4 and CEM-C7-14 cells (Figure 5-8 C, lanes 3 to 6). LC3 II / I ratios were not changed by BTZ alone and combination with Dex treatment in Molt4 and CEM-C7-14 cells (Figure 5-8 D, lanes 3 to 6 light grey bars and grey bars).

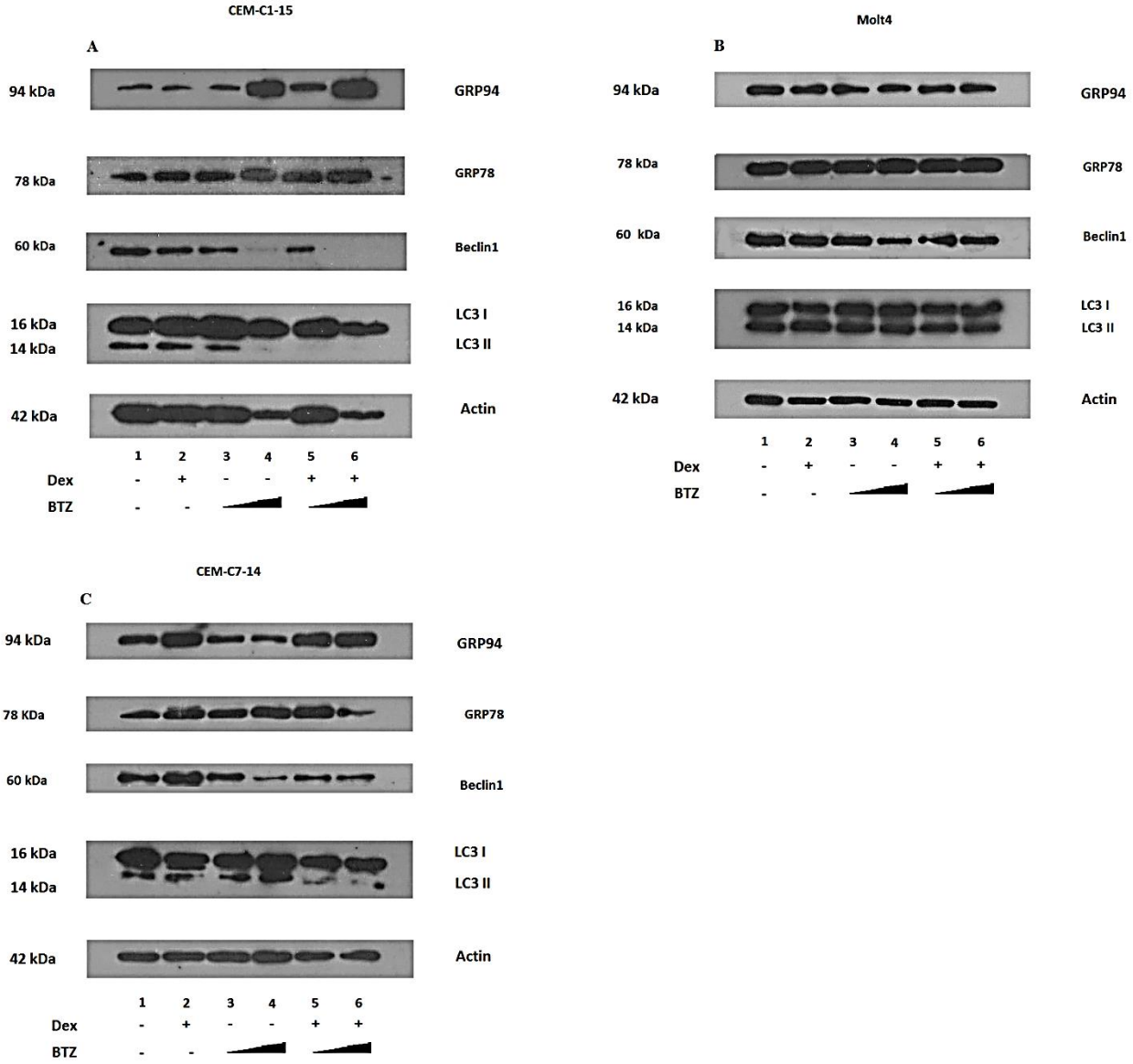

Figure 5-7 Protein levels in CEM-C1-15, CEM-C7-14 and Molt4 cells treated with Bortezomib and Dexamethasone

The figures show representative protein intensities of GRP94, GRP78, Beclin1, LC3 and Actin as loading control protein in CEM-C1-15 (A), Molt4 (B) and CEM-C7-14 (C) cells in different conditions including untreated group (lane 1), 1 μM Dex (lane 2), 2 and 5 nM of Bortezomib (lanes 3-4), and combination treatment of 1 μM Dex with 2 and 5 nM Bortezomib (lanes 5-6), respectively.

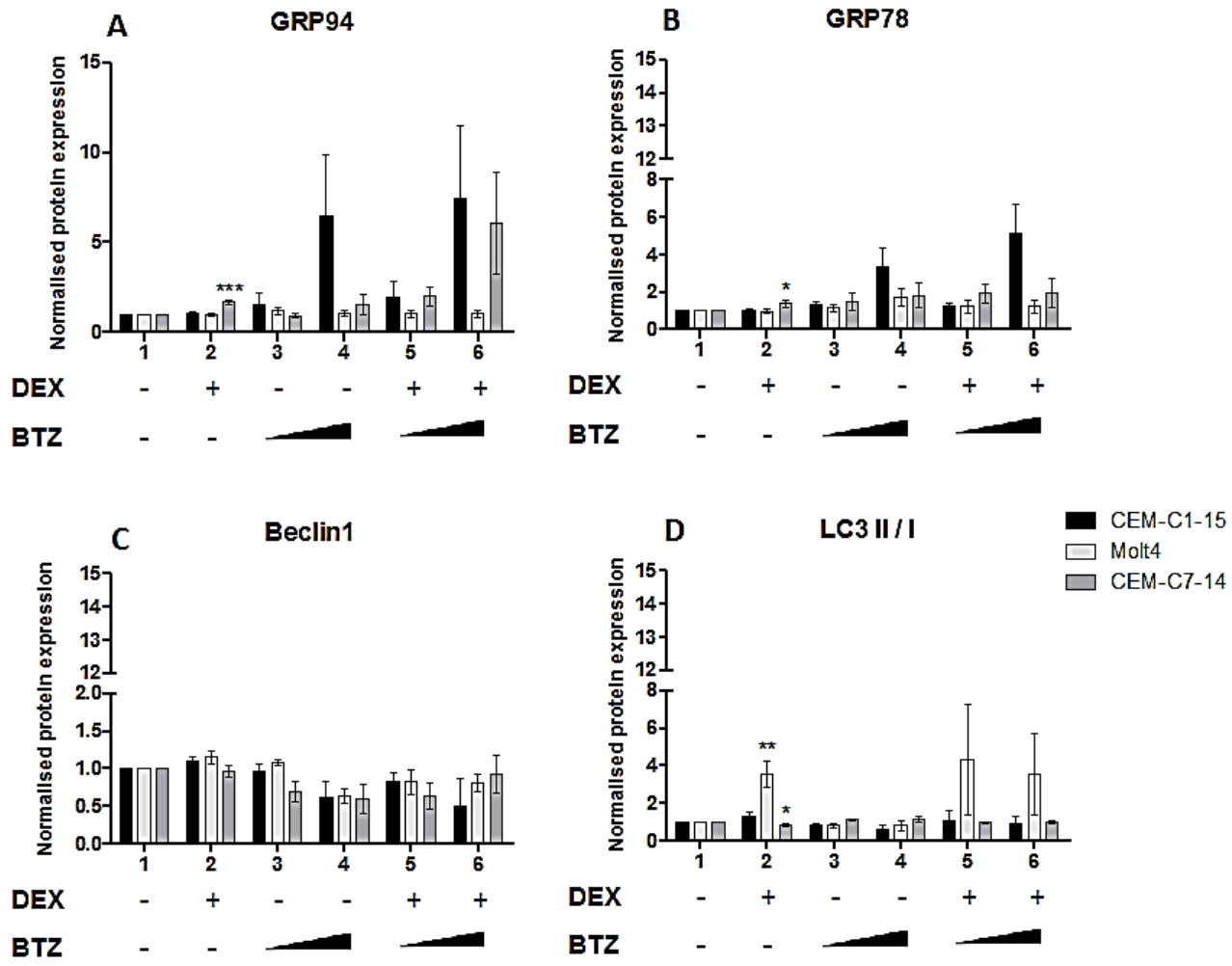

Figure 5-8 Protein expression levels in CEM-C1-15, Molt4 and CEM-C7-14 Bortezomib and Dex treated cells

The figures show the relative protein intensities of GRP94 (A), GRP78 (B), Beclin1 (C) and LC3 II / I (D) in CEM-C1-15 (black bars), Molt4 (light grey bars) and CEM-C7-14 (grey bars) cells in different conditions including untreated group (lane 1), 1 μM Dex (lane 2), 2 and 5 nM Bortezomib (lanes 3-4), and combination treatment of 1 μM Dex with 2 and 5 nM Bortezomib (lanes 5-6). The results are representative of 3 independent experiments. Error bars represent ± SEM. (* $p < 0.05$, ** $p < 0.01$, *** $p < 0.001$, *student t.test*). The values were normalised to the corresponding actin loading control and each sample was compared to untreated control.

5.1.5 Conclusion

In summary, Dexamethasone significantly increased chaperone proteins in GC-sensitive cells while Beclin1 expression levels were not changed. LC3 II / I ratio increased in Molt4 cells treated with Dexamethasone and Chloroquine. GRPs expression levels were increased in combination treatment of Thapsigargin and Dexamethasone in GC-sensitive cells. Rotenone increased GRP94 in CEMs cells while GRP78 levels were increased in GC-sensitive cells. CLQ and BTZ increased chaperones proteins expression levels in CEM-C1-15 cells.

5.2 Determination of individual and combined drugs treatments on mRNA expression levels in leukemia cells

To determine levels of gene expression of above studied proteins, mRNA levels were measured. After 24 hours of incubation time, RNA was isolated from cellular extract and cDNA synthesised. The quantitative polymerase chain reaction was performed to quantify mRNA expression level in desired drugs treatments. The mRNA level quantification was analysed using Rotor Gene Q Series software and statistical analysis done using GraphPad prism software.

5.2.1 The mRNA expression levels in Dexamethasone, Thapsigargin and Bortezomib treated leukemia cells

In order to determine the role of ER stress and unfolded protein response in glucocorticoid mediated transcriptional regulation, Dex, BTZ (5 nM) and TG (10 µM) were used individually and in combination to measure mRNA expression level of GRP94, GRP78 which are markers of ER stress condition and Beclin1 and LC3 which are related to autophagy in ALL cells. After seeding the cells in 6-well plates, Dex, BTZ and TG were added for 24 hrs.

The result showed that GRP94 levels increased in TG treated alone and in combination with Dex CEM-C1-15, Molt4 and CEM-C7-14 cells, when compared to untreated condition (Figure 5-9, lane 4 and 6 compare with lane 1). GRP94 level was not changed by Dex treatment in CEM cells while decrease of GRP94 was observed in Molt4 cells (Figure 5-9 B, lane 2). BTZ affected GPR94 mRNA level in GC-sensitive cells when treated alone (Figure 5-9 C, lane 3).

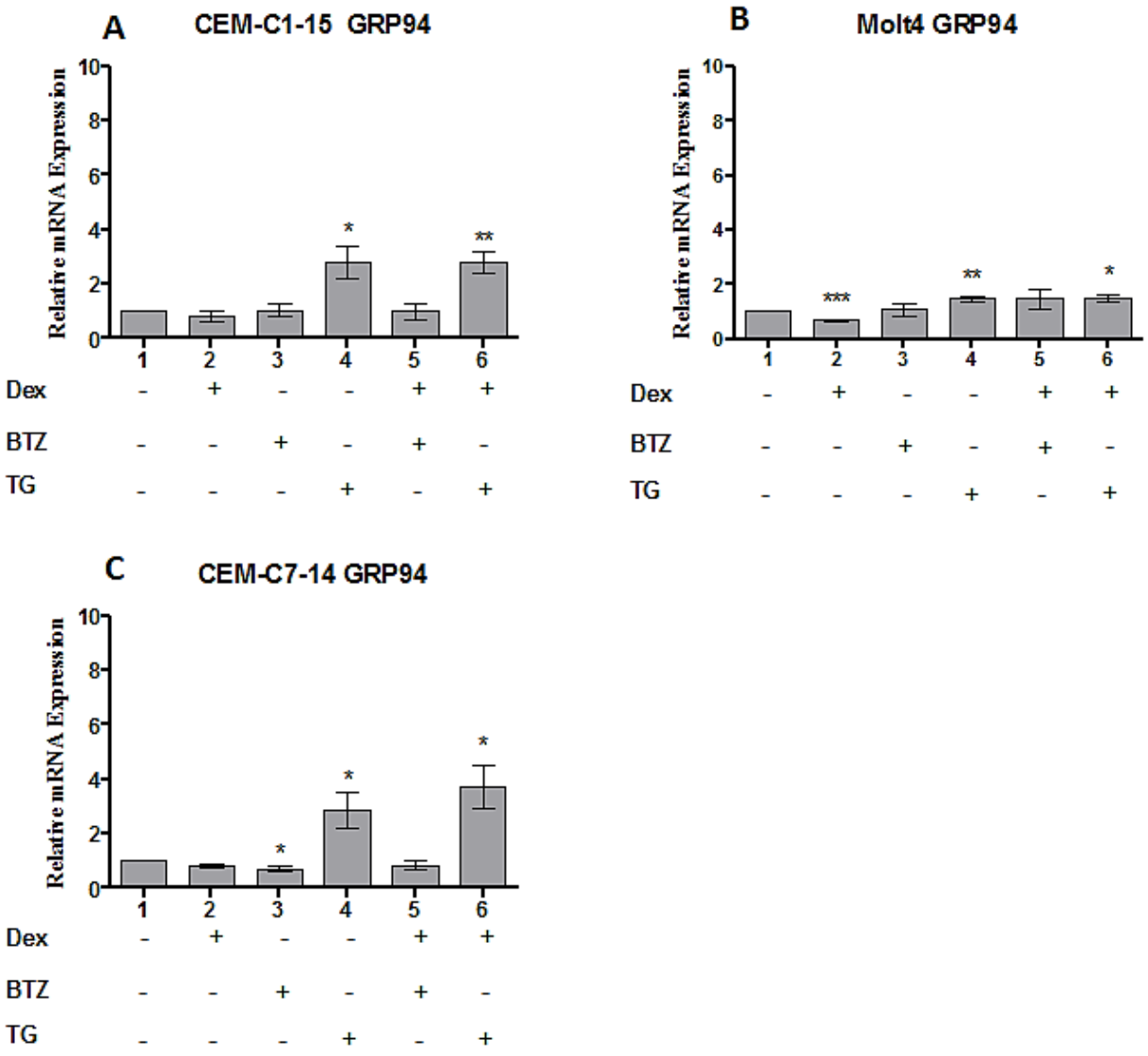

Figure 5-9 mRNA expression levels of GRP94 in Dex, BTZ and TG treated leukemia cells

Bar charts show relative GRP94 mRNA expression levels upon 24 hrs incubation time with 1 µM Dex (lane 2), 5 nM BTZ (lane 3), 10 µM TG (lane 4), combination treatment of Dex with BTZ (lane 5) and TG (lane 6) in CEM-C1-15 (A), Molt4 (B) and CEM-C7-14 (C) cells. The results are representative of 3 independent experiments. Error bars represent ± SEM (* $p < 0.05$, ** $p < 0.01$, *** $p < 0.001$, *student t.test*). The values were normalised to the corresponding *RPL19* internal control and each sample was compared to untreated control.

GRP78 mRNA expression levels substantially increased by TG alone treatment and in combination with Dex in all cells after 24 hrs (Figure 5-10, lane 4 and 6 compare to lane 1). GRP78 mRNA levels in GC-sensitive cell decreased when BTZ alone and in combination with Dex was used (Figure 5-10 C, lane 3 and 5) while GRP78 was not changed in CEM-C1-15 and Molt4 cells.

To determine the level of Beclin1 and LC3 gene expression upon glucocorticoid and ER stress conditions mRNA expression levels were determined. The result showed that Beclin1 mRNA expression levels increased in Dex treated GC-sensitive cell while increase of Beclin1 has been observed in Molt4 cells. Dex had no significant effect on Beclin1 level in CEM-C1-15 cells (Figure 5-11, lane 2 compare to lane 1). BTZ had no effect on the level of Beclin1 mRNA except in CEM-C1-15 cells when Dex and BTZ were used in combination. TG alone and combination treatment significantly increased Beclin1 mRNA level in all cells (Figure 5-11, lane 4 and 6 compare to lane 1).

BTZ alone and combination treatment increased LC3 mRNA expression levels in GC-resistant cells (Figure 5-12 A and B, lane 3 and 5) while only combined treatment with Dex increased LC3 level in CEM-C7-14 cells (Figure 5-12 C, lane 5). LC3 mRNA level substantially increased in TG alone and combination treatment in all cells and the Molt4 cells were more sensitive to TG than CEMs by expressing LC3 levels higher than 10 times when compared to control group (Figure 5-12 B, lane 4 and 6 compare to lane 1).

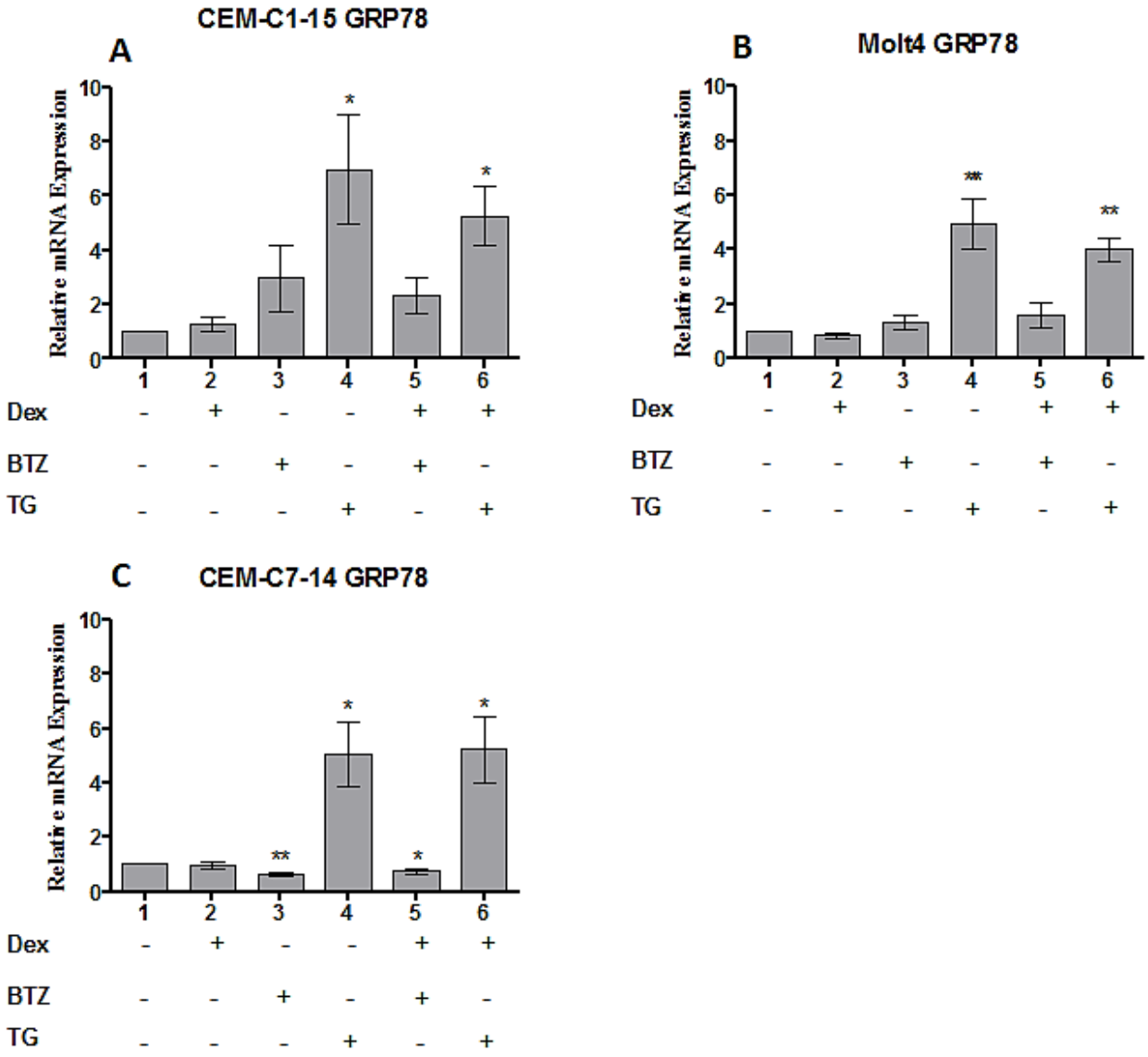

Figure 5-10 mRNA expression levels of GRP78 in Dex, BTZ and TG treated leukemia cells

Bar charts show relative GRP78 mRNA expression levels in 24 hrs incubation time of 1 µM Dex (lane 2), 5 nM BTZ (lane 3), 10 µM TG (lane 4), combination treatment of Dex with BTZ (lane 5) and TG (lane 6) in CEM-C1-15 (A), Molt4 (B) and CEM-C7-14 (C) cells. The results are representative of 3 independent experiments. Error bars represent ± SEM (* $p < 0.05$, ** $p < 0.01$, *** $p < 0.001$, *student t.test*). The values were normalised to the corresponding *RPL19* internal control and each sample was compared to untreated control.

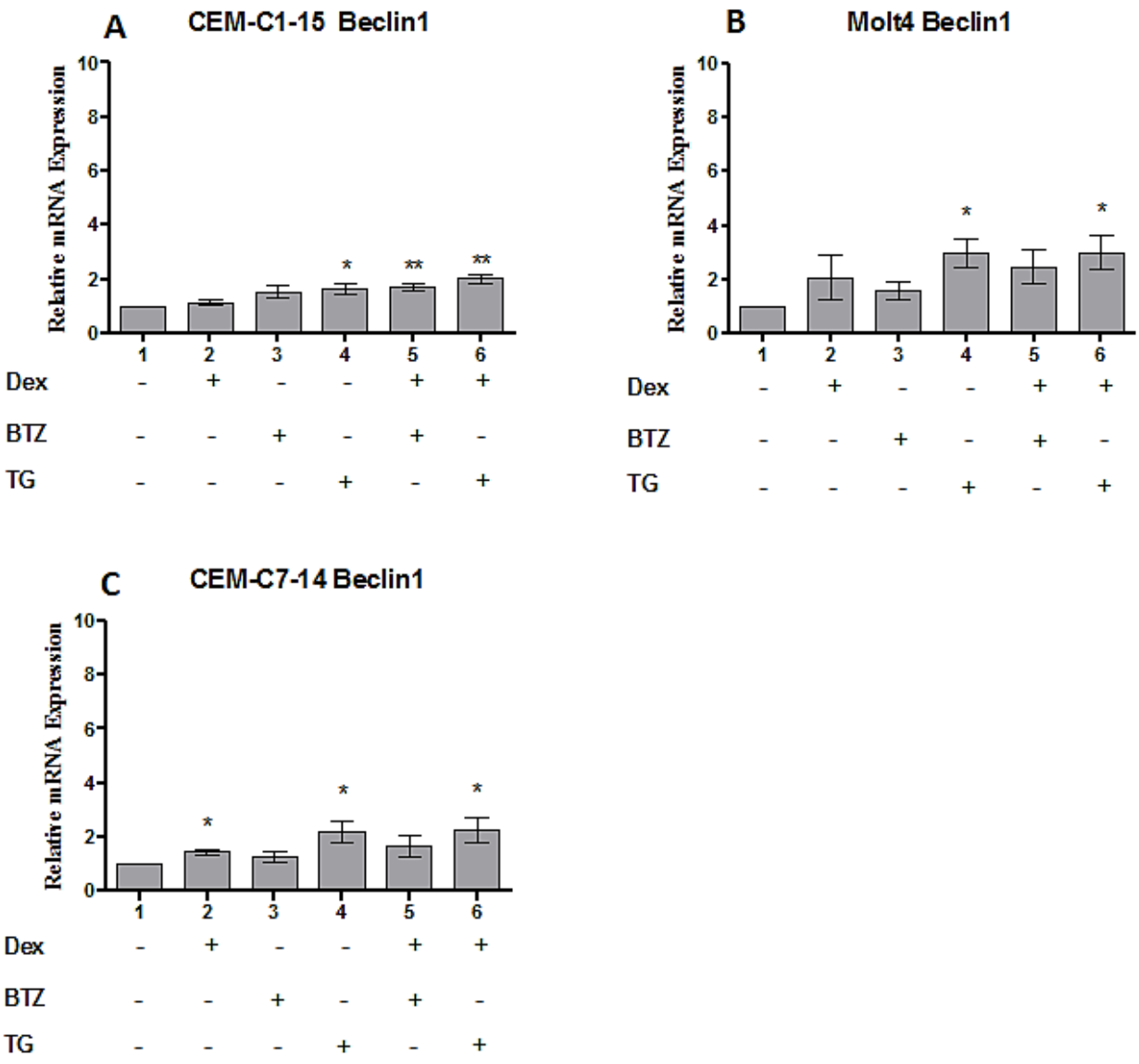

Figure 5-11 mRNA expression levels of Beclin1 in Dex, BTZ and TG treated leukemia cells

Bar charts show relative Beclin1 mRNA expression levels in 24 hrs incubation time of 1 µM Dex (lane 2), 5 nM BTZ (lane 3), 10 µM TG (lane 4), combination treatment of Dex with BTZ (lane 5) and TG (lane 6) in CEM-C1-15 (A), Molt4 (B) and CEM-C7-14 (C) cells. The results are representative of 3 independent experiments. Error bars represent ± SEM (* $p < 0.05$, ** $p < 0.01$, *** $p < 0.001$, *student t.test*). The values were normalised to the corresponding *RPL19* internal control and each sample was compared to untreated control.

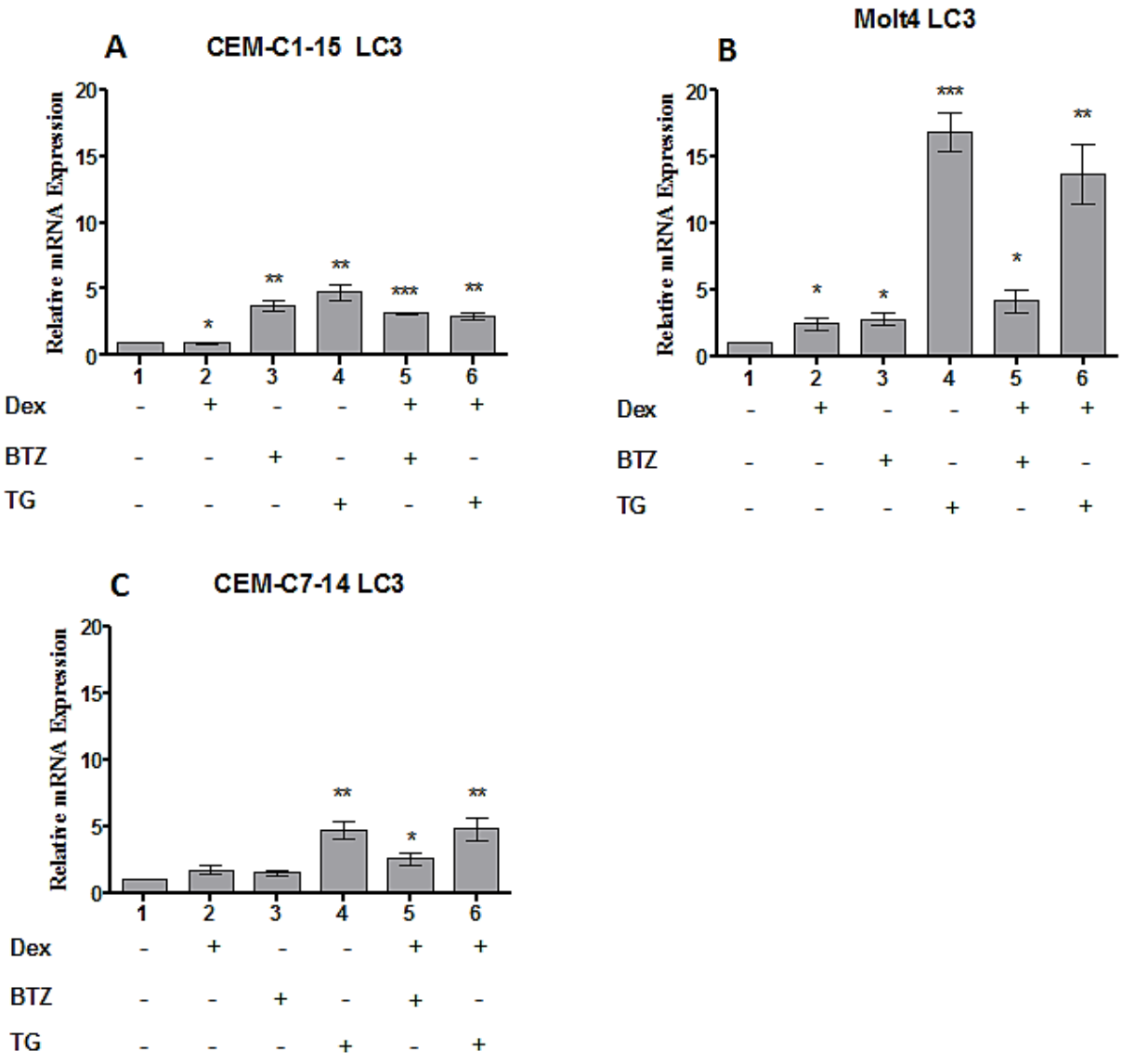

Figure 5-12 mRNA expression levels of LC3 in Dex, BTZ and TG treated leukemia cells

Bar charts show relative LC3 mRNA expression levels in 24 hrs incubation time of 1 µM Dex (lane 2), 5 nM BTZ (lane 3), 10 µM TG (lane 4), combination treatment of Dex with BTZ (lane 5) and TG (lane 6) in CEM-C1-15 (A), Molt4 (B) and CEM-C7-14 (C) cells. The results are representative of 3 independent experiments. Error bars represent ± SEM (* $p < 0.05$, ** $p < 0.01$, *** $p < 0.001$, *student t.test*). The values were normalised to the corresponding *RPL19* internal control and each sample was compared to untreated control.

5.2.2 Conclusion

In summary, Thapsigargin significantly increased GRP94, GRP78, Beclin1 and LC3 mRNA levels when used alone and in combination with Dex to treat CEM-C1-15, Molt4 and CEM-C7-14 cells. Dexamethasone affected CEM-C1-15 and Molt4 cells by decreasing GRP94 and LC3 mRNA expression levels but increasing Beclin1 and LC3 mRNA levels in CEM-C7-14 and Molt4 cells, respectively. Bortezomib decreased GRP94 and GRP78 mRNA levels in GC-sensitive cells, while LC3 levels increased in Molt4 and CEM-C1-15 treated with BTZ.

When comparing effects of studied drugs on mRNA and protein levels of autophagy and ER stress markers, it was observed that Dexamethasone increased Beclin1 protein levels in CEM-C1-15 cells while increase in Beclin1 mRNA level was observed in CEM-C7-14 cells. Dex increased LC3 protein (LC3 II / I ratio) and mRNA levels in Molt4, but the decrease of mRNA and protein expression levels were observed in CEM-C1-15 and CEM-C7-14 cells, respectively. In GC-resistant cells, GRP94 protein levels decreased in Dex treated CEM-C1-15 cells while the mRNA levels were affected in Motl4 cells. Interestingly, Dex increased GRP94 and GRP78 protein levels only in GC-sensitive cells.

Chloroquine alone and in combination with Dex increased LC3 II / I ration in all cells but there were no statistic significant value observed. However, mRNA levels have not been analysed to detect autophagy and ER stress markers. Thapsigargin treatment individually and combined with Dex lead to increased mRNA expression levels of Beclin1, LC3, GRP94, and GRP78 in all cells. However, increased trend but not significant of LC3 protein expression levels were observed in GC-resistant cells while increase of GRP94 and GRP78 protein levels was found in only CEM-C7-14 cells. In rotenone treated cells trend of increase in protein expression levels of GRP94 in CEM-C1-15 and CEM-C7-14 cells was observed and increased GRP78 protein levels in CEM-C7-14 cells was detected. However, no statistically significant values were observed in ROT individual and combination treatments. Bortezomib increased mRNA expression of LC3 in GC-resistant cells and GC-sensitive cells in combination treatment with Dex. GRP94 and GRP78 mRNA levels decreased in only Bortezomib treated CEM-C7-14 cells, but in combined treatment with Dex only GRP78 mRNA levels were reduced.

CHAPTER 6 DISCUSSION

ALL is the most frequent cancer in children. Although the treatment of this disease can be considered as highly successful, compared to other types of cancer, toxicity of therapies and drug resistance still pose substantial problem. In this thesis focus of study is molecular mechanism of action of glucocorticoids that have been used as part of ALL therapy towards developing better understanding how these drugs function, and what could be cause of resistance.

There are several proposed resistance mechanisms observed in different tissues. These include;

1) Down-regulation of GR at both mRNA and protein levels by its own hormone ligand glucocorticoid (Schaaf & Cidlowski, 2002). Post translational modification mechanism are also involved to decrease expression level of GR protein (Dong, Y. et al., 1988). Hormone treatment has been shown to decrease GR protein stability resulting in reduced GR half-life by 50% (Mcintyre & Samuels, 1985)

2) The human GRβ-isoform that is a result of alternative splicing of hGR pre-mRNA and can inhibit hGRα as observed in vitro studies (Bamberger et al., 1995; Oakley et al., 1996; Oakley et al., 1999)

3) Transrepression by NF-κB. Under basal condition, NF-κB heterodimer locates in the cytosol and is inactivated by association with an inhibitory protein IκB α or β. Studies have shown that IκB is affected by inflammatory signals such as tumor necrosis factor- α (TNF- α) and lipopolysaccharide (LPS) resulting in dissociation of the complex of NF-κB and IκB and leading to NF-κB nuclear translocation (Baeuerle & Henkel, 1994; Brown et al., 1995; DiDonato et al., 1997; Krappmann et al., 1996). One mechanism of NF-κB to GR repression is competition binding of p65 subunit and hGRα on GRE site (Caldenhoven et al., 1995; McKay & Cidlowski, 1998; Ray & Prefontaine, 1994).

4) Microenvironment and stem cell niche have been proposed to affect response to drugs (Bakker et al., 2016).

5) Several factors that modulate GR function and its ability to induce apoptosis in leukemia cells and include posttranslational modifications and crosstalk with other less well studied pathways such as autophagy and necroptosis.

In leukemia cells, mechanisms of GR-induced apoptosis are linked with several intrinsic apoptotic molecules such as APAF-1, Bax, Bak, Bim, Puma, and Noxa (Bouillet et al., 1999; Cecconi et al., 1998; Rathmell et al., 2002; Villunger et al., 2003; Yoshida, H. et al., 1998). These regulations subsequently activate downstream apoptosis processes. GR also increases expression of several genes that are involved in GR activities and apoptosis pathway such as FKBP 51, IκB-α, BIM and Dig-2.

Over the past decade, several studies linked the autophagy (macroautophagy) to the cancer therapy as this pathway plays an important role in proteins and organelles degradation and recycling (Mizushima, 2007; Ravikumar et al., 2010a) and many chemotherapeutic agents affect autophagy in both tumor and normal cells. In addition, the role of cellular stress such as ER stress and UPR in modulating GR function has not been described in detail. This topic is not well understood and needs to be investigated further towards future development of beneficial anti-cancer treatment.

In this study, we used several drugs including Dexamethasone, Chloroquine, Thapsigargin, Rotenone and Bortezomib treated in GC-resistant cells (CEM-C1-15 and Molt4) and GC-sensitive cells (CEM-C7-14) to investigate the role of autophagy processes, ER stress, unfolded protein response, and ROS expression levels on the mechanisms of GC-induced leukemia apoptosis. We found that autophagy, mitochondrial and endoplasmic reticulum play an important role in GC-resistant mechanisms. Several drug combination conditions showed increase cell death that may be used in chemotherapy with the aim of minimising side effects from high dose single treatment.

6.1 The role of macroautophagy in glucocorticoid induced ALL cells death

Autophagy plays an important role in maintaining normal cellular homeostasis by removing misfolded protein and neutralising hazardous stimuli. Autophagy has been reported to promote or supress acute lymphoblastic cell proliferation (Evangelisti et al., 2014). To investigate how ALL cells respond to glucocorticoid hormones when autophagy is inhibited, chloroquine individually or combined with Dexamethasone was used to inhibit autophagy with the mechanism of autophago-lysosome formation blockage.

Recent studies showed that autophagy is involved in ALL chemotherapeutic treatment. Both pro-survival and pro-death roles of autophagy in ALL cells have been found and it is still unclear how autophagy process determines cell fate (Evangelisti et al., 2014). It has been reported that autophagy is induced by ER stress, unfolded protein response and reactive oxygen species (He & Klionsky, 2009). However, the mechanisms linking ER stress and autophagy are dependent on the stress stimuli and type of organism. In myeloid leukemia cells, combination treatment of Chloroquine and other therapeutic agents such as Imatinib mesylate (IM), HDACi/SAHA, HDACi/ valproic acid increased cytotoxic effect on cancer cells (Bellodi et al., 2009; Carew et al., 2007; Torgersen et al., 2013). IM inhibits BCR/ABL tyrosine kinase and subsequently triggers apoptosis. While IM induces autophagy, suppression of autophagy enhanced cell death during IM treatment in CML cells (Bellodi et al., 2009). Suberoylanilide hydroxamic acid (SAHA) is a well-tolerated pan-HDAC inhibitor used as anticancer agent. SAHA's effects have been linked to ROS generation and increase of autophagy (Shao et al., 2004). Disruption of autophagy enhanced the anticancer activity of SAHA in CML (Carew et al., 2007).

Our results indicated that Dex alone induced early stage of autophagy, as measured by increase in Beclin1 protein levels, in CEM-C1-15 and induced late stage of autophagy (as suggested by the increase in the ratio of LC3 II / I protein levels) in Molt4, while the opposite effect was observed in GC-sensitive cell (decrease of LC3 II / I) (Figure 5-2, C and D lane 2). These findings suggest that macroautophagy may be involved in the mechanism of GR induced cell death by facilitating pro-survival mechanism in GC-resistant cells. However, Dex induced autophagy is different between leukemic cell types. The preliminary studies in multiple myeloma (MM) cells indicated that Dex induced autophagy and increased percent of cells undergoing apoptosis. The inhibition of autophagy by Beclin1 protein silencing and type III Ptdlns3K inhibitor during Dex treatment resulted in apoptosis inhibition in MM cells (Grander et al., 2009).

We used combination treatment with CLQ, autophagy inhibitor, in ALL cells and found increase in the percent of cell death based on cell viability assays (Chapter 3, sections 3.1-3.3) is increased by dose-dependent manner. Our results suggest that autophagy is involved in the regulation of GC-induced ALL cells apoptosis. These finding have been supported with the report indicating that inhibition of autophagy induces cell apoptosis in glucocorticoid resistant ALL cell lines (Jiang et al., 2015). Recent study indicated that chloroquine can induce lymphoma cell apoptosis and activated ER stress pathway including GRP78 up-regulation, as

well as IRE6α and ATF6 activation (Masud Alam et al., 2016). However, our results show CLQ did not affect ER stress chaperone protein markers, GRP78 and GRP94, in ALL cells. It is possible that different pathways may be activated in CLQ induced ALL death, depending on cell type, experimental or other conditions.

During ER stress, GC-resistant cells respond to stress by increasing autophagic protein marker to a greater extent than GC-sensitive cell (Figure 5-4 D, lanes 3 and 4). After combination with Dex, only CEM-C7-14 cells showed decrease in autophagy (Figure 5-4 D, lanes 5 and 6). This finding suggests that autophagy plays an important role in the ALL cells apoptosis and resistance to Dex treatment. In clinical trials, CLQ has been used with other anti-cancer agents to sensitise solid tumors such as malignant neoplasm, breast cancer, glioblastoma, and multiple myeloma. Phase II multiple myeloma trial indicated that combination treatments of Bortezomib and Chloroquine may induce cancer cells to become more sensitised to the drugs (ClinicalTrials.gov, 2018).

6.2 Role of GRPs chaperone proteins in glucocorticoid induced ALL cells death

Leukemia is characterized by abnormal proliferation and maturation of leukocytes and precursors cells in blood and bone marrow. Although there are several indications that unfolded protein response (UPR) is involved in solid tumor pathogenesis, the role of the UPR in leukemogenesis remains unclear (Schardt et al., 2011).

Early studies showed that XBP1s and GRP78 were up-regulated in Ph^+ leukemia cell lines and this subsequently activated CCAAT/enhancer-binding protein homologous protein (CHOP), inducer of UPR-related apoptosis (Dengler et al., 2011; Tanimura et al., 2009). In our studies, Dexamethasone treatment in GC-sensitive cells but not GC-resistant cells led to increase chaperone proteins levels, especially GRP78 and GRP94 (described in Chapter 5) that is a novel finding in ALL cells. Furthermore, Dex also induced GC-sensitive cell death, as determined by increasing of subG1 phase in cell cycle analysis (Chapter 3, section 3.2), and disrupted the mitochondrial membrane voltage, suggesting effects in early apoptosis (Chapter 3, section 3.3).

GRPs over expression has been reported widely in several cancer cell lines such as breast carcinoma, prostate adenocarcinoma, liver cancer, colorectal cancer, multiple myeloma, and leukemia (Chen, W. T. et al., 2014a; Chen, W. T. et al., 2014b; Dong, D. et al., 2008; Fu et al., 2008; Hua et al., 2013; Morales et al., 2014; Wey et al., 2012). These increases of GRP

expression are associated with cancer cell aggressive and metastasis properties (Lee, A. S., 2007; Miao et al., 2013). While cell surface GRP78 triggers ERK and AKT activation and increase in DNA and protein synthesis in prostate cancer (Misra & Pizzo, 2012) GRP94 binds to IGF-1 or IGF-2 and controls IGFs maturation and secretion leading to PI3K-AKT activation (Wanderling et al., 2007).

GRPs act as apoptosis suppressor proteins (Luo & Lee, 2013). GRP78 binds to caspase-7 and inhibits apoptosis induced by etoposide (Rao et al., 2002; Reddy, R. K. et al., 2003). Recently, it has been reported that interaction of GRP78, BIK and Bcl-2 is associated with the regulation of ER Ca^{2+} and cytochrome *c* release which initiates apoptosis pathway. Overexpression of GRP78 inhibits the suppressing of Bcl-2 by BIK and releases anti-apoptosis properties of Bcl-2 in breast cancer cells (Fu et al., 2007; Zhou, H. et al., 2011). GRP94 also has a role to protect cancer cells from apoptosis by maintaining ER Ca^{2+} homeostasis (Reddy, R. K. et al., 1999). Under ER stress conditions, GRP78 and GRP94 translocate to cell surface for growth and apoptotic signaling regulation and interact with MHC class I molecule to mediate antigen presentation (Lee, A. S., 2014; Luo & Lee, 2013; Triantafilou et al., 2001).

However, it is possible that increase of GRP protein levels, detected by western blotting technique in GC-sensitive CEM cells may be involved in another pathway during Dex mediated apoptotic mechanism.

Out results showed that mRNA expression levels were not altered by Dex as measured by RT-qPCR technique. This finding indicated that post transcriptional mechanism including protein stability, posttranslational modification and others may be involved in GR mediated control of GRP levels in GC-sensitive cell. GR may also induce transcription of other genes that can affect GRPs protein levels. However, some reported showed high expression level of GRP94 is associated with clinical outcome in multiple myeloma (MM) patients. They found that higher expression level of GRP94 is associated with malignant stage of MM patients (International Staging System (ISS) stage III MM patients is higher than those in ISS stage I/II MM patients) (Chhabra et al., 2015).

Several studies have reported that loss of mitochondrial membrane voltage induced cell apoptosis by releasing pro-apoptotic proteins and Cyto *c* to the cytosol (Chang et al., 2010; Ott et al., 2007; Zhang, R. et al., 2008b). Mitochondria are another target organelle of GRP proteins, the disruption of mitochondria also induces GRPs translocation to the cell surface and secretion outside the cell to control apoptosis, cell growth and immune system (Lee, A. S.,

2014). We found that GR-induced cell apoptosis in ALL sensitive cell is correlated with the increase in mitochondrial membrane voltage disruption (Figure 3-10, A to C, lanes 2). This finding suggests that Dexamethasone induced ALL apoptosis may be triggered via mitochondrial pathway. There are several studies that indicated that mitochondria is the target organelle for GC-induced apoptosis and these are in agreement with our findings. Dexamethasone disrupts mitochondrial membrane potential in Nalm-6 and Reh ALL cells, releases cytochrome *c* and increases caspase-3 activities in Dex-induced ALL apoptosis (Abdoul-Azize et al., 2017), In MM cells, Dexamethasone triggers the release of SMAC, a second mitochondria-derived activator of caspases, into cytoplasm and subsequently stimulates cytochrome *c* and Apaf-1 pathway resulting in cell apoptosis precesses activation (Chauhan, D. et al., 2001; Chauhan, D. et al., 1997a; Chauhan, D. et al., 1997b). Eberhart and colleagues demonstrated that Dexamethasone alters the mitochondrial membrane properties and represses mitochondrial respiratory activity resulting in GC-sensitive ALL cells apoptosis (Eberhart et al., 2011; Eberhart et al., 2009).

In addition, ER stress inducer such as Thapsigargin was used to test the role of GR and glucose-regulated proteins 78 and 94 on the cell survival regulation. We found that increasing of GRP proteins in GC-sensitive cells is correlated with increasing of apoptotic cell death in Dex and TG combination treatments (based on MTS, SubG1 detection, and mitochondrial membrane potential assays). The mRNA and protein expression levels of GRP78 and GRP94 were increased by TG treatment alone and combination treatment with Dex in all cells (Figures 5-9 and 5-10, lanes 4 and 6). These findings were supported by Li and colleagues in 1993 and Lee in 2001 who reported that TG was a strong ER stress inducer and activated GRP transcription through decreasing Ca^{2+} concentration in ER (Lee, A. S., 2001; Li, W. W. et al., 1993). Our results also showed the combination treatment, with Dex, enhanced cytotoxic effects observed in CEM-C1-15, Molt4, and CEM-C7-14 cells after 48 hrs treatment. These results could mean that unfolded protein response in GC-resistant cells play a critical role in the regulation of GR induced cell death and could be used as a target for drug development and future clinical use in both sensitive and resistant leukemia. In medicine, the first clinical trials of thapsigargin started in 2008 under the generic name Mipsagargin (G-202) (Andersen et al., 2015). Several trial studies reported that Thapsigargin has been used to induce glioblastoma (GBM), cancer of nervous system, renal cell carcinoma, prostate cancer, and hepatocellular carcinoma (HCC) apoptosis. G-202 is activated by prostate specific membrane antigen (PSMA), which is expressed in most solid tumor vessels (NIH, 2018).

However, the link between ER stress and Autophagy in ALL cells remains unclear. The results showed that TG activated autophagy by increasing protein levels of LC3 II / I ratio and mRNA levels of Beclin1 and LC3 in all cells (Figure 5-11, A to C lanes 4, Figure 5-12, A to C lanes 4). The decrease of LC3 protein expression levels was observed in only GC-sensitive cell when Dex and TG were applied.

6.3 Role of reactive oxygen species in glucocorticoid induced ALL cells death

Under normal condition, intracellular ROS levels are stable and are maintained by non-enzymatic molecules including glutathione, flavonoids, vitamins A, C and E to prevent ROS induced cellular damage. In cancer cells, high metabolic activity, mitochondrial dysfunction, and peroxisome over expression elevate the level of reactive oxygen species. These can lead to increased cellular receptor signalling, activity of oncogenes and oxidative activity (Babior, 1999; Storz, 2005; Szatrowski & Nathan, 1991). Mitochondria are the source of reactive oxygen species such as superoxide radicals that generate during electron transport chain activation and they release into mitochondrial matrix or cytoplasm via mitochondrial permeability transition pores (MPTP) (Liou & Storz, 2010). The elevated basal level of ROS promotes development and progression of tumor cells, whereas the cells also express high level of antioxidant proteins to neutralize high level of ROS. Several signalling pathways have been found that were regulated by ROS in cancer cell such as mitogen-activated protein (MAP) kinase/Erk cascade, phosphoinositide-3-kinase (PI3K)/Akt-regulated signalling cascades, and NF-κB-activating pathways (Irani et al., 1997; Khavari & Rinn, 2007; Reddy, K. B. & Glaros, 2007; Roberts & Der, 2007). Increased ROS levels by chemotherapeutic agents can also induce cell cycle arrest and promote tumor cell death (Liou & Storz, 2010). Our studies showed that high levels of ROS (ROT treatment) increased accumulation of cells in G2/M phase (Figure 3-8 D lanes 3 and 4), interrupted mitochondrial membrane integrity and induced cell death.

The results obtained from MMPA indicated that Rotenone increased the proportion of cells that altered mitochondrial membrane potential in CEM-C7-14, CEM-C1-15 and Molt4 cells (Figure 3-12, A to C lanes 3 and 4) and these alterations mostly supported results obtained using MTS assay that determined cell survival (Figure 3-3 D to F). The combination with Dex increased MMP disruption and enhanced cytotoxic effect as indicated by viability assays in CEMs cell, whereas effects in Molt4 cells were marginal. High ROS levels in CEM cells is correlated with the increase in cell death (Figure 4-3, A and B lanes 3-4 and Figure 3-3, A, B, D, and E), suggesting that reactive oxygen species can induce apoptosis pathway in CEM cells.

Moreover, the synergistic effects observed in combination treatment with Dex treated CEM cells indicated that high ROS levels may be beneficial in GC-induced CEM cells death. However, the sensitivity to ROS levels depend on leukemia cell type and incubation time. Molt4 cells did not respond to ROT treatment in 24 hrs but marginal effect can be observed in 48 hrs.

Previous studies showed that rotenone induced ER stress and increased ROS production in rat retinal cells (Han et al., 2014). Rotenone also induced human promyelocytic leukemia cell line (HL-60) apoptosis through ROS production (Li et al., 2003).

The ROS levels in glucocorticoid treated cells are different across the cell lines. CEM-C7-14 and Molt4 cells have the low level of ROS during Dex treatment while the ROS level is not changed in CEM-C1-15 cells and the mechanisms of ROS production on response to glucocorticoid treatment are unclear. Some studies indicated that Dexamethasone induced ROS production in Nalm-6 and Reh leukemia cell lines (Abdoul-Azize et al., 2017). However, the combined treatment between ROS modulator and ROS generating agents may lead to increase apoptosis of cancer cells and enhance cytotoxic effect in resistant cells that do not respond to ROS generating drug alone (Lau et al., 2008).

6.4 Role of protein degradation inhibition in glucocorticoid induced ALL cells death

Protein degradation is the main pathway for maintenance of protein homeostasis in the intracellular proteins. The multi-complexed structure, proteasome, regulates protein clearance of misfolded and /or unfolded and cytotoxic proteins (Adams, J., 2004). Proteasome inhibitor, bortezomib, blocks protein degradation processes by inhibiting 26S proteasome complex resulting in induction of ER stress response. Bortezomib has been used to treat multiple myeloma (MM) and mantle cell lymphoma while the mechanism of anticancer action is still unclear (Du and Chen, 2013).

Our results indicate that CEM-C1-15 and Molt4 cells are highly sensitive to Bortezomib, which enhances the cytotoxic effects of Dexamethasone as observed in MTS assay (Figure 3-4 D and F) and this finding suggest that UPR to restore protein folding in GC-resistant cells may be altered subsequently to trigger ER stress induced cell apoptosis. The previous study was performed by Horton and colleague in 2006 and they found that several leukemic cell lines are sensitive to bortezomib, especially CEM, which was sensitive to Bortezomib with IC_{50} at 2 nM

(Horton et al., 2006). However, GC-sensitive cells were not affected by Bortezomib at the maximal dose of 10 nM, while Our western blot results indicated that 5 nM bortezomib treatment increased the GRP94 and GRP78 chaperone proteins in CEM-C1-15 cell more than in CEM-C7-14 (Figure 5-8 A and B, lanes 4 and 6). The LC3 mRNA levels increased in CEM-C1-15 and Molt4 cells but not in CEM-C7-14 (Figure 5-12 A to C, lane 3). These findings suggested that CEM-C1-15 and Molt4 cells are sensitive to ER stress and unfolded protein response when the protein degradation mechanism is disrupted while GC-sensitive cells may use alternative pathways to restore misfolded proteins. Pre-clinical studies in AML have indicated that proteasome inhibition disrupts pathways in cell proliferation, enhances cytotoxic effects of other anti-cancer agents, and induces autophagy. Bortezomib inhibits the degradation of NFκB inhibitor (IκBα) leading to decrease in the expression of NFκB target genes involved in pro-survival and expression of proliferative pathways resulting in apoptosis (Csizmar et al., 2016).

In clinical trials, Bortezomib is used to achieve complete remission (CR) in relapsed ALL. Bortezomib was used with other chemotherapy agents including Dexamethasone, Doxorubicin, Vincristine and PEGylated asparaginase in 30 and 7 children with B-cell precursor (BCP) and T-cell ALL, respectively. The results of the trial indicated that more than 70% of patients were curable (Bertaina et al., 2017).

6.5 Overall conclusions

GC-induced ALL cells apoptosis is the beneficial process for anti-leukemia therapy. Several pathways are linked and involved in the GC-induced apoptosis mechanisms. This study demonstrated that chaperone proteins, GRP78 and GRP94 are stimulated by dexamethasone in GC-sensitive cells but no change of mRNA expression levels was detected suggesting that the regulation of GRPs by GC is not by direct effect on GRPs mRNA but occurs via other pathways

Autophagy is an important process to consider in studies of GC resistance. We found that autophagy marker, LC3 II / I ratio, is activated in Dex treated Molt4 cells and Beclin1 expression levels is increased in Dex treated CEM-C1-15 cells. These autophagic responses are related with increase in cell death in GC-resistant cells after autophagy is inhibited, which indicated that autophagy may be a pro-survival mechanism in GC-resistant cells (Figure 6-1 A).

Mitochondria may be the target organelle involved in GC-induced cell apoptosis and this phenomenon is observed by MMP assay in Dex treated CEM-C7-14 cells. This mitochondrial membrane disruption may trigger several apoptotic molecules release and subsequently induces leukemia cellapoptosis (Figure 6-1 B).

Combination between Dex and the drugs that regulate ER stress showed enhanced cytotoxic effects in all cells. TG increased mRNA levels of autophagy markers, Beclin1 and LC3 and ER stress markers chaperone proteins, GRP78 and GRP94, in all cell lines. These findings indicated that distruption of ER hoeostasis during Dex treatment has potential to inhibit ALL cell proliferation. However, autophagy is also activated during ER stress and that could be pro-death or prosurvival mechanisms.

Increase of ROS levels exerted cytotoxic effects and induced cell death in CEM cells higher than Molt4 cells. And high ROS levels can activate autophagy in only Molt4 cells. The sensitivity to ROS levels depends on leukemia cell type and incubation time.

Finaly, numerous pathways are linked and important for ALL cells apoptosis and this could be usedd to improve the anti-cancer therapy and alleviate side effects from high dose of chemotherapy used.

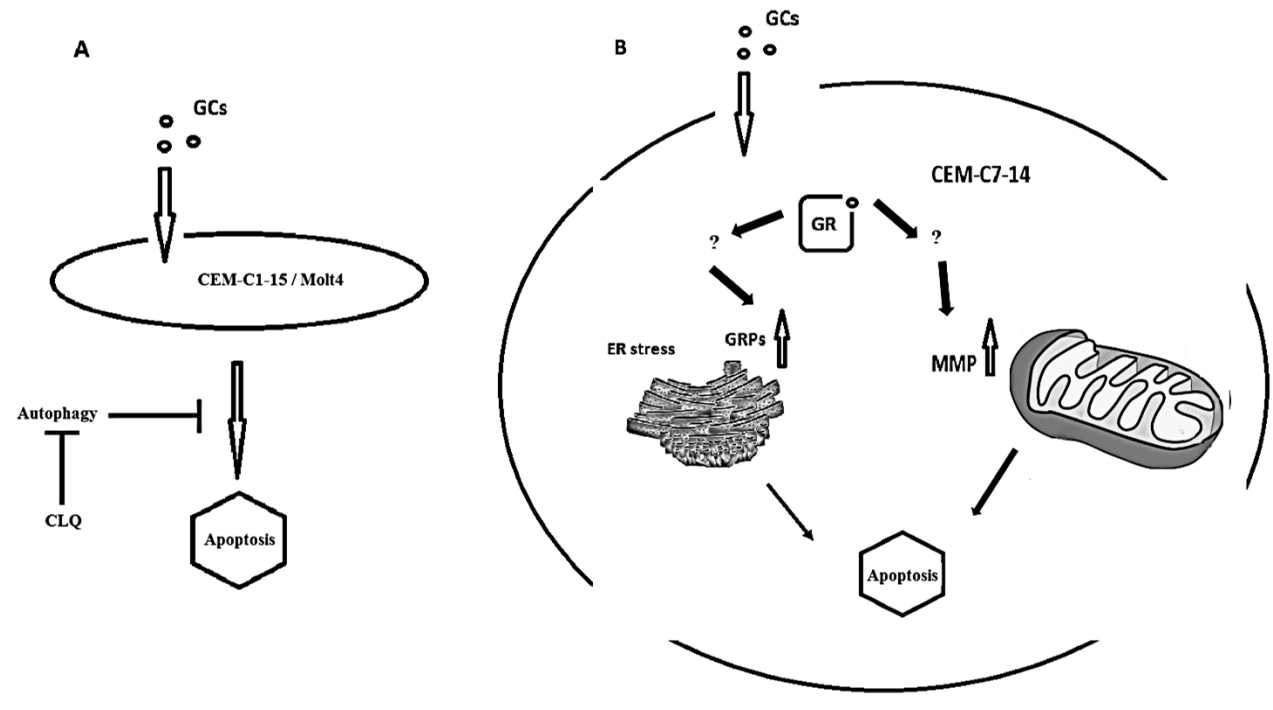

Figure 6-1 Proposed model in GCs induced ALL apoptosis

The figures show autophagy may have a role as anti-apoptotic process in CEM-C1-15 / Molt4 (A) while in CEM-C7-14, mitochondria and ER are the important organelles in GCs induced cell death (B). GRPs activation may regulate ER stress mediated cell apoptosis and mitochondrial membrane potential alteration may be involved in mitochondrial mediated cell apoptosis.

6.6 Limitations of the study

One limitation of this study is the specificity of drugs used in different leukemia cell types (CEMs and Molt4 cells). It is possible that drugs used to study effects on one process (for example ER stress) could affect other processes as well. In addition, the sensitivity of leukemia cells to drug treatment varies and the minimum doses used to approach the maximum effects are different across leukemia cells.

There are some limitations of laboratory techniques and the systems used in this study. Cells growing in suspension (such as leukemia cells) are difficulty to transfect and carry out immunofluorescence and immunohistochemistry studies. However, the availability of GC-sensitive and GC-resitant cell lines provides certain advantage for analysis of resistant phenotype, given that mouse models of ALL are difficult to obtain and study.

Some other technical difficulties include potential false positive results when using RT-qPCR, SYBR Green system, although this possibility was minimised by exon-exon junction primer design and by melting curve analysis.

In vitro assays are limited when predicting and extrapolating the in vivo responses. Therefore, 3D systems, experiments in mice as well as clinical triels will be needed to confirm data obtained in this project as well as to explore in clinical use of these findings.

6.7 Future Directions

Although Dexamethasone and several compounds have been used to explore the relationship between autophagy, ER stress and unfolded protein response, the mechanism of glucocorticoid-resistant ALL cells remains unclear. These issues have become interesting study topics for the potential improvement of ALL treatment. The role of GR induced cell death and the novel mechanism we found here of increasing chaperone proteins GRP78 and GRP94 in GC-sensitive cell lacks mechanistic details. Novel approaches to analyse these at molecular levels are needed including analysis of promoter region of GRPs and modulation of potential transcription factors involved in their regulation. The mechanism of protein stability of GRPs could also lead to finding out the link with glucocorticoid effects.

Our results suggested that GRP78 and GRP94 may have an important role in GR function, while chloroquine induced glucocorticoid sensitive and resistant ALL cells death and increased ER stress protein levels. The further studies such as detection of secreted form and

cell surface expression of GRP proteins in cell lines and patient's samples will be needed to elucidate these mechanisms. We are currently developing flow cytometry based assay to detect intracellular and membrane based GRPs in cells treated as above. Complete picture of GRPs distribution could be obtained if extracellular levels of GRPs are also determined using ELISA method. Future experiments can also address GRP's role in antigen presentation and potentially link their expression to immunotherapy of ALL.

Finally, in order for these findings to be translated into clinical practice expression of GRPs needs to be detected in patient's samples. This can potentially be carried out in Thailand and results correlated with clinical parameters including stage and grade of the cancer, resistance and type to therapy, weight, age and gender of patients. Ultimately, these results may find application in clinical practice by combining Dexamethasone treatment with other drugs that potentially could kill resistant leukemia or lower down Dex dose therefore lowering side effects.

REFERENCES

Abbinante-Nissen, J. M., Simpson, L. G., & Leikauf, G. D. (1995). Corticosteroids increase secretory leukocyte protease inhibitor transcript levels in airway epithelial cells. *Am J Physiol, 268*(4 Pt 1), L601-606. doi:10.1152/ajplung.1995.268.4.L601

Abdoul-Azize, S., Dubus, I., & Vannier, J. P. (2017). Improvement of dexamethasone sensitivity by chelation of intracellular Ca2+ in pediatric acute lymphoblastic leukemia cells through the prosurvival kinase ERK1/2 deactivation. *Oncotarget, 8*(16), 27339-27352. doi:10.18632/oncotarget.16039

Abrahamsen, H., Stenmark, H., & Platta, H. W. (2012). Ubiquitination and phosphorylation of Beclin 1 and its binding partners: Tuning class III phosphatidylinositol 3-kinase activity and tumor suppression. *FEBS Lett, 586*(11), 1584-1591. doi:10.1016/j.febslet.2012.04.046

Acosta-Alvear, D., Zhou, Y., Blais, A., Tsikitis, M., Lents, N. H., Arias, C., . . . Dynlacht, B. D. (2007). XBP1 controls diverse cell type- and condition-specific transcriptional regulatory networks. *Mol Cell, 27*(1), 53-66. doi:10.1016/j.molcel.2007.06.011

Adams, J. (2004). The proteasome: a suitable antineoplastic target. *Nat Rev Cancer, 4*(5), 349-360. doi:10.1038/nrc1361

Adams, J. M., & Cory, S. (1998). The Bcl-2 protein family: arbiters of cell survival. *Science, 281*(5381), 1322-1326.

Alnemri, E. S., Fernandes, T. F., Haldar, S., Croce, C. M., & Litwack, G. (1992a). Involvement of BCL-2 in glucocorticoid-induced apoptosis of human pre-B-leukemias. *Cancer Res, 52*(2), 491-495.

Alnemri, E. S., Robertson, N. M., Fernandes, T. F., Croce, C. M., & Litwack, G. (1992b). Overexpressed full-length human BCL2 extends the survival of baculovirus-infected Sf9 insect cells. *Proc Natl Acad Sci U S A, 89*(16), 7295-7299.

Andersen, T. B., Lopez, C. Q., Manczak, T., Martinez, K., & Simonsen, H. T. (2015). Thapsigargin--from Thapsia L. to mipsagargin. *Molecules, 20*(4), 6113-6127. doi:10.3390/molecules20046113

Antakly, T., Thompson, E. B., & O'Donnell, D. (1989). Demonstration of the intracellular localization and up-regulation of glucocorticoid receptor by in situ hybridization and immunocytochemistry. *Cancer Res, 49*(8 Suppl), 2230s-2234s.

Arnold, R. S., He, J., Remo, A., Ritsick, D., Yin-Goen, Q., Lambeth, J. D., . . . Petros, J. A. (2007). Nox1 expression determines cellular reactive oxygen and modulates c-fos-induced growth factor, interleukin-8, and Cav-1. *Am J Pathol, 171*(6), 2021-2032. doi:10.2353/ajpath.2007.061144

Ashkenazi, A., & Dixit, V. M. (1998). Death receptors: signaling and modulation. *Science, 281*(5381), 1305-1308.

Ashraf, J., Kunapuli, S., Chilton, D., & Thompson, E. B. (1991). Cortivazol mediated induction of glucocorticoid receptor messenger ribonucleic acid in wild-type and dexamethasone-resistant human leukemic (CEM) cells. *J Steroid Biochem Mol Biol, 38*(5), 561-568.

Babior, B. M. (1999). NADPH oxidase: an update. *Blood, 93*(5), 1464-1476.

Baeuerle, P. A., & Henkel, T. (1994). Function and activation of NF-kappa B in the immune system. *Annu Rev Immunol, 12*, 141-179. doi:10.1146/annurev.iy.12.040194.001041

Bakker, E., Qattan, M., Mutti, L., Demonacos, C., & Krstic-Demonacos, M. (2016). The role of microenvironment and immunity in drug response in leukemia. *Biochim Biophys Acta, 1863*(3), 414-426. doi:10.1016/j.bbamcr.2015.08.003

Ballard, P. L. (1979). Delivery and transport of glucocorticoids to target cells. *Monogr Endocrinol, 12*, 25-48.

Bamberger, C. M., Bamberger, A. M., de Castro, M., & Chrousos, G. P. (1995). Glucocorticoid receptor beta, a potential endogenous inhibitor of glucocorticoid action in humans. *J Clin Invest, 95*(6), 2435-2441. doi:10.1172/JCI117943

Barnes, P. J. (1999). Therapeutic strategies for allergic diseases. *Nature, 402*(6760 Suppl), B31-38.

Barnes, P. J., & Karin, M. (1997). Nuclear factor-kappaB: a pivotal transcription factor in chronic inflammatory diseases. *N Engl J Med, 336*(15), 1066-1071. doi:10.1056/NEJM199704103361506

Battisti, V., Maders, L. D., Bagatini, M. D., Santos, K. F., Spanevello, R. M., Maldonado, P. A., . . . Morsch, V. M. (2008). Measurement of oxidative stress and antioxidant status in acute lymphoblastic leukemia patients. *Clin Biochem, 41*(7-8), 511-518. doi:10.1016/j.clinbiochem.2008.01.027

Beato, M., & Sánchez-Pacheco, A. (1996). Interaction of steroid hormone receptors with the transcription initiation complex. *Endocr Rev, 17*(6), 587-609. doi:10.1210/edrv-17-6-587

Bellodi, C., Lidonnici, M. R., Hamilton, A., Helgason, G. V., Soliera, A. R., Ronchetti, M., . . . Calabretta, B. (2009). Targeting autophagy potentiates tyrosine kinase inhibitor-induced

cell death in Philadelphia chromosome-positive cells, including primary CML stem cells. *J Clin Invest, 119*(5), 1109-1123. doi:10.1172/JCI35660

Berridge, M. V., Herst, P. M., & Tan, A. S. (2005). Tetrazolium dyes as tools in cell biology: new insights into their cellular reduction. *Biotechnol Annu Rev, 11*, 127-152. doi:10.1016/S1387-2656(05)11004-7

Bertaina, A., Vinti, L., Strocchio, L., Gaspari, S., Caruso, R., Algeri, M., . . . Locatelli, F. (2017). The combination of bortezomib with chemotherapy to treat relapsed/refractory acute lymphoblastic leukaemia of childhood. *Br J Haematol, 176*(4), 629-636. doi:10.1111/bjh.14505

Bertram, J. S. (2001). The molecular biology of cancer. *Molecular Aspects of Medicine, 21*, 167-223.

Bestebroer, J., V'Kovski, P., Mauthe, M., & Reggiori, F. (2013). Hidden behind autophagy: the unconventional roles of ATG proteins. *Traffic, 14*(10), 1029-1041. doi:10.1111/tra.12091

Bledsoe, R. K., Montana, V. G., Stanley, T. B., Delves, C. J., Apolito, C. J., McKee, D. D., . . . Xu, H. E. (2002). Crystal structure of the glucocorticoid receptor ligand binding domain reveals a novel mode of receptor dimerization and coactivator recognition. *Cell, 110*(1), 93-105.

Bonapace, L., Bornhauser, B. C., Schmitz, M., Cario, G., Ziegler, U., Niggli, F. K., . . . Bourquin, J. P. (2010). Induction of autophagy-dependent necroptosis is required for childhood acute lymphoblastic leukemia cells to overcome glucocorticoid resistance. *J Clin Invest, 120*(4), 1310-1323. doi:10.1172/JCI39987

Bouillet, P., Metcalf, D., Huang, D. C., Tarlinton, D. M., Kay, T. W., Kontgen, F., . . . Strasser, A. (1999). Proapoptotic Bcl-2 relative Bim required for certain apoptotic responses, leukocyte homeostasis, and to preclude autoimmunity. *Science, 286*(5445), 1735-1738.

Breslin, M. B., Geng, C. D., & Vedeckis, W. V. (2001). Multiple promoters exist in the human GR gene, one of which is activated by glucocorticoids. *Mol Endocrinol, 15*(8), 1381-1395. doi:10.1210/mend.15.8.0696

Brink, R., & Lodish, H. F. (1998). Tumor necrosis factor receptor (TNFR)-associated factor 2A (TRAF2A), a TRAF2 splice variant with an extended RING finger domain that inhibits TNFR2-mediated NF-kappaB activation. *J Biol Chem, 273*(7), 4129-4134.

Bröker, L. E., Kruyt, F. A., & Giaccone, G. (2005). Cell death independent of caspases: a review. *Clin Cancer Res, 11*(9), 3155-3162. doi:10.1158/1078-0432.CCR-04-2223

Brown, K., Gerstberger, S., Carlson, L., Franzoso, G., & Siebenlist, U. (1995). Control of I kappa B-alpha proteolysis by site-specific, signal-induced phosphorylation. *Science, 267*(5203), 1485-1488.

Cabal-Hierro, L., & Lazo, P. S. (2012). Signal transduction by tumor necrosis factor receptors. *Cell Signal, 24*(6), 1297-1305. doi:10.1016/j.cellsig.2012.02.006

Caldenhoven, E., Liden, J., Wissink, S., Van de Stolpe, A., Raaijmakers, J., Koenderman, L., . . . Van der Saag, P. T. (1995). Negative cross-talk between RelA and the glucocorticoid receptor: a possible mechanism for the antiinflammatory action of glucocorticoids. *Mol Endocrinol, 9*(4), 401-412. doi:10.1210/mend.9.4.7659084

Cao, Z., Xiong, J., Takeuchi, M., Kurama, T., & Goeddel, D. V. (1996). TRAF6 is a signal transducer for interleukin-1. *Nature, 383*(6599), 443-446. doi:10.1038/383443a0

Carew, J. S., Nawrocki, S. T., Kahue, C. N., Zhang, H., Yang, C., Chung, L., . . . Cleveland, J. L. (2007). Targeting autophagy augments the anticancer activity of the histone deacetylase inhibitor SAHA to overcome Bcr-Abl-mediated drug resistance. *Blood, 110*(1), 313-322. doi:10.1182/blood-2006-10-050260

Carew, J. S., Zhou, Y., Albitar, M., Carew, J. D., Keating, M. J., & Huang, P. (2003). Mitochondrial DNA mutations in primary leukemia cells after chemotherapy: clinical significance and therapeutic implications. *Leukemia, 17*(8), 1437-1447. doi:10.1038/sj.leu.2403043

Cecconi, F., Alvarez-Bolado, G., Meyer, B. I., Roth, K. A., & Gruss, P. (1998). Apaf1 (CED-4 homolog) regulates programmed cell death in mammalian development. *Cell, 94*(6), 727-737.

Chan, S. L., & Yu, V. C. (2004). Proteins of the bcl-2 family in apoptosis signalling: from mechanistic insights to therapeutic opportunities. *Clin Exp Pharmacol Physiol, 31*(3), 119-128.

Chance, B., & Williams, G. R. (1956). The respiratory chain and oxidative phosphorylation. *Adv Enzymol Relat Subj Biochem, 17*, 65-134.

Chang, C., Zhu, Y. Q., Mei, J. J., Liu, S. Q., & Luo, J. (2010). Involvement of mitochondrial pathway in NCTD-induced cytotoxicity in human hepG2 cells. *J Exp Clin Cancer Res, 29*, 145. doi:10.1186/1756-9966-29-145

Charmandari, E., Kino, T., & Chrousos, G. P. (2004). Familial/sporadic glucocorticoid resistance: clinical phenotype and molecular mechanisms. *Ann N Y Acad Sci, 1024*, 168-181. doi:10.1196/annals.1321.014

Chauhan, D., Auclair, D., Robinson, E. K., Hideshima, T., Li, G., Podar, K., . . . Anderson, K. C. (2002). Identification of genes regulated by dexamethasone in multiple myeloma cells using oligonucleotide arrays. *Oncogene, 21*(9), 1346-1358. doi:10.1038/sj.onc.1205205

Chauhan, D., Hideshima, T., Rosen, S., Reed, J. C., Kharbanda, S., & Anderson, K. C. (2001). Apaf-1/cytochrome c-independent and Smac-dependent induction of apoptosis in multiple myeloma (MM) cells. *J Biol Chem, 276*(27), 24453-24456. doi:10.1074/jbc.C100074200

Chauhan, D., Pandey, P., Ogata, A., Teoh, G., Krett, N., Halgren, R., . . . Anderson, K. (1997a). Cytochrome c-dependent and -independent induction of apoptosis in multiple myeloma cells. *J Biol Chem, 272*(48), 29995-29997.

Chauhan, D., Pandey, P., Ogata, A., Teoh, G., Treon, S., Urashima, M., . . . Anderson, K. C. (1997b). Dexamethasone induces apoptosis of multiple myeloma cells in a JNK/SAP kinase independent mechanism. *Oncogene, 15*(7), 837-843. doi:10.1038/sj.onc.1201253

Chauhan, S., Leach, C. H., Kunz, S., Bloom, J. W., & Miesfeld, R. L. (2003). Glucocorticoid regulation of human eosinophil gene expression. *J Steroid Biochem Mol Biol, 84*(4), 441-452.

Chazotte, B. (2011). Labeling mitochondria with JC-1. *Cold Spring Harb Protoc, 2011*(9). doi:10.1101/pdb.prot065490

Chen, L. B. (1988). Mitochondrial membrane potential in living cells. *Annu Rev Cell Biol, 4*, 155-181. doi:10.1146/annurev.cb.04.110188.001103

Chen, W. T., Tseng, C. C., Pfaffenbach, K., Kanel, G., Luo, B., Stiles, B. L., & Lee, A. S. (2014a). Liver-specific knockout of GRP94 in mice disrupts cell adhesion, activates liver progenitor cells, and accelerates liver tumorigenesis. *Hepatology, 59*(3), 947-957. doi:10.1002/hep.26711

Chen, W. T., Zhu, G., Pfaffenbach, K., Kanel, G., Stiles, B., & Lee, A. S. (2014b). GRP78 as a regulator of liver steatosis and cancer progression mediated by loss of the tumor suppressor PTEN. *Oncogene, 33*(42), 4997-5005. doi:10.1038/onc.2013.437

Chen, Y., McMillan-Ward, E., Kong, J., Israels, S. J., & Gibson, S. B. (2007). Mitochondrial electron-transport-chain inhibitors of complexes I and II induce autophagic cell death mediated by reactive oxygen species. *J Cell Sci, 120*(Pt 23), 4155-4166. doi:10.1242/jcs.011163

Chen, Y., McMillan-Ward, E., Kong, J., Israels, S. J., & Gibson, S. B. (2008). Oxidative stress induces autophagic cell death independent of apoptosis in transformed and cancer cells. *Cell Death Differ, 15*(1), 171-182. doi:10.1038/sj.cdd.4402233

Cheng, J., & Haas, M. (1990). Frequent mutations in the p53 tumor suppressor gene in human leukemia T-cell lines. *Mol Cell Biol, 10*(10), 5502-5509.

Chhabra, S., Jain, S., Wallace, C., Hong, F., & Liu, B. (2015). High expression of endoplasmic reticulum chaperone grp94 is a novel molecular hallmark of malignant plasma cells in multiple myeloma. *J Hematol Oncol, 8*, 77. doi:10.1186/s13045-015-0177-6

Chicheportiche, Y., Bourdon, P. R., Xu, H., Hsu, Y. M., Scott, H., Hession, C., . . . Browning, J. L. (1997). TWEAK, a new secreted ligand in the tumor necrosis factor family that weakly induces apoptosis. *J Biol Chem, 272*(51), 32401-32410.

Chinnaiyan, A. M. (1999). The apoptosome: heart and soul of the cell death machine. *Neoplasia, 1*(1), 5-15.

Chrousos, G. P., Charmandari, E., & Kino, T. (2004). Glucocorticoid action networks--an introduction to systems biology. *J Clin Endocrinol Metab, 89*(2), 563-564. doi:10.1210/jc.2003-032026

Chrousos, G. P., & Kino, T. (2005). Intracellular glucocorticoid signaling: a formerly simple system turns stochastic. *Sci STKE, 2005*(304), pe48. doi:10.1126/stke.3042005pe48

Chung, S., Son, G. H., & Kim, K. (2011). Circadian rhythm of adrenal glucocorticoid: its regulation and clinical implications. *Biochim Biophys Acta, 1812*(5), 581-591. doi:10.1016/j.bbadis.2011.02.003

Claman, H. N. (1972). Corticosteroids and lymphoid cells. *N Engl J Med, 287*(8), 388-397. doi:10.1056/NEJM197208242870806

Clark, J. K., Schrader, W. T., & O'Malley, B. W. (1992). *Mechanism of Steroid hormones*. Philadelphia: WB Sanders Co.

ClinicalTrials.gov. (2018). Chloroquine in Combination With VELCADE and Cyclophosphamide for Relapsed and Refractory Multiple Myeloma. Retrieved from https://clinicaltrials.gov/ct2/show/NCT01438177?term=chloroquine&draw=2&rank=37

Corrigall, V. M., Vittecoq, O., & Panayi, G. S. (2009). Binding immunoglobulin protein-treated peripheral blood monocyte-derived dendritic cells are refractory to maturation and induce regulatory T-cell development. *Immunology, 128*(2), 218-226. doi:10.1111/j.1365-2567.2009.03103.x

Cory, S. (1995). Regulation of lymphocyte survival by the bcl-2 gene family. *Annu Rev Immunol, 13*, 513-543. doi:10.1146/annurev.iy.13.040195.002501

CRUK. (2013 - 2015). Acute Lymphoblastic Leukemia, Average number of New Cases per year. Retrieved from http://www.cancerresearchuk.org/health-professional/cancer-statistics/statistics-by-cancer-type/leukaemia-all/incidence#heading-One

CRUK. (2015). Acute Lymphoblastic Leukemia, European Age-Standardised incidence Rates, UK, 1993-2015.

Csizmar, C. M., Kim, D. H., & Sachs, Z. (2016). The role of the proteasome in AML. *Blood Cancer J, 6*(12), e503. doi:10.1038/bcj.2016.112

Cuervo, A. M., & Dice, J. F. (1996). A receptor for the selective uptake and degradation of proteins by lysosomes. *Science, 273*(5274), 501-503.

Dadgostar, H., & Cheng, G. (1998). An intact zinc ring finger is required for tumor necrosis factor receptor-associated factor-mediated nuclear factor-kappaB activation but is dispensable for c-Jun N-terminal kinase signaling. *J Biol Chem, 273*(38), 24775-24780.

Dai, Y., Chen, S., Wang, L., Pei, X. Y., Kramer, L. B., Dent, P., & Grant, S. (2011). Bortezomib interacts synergistically with belinostat in human acute myeloid leukaemia and acute lymphoblastic leukaemia cells in association with perturbations in NF-κB and Bim. *Br J Haematol, 153*(2), 222-235. doi:10.1111/j.1365-2141.2011.08591.x

Davies, L., Karthikeyan, N., Lynch, J. T., Sial, E. A., Gkourtsa, A., Demonacos, C., & Krstic-Demonacos, M. (2008). Cross talk of signaling pathways in the regulation of the glucocorticoid receptor function. *Mol Endocrinol, 22*(6), 1331-1344. doi:10.1210/me.2007-0360

Demonacos, C., Djordjevic-Markovic, R., Tsawdaroglou, N., & Sekeris, C. E. (1995). The mitochondrion as a primary site of action of glucocorticoids: the interaction of the glucocorticoid receptor with mitochondrial DNA sequences showing partial similarity to the nuclear glucocorticoid responsive elements. *J Steroid Biochem Mol Biol, 55*(1), 43-55.

Dempsey, P. W., Doyle, S. E., He, J. Q., & Cheng, G. (2003). The signaling adaptors and pathways activated by TNF superfamily. *Cytokine Growth Factor Rev, 14*(3-4), 193-209.

Deng, Y., Ren, X., Yang, L., Lin, Y., & Wu, X. (2003). A JNK-dependent pathway is required for TNFalpha-induced apoptosis. *Cell, 115*(1), 61-70.

Dengler, M. A., Staiger, A. M., Gutekunst, M., Hofmann, U., Doszczak, M., Scheurich, P., . . . van der Kuip, H. (2011). Oncogenic stress induced by acute hyper-activation of Bcr-Abl leads to cell death upon induction of excessive aerobic glycolysis. *PLoS One, 6*(9), e25139. doi:10.1371/journal.pone.0025139

Dennis, A. P., & O'Malley, B. W. (2005). Rush hour at the promoter: how the ubiquitin-proteasome pathway polices the traffic flow of nuclear receptor-dependent transcription. *J Steroid Biochem Mol Biol, 93*(2-5), 139-151. doi:10.1016/j.jsbmb.2004.12.015

Denton, D., Nicolson, S., & Kumar, S. (2012). Cell death by autophagy: facts and apparent artefacts. *Cell Death Differ, 19*(1), 87-95. doi:10.1038/cdd.2011.146

Deroo, B. J., Rentsch, C., Sampath, S., Young, J., DeFranco, D. B., & Archer, T. K. (2002). Proteasomal inhibition enhances glucocorticoid receptor transactivation and alters its subnuclear trafficking. *Mol Cell Biol, 22*(12), 4113-4123.

Dice, J. F. (1990). Peptide sequences that target cytosolic proteins for lysosomal proteolysis. *Trends Biochem Sci, 15*(8), 305-309.

DiDonato, J. A., Hayakawa, M., Rothwarf, D. M., Zandi, E., & Karin, M. (1997). A cytokine-responsive IkappaB kinase that activates the transcription factor NF-kappaB. *Nature, 388*(6642), 548-554. doi:10.1038/41493

Diederich, S., Eigendorff, E., Burkhardt, P., Quinkler, M., Bumke-Vogt, C., Rochel, M., . . . Bahr, V. (2002). 11beta-hydroxysteroid dehydrogenase types 1 and 2: an important pharmacokinetic determinant for the activity of synthetic mineralo- and glucocorticoids. *J Clin Endocrinol Metab, 87*(12), 5695-5701. doi:10.1210/jc.2002-020970

Ding, W. X., Ni, H. M., Gao, W., Yoshimori, T., Stolz, D. B., Ron, D., & Yin, X. M. (2007). Linking of autophagy to ubiquitin-proteasome system is important for the regulation of endoplasmic reticulum stress and cell viability. *Am J Pathol, 171*(2), 513-524. doi:10.2353/ajpath.2007.070188

Doan, N. T., Paulsen, E. S., Sehgal, P., Møller, J. V., Nissen, P., Denmeade, S. R., . . . Christensen, S. B. (2015). Targeting thapsigargin towards tumors. *Steroids, 97*, 2-7. doi:10.1016/j.steroids.2014.07.009

Dong, D., Ni, M., Li, J., Xiong, S., Ye, W., Virrey, J. J., . . . Lee, A. S. (2008). Critical role of the stress chaperone GRP78/BiP in tumor proliferation, survival, and tumor angiogenesis in transgene-induced mammary tumor development. *Cancer Res, 68*(2), 498-505. doi:10.1158/0008-5472.CAN-07-2950

Dong, Y., Poellinger, L., Gustafsson, J. A., & Okret, S. (1988). Regulation of glucocorticoid receptor expression: evidence for transcriptional and posttranslational mechanisms. *Mol Endocrinol, 2*(12), 1256-1264. doi:10.1210/mend-2-12-1256

Drouin, J., Trifiro, M. A., Plante, R. K., Nemer, M., Eriksson, P., & Wrange, O. (1989). Glucocorticoid receptor binding to a specific DNA sequence is required for hormone-

dependent repression of pro-opiomelanocortin gene transcription. *Mol Cell Biol, 9*(12), 5305-5314.

Druker, J., Liberman, A. C., Antunica-Noguerol, M., Gerez, J., Paez-Pereda, M., Rein, T., . . . Arzt, E. (2013). RSUME enhances glucocorticoid receptor SUMOylation and transcriptional activity. *Mol Cell Biol, 33*(11), 2116-2127. doi:10.1128/MCB.01470-12

Du, C., Fang, M., Li, Y., Li, L., & Wang, X. (2000). Smac, a mitochondrial protein that promotes cytochrome c-dependent caspase activation by eliminating IAP inhibition. *Cell, 102*(1), 33-42.

Duma, D., Jewell, C. M., & Cidlowski, J. A. (2006). Multiple glucocorticoid receptor isoforms and mechanisms of post-translational modification. *J Steroid Biochem Mol Biol, 102*(1-5), 11-21. doi:10.1016/j.jsbmb.2006.09.009

Dunlop, E. A., & Tee, A. R. (2013). The kinase triad, AMPK, mTORC1 and ULK1, maintains energy and nutrient homoeostasis. *Biochem Soc Trans, 41*(4), 939-943. doi:10.1042/BST20130030

Eberhart, K., Rainer, J., Bindreither, D., Ritter, I., Gnaiger, E., Kofler, R., . . . Renner, K. (2011). Glucocorticoid-induced alterations in mitochondrial membrane properties and respiration in childhood acute lymphoblastic leukemia. *Biochim Biophys Acta, 1807*(6), 719-725. doi:10.1016/j.bbabio.2010.12.010

Eberhart, K., Renner, K., Ritter, I., Kastenberger, M., Singer, K., Hellerbrand, C., . . . Oefner, P. J. (2009). Low doses of 2-deoxy-glucose sensitize acute lymphoblastic leukemia cells to glucocorticoid-induced apoptosis. *Leukemia, 23*(11), 2167-2170. doi:10.1038/leu.2009.154

Eisen, L. P., Elsasser, M. S., & Harmon, J. M. (1988). Positive regulation of the glucocorticoid receptor in human T-cells sensitive to the cytolytic effects of glucocorticoids. *J Biol Chem, 263*(24), 12044-12048.

Elmore, S. (2007). Apoptosis: a review of programmed cell death. *Toxicol Pathol, 35*(4), 495-516. doi:10.1080/01926230701320337

Enari, M., Sakahira, H., Yokoyama, H., Okawa, K., Iwamatsu, A., & Nagata, S. (1998). A caspase-activated DNase that degrades DNA during apoptosis, and its inhibitor ICAD. *Nature, 391*(6662), 43-50. doi:10.1038/34112

English, L., Chemali, M., Duron, J., Rondeau, C., Laplante, A., Gingras, D., . . . Desjardins, M. (2009). Autophagy enhances the presentation of endogenous viral antigens on MHC class I molecules during HSV-1 infection. *Nat Immunol, 10*(5), 480-487. doi:10.1038/ni.1720

Espindola-Antunes, D., & Kater, C. E. (2007). Adipose tissue expression of 11beta-hydroxysteroid dehydrogenase type 1 in Cushing's syndrome and in obesity. *Arq Bras Endocrinol Metabol, 51*(8), 1397-1403.

Evangelisti, C., Chiarini, F., Lonetti, A., Buontempo, F., Neri, L. M., McCubrey, J. A., & Martelli, A. M. (2014). Autophagy in acute leukemias: A double-edged sword with important therapeutic implications. *Biochim Biophys Acta, 1853*(1), 14-26. doi:10.1016/j.bbamcr.2014.09.023

Farquhar, M. J., & Bowen, D. T. (2003). Oxidative stress and the myelodysplastic syndromes. *Int J Hematol, 77*(4), 342-350.

Finkel, T. (2003). Oxidant signals and oxidative stress. *Curr Opin Cell Biol, 15*(2), 247-254.

Flora, S. J. (2009). Structural, chemical and biological aspects of antioxidants for strategies against metal and metalloid exposure. *Oxid Med Cell Longev, 2*(4), 191-206. doi:10.4161/oxim.2.4.9112

Flower, R. J., & Rothwell, N. J. (1994). Lipocortin-1: cellular mechanisms and clinical relevance. *Trends Pharmacol Sci, 15*(3), 71-76.

Foley, G. E., Lazarus, H., Farber, S., Uzman, B. G., Boone, B. A., & Mccarthy, R. E. (1965). Ccontinuous Culture of Human Lymphoblsts from Peripheral Blood of a Child with Acute Leukemia. *Cancer, 18*, 522-529.

Fried, L., & Arbiser, J. L. (2008). The reactive oxygen-driven tumor: relevance to melanoma. *Pigment Cell Melanoma Res, 21*(2), 117-122. doi:10.1111/j.1755-148X.2008.00451.x

Fu, Y., Li, J., & Lee, A. S. (2007). GRP78/BiP inhibits endoplasmic reticulum BIK and protects human breast cancer cells against estrogen starvation-induced apoptosis. *Cancer Res, 67*(8), 3734-3740. doi:10.1158/0008-5472.CAN-06-4594

Fu, Y., Wey, S., Wang, M., Ye, R., Liao, C. P., Roy-Burman, P., & Lee, A. S. (2008). Pten null prostate tumorigenesis and AKT activation are blocked by targeted knockout of ER chaperone GRP78/BiP in prostate epithelium. *Proc Natl Acad Sci U S A, 105*(49), 19444-19449. doi:10.1073/pnas.0807691105

Fujita, E., Kouroku, Y., Isoai, A., Kumagai, H., Misutani, A., Matsuda, C., . . . Momoi, T. (2007). Two endoplasmic reticulum-associated degradation (ERAD) systems for the novel variant of the mutant dysferlin: ubiquitin/proteasome ERAD(I) and autophagy/lysosome ERAD(II). *Hum Mol Genet, 16*(6), 618-629. doi:10.1093/hmg/ddm002

Galon, J., Franchimont, D., Hiroi, N., Frey, G., Boettner, A., Ehrhart-Bornstein, M., . . . Bornstein, S. R. (2002). Gene profiling reveals unknown enhancing and suppressive

actions of glucocorticoids on immune cells. *FASEB J, 16*(1), 61-71. doi:10.1096/fj.01-0245com

Gaynon, P. S., & Carrel, A. L. (1999). Glucocorticosteroid therapy in childhood acute lymphoblastic leukemia. *Adv Exp Med Biol, 457*, 593-605.

Geley, S., Hartmann, B. L., Kapelari, K., Egle, A., Villunger, A., Heidacher, D., . . . Kofler, R. (1997). The interleukin 1beta-converting enzyme inhibitor CrmA prevents Apo1/Fas- but not glucocorticoid-induced poly(ADP-ribose) polymerase cleavage and apoptosis in lymphoblastic leukemia cells. *FEBS Lett, 402*(1), 36-40.

George, P., Hernandez, K., Hustu, O., Borella, L., Holton, C., & Pinkel, D. (1968). A study of "total therapy" of acute lymphocytic leukemia in children. *J Pediatr, 72*(3), 399-408.

Goldin, A., Sandberg, J. S., Henderson, E. S., Newman, J. W., Frei, E., & Holland, J. F. (1971). The chemotherapy of human and animal acute leukemia. *Cancer Chemother Rep, 55*(4), 309-505.

Goldman, S. R., Ebright, R. H., & Nickels, B. E. (2009). Direct detection of abortive RNA transcripts in vivo. *Science, 324*(5929), 927-928. doi:10.1126/science.1169237

Gomi, M., Moriwaki, K., Katagiri, S., Kurata, Y., & Thompson, E. B. (1990). Glucocorticoid effects on myeloma cells in culture: correlation of growth inhibition with induction of glucocorticoid receptor messenger RNA. *Cancer Res, 50*(6), 1873-1878.

Gonzalez-Gronow, M., Selim, M. A., Papalas, J., & Pizzo, S. V. (2009). GRP78: a multifunctional receptor on the cell surface. *Antioxid Redox Signal, 11*(9), 2299-2306. doi:10.1089/ARS.2009.2568

Grander, D., Kharaziha, P., Laane, E., Pokrovskaja, K., & Panaretakis, T. (2009). Autophagy as the main means of cytotoxicity by glucocorticoids in hematological malignancies. *Autophagy, 5*(8), 1198-1200.

Gray, P. C., & Vale, W. (2012). Cripto/GRP78 modulation of the TGF-beta pathway in development and oncogenesis. *FEBS Lett, 586*(14), 1836-1845. doi:10.1016/j.febslet.2012.01.051

Greaves, M. (2006). Infection, immune responses and the aetiology of childhood leukaemia. *Nat Rev Cancer, 6*(3), 193-203. doi:10.1038/nrc1816

Greaves, M. F., & Wiemels, J. (2003). Origins of chromosome translocations in childhood leukaemia. *Nat Rev Cancer, 3*(9), 639-649. doi:10.1038/nrc1164

Greenstein, S., Ghias, K., Krett, N. L., & Rosen, S. T. (2002). Mechanisms of glucocorticoid-mediated apoptosis in hematological malignancies. *Clin Cancer Res, 8*(6), 1681-1694.

Grigoropoulos, N. F., Petter, R., Van 't Veer, M. B., Scott, M. A., & Follows, G. A. (2013). Leukaemia update. Part 1: diagnosis and management. *BMJ, 346*, f1660. doi:10.1136/bmj.f1660

Gross, K. L., & Cidlowski, J. A. (2008). Tissue-specific glucocorticoid action: a family affair. *Trends Endocrinol Metab, 19*(9), 331-339. doi:10.1016/j.tem.2008.07.009

Gruol, D. J., Rajah, F. M., & Bourgeois, S. (1989). Cyclic AMP-dependent protein kinase modulation of the glucocorticoid-induced cytolytic response in murine T-lymphoma cells. *Mol Endocrinol, 3*(12), 2119-2127. doi:10.1210/mend-3-12-2119

Guo, X. L., Li, D., Sun, K., Wang, J., Liu, Y., Song, J. R., . . . Wei, L. X. (2013). Inhibition of autophagy enhances anticancer effects of bevacizumab in hepatocarcinoma. *J Mol Med (Berl), 91*(4), 473-483. doi:10.1007/s00109-012-0966-0

Gupta, R. C. (2012). Rotenone. In R. C. Gupta (Ed.), *Veterinary Toxicology (Second Edition) Basic and Clinical Principle* (Second Edition ed., pp. 620-623): Elsevier Inc.

Häcker, G. (2000). The morphology of apoptosis. *Cell Tissue Res, 301*(1), 5-17.

Hammond, G. L., Smith, C. L., Goping, I. S., Underhill, D. A., Harley, M. J., Reventos, J., . . . Bardin, C. W. (1987). Primary structure of human corticosteroid binding globulin, deduced from hepatic and pulmonary cDNAs, exhibits homology with serine protease inhibitors. *Proc Natl Acad Sci U S A, 84*(15), 5153-5157.

Hammond, G. L., Smith, C. L., Paterson, N. A., & Sibbald, W. J. (1990). A role for corticosteroid-binding globulin in delivery of cortisol to activated neutrophils. *J Clin Endocrinol Metab, 71*(1), 34-39. doi:10.1210/jcem-71-1-34

Hanahan, D., & Weinberg, R. A. (2011). Hallmarks of cancer: the next generation. *Cell, 144*(5), 646-674. doi:10.1016/j.cell.2011.02.013

Hancock, J. T., Desikan, R., & Neill, S. J. (2001). Role of reactive oxygen species in cell signalling pathways. *Biochem Soc Trans, 29*(Pt 2), 345-350.

Hann, I., Vora, A., Richards, S., Hill, F., Gibson, B., Lilleyman, J., . . . Eden, O. B. (2000). Benefit of intensified treatment for all children with acute lymphoblastic leukaemia: results from MRC UKALL XI and MRC ALL97 randomised trials. UK Medical Research Council's Working Party on Childhood Leukaemia. *Leukemia, 14*(3), 356-363.

Harding, H. P., Novoa, I., Zhang, Y., Zeng, H., Wek, R., Schapira, M., & Ron, D. (2000). Regulated translation initiation controls stress-induced gene expression in mammalian cells. *Mol Cell, 6*(5), 1099-1108.

Harmon, J. M., & Thompson, E. B. (1981). Isolation and characterization of dexamethasone-resistant mutants from human lymphoid cell line CEM-C7. *Mol Cell Biol, 1*(6), 512-521.

Harrison, C. J. (2009). Cytogenetics of paediatric and adolescent acute lymphoblastic leukaemia. *Br J Haematol, 144*(2), 147-156. doi:10.1111/j.1365-2141.2008.07417.x

Hartmann, B. L., Geley, S., Loffler, M., Hattmannstorfer, R., Strasser-Wozak, E. M., Auer, B., & Kofler, R. (1999). Bcl-2 interferes with the execution phase, but not upstream events, in glucocorticoid-induced leukemia apoptosis. *Oncogene, 18*(3), 713-719. doi:10.1038/sj.onc.1202339

He, C., & Klionsky, D. J. (2009). Regulation mechanisms and signaling pathways of autophagy. *Annu Rev Genet, 43*, 67-93. doi:10.1146/annurev-genet-102808-114910

Heck, S., Kullmann, M., Gast, A., Ponta, H., Rahmsdorf, H. J., Herrlich, P., & Cato, A. C. (1994). A distinct modulating domain in glucocorticoid receptor monomers in the repression of activity of the transcription factor AP-1. *EMBO J, 13*(17), 4087-4095.

Heery, D. M., Kalkhoven, E., Hoare, S., & Parker, M. G. (1997). A signature motif in transcriptional co-activators mediates binding to nuclear receptors. *Nature, 387*(6634), 733-736. doi:10.1038/42750

Henley, D., Lightman, S., & Carrell, R. (2016). Cortisol and CBG - Getting cortisol to the right place at the right time. *Pharmacol Ther, 166*, 128-135. doi:10.1016/j.pharmthera.2016.06.020

Hetz, C., Bernasconi, P., Fisher, J., Lee, A. H., Bassik, M. C., Antonsson, B., . . . Korsmeyer, S. J. (2006). Proapoptotic BAX and BAK modulate the unfolded protein response by a direct interaction with IRE1alpha. *Science, 312*(5773), 572-576. doi:10.1126/science.1123480

Hill, M. M., Adrain, C., Duriez, P. J., Creagh, E. M., & Martin, S. J. (2004). Analysis of the composition, assembly kinetics and activity of native Apaf-1 apoptosomes. *EMBO J, 23*(10), 2134-2145. doi:10.1038/sj.emboj.7600210

Ho, J. T., Al-Musalhi, H., Chapman, M. J., Quach, T., Thomas, P. D., Bagley, C. J., . . . Torpy, D. J. (2006). Septic shock and sepsis: a comparison of total and free plasma cortisol levels. *J Clin Endocrinol Metab, 91*(1), 105-114. doi:10.1210/jc.2005-0265

Hollenberg, S. M., Weinberger, C., Ong, E. S., Cerelli, G., Oro, A., Lebo, R., . . . Evans, R. M. (1985). Primary structure and expression of a functional human glucocorticoid receptor cDNA. *Nature, 318*(6047), 635-641.

Hom, J. R., Gewandter, J. S., Michael, L., Sheu, S. S., & Yoon, Y. (2007). Thapsigargin induces biphasic fragmentation of mitochondria through calcium-mediated mitochondrial fission and apoptosis. *J Cell Physiol, 212*(2), 498-508. doi:10.1002/jcp.21051

Horton, T. M., Gannavarapu, A., Blaney, S. M., D'Argenio, D. Z., Plon, S. E., & Berg, S. L. (2006). Bortezomib interactions with chemotherapy agents in acute leukemia in vitro. *Cancer Chemother Pharmacol, 58*(1), 13-23. doi:10.1007/s00280-005-0135-z

Hsu, H., Huang, J., Shu, H. B., Baichwal, V., & Goeddel, D. V. (1996). TNF-dependent recruitment of the protein kinase RIP to the TNF receptor-1 signaling complex. *Immunity, 4*(4), 387-396.

Hua, Y., White-Gilbertson, S., Kellner, J., Rachidi, S., Usmani, S. Z., Chiosis, G., . . . Liu, B. (2013). Molecular chaperone gp96 is a novel therapeutic target of multiple myeloma. *Clin Cancer Res, 19*(22), 6242-6251. doi:10.1158/1078-0432.CCR-13-2083

Hunger, S. P., Lu, X., Devidas, M., Camitta, B. M., Gaynon, P. S., Winick, N. J., . . . Carroll, W. L. (2012). Improved survival for children and adolescents with acute lymphoblastic leukemia between 1990 and 2005: a report from the children's oncology group. *J Clin Oncol, 30*(14), 1663-1669. doi:10.1200/JCO.2011.37.8018

Hunger, S. P., & Mullighan, C. G. (2015a). Acute Lymphoblastic Leukemia in Children. *N Engl J Med, 373*(16), 1541-1552. doi:10.1056/NEJMra1400972

Hunger, S. P., & Mullighan, C. G. (2015b). Redefining ALL classification: toward detecting high-risk ALL and implementing precision medicine. *Blood, 125*(26), 3977-3987. doi:10.1182/blood-2015-02-580043

Igney, F. H., & Krammer, P. H. (2002). Death and anti-death: tumour resistance to apoptosis. *Nat Rev Cancer, 2*(4), 277-288. doi:10.1038/nrc776

Imran, A., Qamar, H. Y., Ali, Q., Naeem, H., Riaz, M., Amin, S., . . . Nasir, I. A. (2017). Role of Molecular Biology in Cancer Treatment: A Review Article. *Iran J Public Health, 46*(11), 1475-1485.

Inaba, H., Greaves, M., & Mullighan, C. G. (2013). Acute lymphoblastic leukaemia. *Lancet, 381*(9881), 1943-1955. doi:10.1016/S0140-6736(12)62187-4

Inaba, H., & Pui, C. H. (2010). Glucocorticoid use in acute lymphoblastic leukaemia. *Lancet Oncol, 11*(11), 1096-1106. doi:10.1016/S1470-2045(10)70114-5

Irani, K., Xia, Y., Zweier, J. L., Sollott, S. J., Der, C. J., Fearon, E. R., . . . Goldschmidt-Clermont, P. J. (1997). Mitogenic signaling mediated by oxidants in Ras-transformed fibroblasts. *Science, 275*(5306), 1649-1652.

Irving, J. A., Pike, R. N., Lesk, A. M., & Whisstock, J. C. (2000). Phylogeny of the serpin superfamily: implications of patterns of amino acid conservation for structure and function. *Genome Res, 10*(12), 1845-1864.

Irwin, M. E., Rivera-Del Valle, N., & Chandra, J. (2013). Redox control of leukemia: from molecular mechanisms to therapeutic opportunities. *Antioxid Redox Signal, 18*(11), 1349-1383. doi:10.1089/ars.2011.4258

Ismaili, N., & Garabedian, M. J. (2004). Modulation of glucocorticoid receptor function via phosphorylation. *Ann N Y Acad Sci, 1024*, 86-101. doi:10.1196/annals.1321.007

Itoh, M., Adachi, M., Yasui, H., Takekawa, M., Tanaka, H., & Imai, K. (2002). Nuclear export of glucocorticoid receptor is enhanced by c-Jun N-terminal kinase-mediated phosphorylation. *Mol Endocrinol, 16*(10), 2382-2392. doi:10.1210/me.2002-0144

Jia, G., & Sowers, J. R. (2015). Autophagy: a housekeeper in cardiorenal metabolic health and disease. *Biochim Biophys Acta, 1852*(2), 219-224. doi:10.1016/j.bbadis.2014.06.025

Jiang, L., Xu, L., Xie, J., Li, S., Guan, Y., Zhang, Y., . . . Liu, Q. (2015). Inhibition of autophagy overcomes glucocorticoid resistance in lymphoid malignant cells. *Cancer Biol Ther, 16*(3), 466-476. doi:10.1080/15384047.2015.1016658

Joza, N., Susin, S. A., Daugas, E., Stanford, W. L., Cho, S. K., Li, C. Y., . . . Penninger, J. M. (2001). Essential role of the mitochondrial apoptosis-inducing factor in programmed cell death. *Nature, 410*(6828), 549-554. doi:10.1038/35069004

Kelly, K. R., Rowe, J. H., Padmanabhan, S., Nawrocki, S. T., & Carew, J. S. (2011). Mammalian target of rapamycin as a target in hematological malignancies. *Target Oncol, 6*(1), 53-61. doi:10.1007/s11523-011-0175-8

Kerr, J. F., Wyllie, A. H., & Currie, A. R. (1972). Apoptosis: a basic biological phenomenon with wide-ranging implications in tissue kinetics. *Br J Cancer, 26*(4), 239-257.

Khan, M. S., Aden, D., & Rosner, W. (1984). Human corticosteroid binding globulin is secreted by a hepatoma-derived cell line. *J Steroid Biochem, 20*(2), 677-678.

Khavari, T. A., & Rinn, J. (2007). Ras/Erk MAPK signaling in epidermal homeostasis and neoplasia. *Cell Cycle, 6*(23), 2928-2931. doi:10.4161/cc.6.23.4998

Kimura, T., Takabatake, Y., Takahashi, A., & Isaka, Y. (2013). Chloroquine in cancer therapy: a double-edged sword of autophagy. *Cancer Res, 73*(1), 3-7. doi:10.1158/0008-5472.CAN-12-2464

Kino, T. (2000). Glucocorticoid Receptor. In L. J. De Groot, G. Chrousos, K. Dungan, K. R. Feingold, A. Grossman, J. M. Hershman, C. Koch, M. Korbonits, R. McLachlan, M.

New, J. Purnell, R. Rebar, F. Singer, & A. Vinik (Eds.), *Endotext*. South Dartmouth (MA).

Kino, T., Liou, S. H., Charmandari, E., & Chrousos, G. P. (2004). Glucocorticoid receptor mutants demonstrate increased motility inside the nucleus of living cells: time of fluorescence recovery after photobleaching (FRAP) is an integrated measure of receptor function. *Mol Med, 10*(7-12), 80-88. doi:10.2119/2005-00026.Kino

Kinyamu, H. K., Chen, J., & Archer, T. K. (2005). Linking the ubiquitin-proteasome pathway to chromatin remodeling/modification by nuclear receptors. *J Mol Endocrinol, 34*(2), 281-297. doi:10.1677/jme.1.01680

Klieber, M. A., Underhill, C., Hammond, G. L., & Muller, Y. A. (2007). Corticosteroid-binding globulin, a structural basis for steroid transport and proteinase-triggered release. *J Biol Chem, 282*(40), 29594-29603. doi:10.1074/jbc.M705014200

Kluck, R. M., Bossy-Wetzel, E., Green, D. R., & Newmeyer, D. D. (1997). The release of cytochrome c from mitochondria: a primary site for Bcl-2 regulation of apoptosis. *Science, 275*(5303), 1132-1136.

Koong, A. C., Chauhan, V., & Romero-Ramirez, L. (2006). Targeting XBP-1 as a novel anti-cancer strategy. *Cancer Biol Ther, 5*(7), 756-759.

Koufali, M. M., Moutsatsou, P., Sekeris, C. E., & Breen, K. C. (2003). The dynamic localization of the glucocorticoid receptor in rat C6 glioma cell mitochondria. *Mol Cell Endocrinol, 209*(1-2), 51-60.

Koumenis, C., Naczki, C., Koritzinsky, M., Rastani, S., Diehl, A., Sonenberg, N., . . . Wouters, B. G. (2002). Regulation of protein synthesis by hypoxia via activation of the endoplasmic reticulum kinase PERK and phosphorylation of the translation initiation factor eIF2alpha. *Mol Cell Biol, 22*(21), 7405-7416.

Kouroku, Y., Fujita, E., Tanida, I., Ueno, T., Isoai, A., Kumagai, H., . . . Momoi, T. (2007). ER stress (PERK/eIF2alpha phosphorylation) mediates the polyglutamine-induced LC3 conversion, an essential step for autophagy formation. *Cell Death Differ, 14*(2), 230-239. doi:10.1038/sj.cdd.4401984

Koyama, D., Kikuchi, J., Hiraoka, N., Wada, T., Kurosawa, H., Chiba, S., & Furukawa, Y. (2014). Proteasome inhibitors exert cytotoxicity and increase chemosensitivity via transcriptional repression of Notch1 in T-cell acute lymphoblastic leukemia. *Leukemia, 28*(6), 1216-1226. doi:10.1038/leu.2013.366

Krappmann, D., Wulczyn, F. G., & Scheidereit, C. (1996). Different mechanisms control signal-induced degradation and basal turnover of the NF-kappaB inhibitor IkappaB alpha in vivo. *EMBO J, 15*(23), 6716-6726.

Kraskiewicz, H., & FitzGerald, U. (2012). InterfERing with endoplasmic reticulum stress. *Trends Pharmacol Sci, 33*(2), 53-63. doi:10.1016/j.tips.2011.10.002

Kroemer, G., Galluzzi, L., Vandenabeele, P., Abrams, J., Alnemri, E. S., Baehrecke, E. H., . . . 2009, N. C. o. C. D. (2009). Classification of cell death: recommendations of the Nomenclature Committee on Cell Death 2009. *Cell Death Differ, 16*(1), 3-11. doi:10.1038/cdd.2008.150

Kroemer, G., Mariño, G., & Levine, B. (2010). Autophagy and the integrated stress response. *Mol Cell, 40*(2), 280-293. doi:10.1016/j.molcel.2010.09.023

Krstic, M. D., Rogatsky, I., Yamamoto, K. R., & Garabedian, M. J. (1997). Mitogen-activated and cyclin-dependent protein kinases selectively and differentially modulate transcriptional enhancement by the glucocorticoid receptor. *Mol Cell Biol, 17*(7), 3947-3954.

Krysov, S., Steele, A. J., Coelho, V., Linley, A., Sanchez Hidalgo, M., Carter, M., . . . Packham, G. (2014). Stimulation of surface IgM of chronic lymphocytic leukemia cells induces an unfolded protein response dependent on BTK and SYK. *Blood, 124*(20), 3101-3109. doi:10.1182/blood-2014-04-567198

Kumar, B., Koul, S., Khandrika, L., Meacham, R. B., & Koul, H. K. (2008). Oxidative stress is inherent in prostate cancer cells and is required for aggressive phenotype. *Cancer Res, 68*(6), 1777-1785. doi:10.1158/0008-5472.CAN-07-5259

Kumar, S., Yedjou, C. G., & Tchounwou, P. B. (2014). Arsenic trioxide induces oxidative stress, DNA damage, and mitochondrial pathway of apoptosis in human leukemia (HL-60) cells. *J Exp Clin Cancer Res, 33*, 42. doi:10.1186/1756-9966-33-42

Lacroix, A., Bonnard, G. D., & Lippman, M. E. (1984). Modulation of glucocorticoid receptors by mitogenic stimuli, glucocorticoids and retinoids in normal human cultured T cells. *J Steroid Biochem, 21*(1), 73-80.

Lamy, L., Ngo, V. N., Emre, N. C., Shaffer, A. L., 3rd, Yang, Y., Tian, E., . . . Staudt, L. M. (2013). Control of autophagic cell death by caspase-10 in multiple myeloma. *Cancer Cell, 23*(4), 435-449. doi:10.1016/j.ccr.2013.02.017

Lau, A. T., Wang, Y., & Chiu, J. F. (2008). Reactive oxygen species: current knowledge and applications in cancer research and therapeutic. *J Cell Biochem, 104*(2), 657-667. doi:10.1002/jcb.21655

Le Drean, Y., Mincheneau, N., Le Goff, P., & Michel, D. (2002). Potentiation of glucocorticoid receptor transcriptional activity by sumoylation. *Endocrinology, 143*(9), 3482-3489. doi:10.1210/en.2002-220135

Lee, A. H., Iwakoshi, N. N., Anderson, K. C., & Glimcher, L. H. (2003). Proteasome inhibitors disrupt the unfolded protein response in myeloma cells. *Proc Natl Acad Sci U S A, 100*(17), 9946-9951. doi:10.1073/pnas.1334037100

Lee, A. S. (2001). The glucose-regulated proteins: stress induction and clinical applications. *Trends Biochem Sci, 26*(8), 504-510.

Lee, A. S. (2007). GRP78 induction in cancer: therapeutic and prognostic implications. *Cancer Res, 67*(8), 3496-3499. doi:10.1158/0008-5472.CAN-07-0325

Lee, A. S. (2014). Glucose-regulated proteins in cancer: molecular mechanisms and therapeutic potential. *Nat Rev Cancer, 14*(4), 263-276. doi:10.1038/nrc3701

Lemasters, J. J., Qian, T., He, L., Kim, J. S., Elmore, S. P., Cascio, W. E., & Brenner, D. A. (2002). Role of mitochondrial inner membrane permeabilization in necrotic cell death, apoptosis, and autophagy. *Antioxid Redox Signal, 4*(5), 769-781. doi:10.1089/152308602760598918

Leung, D. Y., Hamid, Q., Vottero, A., Szefler, S. J., Surs, W., Minshall, E., . . . Klemm, D. J. (1997). Association of glucocorticoid insensitivity with increased expression of glucocorticoid receptor beta. *J Exp Med, 186*(9), 1567-1574.

Levine, B., & Kroemer, G. (2008). Autophagy in the pathogenesis of disease. *Cell, 132*(1), 27-42. doi:10.1016/j.cell.2007.12.018

Levine, B., Mizushima, N., & Virgin, H. W. (2011). Autophagy in immunity and inflammation. *Nature, 469*(7330), 323-335. doi:10.1038/nature09782

Li, J., Ni, M., Lee, B., Barron, E., Hinton, D. R., & Lee, A. S. (2008). The unfolded protein response regulator GRP78/BiP is required for endoplasmic reticulum integrity and stress-induced autophagy in mammalian cells. *Cell Death Differ, 15*(9), 1460-1471. doi:10.1038/cdd.2008.81

Li, L. Y., Luo, X., & Wang, X. (2001). Endonuclease G is an apoptotic DNase when released from mitochondria. *Nature, 412*(6842), 95-99. doi:10.1038/35083620

Li, N., Ragheb, K., Lawler, G., Sturgis, J., Rajwa, B., Melendez, J. A., & Robinson, J. P. (2003). Mitochondrial complex I inhibitor rotenone induces apoptosis through enhancing mitochondrial reactive oxygen species production. *J Biol Chem, 278*(10), 8516-8525. doi:10.1074/jbc.M210432200

Li, W. W., Alexandre, S., Cao, X., & Lee, A. S. (1993). Transactivation of the grp78 promoter by Ca2+ depletion. A comparative analysis with A23187 and the endoplasmic reticulum Ca(2+)-ATPase inhibitor thapsigargin. *J Biol Chem, 268*(16), 12003-12009.

Liou, G. Y., & Storz, P. (2010). Reactive oxygen species in cancer. *Free Radic Res, 44*(5), 479-496. doi:10.3109/10715761003667554

Liu, D., Ahmet, A., Ward, L., Krishnamoorthy, P., Mandelcorn, E. D., Leigh, R., . . . Kim, H. (2013a). A practical guide to the monitoring and management of the complications of systemic corticosteroid therapy. *Allergy Asthma Clin Immunol, 9*(1), 30. doi:10.1186/1710-1492-9-30

Liu, J., & DeFranco, D. B. (2000). Protracted nuclear export of glucocorticoid receptor limits its turnover and does not require the exportin 1/CRM1-directed nuclear export pathway. *Mol Endocrinol, 14*(1), 40-51. doi:10.1210/mend.14.1.0398

Liu, R., Li, X., Gao, W., Zhou, Y., Wey, S., Mitra, S. K., . . . Gill, P. S. (2013b). Monoclonal antibody against cell surface GRP78 as a novel agent in suppressing PI3K/AKT signaling, tumor growth, and metastasis. *Clin Cancer Res, 19*(24), 6802-6811. doi:10.1158/1078-0432.CCR-13-1106

Locksley, R. M., Killeen, N., & Lenardo, M. J. (2001). The TNF and TNF receptor superfamilies: integrating mammalian biology. *Cell, 104*(4), 487-501.

Louis, K. S., & Siegel, A. C. (2011). Cell viability analysis using trypan blue: manual and automated methods. *Methods Mol Biol, 740*, 7-12. doi:10.1007/978-1-61779-108-6_2

Lu, N. Z., & Cidlowski, J. A. (2005). Translational regulatory mechanisms generate N-terminal glucocorticoid receptor isoforms with unique transcriptional target genes. *Mol Cell, 18*(3), 331-342. doi:10.1016/j.molcel.2005.03.025

Luo, B., & Lee, A. S. (2013). The critical roles of endoplasmic reticulum chaperones and unfolded protein response in tumorigenesis and anticancer therapies. *Oncogene, 32*(7), 805-818. doi:10.1038/onc.2012.130

Lykke-Andersen, S., & Jensen, T. H. (2007). Overlapping pathways dictate termination of RNA polymerase II transcription. *Biochimie, 89*(10), 1177-1182. doi:10.1016/j.biochi.2007.05.007

Lynch, J. T., Rajendran, R., Xenaki, G., Berrou, I., Demonacos, C., & Krstic-Demonacos, M. (2010). The role of glucocorticoid receptor phosphorylation in Mcl-1 and NOXA gene expression. *Mol Cancer, 9*, 38. doi:10.1186/1476-4598-9-38

Ma, T., Zhu, J., Chen, X., Zha, D., Singhal, P. C., & Ding, G. (2013). High glucose induces autophagy in podocytes. *Exp Cell Res, 319*(6), 779-789. doi:10.1016/j.yexcr.2013.01.018

Ma, X. C., Liu, C. Y., Sun, X. J., He, J. J., Wan, S. G., & Sun, W. L. (2014). [Genetic characteristics of human acute lymphoblastic leukemia cell line Molt-4]. *Zhongguo Shi Yan Xue Ye Xue Za Zhi, 22*(2), 280-284.

Ma, Y., & Hendershot, L. M. (2004). The role of the unfolded protein response in tumour development: friend or foe? *Nat Rev Cancer, 4*(12), 966-977. doi:10.1038/nrc1505

Maraldi, T., Prata, C., Vieceli Dalla Sega, F., Caliceti, C., Zambonin, L., Fiorentini, D., & Hakim, G. (2009). NAD(P)H oxidase isoform Nox2 plays a prosurvival role in human leukaemia cells. *Free Radic Res, 43*(11), 1111-1121. doi:10.1080/10715760903186132

Martini, M., De Santis, M. C., Braccini, L., Gulluni, F., & Hirsch, E. (2014). PI3K/AKT signaling pathway and cancer: an updated review. *Ann Med, 46*(6), 372-383. doi:10.3109/07853890.2014.912836

Martinon, F. (2012). Targeting endoplasmic reticulum signaling pathways in cancer. *Acta Oncol, 51*(7), 822-830. doi:10.3109/0284186X.2012.689113

Marzec, M., Eletto, D., & Argon, Y. (2012). GRP94: An HSP90-like protein specialized for protein folding and quality control in the endoplasmic reticulum. *Biochim Biophys Acta, 1823*(3), 774-787. doi:10.1016/j.bbamcr.2011.10.013

Masud Alam, M., Kariya, R., Kawaguchi, A., Matsuda, K., Kudo, E., & Okada, S. (2016). Inhibition of autophagy by chloroquine induces apoptosis in primary effusion lymphoma in vitro and in vivo through induction of endoplasmic reticulum stress. *Apoptosis*. doi:10.1007/s10495-016-1277-7

Mathew, R., Karp, C. M., Beaudoin, B., Vuong, N., Chen, G., Chen, H. Y., . . . White, E. (2009). Autophagy suppresses tumorigenesis through elimination of p62. *Cell, 137*(6), 1062-1075. doi:10.1016/j.cell.2009.03.048

Mcintyre, W. R., & Samuels, H. H. (1985). Triamcinolone Acetonide Regulates Glucocorticoid-Receptor Levels by Decreasing the Half-Life of the Activated Nuclear-Receptor Form. *Journal of Biological Chemistry, 260*(1), 418-427.

McKay, L. I., & Cidlowski, J. A. (1998). Cross-talk between nuclear factor-kappa B and the steroid hormone receptors: mechanisms of mutual antagonism. *Mol Endocrinol, 12*(1), 45-56. doi:10.1210/mend.12.1.0044

McKay, L. I., & Cidlowski, J. A. (1999). Molecular control of immune/inflammatory responses: interactions between nuclear factor-kappa B and steroid receptor-signaling pathways. *Endocr Rev, 20*(4), 435-459. doi:10.1210/edrv.20.4.0375

McKenna, N. J., Lanz, R. B., & O'Malley, B. W. (1999). Nuclear receptor coregulators: cellular and molecular biology. *Endocr Rev, 20*(3), 321-344. doi:10.1210/edrv.20.3.0366

McKenna, N. J., & O'Malley, B. W. (2002). Combinatorial control of gene expression by nuclear receptors and coregulators. *Cell, 108*(4), 465-474.

Medh, R. D., Saeed, M. F., Johnson, B. H., & Thompson, E. B. (1998). Resistance of human leukemic CEM-C1 cells is overcome by synergism between glucocorticoid and protein kinase A pathways: correlation with c-Myc suppression. *Cancer Res, 58*(16), 3684-3693.

Medh, R. D., Webb, M. S., Miller, A. L., Johnson, B. H., Fofanov, Y., Li, T., . . . Thompson, E. B. (2003). Gene expression profile of human lymphoid CEM cells sensitive and resistant to glucocorticoid-evoked apoptosis. *Genomics, 81*(6), 543-555.

Mei, Y., Thompson, M. D., Cohen, R. A., & Tong, X. (2015). Autophagy and oxidative stress in cardiovascular diseases. *Biochim Biophys Acta, 1852*(2), 243-251. doi:10.1016/j.bbadis.2014.05.005

Miao, Y. R., Eckhardt, B. L., Cao, Y., Pasqualini, R., Argani, P., Arap, W., . . . Anderson, R. L. (2013). Inhibition of established micrometastases by targeted drug delivery via cell surface-associated GRP78. *Clin Cancer Res, 19*(8), 2107-2116. doi:10.1158/1078-0432.CCR-12-2991

Misra, U. K., Chu, C. T., Rubenstein, D. S., Gawdi, G., & Pizzo, S. V. (1993). Receptor-recognized alpha 2-macroglobulin-methylamine elevates intracellular calcium, inositol phosphates and cyclic AMP in murine peritoneal macrophages. *Biochem J, 290 (Pt 3)*, 885-891.

Misra, U. K., & Pizzo, S. V. (2012). Receptor-recognized alpha(2)-macroglobulin binds to cell surface-associated GRP78 and activates mTORC1 and mTORC2 signaling in prostate cancer cells. *PLoS One, 7*(12), e51735. doi:10.1371/journal.pone.0051735

Misra, U. K., & Pizzo, S. V. (2013). Evidence for a pro-proliferative feedback loop in prostate cancer: the role of Epac1 and COX-2-dependent pathways. *PLoS One, 8*(4), e63150. doi:10.1371/journal.pone.0063150

MITCHELL, P. (1961). Coupling of phosphorylation to electron and hydrogen transfer by a chemi-osmotic type of mechanism. *Nature, 191*, 144-148.

Mizushima, N. (2007). Autophagy: process and function. *Genes Dev, 21*(22), 2861-2873. doi:10.1101/gad.1599207

Mizushima, N., Levine, B., Cuervo, A. M., & Klionsky, D. J. (2008). Autophagy fights disease through cellular self-digestion. *Nature, 451*(7182), 1069-1075. doi:10.1038/nature06639

Moenner, M., Pluquet, O., Bouchecareilh, M., & Chevet, E. (2007). Integrated endoplasmic reticulum stress responses in cancer. *Cancer Res, 67*(22), 10631-10634. doi:10.1158/0008-5472.CAN-07-1705

Molitoris, J. K., McColl, K. S., Swerdlow, S., Matsuyama, M., Lam, M., Finkel, T. H., . . . Distelhorst, C. W. (2011). Glucocorticoid elevation of dexamethasone-induced gene 2 (Dig2/RTP801/REDD1) protein mediates autophagy in lymphocytes. *J Biol Chem, 286*(34), 30181-30189. doi:10.1074/jbc.M111.245423

Møller, J. V., Olesen, C., Winther, A. M., & Nissen, P. (2010). The sarcoplasmic Ca2+-ATPase: design of a perfect chemi-osmotic pump. *Q Rev Biophys, 43*(4), 501-566. doi:10.1017/S003358351000017X

Morales, C., Rachidi, S., Hong, F., Sun, S., Ouyang, X., Wallace, C., . . . Li, Z. (2014). Immune chaperone gp96 drives the contributions of macrophages to inflammatory colon tumorigenesis. *Cancer Res, 74*(2), 446-459. doi:10.1158/0008-5472.CAN-13-1677

Nader, N., Chrousos, G. P., & Kino, T. (2009). Circadian rhythm transcription factor CLOCK regulates the transcriptional activity of the glucocorticoid receptor by acetylating its hinge region lysine cluster: potential physiological implications. *FASEB J, 23*(5), 1572-1583. doi:10.1096/fj.08-117697

Nakatogawa, H., Suzuki, K., Kamada, Y., & Ohsumi, Y. (2009). Dynamics and diversity in autophagy mechanisms: lessons from yeast. *Nat Rev Mol Cell Biol, 10*(7), 458-467. doi:10.1038/nrm2708

Naughton, R., Quiney, C., Turner, S. D., & Cotter, T. G. (2009). Bcr-Abl-mediated redox regulation of the PI3K/AKT pathway. *Leukemia, 23*(8), 1432-1440. doi:10.1038/leu.2009.49

Nenke, M. A., Holmes, M., Rankin, W., Lewis, J. G., & Torpy, D. J. (2016). Corticosteroid-binding globulin cleavage is paradoxically reduced in alpha-1 antitrypsin deficiency: Implications for cortisol homeostasis. *Clin Chim Acta, 452*, 27-31. doi:10.1016/j.cca.2015.10.028

Newton, R. (2000). Molecular mechanisms of glucocorticoid action: what is important? *Thorax, 55*(7), 603-613.

Ngoka, L. C. (2008). Sample prep for proteomics of breast cancer: proteomics and gene ontology reveal dramatic differences in protein solubilization preferences of radioimmunoprecipitation assay and urea lysis buffers. *Proteome Sci, 6,* 30. doi:10.1186/1477-5956-6-30

Ni, M., & Lee, A. S. (2007). ER chaperones in mammalian development and human diseases. *FEBS Lett, 581*(19), 3641-3651. doi:10.1016/j.febslet.2007.04.045

Ni, M., Zhang, Y., & Lee, A. S. (2011). Beyond the endoplasmic reticulum: atypical GRP78 in cell viability, signalling and therapeutic targeting. *Biochem J, 434*(2), 181-188. doi:10.1042/BJ20101569

Ni, M., Zhou, H., Wey, S., Baumeister, P., & Lee, A. S. (2009). Regulation of PERK signaling and leukemic cell survival by a novel cytosolic isoform of the UPR regulator GRP78/BiP. *PLoS One, 4*(8), e6868. doi:10.1371/journal.pone.0006868

Nicolaides, N. C., Galata, Z., Kino, T., Chrousos, G. P., & Charmandari, E. (2010). The human glucocorticoid receptor: molecular basis of biologic function. *Steroids, 75*(1), 1-12. doi:10.1016/j.steroids.2009.09.002 S0039-128X(09)00208-6 [pii]

NIH. (2018). Study of G-202 (Mipsagargin) Retrieved from https://clinicaltrials.gov/

Norman, M. R., & Thompson, E. B. (1977). Characterization of a glucocorticoid-sensitive human lymphoid cell line. *Cancer Res, 37*(10), 3785-3791.

Nowell, P. C., & Hungerford, D. A. (1960). Chromosome studies on normal and leukemic human leukocytes. *J Natl Cancer Inst, 25*, 85-109.

Nunes, T., Bernardazzi, C., & de Souza, H. S. (2014). Cell death and inflammatory bowel diseases: apoptosis, necrosis, and autophagy in the intestinal epithelium. *Biomed Res Int, 2014*, 218493. doi:10.1155/2014/218493

Oakley, R. H., Sar, M., & Cidlowski, J. A. (1996). The human glucocorticoid receptor beta isoform. Expression, biochemical properties, and putative function. *J Biol Chem, 271*(16), 9550-9559.

Oakley, R. H., Webster, J. C., Jewell, C. M., Sar, M., & Cidlowski, J. A. (1999). Immunocytochemical analysis of the glucocorticoid receptor alpha isoform (GRalpha) using GRalpha-specific antibody. *Steroids, 64*(10), 742-751.

Obexer, P., Certa, U., Kofler, R., & Helmberg, A. (2001). Expression profiling of glucocorticoid-treated T-ALL cell lines: rapid repression of multiple genes involved in RNA-, protein- and nucleotide synthesis. *Oncogene, 20*(32), 4324-4336.

Ogata, M., Hino, S., Saito, A., Morikawa, K., Kondo, S., Kanemoto, S., . . . Imaizumi, K. (2006). Autophagy is activated for cell survival after endoplasmic reticulum stress. *Mol Cell Biol, 26*(24), 9220-9231. doi:10.1128/MCB.01453-06

Oida, T., & Weiner, H. L. (2010). TGF-beta induces surface LAP expression on murine CD4 T cells independent of Foxp3 induction. *PLoS One, 5*(11), e15523. doi:10.1371/journal.pone.0015523

Orenstein, S. J., & Cuervo, A. M. (2010). Chaperone-mediated autophagy: molecular mechanisms and physiological relevance. *Semin Cell Dev Biol, 21*(7), 719-726. doi:10.1016/j.semcdb.2010.02.005

Orphanides, G., Lagrange, T., & Reinberg, D. (1996). The general transcription factors of RNA polymerase II. *Genes Dev, 10*(21), 2657-2683.

Orti, E., Hu, L. M., & Munck, A. (1993). Kinetics of glucocorticoid receptor phosphorylation in intact cells. Evidence for hormone-induced hyperphosphorylation after activation and recycling of hyperphosphorylated receptors. *J Biol Chem, 268*(11), 7779-7784.

Ott, M., Gogvadze, V., Orrenius, S., & Zhivotovsky, B. (2007). Mitochondria, oxidative stress and cell death. *Apoptosis, 12*(5), 913-922. doi:10.1007/s10495-007-0756-2

Parkin, D. M. (2006). The global health burden of infection-associated cancers in the year 2002. *Int J Cancer, 118*(12), 3030-3044. doi:10.1002/ijc.21731

Parzych, K. R., & Klionsky, D. J. (2014). An overview of autophagy: morphology, mechanism, and regulation. *Antioxid Redox Signal, 20*(3), 460-473. doi:10.1089/ars.2013.5371

Pattingre, S., Tassa, A., Qu, X., Garuti, R., Liang, X. H., Mizushima, N., . . . Levine, B. (2005). Bcl-2 antiapoptotic proteins inhibit Beclin 1-dependent autophagy. *Cell, 122*(6), 927-939. doi:10.1016/j.cell.2005.07.002

Peirson, S. N., & Butler, J. N. (2007). Quantitative polymerase chain reaction. *Methods Mol Biol, 362*, 349-362. doi:10.1007/978-1-59745-257-1_25

Pemberton, P. A., Stein, P. E., Pepys, M. B., Potter, J. M., & Carrell, R. W. (1988). Hormone binding globulins undergo serpin conformational change in inflammation. *Nature, 336*(6196), 257-258. doi:10.1038/336257a0

Perez-Andreu, V., Roberts, K. G., Harvey, R. C., Yang, W., Cheng, C., Pei, D., . . . Yang, J. J. (2013). Inherited GATA3 variants are associated with Ph-like childhood acute lymphoblastic leukemia and risk of relapse. *Nat Genet, 45*(12), 1494-1498. doi:10.1038/ng.2803

Peter, M. E., & Krammer, P. H. (1998). Mechanisms of CD95 (APO-1/Fas)-mediated apoptosis. *Curr Opin Immunol, 10*(5), 545-551.

Ploner, C., Schmidt, S., Presul, E., Renner, K., Schrocksnadel, K., Rainer, J., . . . Kofler, R. (2005). Glucocorticoid-induced apoptosis and glucocorticoid resistance in acute lymphoblastic leukemia. *J Steroid Biochem Mol Biol, 93*(2-5), 153-160. doi:10.1016/j.jsbmb.2004.12.017

Polivka, J., & Janku, F. (2014). Molecular targets for cancer therapy in the PI3K/AKT/mTOR pathway. *Pharmacol Ther, 142*(2), 164-175. doi:10.1016/j.pharmthera.2013.12.004

Pozarowski, P., & Darzynkiewicz, Z. (2004). Analysis of cell cycle by flow cytometry. *Methods Mol Biol, 281*, 301-311. doi:10.1385/1-59259-811-0:301

Psarra, A. M., Solakidi, S., Trougakos, I. P., Margaritis, L. H., Spyrou, G., & Sekeris, C. E. (2005). Glucocorticoid receptor isoforms in human hepatocarcinoma HepG2 and SaOS-2 osteosarcoma cells: presence of glucocorticoid receptor alpha in mitochondria and of glucocorticoid receptor beta in nucleoli. *Int J Biochem Cell Biol, 37*(12), 2544-2558. doi:10.1016/j.biocel.2005.06.015

Pui, C. H., Mullighan, C. G., Evans, W. E., & Relling, M. V. (2012). Pediatric acute lymphoblastic leukemia: where are we going and how do we get there? *Blood, 120*(6), 1165-1174. doi:10.1182/blood-2012-05-378943

Pui, C. H., Robison, L. L., & Look, A. T. (2008). Acute lymphoblastic leukaemia. *Lancet, 371*(9617), 1030-1043. doi:10.1016/S0140-6736(08)60457-2

Pullen, S. S., Miller, H. G., Everdeen, D. S., Dang, T. T., Crute, J. J., & Kehry, M. R. (1998). CD40-tumor necrosis factor receptor-associated factor (TRAF) interactions: regulation of CD40 signaling through multiple TRAF binding sites and TRAF hetero-oligomerization. *Biochemistry, 37*(34), 11836-11845. doi:10.1021/bi981067q

Puthalakath, H., O'Reilly, L. A., Gunn, P., Lee, L., Kelly, P. N., Huntington, N. D., . . . Strasser, A. (2007). ER stress triggers apoptosis by activating BH3-only protein Bim. *Cell, 129*(7), 1337-1349. doi:10.1016/j.cell.2007.04.027

Quillet-Mary, A., Jaffrézou, J. P., Mansat, V., Bordier, C., Naval, J., & Laurent, G. (1997). Implication of mitochondrial hydrogen peroxide generation in ceramide-induced apoptosis. *J Biol Chem, 272*(34), 21388-21395.

Ramakrishnan, S., & Houston, L. L. (1984). Inhibition of human acute lymphoblastic leukemia cells by immunotoxins: potentiation by chloroquine. *Science, 223*(4631), 58-61.

Rao, R. V., Peel, A., Logvinova, A., del Rio, G., Hermel, E., Yokota, T., . . . Bredesen, D. E. (2002). Coupling endoplasmic reticulum stress to the cell death program: role of the ER chaperone GRP78. *FEBS Lett, 514*(2-3), 122-128.

Rathmell, J. C., Lindsten, T., Zong, W. X., Cinalli, R. M., & Thompson, C. B. (2002). Deficiency in Bak and Bax perturbs thymic selection and lymphoid homeostasis. *Nat Immunol, 3*(10), 932-939. doi:10.1038/ni834

Ravikumar, B., Moreau, K., Jahreiss, L., Puri, C., & Rubinsztein, D. C. (2010a). Plasma membrane contributes to the formation of pre-autophagosomal structures. *Nat Cell Biol, 12*(8), 747-757. doi:10.1038/ncb2078

Ravikumar, B., Sarkar, S., Davies, J. E., Futter, M., Garcia-Arencibia, M., Green-Thompson, Z. W., . . . Rubinsztein, D. C. (2010b). Regulation of mammalian autophagy in physiology and pathophysiology. *Physiol Rev, 90*(4), 1383-1435. doi:10.1152/physrev.00030.2009

Ray, A., & Prefontaine, K. E. (1994). Physical association and functional antagonism between the p65 subunit of transcription factor NF-kappa B and the glucocorticoid receptor. *Proc Natl Acad Sci U S A, 91*(2), 752-756.

Reddy, K. B., & Glaros, S. (2007). Inhibition of the MAP kinase activity suppresses estrogen-induced breast tumor growth both in vitro and in vivo. *Int J Oncol, 30*(4), 971-975.

Reddy, R. K., Lu, J., & Lee, A. S. (1999). The endoplasmic reticulum chaperone glycoprotein GRP94 with Ca(2+)-binding and antiapoptotic properties is a novel proteolytic target of calpain during etoposide-induced apoptosis. *J Biol Chem, 274*(40), 28476-28483.

Reddy, R. K., Mao, C., Baumeister, P., Austin, R. C., Kaufman, R. J., & Lee, A. S. (2003). Endoplasmic reticulum chaperone protein GRP78 protects cells from apoptosis induced by topoisomerase inhibitors: role of ATP binding site in suppression of caspase-7 activation. *J Biol Chem, 278*(23), 20915-20924. doi:10.1074/jbc.M212328200

Reed, J. C. (1994). Bcl-2 and the regulation of programmed cell death. *J Cell Biol, 124*(1-2), 1-6.

Renschler, M. F. (2004). The emerging role of reactive oxygen species in cancer therapy. *Eur J Cancer, 40*(13), 1934-1940. doi:10.1016/j.ejca.2004.02.031

Roberts, P. J., & Der, C. J. (2007). Targeting the Raf-MEK-ERK mitogen-activated protein kinase cascade for the treatment of cancer. *Oncogene, 26*(22), 3291-3310. doi:10.1038/sj.onc.1210422

Roedding, A. S., Gao, A. F., Au-Yeung, W., Scarcelli, T., Li, P. P., & Warsh, J. J. (2012). Effect of oxidative stress on TRPM2 and TRPC3 channels in B lymphoblast cells in bipolar disorder. *Bipolar Disord, 14*(2), 151-161. doi:10.1111/j.1399-5618.2012.01003.x

Rogatsky, I., Waase, C. L., & Garabedian, M. J. (1998). Phosphorylation and inhibition of rat glucocorticoid receptor transcriptional activation by glycogen synthase kinase-3 (GSK-

3). Species-specific differences between human and rat glucocorticoid receptor signaling as revealed through GSK-3 phosphorylation. *J Biol Chem, 273*(23), 14315-14321.

Rosati, E., Sabatini, R., Rampino, G., De Falco, F., Di Ianni, M., Falzetti, F., . . . Marconi, P. (2010). Novel targets for endoplasmic reticulum stress-induced apoptosis in B-CLL. *Blood, 116*(15), 2713-2723. doi:10.1182/blood-2010-03-275628

Rothe, M., Sarma, V., Dixit, V. M., & Goeddel, D. V. (1995). TRAF2-mediated activation of NF-kappa B by TNF receptor 2 and CD40. *Science, 269*(5229), 1424-1427.

Rothe, M., Wong, S. C., Henzel, W. J., & Goeddel, D. V. (1994). A novel family of putative signal transducers associated with the cytoplasmic domain of the 75 kDa tumor necrosis factor receptor. *Cell, 78*(4), 681-692.

Roussel, D., Dumas, J. F., Simard, G., Malthiery, Y., & Ritz, P. (2004). Kinetics and control of oxidative phosphorylation in rat liver mitochondria after dexamethasone treatment. *Biochem J, 382*(Pt 2), 491-499. doi:10.1042/BJ20040696

Rubio-Moscardo, F., Blesa, D., Mestre, C., Siebert, R., Balasas, T., Benito, A., . . . Martinez-Climent, J. A. (2005). Characterization of 8p21.3 chromosomal deletions in B-cell lymphoma: TRAIL-R1 and TRAIL-R2 as candidate dosage-dependent tumor suppressor genes. *Blood, 106*(9), 3214-3222. doi:10.1182/blood-2005-05-2013

Saelens, X., Festjens, N., Vande Walle, L., van Gurp, M., van Loo, G., & Vandenabeele, P. (2004). Toxic proteins released from mitochondria in cell death. *Oncogene, 23*(16), 2861-2874. doi:10.1038/sj.onc.1207523

Sakamuru, S., Attene-Ramos, M. S., & Xia, M. (2016). Mitochondrial Membrane Potential Assay. *Methods Mol Biol, 1473*, 17-22. doi:10.1007/978-1-4939-6346-1_2

Sakamuru, S., Li, X., Attene-Ramos, M. S., Huang, R., Lu, J., Shou, L., . . . Xia, M. (2012). Application of a homogenous membrane potential assay to assess mitochondrial function. *Physiol Genomics, 44*(9), 495-503. doi:10.1152/physiolgenomics.00161.2011

Sandoval, H., Thiagarajan, P., Dasgupta, S. K., Schumacher, A., Prchal, J. T., Chen, M., & Wang, J. (2008). Essential role for Nix in autophagic maturation of erythroid cells. *Nature, 454*(7201), 232-235. doi:10.1038/nature07006

Sapolsky, R. M., Krey, L. C., & McEwen, B. S. (1984). Stress down-regulates corticosterone receptors in a site-specific manner in the brain. *Endocrinology, 114*(1), 287-292. doi:10.1210/endo-114-1-287

Sato, M., Yao, V. J., Arap, W., & Pasqualini, R. (2010). GRP78 signaling hub a receptor for targeted tumor therapy. *Adv Genet, 69*, 97-114. doi:10.1016/S0065-2660(10)69006-2

Schaaf, M. J., & Cidlowski, J. A. (2002). Molecular mechanisms of glucocorticoid action and resistance. *J Steroid Biochem Mol Biol, 83*(1-5), 37-48.

Schardt, J. A., Mueller, B. U., & Pabst, T. (2011). Activation of the unfolded protein response in human acute myeloid leukemia. *Methods Enzymol, 489*, 227-243. doi:10.1016/B978-0-12-385116-1.00013-3

Scheller, K., Seibel, P., & Sekeris, C. E. (2003). Glucocorticoid and thyroid hormone receptors in mitochondria of animal cells. *Int Rev Cytol, 222*, 1-61.

Scheller, K., Sekeris, C. E., Krohne, G., Hock, R., Hansen, I. A., & Scheer, U. (2000). Localization of glucocorticoid hormone receptors in mitochondria of human cells. *Eur J Cell Biol, 79*(5), 299-307. doi:10.1078/S0171-9335(04)70033-3

Schindler, A. J., & Schekman, R. (2009). In vitro reconstitution of ER-stress induced ATF6 transport in COPII vesicles. *Proc Natl Acad Sci U S A, 106*(42), 17775-17780. doi:10.1073/pnas.0910342106

Schlechte, J. A., Ginsberg, B. H., & Sherman, B. M. (1982). Regulation of the glucocorticoid receptor in human lymphocytes. *J Steroid Biochem, 16*(1), 69-74.

Schweers, R. L., Zhang, J., Randall, M. S., Loyd, M. R., Li, W., Dorsey, F. C., . . . Ney, P. A. (2007). NIX is required for programmed mitochondrial clearance during reticulocyte maturation. *Proc Natl Acad Sci U S A, 104*(49), 19500-19505. doi:10.1073/pnas.0708818104

Secker-Walker, L. M., Lawler, S. D., & Hardisty, R. M. (1978). Prognostic implications of chromosomal findings in acute lymphoblastic leukaemia at diagnosis. *Br Med J, 2*(6151), 1529-1530.

Seibel, N. L., Steinherz, P. G., Sather, H. N., Nachman, J. B., Delaat, C., Ettinger, L. J., . . . Gaynon, P. S. (2008). Early postinduction intensification therapy improves survival for children and adolescents with high-risk acute lymphoblastic leukemia: a report from the Children's Oncology Group. *Blood, 111*(5), 2548-2555. doi:10.1182/blood-2007-02-070342

Shah, S., Schrader, K. A., Waanders, E., Timms, A. E., Vijai, J., Miething, C., . . . Offit, K. (2013). A recurrent germline PAX5 mutation confers susceptibility to pre-B cell acute lymphoblastic leukemia. *Nat Genet, 45*(10), 1226-1231. doi:10.1038/ng.2754

Shao, Y., Gao, Z., Marks, P. A., & Jiang, X. (2004). Apoptotic and autophagic cell death induced by histone deacetylase inhibitors. *Proc Natl Acad Sci U S A, 101*(52), 18030-18035. doi:10.1073/pnas.0408345102

Sheriff, M. J., Dantzer, B., Delehanty, B., Palme, R., & boonstra, R. (2011). Measuring stress in wildlife: techniques for quantifying glucocorticoids. *Oecologia, 166*(4), 869-887. doi:10.1007/s00442-011-1943-y

Shi, Y., Vattem, K. M., Sood, R., An, J., Liang, J., Stramm, L., & Wek, R. C. (1998). Identification and characterization of pancreatic eukaryotic initiation factor 2 alpha-subunit kinase, PEK, involved in translational control. *Mol Cell Biol, 18*(12), 7499-7509.

Shu, C. W., Sun, F. C., Cho, J. H., Lin, C. C., Liu, P. F., Chen, P. Y., . . . Lai, Y. K. (2008). GRP78 and Raf-1 cooperatively confer resistance to endoplasmic reticulum stress-induced apoptosis. *J Cell Physiol, 215*(3), 627-635. doi:10.1002/jcp.21340

Siegel, R. L., Miller, K. D., & Jemal, A. (2016). Cancer statistics, 2016. *CA Cancer J Clin, 66*(1), 7-30. doi:10.3322/caac.21332

Siiteri, P. K., Murai, J. T., Hammond, G. L., Nisker, J. A., Raymoure, W. J., & Kuhn, R. W. (1982). The serum transport of steroid hormones. *Recent Prog Horm Res, 38*, 457-510.

Silva, A., Gírio, A., Cebola, I., Santos, C. I., Antunes, F., & Barata, J. T. (2011). Intracellular reactive oxygen species are essential for PI3K/Akt/mTOR-dependent IL-7-mediated viability of T-cell acute lymphoblastic leukemia cells. *Leukemia, 25*(6), 960-967. doi:10.1038/leu.2011.56

Sionov, R. V., Cohen, O., Kfir, S., Zilberman, Y., & Yefenof, E. (2006a). Role of mitochondrial glucocorticoid receptor in glucocorticoid-induced apoptosis. *J Exp Med, 203*(1), 189-201. doi:10.1084/jem.20050433

Sionov, R. V., Kfir, S., Zafrir, E., Cohen, O., Zilberman, Y., & Yefenof, E. (2006b). Glucocorticoid-induced apoptosis revisited: a novel role for glucocorticoid receptor translocation to the mitochondria. *Cell Cycle, 5*(10), 1017-1026. doi:10.4161/cc.5.10.2738

Smets, L. A., Salomons, G., & van den Berg, J. (1999). Glucocorticoid induced apoptosis in leukemia. *Adv Exp Med Biol, 457*, 607-614.

Smets, L. A., Van den Berg, J., Acton, D., Top, B., Van Rooij, H., & Verwijs-Janssen, M. (1994). BCL-2 expression and mitochondrial activity in leukemic cells with different sensitivity to glucocorticoid-induced apoptosis. *Blood, 84*(5), 1613-1619.

Smets, L. A., & van den Berg, J. D. (1996). Bcl-2 expression and glucocorticoid-induced apoptosis of leukemic and lymphoma cells. *Leuk Lymphoma, 20*(3-4), 199-205. doi:10.3109/10428199609051608

Smith, K. G., Strasser, A., & Vaux, D. L. (1996). CrmA expression in T lymphocytes of transgenic mice inhibits CD95 (Fas/APO-1)-transduced apoptosis, but does not cause lymphadenopathy or autoimmune disease. *EMBO J, 15*(19), 5167-5176.

Smith, M. A., Seibel, N. L., Altekruse, S. F., Ries, L. A., Melbert, D. L., O'Leary, M., . . . Reaman, G. H. (2010). Outcomes for children and adolescents with cancer: challenges for the twenty-first century. *J Clin Oncol, 28*(15), 2625-2634. doi:10.1200/JCO.2009.27.0421

Stanger, B. Z., Leder, P., Lee, T. H., Kim, E., & Seed, B. (1995). RIP: a novel protein containing a death domain that interacts with Fas/APO-1 (CD95) in yeast and causes cell death. *Cell, 81*(4), 513-523.

Stanulla, M., & Schrappe, M. (2009). Treatment of childhood acute lymphoblastic leukemia. *Semin Hematol, 46*(1), 52-63. doi:10.1053/j.seminhematol.2008.09.007

Stocklin, E., Wissler, M., Gouilleux, F., & Groner, B. (1996). Functional interactions between Stat5 and the glucocorticoid receptor. *Nature, 383*(6602), 726-728. doi:10.1038/383726a0

Storz, P. (2005). Reactive oxygen species in tumor progression. *Front Biosci, 10*, 1881-1896.

Strickland, I., Kisich, K., Hauk, P. J., Vottero, A., Chrousos, G. P., Klemm, D. J., & Leung, D. Y. (2001). High constitutive glucocorticoid receptor beta in human neutrophils enables them to reduce their spontaneous rate of cell death in response to corticosteroids. *J Exp Med, 193*(5), 585-593.

Suliman, A., Lam, A., Datta, R., & Srivastava, R. K. (2001). Intracellular mechanisms of TRAIL: apoptosis through mitochondrial-dependent and -independent pathways. *Oncogene, 20*(17), 2122-2133. doi:10.1038/sj.onc.1204282

Sumer-Bayraktar, Z., Kolarich, D., Campbell, M. P., Ali, S., Packer, N. H., & Thaysen-Andersen, M. (2011). N-glycans modulate the function of human corticosteroid-binding globulin. *Mol Cell Proteomics, 10*(8), M111 009100. doi:10.1074/mcp.M111.009100

Swerdlow, S., Campo, E., Harris, N., Jaffe, E., Pilleri, S., & Stein, H. (2008). WHO classification of tumours of haematopoietic and lymphoid tissures. *IARC Press, 4th ed*.

Szatrowski, T. P., & Nathan, C. F. (1991). Production of large amounts of hydrogen peroxide by human tumor cells. *Cancer Res, 51*(3), 794-798.

Szegezdi, E., Logue, S. E., Gorman, A. M., & Samali, A. (2006). Mediators of endoplasmic reticulum stress-induced apoptosis. *EMBO Rep, 7*(9), 880-885. doi:10.1038/sj.embor.7400779

Tabas, I., & Ron, D. (2011). Integrating the mechanisms of apoptosis induced by endoplasmic reticulum stress. *Nat Cell Biol, 13*(3), 184-190. doi:10.1038/ncb0311-184

Takahashi, J. S., Hong, H. K., Ko, C. H., & McDearmon, E. L. (2008). The genetics of mammalian circadian order and disorder: implications for physiology and disease. *Nat Rev Genet, 9*(10), 764-775. doi:10.1038/nrg2430

Takeuchi, M., Rothe, M., & Goeddel, D. V. (1996). Anatomy of TRAF2. Distinct domains for nuclear factor-kappaB activation and association with tumor necrosis factor signaling proteins. *J Biol Chem, 271*(33), 19935-19942.

Tanenbaum, D. M., Wang, Y., Williams, S. P., & Sigler, P. B. (1998). Crystallographic comparison of the estrogen and progesterone receptor's ligand binding domains. *Proc Natl Acad Sci U S A, 95*(11), 5998-6003.

Tanida, I., Ueno, T., & Kominami, E. (2004). LC3 conjugation system in mammalian autophagy. *Int J Biochem Cell Biol, 36*(12), 2503-2518. doi:10.1016/j.biocel.2004.05.009

Tanimura, A., Yujiri, T., Tanaka, Y., Hatanaka, M., Mitani, N., Nakamura, Y., . . . Tanizawa, Y. (2009). The anti-apoptotic role of the unfolded protein response in Bcr-Abl-positive leukemia cells. *Leuk Res, 33*(7), 924-928. doi:10.1016/j.leukres.2009.01.027

Terry L Riss, P., Richard A Moravec, BS, Andrew L Niles, MS, Sarah Duellman, PhD, Hélène A Benink, PhD, Tracy J Worzella, MS, and Lisa Minor. (Published May 1, 2013; Last Update: July 1, 2016.). Cell Viability Assays. In C. N. Sittampalam GS, Brimacombe K, et al., (Ed.), *Assay Guidance Manual*: Eli Lilly & Company and the National Center for Advancing Translational Sciences; NCBI.

Tian, S., Poukka, H., Palvimo, J. J., & Janne, O. A. (2002). Small ubiquitin-related modifier-1 (SUMO-1) modification of the glucocorticoid receptor. *Biochem J, 367*(Pt 3), 907-911. doi:10.1042/BJ20021085

Tome, M. E., Lutz, N. W., & Briehl, M. M. (2004). Overexpression of catalase or Bcl-2 alters glucose and energy metabolism concomitant with dexamethasone resistance. *Biochim Biophys Acta, 1693*(1), 57-72. doi:10.1016/j.bbamcr.2004.05.004

Tonko, M., Ausserlechner, M. J., Bernhard, D., Helmberg, A., & Kofler, R. (2001). Gene expression profiles of proliferating vs. G1/G0 arrested human leukemia cells suggest a mechanism for glucocorticoid-induced apoptosis. *FASEB J, 15*(3), 693-699. doi:10.1096/fj.00-0327com

Torgersen, M. L., Engedal, N., Boe, S. O., Hokland, P., & Simonsen, A. (2013). Targeting autophagy potentiates the apoptotic effect of histone deacetylase inhibitors in t(8;21) AML cells. *Blood, 122*(14), 2467-2476. doi:10.1182/blood-2013-05-500629

Trachootham, D., Alexandre, J., & Huang, P. (2009). Targeting cancer cells by ROS-mediated mechanisms: a radical therapeutic approach? *Nat Rev Drug Discov, 8*(7), 579-591. doi:10.1038/nrd2803

Trevino, L. R., Yang, W., French, D., Hunger, S. P., Carroll, W. L., Devidas, M., . . . Relling, M. V. (2009). Germline genomic variants associated with childhood acute lymphoblastic leukemia. *Nat Genet, 41*(9), 1001-1005. doi:10.1038/ng.432

Triantafilou, M., Fradelizi, D., & Triantafilou, K. (2001). Major histocompatibility class one molecule associates with glucose regulated protein (GRP) 78 on the cell surface. *Hum Immunol, 62*(8), 764-770.

Udensi, U. K., & Tchounwou, P. B. (2014). Dual effect of oxidative stress on leukemia cancer induction and treatment. *J Exp Clin Cancer Res, 33*, 106. doi:10.1186/s13046-014-0106-5

Veis, D. J., Sorenson, C. M., Shutter, J. R., & Korsmeyer, S. J. (1993). Bcl-2-deficient mice demonstrate fulminant lymphoid apoptosis, polycystic kidneys, and hypopigmented hair. *Cell, 75*(2), 229-240.

Veleiro, A. S., Alvarez, L. D., Eduardo, S. L., & Burton, G. (2010). Structure of the glucocorticoid receptor, a flexible protein that can adapt to different ligands. *ChemMedChem, 5*(5), 649-659. doi:10.1002/cmdc.201000014

Velez, J., Pan, R., Lee, J. T., Enciso, L., Suarez, M., Duque, J. E., . . . Samudio, I. (2016). Biguanides sensitize leukemia cells to ABT-737-induced apoptosis by inhibiting mitochondrial electron transport. *Oncotarget, 7*(32), 51435-51449. doi:10.18632/oncotarget.9843

Vermeulen, K., Van Bockstaele, D. R., & Berneman, Z. N. (2003). The cell cycle: a review of regulation, deregulation and therapeutic targets in cancer. *Cell Prolif, 36*(3), 131-149.

Verras, M., Papandreou, I., & Denko, N. C. (2015). WNT16-expressing Acute Lymphoblastic Leukemia Cells are Sensitive to Autophagy Inhibitors after ER Stress Induction. *Anticancer Res, 35*(9), 4625-4631.

Villunger, A., Michalak, E. M., Coultas, L., Mullauer, F., Bock, G., Ausserlechner, M. J., . . . Strasser, A. (2003). p53- and drug-induced apoptotic responses mediated by BH3-only proteins puma and noxa. *Science, 302*(5647), 1036-1038. doi:10.1126/science.1090072

Wadhwa, R., Taira, K., & Kaul, S. C. (2002). An Hsp70 family chaperone, mortalin/mthsp70/PBP74/Grp75: what, when, and where? *Cell Stress Chaperones, 7*(3), 309-316.

Walczak, M., & Martens, S. (2013). Dissecting the role of the Atg12-Atg5-Atg16 complex during autophagosome formation. *Autophagy, 9*(3), 424-425. doi:10.4161/auto.22931

Walter, L., & Hajnoczky, G. (2005). Mitochondria and endoplasmic reticulum: the lethal interorganelle cross-talk. *J Bioenerg Biomembr, 37*(3), 191-206. doi:10.1007/s10863-005-6600-x

Wanderling, S., Simen, B. B., Ostrovsky, O., Ahmed, N. T., Vogen, S. M., Gidalevitz, T., & Argon, Y. (2007). GRP94 is essential for mesoderm induction and muscle development because it regulates insulin-like growth factor secretion. *Mol Biol Cell, 18*(10), 3764-3775. doi:10.1091/mbc.e07-03-0275

Wang, A. H., Wei, L., Chen, L., Zhao, S. Q., Wu, W. L., Shen, Z. X., & Li, J. M. (2011a). Synergistic effect of bortezomib and valproic acid treatment on the proliferation and apoptosis of acute myeloid leukemia and myelodysplastic syndrome cells. *Ann Hematol, 90*(8), 917-931. doi:10.1007/s00277-011-1175-6

Wang, C., Tian, L., Popov, V. M., & Pestell, R. G. (2011b). Acetylation and nuclear receptor action. *J Steroid Biochem Mol Biol, 123*(3-5), 91-100. doi:10.1016/j.jsbmb.2010.12.003

Wang, M., Wey, S., Zhang, Y., Ye, R., & Lee, A. S. (2009). Role of the unfolded protein response regulator GRP78/BiP in development, cancer, and neurological disorders. *Antioxid Redox Signal, 11*(9), 2307-2316. doi:10.1089/ARS.2009.2485

Wang, X. Y., & Subjeck, J. R. (2013). High molecular weight stress proteins: Identification, cloning and utilisation in cancer immunotherapy. *Int J Hyperthermia, 29*(5), 364-375. doi:10.3109/02656736.2013.803607

Wang, Y., Alam, G. N., Ning, Y., Visioli, F., Dong, Z., Nör, J. E., & Polverini, P. J. (2012). The unfolded protein response induces the angiogenic switch in human tumor cells through the PERK/ATF4 pathway. *Cancer Res, 72*(20), 5396-5406. doi:10.1158/0008-5472.CAN-12-0474

Wang, Z., Frederick, J., & Garabedian, M. J. (2002). Deciphering the phosphorylation "code" of the glucocorticoid receptor in vivo. *J Biol Chem, 277*(29), 26573-26580. doi:10.1074/jbc.M110530200

Webb, M. S., Miller, A. L., Johnson, B. H., Fofanov, Y., Li, T., Wood, T. G., & Thompson, E. B. (2003). Gene networks in glucocorticoid-evoked apoptosis of leukemic cells. *J Steroid Biochem Mol Biol, 85*(2-5), 183-193.

Weinberg, F., & Chandel, N. S. (2009). Reactive oxygen species-dependent signaling regulates cancer. *Cell Mol Life Sci, 66*(23), 3663-3673. doi:10.1007/s00018-009-0099-y

Wey, S., Luo, B., Tseng, C. C., Ni, M., Zhou, H., Fu, Y., . . . Lee, A. S. (2012). Inducible knockout of GRP78/BiP in the hematopoietic system suppresses Pten-null leukemogenesis and AKT oncogenic signaling. *Blood, 119*(3), 817-825. doi:10.1182/blood-2011-06-357384

Winslow, A. R., & Rubinsztein, D. C. (2008). Autophagy in neurodegeneration and development. *Biochim Biophys Acta, 1782*(12), 723-729. doi:10.1016/j.bbadis.2008.06.010

Wu, W. S., Wu, J. R., & Hu, C. T. (2008). Signal cross talks for sustained MAPK activation and cell migration: the potential role of reactive oxygen species. *Cancer Metastasis Rev, 27*(2), 303-314. doi:10.1007/s10555-008-9112-4

Xi, G., Hu, X., Wu, B., Jiang, H., Young, C. Y., Pang, Y., & Yuan, H. (2011). Autophagy inhibition promotes paclitaxel-induced apoptosis in cancer cells. *Cancer Lett, 307*(2), 141-148. doi:10.1016/j.canlet.2011.03.026

Xu, C., Zhu, L., Chan, T., Lu, X., Shen, W., Madigan, M. C., . . . Zhou, F. (2016). Chloroquine and Hydroxychloroquine Are Novel Inhibitors of Human Organic Anion Transporting Polypeptide 1A2. *J Pharm Sci, 105*(2), 884-890. doi:10.1002/jps.24663

Yadav, R. K., Chae, S. W., Kim, H. R., & Chae, H. J. (2014). Endoplasmic reticulum stress and cancer. *J Cancer Prev, 19*(2), 75-88. doi:10.15430/JCP.2014.19.2.75

Yang, L., Zhao, D., Ren, J., & Yang, J. (2015). Endoplasmic reticulum stress and protein quality control in diabetic cardiomyopathy. *Biochim Biophys Acta, 1852*(2), 209-218. doi:10.1016/j.bbadis.2014.05.006

Yang, Z., & Klionsky, D. J. (2010). Mammalian autophagy: core molecular machinery and signaling regulation. *Curr Opin Cell Biol, 22*(2), 124-131. doi:10.1016/j.ceb.2009.11.014

Yao, X. L., Cowan, M. J., Gladwin, M. T., Lawrence, M. M., Angus, C. W., & Shelhamer, J. H. (1999). Dexamethasone alters arachidonate release from human epithelial cells by induction of p11 protein synthesis and inhibition of phospholipase A2 activity. *J Biol Chem, 274*(24), 17202-17208.

Ying, M., Zhou, X., Zhong, L., Lin, N., Jing, H., Luo, P., . . . He, Q. (2013). Bortezomib sensitizes human acute myeloid leukemia cells to all-trans-retinoic acid-induced differentiation by modifying the RARα/STAT1 axis. *Mol Cancer Ther, 12*(2), 195-206. doi:10.1158/1535-7163.MCT-12-0433

Yoo, K., & Chin, H. (2003). Cancer epidermiology and prevention. *Korean J epidermiol, 25*, 1-15.

Yoshida, H., Kong, Y. Y., Yoshida, R., Elia, A. J., Hakem, A., Hakem, R., . . . Mak, T. W. (1998). Apaf1 is required for mitochondrial pathways of apoptosis and brain development. *Cell, 94*(6), 739-750.

Yoshida, N. L., Miyashita, T., U, M., Yamada, M., Reed, J. C., Sugita, Y., & Oshida, T. (2002). Analysis of gene expression patterns during glucocorticoid-induced apoptosis using oligonucleotide arrays. *Biochem Biophys Res Commun, 293*(4), 1254-1261. doi:10.1016/S0006-291X(02)00361-3

Zawydiwski, R., Harmon, J. M., & Thompson, E. B. (1983). Glucocorticoid-resistant human acute lymphoblastic leukemic cell line with functional receptor. *Cancer Res, 43*(8), 3865-3873.

Zhang, H., Bosch-Marce, M., Shimoda, L. A., Tan, Y. S., Baek, J. H., Wesley, J. B., . . . Semenza, G. L. (2008a). Mitochondrial autophagy is an HIF-1-dependent adaptive metabolic response to hypoxia. *J Biol Chem, 283*(16), 10892-10903. doi:10.1074/jbc.M800102200

Zhang, L., Zhou, R., Li, X., Ursano, R. J., & Li, H. (2006). Stress-induced change of mitochondria membrane potential regulated by genomic and non-genomic GR signaling: a possible mechanism for hippocampus atrophy in PTSD. *Med Hypotheses, 66*(6), 1205-1208. doi:10.1016/j.mehy.2005.11.041

Zhang, M. Y., Churpek, J. E., Keel, S. B., Walsh, T., Lee, M. K., Loeb, K. R., . . . Shimamura, A. (2015). Germline ETV6 mutations in familial thrombocytopenia and hematologic malignancy. *Nat Genet, 47*(2), 180-185. doi:10.1038/ng.3177

Zhang, N., Fu, J. N., & Chou, T. C. (2016). Synergistic combination of microtubule targeting anticancer fludelone with cytoprotective panaxytriol derived from panax ginseng against MX-1 cells in vitro: experimental design and data analysis using the combination index method. *Am J Cancer Res, 6*(1), 97-104.

Zhang, R., Humphreys, I., Sahu, R. P., Shi, Y., & Srivastava, S. K. (2008b). In vitro and in vivo induction of apoptosis by capsaicin in pancreatic cancer cells is mediated through ROS generation and mitochondrial death pathway. *Apoptosis, 13*(12), 1465-1478. doi:10.1007/s10495-008-0278-6

Zhang, Y., Liu, R., Ni, M., Gill, P., & Lee, A. S. (2010). Cell surface relocalization of the endoplasmic reticulum chaperone and unfolded protein response regulator GRP78/BiP. *J Biol Chem, 285*(20), 15065-15075. doi:10.1074/jbc.M109.087445

Zhang, Y., Tseng, C. C., Tsai, Y. L., Fu, X., Schiff, R., & Lee, A. S. (2013). Cancer cells resistant to therapy promote cell surface relocalization of GRP78 which complexes with PI3K and enhances PI(3,4,5)P3 production. *PLoS One, 8*(11), e80071. doi:10.1371/journal.pone.0080071

Zhou, A., Wei, Z., Read, R. J., & Carrell, R. W. (2006). Structural mechanism for the carriage and release of thyroxine in the blood. *Proc Natl Acad Sci U S A, 103*(36), 13321-13326. doi:10.1073/pnas.0604080103

Zhou, H., Zhang, Y., Fu, Y., Chan, L., & Lee, A. S. (2011). Novel mechanism of anti-apoptotic function of 78-kDa glucose-regulated protein (GRP78): endocrine resistance factor in breast cancer, through release of B-cell lymphoma 2 (BCL-2) from BCL-2-interacting killer (BIK). *J Biol Chem, 286*(29), 25687-25696. doi:10.1074/jbc.M110.212944

Zhou, J., & Cidlowski, J. A. (2005). The human glucocorticoid receptor: one gene, multiple proteins and diverse responses. *Steroids, 70*(5-7), 407-417. doi:10.1016/j.steroids.2005.02.006

Zhu, L. (2005). Tumour suppressor retinoblastoma protein Rb: a transcriptional regulator. *Eur J Cancer, 41*(16), 2415-2427. doi:10.1016/j.ejca.2005.08.009